STUDIES ON GLUON DISTRIBUTION FUNCTION AT LOW-X

A thesis submitted to
Tezpur University
in fulfillment of the requirements
for the degree of
Doctor of Philosophy

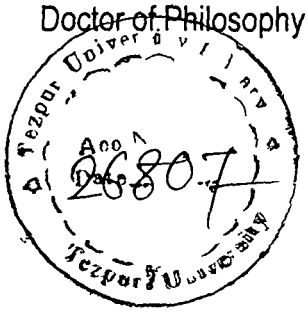

By

Ghana Kanta Medhi

Department of Physics
School of Science and Technology
Tezpur University
Napaam, Tezpur – 784 028
Assam, India

Dedicated to
my beloved father
Ramesh Chandra Medhi

And

my beloved mother
Late Labanya Medhi

CERTIFICATE

Dr. Jayanta Kumar Sarma
Reader
Department of Physics
Tezpur University
Napaam, Tezpur- 784 028
Assam, India

This is to certify that **Mr. Ghana Kanta Medhi** has worked under my supervision for the thesis entitled **"Studies on Gluon Distribution Function at Low-x"** which is being submitted to Tezpur University in fulfillment of the requirements for the degree of Doctor of Philosophy. The thesis is Mr. Medhi's own work. He has fulfilled all the requirements under the Ph. D. rules and regulations of Tezpur University and to the best of my knowledge, the thesis as a whole or a part thereof has not been submitted to any other university for any degree or diploma.

Date : 07-11-2002
Place : Napaam, Tezpur

Jayanta Kr Sarma
(Dr. Jayanta Kumar Sarma)
Supervisor

PREFACE

This thesis deals with gluon distribution function at low-x. Gluon distribution function can not be determined directly from experiment. On the otherhand, it is important as it may be an essential input in many high energy processes. Here, various methods for determination of gluon distribution function from proton and deuteron structure functions are presented. For this purpose, mainly GLDAP evolution equations are used and results are compared with those of other authors.

I am deeply indebted and grateful to my supervisor Dr. Jayanta Kumar Sarma, Reader, Physics Department, Tezpur University for his inspiring and painstaking guidance and constant encouragement throughout the course of this work.

My grateful thanks are due to Professor A. Choudhury and Dr. A. Kumar, Reader, for their kind interest and providing me necessary facilities of research as the heads of the department of Physics Department, Tezpur University during my work.

I acknowledge my gratefulness to Dr. D. K. Choudhury, Dr. N. Nimai Shingh, Dr. P. M. Kalita, Dr. B. Das, Mrs. K. Deka and all the faculty members of Physics Department of Tezpur University for their kind encouragement in performing the research work.

I feel immense pleasure to acknowledge my wife Mrs. Mrinalini Deka Medhi and my son Bittu for their constant support, love, inspiration and encouragement during the arduous time of my life.

My warm appreciation goes to Anjan, Mukesh, Ranjit, Siddhartha, Diganta, Abu, Naba, Juti, Syamalima, Anjali, Rasna, Supriya, Hupesh, Biswanath, Rubul, Bobbyma, Mani, M. Das, K. Nath, Kananba, Parulba, B. Barman, Bhanuba, Khagen, Putul, K. Das, Jyotshna, Jogen, Neelima, Kalpana, Bhabesh, Bijuba, M. Rajbangshi, Deepaba, N. K. Talukdar, Gitiba, Dhan, A. Sarma, Amal and Deepa for their love, inspiration and close friendship.

My thanks are due to all the members of the teaching staff of the Department of Physics of Birjhora Mahavidyalaya, Bongaigaon, all the members of Sangeet Tirtha, all the boarders of Assam Type Hostel of Tezpur University for their inspiration and keen interest to my work.

Financial support from the University Grants Commission, New Delhi, India as a minor research project is gratefully acknowledged.

Ghana Kanta Medhi.

Date . 07-11-2002
Place . Napaam, Tezpur

(Ghana Kanta Medhi)

STUDIES ON GLUON DISTRIBUTION FUNCTION AT LOW-X

CONTENTS

Chapter-1

INTRODUCTION

1.1. Structure of Matter:

The end of the nineteenth century, in1897, J. J. Thomson discovered the electron, a negatively charged particle. The study was started by J. Dalton in his atomic theory. According to him, each element consists of atoms, indivisible objects. But that the atom cannot hold the claim of being indivisible became clear in 1895, when J. J. Thomson showed that all atoms contain electrons. The electron is, therefore, an element of all atoms and hence of all substances. In addition to the electron, each atom consists of a nucleus which is located at the center of the atom with most of its mass. The electrons and the nucleus of each atom are bound together by the coulomb force or in general the electromagnetic force.

In 1911, E. Rutherford showed that all nuclei contain protons which are positively charged particles. In 1932, J. Chadwick discovered the neutron, a particle with mass nearly equal to the mass of the proton but with no electric charge, as a companion constituent of nuclei along with the proton. Thus nuclei are made up of protons and neutrons. In 1934, E. Fermi wrote down a beta nuclear decay Hamiltonian which with slight modification is still believed to be the correct weak interaction Hamiltonian in the low energy limit. In 1935, H. Yukawa introduced yet another force known as strong force responsible for binding together of the proton and the neutron inside the nucleus.

In the 1950's and 1960's, experiments were done at higher and higher energies taking advantages of the existence of new and very powerful particle accelerators. In the subsequent probing of the neutron and the proton, a whole zoo of new particles were found. Following the ideas, that led to the reduction of 100 atoms to only three fundamental particles, physicists suspected that this new, huge number of particle really indicated that even smaller, more fundamental particles existed. Experiments in

the 1970's proved that three smaller particles called Quark could be combined to make up neutrons, protons and many of the multitude of other particles.

The picture of fundamental constituents of matter and the interactions among them that has emerged in recent years is one of great beauty and simplicity. All matter seems to be composed of Quarks and Leptons which are supposedly point like that is structureless, spin half particles. Leaving aside gravitation, which is a negligible perturbation at the energy scales usually considered, all the three interactions namely weak, electromagnetic and strong, are described by gauge theories, and are mediated by spin one gauge bosons. Now there are three generations of Quarks and Leptons as follows:

Particles	First Generation	Second Generation	Third Generation
Quarks	u , d	s , c	b , t
Leptons	e , ν_e	μ , ν_μ	τ , ν_τ

where, u, d, s, c, b, t are up, down, strange, charm, bottom and top quarks respectively and $e, \mu, \tau, \nu_e, \nu_\mu, \mu_\tau$ are electron, muon, tau, electron-neutrino, muon-neutrino and tau-neutrino respectively.

Matter seems of require three kinds of interactions to behave as it does: electromagnetic, which holds the electrons to nuclei; strong which holds the quarks to one another and the weak which can change one kind of quark into another or equivalently, a neutron into a proton or a proton into a neutron. The masses of single atoms are so small that the gravitational force is negligible at the atomic level. At this level the other three forces are much more important.

Each flavour quark comes in three colours: Red (R), Green (G) and Blue (B). Colour is just a quantum number like the charge and bears no similarity with the visual colours. The colour structure tells us also about the properties of gluons. Since they

are absorbed and emitted by quarks, they can change the colour of quarks, that is, a red-blue gluon changes a red quark to a blue quark and so forth. There are also red-red, blue-blue and green-green gluons, so that there are nine possible gluon states in all altogether mathematically only eight of them are independent. Thus we see a kind of pattern: the electromagnetic force requires one photon; the weak force requires three intermediate bosons and the strong force requires eight gluons, each labeled by two colours. Gluons actually carry one colour and one anticolour. The properties of the weak force indicated that the weak force carriers are massive. Photons, intermediate bosons and gluons are all spin one particles.

Forces in the Standard Model

Force	Range	Strength at Fermi distance	Carrier	Mass at rest (GeV/c^2)	Spin	Electric charge
Gravitational	Infinite	10^{-38}	Graviton: g*	0	2	0
Weak	$<10^{-16}$cm	10^{-13}	Intermediate bosons:			
			W^+	81	1	+1
			W^-	81	1	-1
			Z^0	93	1	0
Electromagnetic	Infinite	10^{-2}	Photon: γ	0	1	0
Strong	$\simeq 10^{-13}$cm	1	Gluon: g	0	1	0

Since quarks have colours, antiquarks must possess negative colours ($\bar{R}$, $\bar{G}$, $\bar{B}$) having characteristics exactly opposite to the colour triplet (R, G, B). Since gluons are supposed to mediate interaction between all possible coloured pairs (qq), (q $\bar{q}$) and ($\bar{q}$ $\bar{q}$), they must also carry quantum numbers corresponding colour transitions, for example, $R \rightarrow G$, $R \rightarrow B$, apart from colourless transitions such as $R \rightarrow R$. In other words, gluons must exhibit a rich colour structure so that a particular gluon state must

in general be distinct, in terms of colour content, from the corresponding antigluon state. This necessitates a generalization of the concept of charge. With the quark model, hadrons, that is baryons and mesons are made of quarks which are strongly bound together. The exchange particle between quarks, and the true carrier of the strong force is the gluon. The properties of the gluon come out of the standard model theory. Evidence for gluons came in 1978 from an electron-positron machine at Hamburg in Germany. The machine, called PETRA, was able, like its Stanford twin PEP, to observe collisions up to 30 GeV and in the pattern of produced particles, the gluon was read.

Some people may still doubt the existence of the quark. The primary reason for this doubt is that quarks cannot be seen. To be able to justify treating quarks in the same way as the other elementary particles, the theoretical test, other than directly seeing them, would be necessary; and we must examine the characteristics of quarks in detail and refine the theory if need be. According to the Gell Mann-Zweing theory, quarks are a triplet of spin half fermions that carry SU_3 quantum numbers. In other words, they are particles similar to leptons. Since hadrons are compounds of quarks, not only their isospin and strangeness, but also their spin should be determined by the way the quarks are combined and one should also be able to predict the properties of the excited states of the hadrons. The spectra of hadrons should also be an important indication of the nature of interaction of quarks.

The theory of a Yang-Mills field with colour as the quantum number is called Chromodynamics; that is to say, the dynamics is colour. By assumption, there are three colours: Red, Green and Blue, and the strong force acts between coloured quarks. The hadrons are supposed to be a system in which the colours have cancelled themselves out and become white. The quantum of the colour gauge field is called Gluon, meaning the glue that holds quarks together. Now let us think of a process in which a gluon is emitted by a quark. If, as a result of this process, the red (R) quark changes to a blue (B) one, then the gluon took red from the quark and gave blue. Equivalently, one can think of the gluon as having taken away red (R) and anti-blue ($\bar{B}$); thus this gluon is carrying a composite colour of R $\bar{B}$ (Fig.1.1).

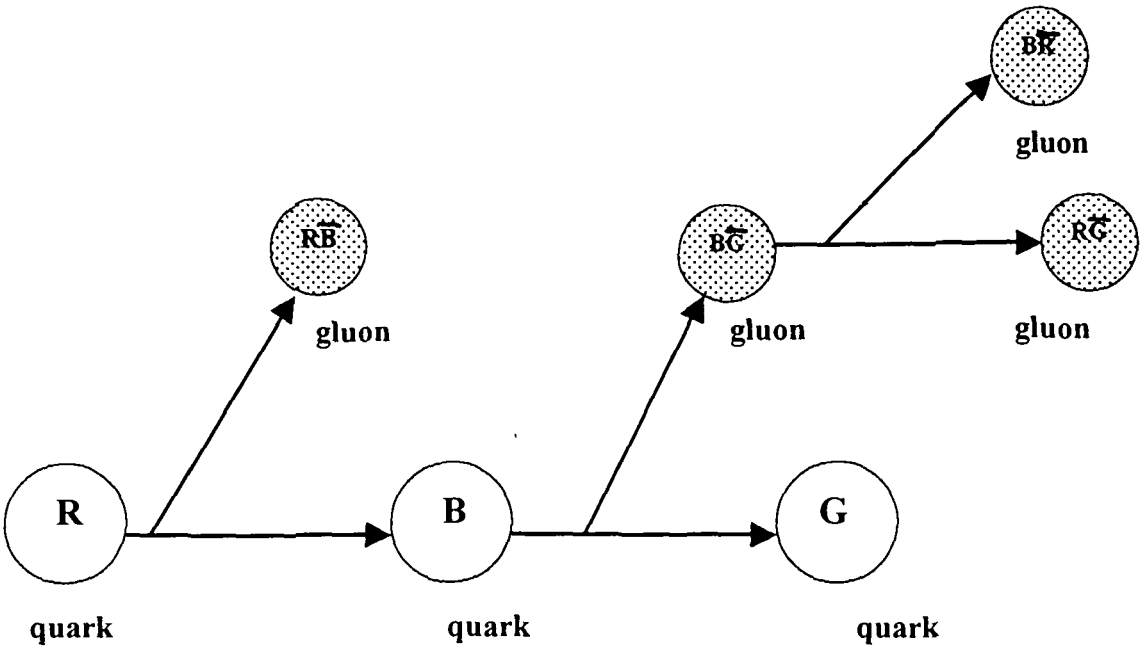

Fig.1.1: Quarks have colours and emit coloured gluons.

In general, the gluon, G_{ij}, that is released when q_i becomes q_j acts exactly like the compound state of q_i and $\bar{q}_j$, $G_{ij} \sim q_i \bar{q}_j$. There are $3 \times 3 = 9$ such combinations and one of the nine gluons is a special combination corresponding to the colour white, $G_w \sim q_R \bar{q}_R + q_G \bar{q}_G + q_B \bar{q}_B = 0$. But since it was required, to begin with, that the glue does not work on a white state, one must have $G_w = 0$. Thus the number of independent gluons must be eight. QCD (Quantum Chromodynamics) refers to the quantum theory of colour gauge fields. One can think of this theory as QED (Quantum Electrodynamics) with the electron replaced by the quarks and photon by the gluons.

1.2. Deep Inelastic Scattering:

High energy Deep Inelastic lepton-nucleon Scattering (DIS) has been recognized as an important testing ground for the understanding of the structure of matter.

Pioneering experiments in this direction started more than twenty years ago. Since then, DIS has been served as the experimental area where QCD is being tested progressively. The complete kinematics of the process is determined measuring the angle and energy of the scattered lepton and two variables which are directly accessible from the experiments. However the results are usually presented and interpreted through the variables Q^2, x and y (Fig.1.2).

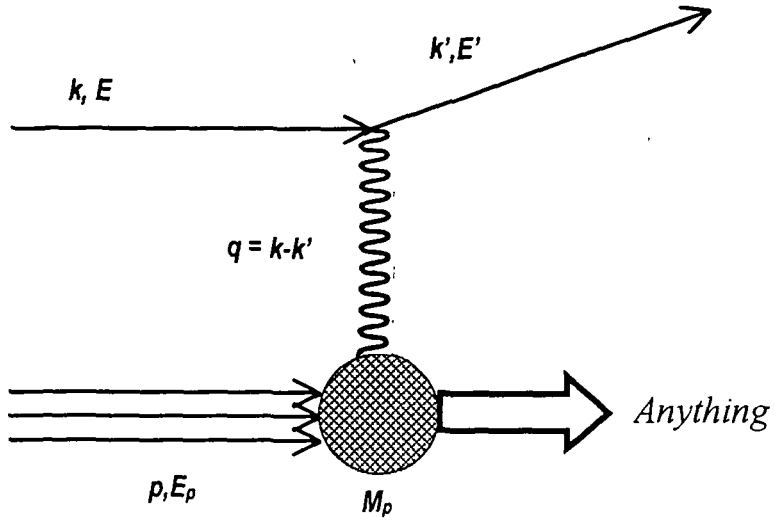

Fig.1.2: Kinematics of deep inelastic scattering process.

Defining,

k_μ = four momentum of the incoming lepton,

k'_μ = four momentum of the scattered lepton,

E = energy of the incoming lepton,

E' = energy of the scattered lepton,

E_p = energy of the nucleon,

M_p = rest mass of the nucleon,

P_μ = four momentum of the nucleon,

S = available squared energy in the CM system,

$$S = (k+P)^2 \approx 4EE',$$

$$Q^2 = -q^2 = -(k-k')^2 \approx 4EE'Cos^2\theta/2,$$

$$x = \frac{Q^2}{2p.q} = \frac{EE'Cos^2\theta/2}{E_p(E-E'Sin^2\theta/2)},$$

$$y = \frac{p.q}{p.k} \approx \frac{2p.q}{S} \approx \frac{E-E'Sin^2\theta/2}{E},$$

where, θ = angle of the scattered lepton measured with respect to the nucleon direction. Physically x is the fraction of the nucleon momentum carried by the struck quark while y represents the fraction of the lepton energy transferred to the nucleon in the nucleon rest frame. The relation between Q^2, x, y and S is $Q^2 \approx xyS$. The differential cross section for deep inelastic scattering from a nuclear target is completely calculable in QED. This cross section is expressible in terms of two structure functions W_1 and W_2 which parametrize the virtual photon nucleon coupling and contain all the interesting physics.

1.3. Structure Function:

Consider the case of electron scattering from a target composed of N well defined constituents which is characterized by the initial state vector $|\psi_i>$, and the final state $|\psi_f>$. Let the final state is unobserved. The invariant scattering cross section can be expressed in the form

$$\frac{\partial^2\sigma}{\partial\Omega\partial E'} = \frac{\alpha^2}{Q^4}\cdot\frac{E'}{E}L_{\mu\vartheta}W^{\mu\nu},$$

where, $L_{\mu\nu} = 2k_\mu k'_\nu + 2k_\nu k'_\mu - g_{\mu\nu}Q^2$ is the electron polarization tensor averaged over initial spin states, while

$$W^{\mu\nu} = \sum_f <p|J^{\mu^*}|f><f|J^\nu|p>\partial^4(p-p_f-Q)$$

is the unpolarised hadronic tensor averaged over initial spins, and J^μ is the hadronic transition current.

All the interesting target physics is contained with $W^{\mu\nu}$. Without any a prior knowledge of nucleon structure, it is possible to place strong constraints of the form of $W^{\mu\nu}$ and thus on the cross section. The most general form of $W^{\mu\nu}$ consistent with Lorentz and gauge invariances, and parity is

$$W_{\mu\nu} = W_1(\nu, Q^2)\left[\frac{Q^\mu Q^\nu}{Q^2} - g^{\mu\nu}\right] + W_2(\nu, Q^2)\frac{1}{M_p^2}\left[p^\mu + \frac{p.Q}{Q^2}.Q^\mu\right]\left[p^\nu + \frac{p.Q}{Q^2}Q^\nu\right],$$

where, W_1 and W_2 are independent scalar functions of ν and Q^2. Using this form, the invariant cross section can be expressed as

$$\sigma \equiv \frac{\partial^2\sigma}{\partial\Omega\,\partial E'} = \sigma^{mott}\left[W_1(\nu, Q^2) + 2W_1(\nu, Q^2)\tan^2\left(\frac{\phi}{2}\right)\right],$$

where,

$\sigma^{mott} = \frac{4\alpha^2 E'}{Q^4}Cos^2\left(\frac{\phi}{2}\right)$, $\nu = E - E'$ and, ϕ and θ are related by $\theta = \pi - \phi$.

Here W_1 and W_2 are the two nucleon structure functions reflecting the possibility of magnetic as well as electric scattering, or alternatively, the possibility of photo absorption of either transverse (helicity = $\pm$ 1) or longitudinal (helicity = 0) photons.

It was suggested by Bjorken that for large ν and Q^2 ($\nu \to \infty, Q^2 \to \infty, \nu/Q^2$ fixed), νW_2 and $M_p W_1$ should become functions solely of the ratio $x = Q^2/2M_p^\nu$. This functional dependence was indeed observed in the very early SLAC data, at least approximately and is called scaling (Fig.1.3). If the nucleon constituents had internal structure denoted by $F_C(q^2)$, then we would expect the data is to be damped by an additional factor of $|F_C(q^2)|^2$. Thus the lack of pronounced Q^2 dependence, known as scaling, suggests that the nucleon constituents are pointlike.

A simple approach for understanding this scaling phenomenon is offered by the naive parton model. In this model, the nucleon is assumed to consist of a collection of pointlike constituent partons with well defined quantum numbers. Viewed from a

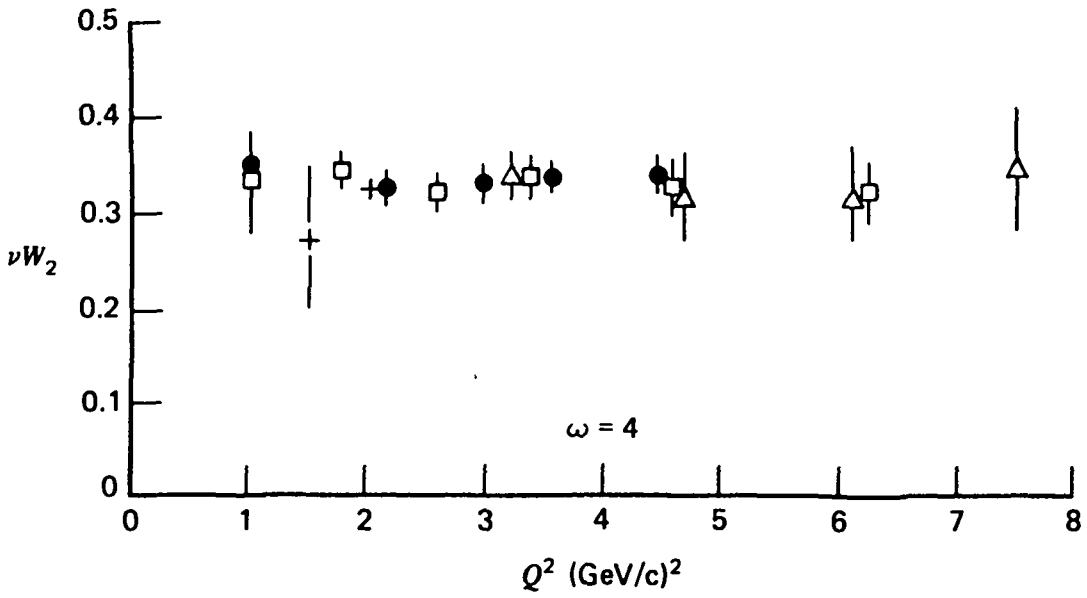

Fig.1.3 Scaling at x = 0 25 as observed in very early SLAC data

frame in which the nucleon is highly relativistic, the so called infinite momentum frame, deep inelastic scattering is seen to be simply incoherent scattering from the individual partons. In this highly boosted frame, the partons recombine to form the final hadronic state over a much longer time scale than that of the collision, and so, it is precise to consider these as quasi-free non-interacting particles. In this frame, the Bjorken scalling quantity, x, is identifiable as the momentum fraction of the elastically scattered partons. Spin half partons thus contributing incoherently to the Dirac cross section yield the observable structure functions,

$$F_1(x) \equiv M_p W_1 = \sum_i f_i(x) e_i^2 \quad \text{and} \quad F_2(x) \equiv \nu W_2 = x \sum_i f_i(x) e_i^2 ,$$

where, $f_i(x)$ is the probability density of finding the i-th parton with fractional momentum x and charge e_i. The Callan-Gross relation $F_2 = 2xF_1$ is a direct consequence of spin half partons and is strongly supported experimentally. To complete the identification of these partons with the quarks of Gell Mann and Zweing, one compares electron and neutrino scattering results for F_1 and F_2 to infer the fractional charge assignment of the quark model.

1.4. Low-x Physics:

According to QCD, at low values of x ($x \sim 10^{-4}$) and at large values of Q^2, a nucleon consists predominantly of gluons and sea quarks. Their densities grow rapidly in the limit $x = 0$ leading to possible spatial overlap and to interactions between the partons. Several interesting physical phenomena are thus expected when the parton densities are high, such as for example, shadowing or semihard processes appearing with large cross-sections in the high energy hadronic reactions [1,2]. Several DIS experiments have been performed on nuclear targets and various nuclear effects have shown up at low-x, as for example, shadowing which depletes the bound nucleon structure function relative to that measured from free nucleons. The low-x physics is a very complicated subject with scare data and a variety of different theoretical approaches.

The low-x region of Deep Inelastic Scattering offers a unique possibility to explore the Regge limit of perturbative QCD [1-14]. Deep Inelastic Scattering corresponds to the region where both ν and Q^2 are large and x is finite. The low-x limit of deep in elastic scattering corresponds to the case when $2M\nu >> Q^2$, yet Q^2 is still large, that is at least a couple of GeV^2. The limit $2M\nu >> Q^2$ is equivalent to $S >> Q^2$, that is to the limit when the center of mass energy squared S is large and much greater than Q^2. The high energy limit, when the scattering energy is kept much greater than the external masses, is by definition the Regge limit. In deep inelastic scattering Q^2 is by definition also kept large, that is $Q^2 >> \Lambda^2$, where Λ is the QCD scale parameter. The limit of energy ν and $2M\nu >> Q^2$ is therefore the Regge limit of deep inelastic scattering [3]. The fact that Q^2 is large allows to use perturbative QCD.

Low energy charged lepton scattering is mediated by a pure electromagnetic interaction. This is also the dominant contribution at low and medium Q^2 at large energies. Therefore it is natural to focus the discussion on one photon exchange. The differential cross section is then given by the formula:

$$\frac{\partial^2 \sigma(x,Q^2)}{\partial Q^2 \partial x} = \frac{4\pi\alpha^2}{Q^4}\left[\left(1 - y - \frac{Mxy}{2E}\right)\frac{F_2(x,Q^2)}{x} + y^2 F_1(x,Q^2)\right],$$

where, due to parity conservation only two structure functions F_1 and F_2 appear. At much higher Q^2, $Q^2 > M_Z^2$, where M_Z is the Z bosons mass, an admixture of the weak interaction and thus axial vector current may appear which introduces a third structure function F_3. Thus when discussing existing DIS data, only the structure functions F_1 and F_2 will be mentioned except for neutrino scattering data where the function F_3 will also be referred to.

Since the low-x limit of DIS corresponds to the Regge limit the concepts of the old Regge theory and Regge phenomenology appear and acquire a new content within perturbative QCD. Since a long time it has been known that two-body scattering of hadrons is strongly dominated by small momentum transfers t or equivalently by small scattering angles. This is successfully described by the exchange of a particle with appropriate quantum numbers. Regge pole exchange is a generalization of a single particle exchange (Fig.1.4).

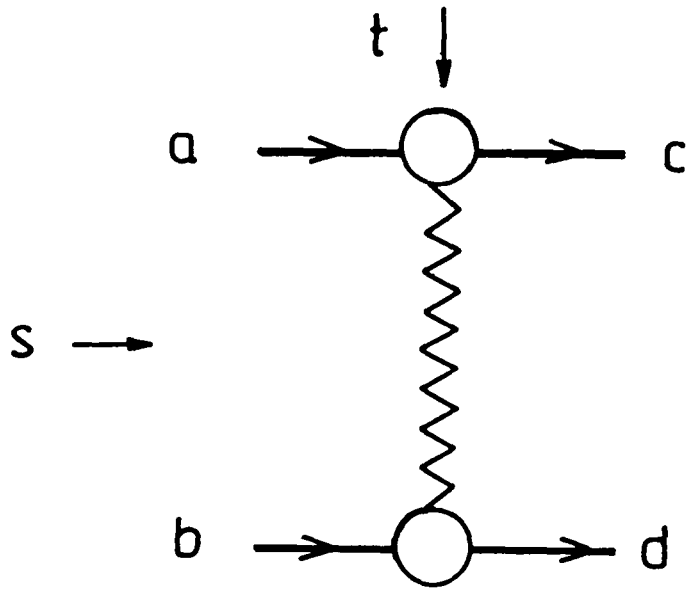

Fig.1.4 Regge pole exchange

The Regge poles, like elementary particles, are characterized by quantum numbers like charge, isospin, strangeness, etc. The Regge pole carrying the quantum numbers of the vacuum and describing diffractive scattering is called the pomeron. Other

Regge poles are called reggeons. It is useful to represent Regge pole exchange in terms of quarks and gluons. Regge pole exchange describes the exchange of states with appropriate quantum numbers and different virtuality t and spin α. The relation between t and α is called the Regge trajectory, $\alpha(t)$. Whenever this function passes through an integer (for bosonic Regge poles) or a half integer (for fermionic Regge poles), that is $\alpha(t)=n$, $n=1,2,.....$or $n=1/2,3/2,.....$,there should exist a particle of spin n and mass $M_n=\sqrt{t}$. The trajectory $\alpha(t)$ thus interpolates between particles of different spins. The increase of the total cross sections with energy and so the possible nature of the pomeron, is strongly constrained by the Froissart bound implying that asymptotically the total cross sections cannot increase faster than $\ln^2 S$ [15]. This bound is a consequence of unitarity and analyticity. The natural quantities to consider are the structure functions F_1 and F_2 which are proportional to the total virtual photon-nucleon cross section and which are expected to have Regge behaviour corresponding to pomeron or region exchange [3].

The predictions obtained in this way for the production of the hadronic system in DIS can be used to estimate the low-x behavour of the structure functions, since the limit of large $S >> Q^2$ discussed above corresponds to low-x ~ Q^2/S. In the parton model, which is appropriate in the large Q^2 limit the structure functions, are related to the quark and antiquark distributions in the nucleon. The Regge behaviour of the structure function $F_2(x)$ in the large Q^2 region reflects itself in the low-x behaviour of the quark and antiquark distributions. Thus a $1/x$ behaviour of the sea quark and antiquark distributions for low-x $q_{sea}(x)\sim 1/x$ corresponds to a Compton amplitude with a pomeron exchange while a behaviour of the valence quark distributions corresponds to a mesonic Regge pole exchange, that is $q_{val}(x)\sim 1/\sqrt{x}$. Since the same processes lead to gluon and sea quarks distributions in the nucleon, we expect that for low-x $G(x)\sim 1/x$. The x dependence of the parton densities given above are often assumed also for the Q^2 dependent parton densities at moderate Q^2.

1.5. Evolution Equations:

Let us now discuss the pertubative QCD predictions for the low-x behaviour of parton distributions. We shall consider the sea quark and gluon distributions which dominate the valence quarks in the low-x limit. Perturbative QCD becomes applicable in the large Q^2 region leading to the evolution of the parton densities with Q^2, expressed in a form of evolution equations. The exact form of these equations depends upon the accuracy with which one treats the large logarithms $\ln(Q^2/\Lambda^2)$ or $\ln(1/x)$.

1.5.1. GLDAP Evolution Equations:

In the leading $\ln(Q^2)$ approximation (LLQ^2) which corresponds to keeping only those terms in the perturbative expansion which have the leading power of $\ln(Q^2)$, that is $\alpha_s^n \ln^n(Q^2)$, the equations have the familiar form of the Gribov-Lipatov-Dokshitzer-Altarelli-Parisi (GLDAP) evolution equations [16-19],

$$\frac{\partial q_i(x,Q^2)}{\partial \ln(Q^2/\Lambda^2)} = \frac{\alpha_s(Q^2)}{2\pi}\int_x^1 \frac{dy}{y}\left[P_{qq}(x/y)q_i(y,Q^2) + P_{qG}(x/y)G(y,Q^2)\right], \qquad (1.1)$$

$$\frac{\partial G(x,Q^2)}{\partial \ln(Q^2/\Lambda^2)} = \frac{\alpha_s(Q^2)}{2\pi}\int_x^1 \frac{dy}{y}\left[\sum_i P_{Gq}(x/y)q_i(y,Q^2) + P_{GG}(x/y)G(y,Q^2)\right], \qquad (1.2)$$

where, P_{ab} are the one loop splitting functions. When the appropriate gauge is chosen, the diagrams which contribute in this approximation are the ladder diagrams with gluon and quark exchange (Fig.1.5). In those diagrams, the longitudinal momenta $\sim x_i$ are ordered along the chain $(x_i \geq x_{i+1})$ and the transverse momenta are strongly ordered, that is, $k_{\perp,i}^2 << k_{\perp,i+1}^2$. It is this strong ordering of transverse momenta towards Q^2 which gives the maximal power of $\ln(Q^2)$, since the integration over transverse momentum in each cell is logarithmic. When the terms with higher powers of the coupling $\alpha_s(Q^2)$ are included in the right hand side of these equations, one obtains the next-to-leading logarithmic approximation $(NLLQ^2)$.

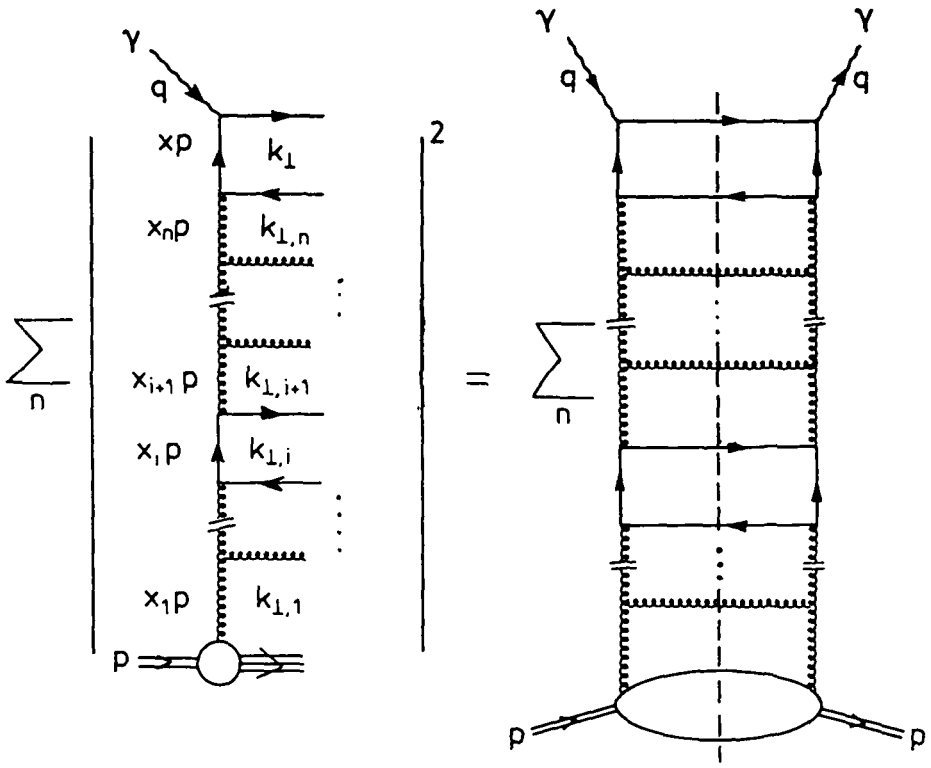

Fig.1.5: Ladder diagram for the deep inelastic scattering in leading $\ln(Q^2)$.

Let us now look at the low-x limit of the distributions generated by these equations. To this end, one notices that the term $P_{GG}(z)$behaves as $6/z$ at low-z which is relevant at low-x, where $z = x/y$. Retainig in the above equations only these terms, one gets the product of maximal powers of both large logarithms $\ln(Q^2)$ and $\ln(1/x)$ which leads to the so-called double logarithmic approximation (DLA).

This predicts the gluon distribution (multiplied by x) to grow faster than any power of $\ln(1/x)$ in the low-x limit. The same applies to the sea quarks since the dominant contribution to sea quark distributions at low-x comes from the $q\bar{q}$ pairs emitted from gluons (Fig.1.6).

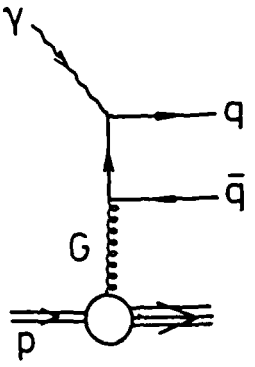

Fig.1.6. Sea quark distribution related to the gluon distribution in the deep inelastic scattering.

1.5.2. BKFL Evolution Equations:

The double logarithmic approximation does not however take into account all leading terms in the parton densities in the low-x limit. By definition it neglects those terms in the perturbative expansion which contain the leading power of $\ln(1/x)$ but which are not accompanied by the leading power of $\ln(Q^2)$. The sum of leading power of $\ln(1/x)$ and arbitrary powers of $\ln(Q^2)$ corresponds to the leading $\ln(1/x)$ approximation ($LL(1/x)$) [2,8,20-22]. This approximation is equivalent to the leading $\ln(S)$ approximation. Equivalence of the leading $\ln(S)$ and leading $\ln(1/x)$ approximation follows from the fact mentioned above that in the limit $S>>Q^2$, $x\sim Q^2/S$, and so $\ln(1/x) \sim \ln(S/Q^2)$. This approximation gives the bare pomeron is perturbative QCD. The corresponding diagrams which contribute in this approximation are ladder like diagrams, yet the exchange mechanism along the ladder is slightly more complicated. Instead of the elementary gluon exchange, one has the exchange of the reggeised gluon (Fig.1.7). The term 'reggeised gluon' means that one can associate the Regge trajectory with the gluon which is calculable in perturbative QCD [2,8,9,10,20]. The Balitskij-Kuraev-Fadin-Lipatov (BKFL) evolution equation which sum these diagrams has the form [8,2,9,23]

$$f(x,k^2)=f^0(x,k^2)+\frac{3\alpha_s(k^2)}{\pi}k^2\int_x^1\frac{dx'}{x'}\int_{k_0^2}^{\infty}\frac{dk'^2}{k'^2}\left\{\frac{f(x',k'^2)-f(x',k^2)}{|k'^2-k^2|}+\frac{f(x',k^2)}{\sqrt{4k'^4+k^4}}\right\},$$

where, the function $f(x,k^2)$ is the nonintegrated gluon distribution, that is

$$f(x,k^2)=\frac{\partial xG(x,k^2)}{\partial \ln k^2},$$

$f^0(x,k^2)$ is a suitably defined inhomogeneous term; k^2,k'^2 are the transverse momenta squared of the gluon in the final and initial states respectively, and k_o^2 is the lower limit cut-off. The important point here is that, unlike the case of the leading $\ln(Q^2)$ approximation, the transverse momenta are no longer ordered along the chain. As before the dominant contribution to sea quark distributions comes from the $q\bar{q}$ pairs emitted from gluons.

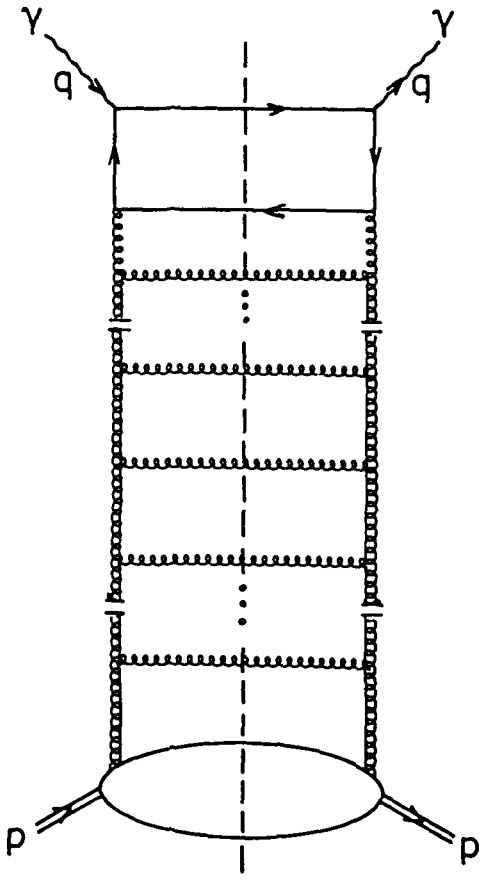

Fig.1.7 The ladder diagram for the deep inelastic scattering in leading ln(1/x) approximation

It is also possible to generalize the $LL(1/x)$ equation in a way which treats both large logarithms, that is $\ln(Q^2)$ and $\ln(1/x)$, on equal footing [2]. The numerical study of

these equations suggests however that the results do not differ substantially when compared with the solution of the conventional GLDAP equations, at least in the region of not too small values of $x>10^{-4}$ [27,28,29].

1.6. Screening Corrections:

The unlimited increase of the parton distributions (multiplied by x) leads to a conflict with unitarity, that is, too rapid S dependence of high energy cross sections violating the Froissart bound [15]. Assume the gluon density $G(x,Q^2)$ to be dominant in the low-x region. Unfortunately we have no direct DIS type of measurement with photonic or W/Z probes for gluons. There exists however the strong interaction analogue to DIS which is the hadron-nualeon interaction where a highly virtual gluon from a hadron probes the structure of the nucleon.

Within the QCD improved parton model, when one counts incoherently the individual probe gluon cross sections, the cross section corresponding to the virtual gluon-nucleon interaction per unit rapidity is $\sigma_{G\cdot N} = \sigma_0 xG(x,Q^2)$, where σ_0 is the total cross-section corresponding to the interaction of the probe with the gluon in a nucleon, that is,

$$\sigma_0 = \sigma_{G\cdot G\to r} = \text{Const.}\frac{\alpha_S(Q^2)}{Q^2}.$$

This can be illustrated in a simple geometrical picture [2]. Assuming that the cross section σ_0 on the parton level is equal to the transverse size of the probed parton, the cross section $\sigma_{G\cdot N}$ is equal to the transverse area occupied by partons (gluons) per unit of their rapidity. Since the number of gluons per unit rapidity, xG, can grow indefinitely for $x\to 0$, the total transverse area occupied by gluons can become comparable or larger than the transverse area of a nucleon, πR^2, for sufficiently small values of x or Q^2. When this happens, then gluons begin to overlap spatially in the transverse direction and so can no longer be regarded as free partons [2]. This is in conflict with the basic assumption of the QCD improved parton model.

The QCD evolution described by the equations (1.1, 1.2) and corresponding to ladder diagrams simply takes care of the evolution of the individual partonic cascades. The important point here is that the interaction of partons from different cascades can be neglected. This interaction of partons leads to non-linear screening or shadowing corrections to the evolution equations (1.1, 1.2). In the simplest version the corrected evolution equation takes the form [30,31]

$$\frac{\partial xG(x,Q^2)}{\partial \ln Q^2} = \frac{3\alpha_s(Q^2)}{\pi}\int_x^1 \frac{dy}{y}\left(yG(y,Q^2)\right) - \frac{9}{16R^2}\left(\frac{3\alpha_s(Q^2)}{Q}\right)^2 \int_x^1 \frac{dy}{y}\left(yG(y,Q^2)\right)^2 . \quad (1.3)$$

In this equation, the linear term on right hand side was obtained from the standard evolution equation for gluons, equation (1.2), by neglecting the quark contribution and keeping only the most singular term of the $P_{GG} \sim 6/z$. That means that, in fact $G(x,Q^2)$ is treated here in the double logarithmic approximation. The second term in equation (1.3) is the screening correction. Note that this equation is written for $G(x,Q^2)$ times x. The most dramatic consequence of parton saturation is a linear scaling violation in parton distributions to be contrasted with the mild logarithmic scaling violation given by perturbative QCD.□

Chapter-2

TAYLOR EXPANSION METHOD

2.1. Taylor's Theorem:

It is frequently easier to find the numerical value of a function by expanding into a power series and evaluating the first few terms than by any other method. In fact, this is sometimes the only possible method of computing it. If a function f defined on $[a,a+h]$, is such that (i)the $(n-1)$-th derivative f^{n-1} is continuous on $[a,a+h]$ and (ii)the n-th derivative f^n exists on $]a,a+h[$, then there exist at least one real number θ between 0 and 1 $(0<\theta<1)$ such that [32]

$$f(a+h)=f(a)+hf'(a)+\frac{h^2}{2!}f''(a)+\frac{h^3}{3!}f'''(a)+ \ldots\ldots\ldots\ldots$$

$$\ldots\ldots+\frac{h^{n-1}}{(n-1)!}f^{n-1}(a)+\frac{h^n(1-\theta)^{n-p}}{p[(n-1)!]}f^n(a+\theta h), \qquad (2.1)$$

where, p is a given positive integer. First of all, we observe that the condition (i) in the statement implies that all the derivatives $f',f'',\ldots\ldots\ldots\ldots f^{n-1}$ exist and are continuous on $[a,a+h]$. Consider the function ϕ defined on $[a,a+h]$ as

$$\phi(x)=f(x)+(a+h-x)f'(x)+\frac{(a+h-x)^2}{2!}f''(x)+\ldots\ldots\ldots\ldots$$

$$\ldots\ldots\ldots+\frac{(a+h-x)^{n-1}}{(n-1)!}f^{n-1}(x)+A(a+h-x)^p,$$

where, A is a constant to be determined such that $\phi(a+h)=\phi(a)$. Therefore,

$$f(a+h)=f(a)+hf'(a)+\frac{h^2}{2!}f''(a)+\ldots\ldots\ldots\ldots\ldots$$

$$\ldots\ldots\ldots\ldots+\frac{h^{n-1}}{(n-1)!}f^{n-1}(a)+Ah^p. \qquad (2.2)$$

Now,

(i) $f, f', f'', \ldots\ldots\ldots, f^{n-1}$ being all continuous on $[a, a+h]$, the function $\phi(x)$ is continuous on $[a, a+h]$,

(ii) $f, f', \ldots\ldots\ldots, f^{n-1}$ and $(a+h-x)^r$ for all r being all derivable in $]a, a+h[$ and the function $\phi(x)$ is derivable in $]a, a+h[$, and

(iii) $\phi(a+h) = \phi(a)$.

Thus the function $\phi(x)$ satisfies all the conditions of Rolle's theorem [33] and hence there exists at least one real number θ between 0 and 1 such that $\phi'(a+\theta h) = 0$. But

$$\phi'(x) = \frac{(a+h-x)^{n-1}}{(n-1)!} f^n(x) - Ap(a+h-x)^{p-1}.$$

Therefore,

$$\phi'(a+\theta h) = \frac{h^{n-1}(1-\theta)^{n-1}}{(n-1)!} f^n(a+\theta h) - Aph^{p-1}(1-\theta)^{p-1} = 0$$

$$\Rightarrow A = \frac{h^{n-p}(1-\theta)^{n-p}}{p(n-1)!} f^n(a+\theta h), \quad h \neq 0, \quad \theta \neq 1. \tag{2.3}$$

Substituting A from equation (2.3) in equation (2.2), we get the required result, that is equation (2.1). If f satisfies the conditions of Taylor's Theorem in $[a, a+h]$ and x is any point of $[a, a+h]$ then it satisfies the conditions in the interval $[a, x]$ also. Replacing $(a+h)$ by x or h by $(x-a)$ in equation (2.1), we get

$$f(x) = f(a) + (x-a)f'(a) + \frac{(x-a)^2}{2!} f''(a) + \ldots\ldots\ldots\ldots$$

$$\ldots\ldots + \frac{(x-a)^{n-1}}{(n-1)!} f^{n-1}(a) + \frac{(x-a)^n}{p[(n-1)!]} (1-\theta)^{n-p} f^n(a+\theta(x-a)), \tag{2.4}$$

where, $0 < \theta < 1$. The remainder after n terms can thus be written as

$$R_n = \frac{(x-a)^n (1-\theta)^{n-p}}{p[(n-1)!]} f^n(c),$$

where, c lies between a and x, and depends on the selection of x. We have seen that

$$f(a+h)=f(a)+hf'(a)+\frac{h^2}{2!}f''(a)+....+\frac{h^{n-1}}{(n-1)!}f^{n-1}(a)+R_n, \qquad (2.5)$$

where, R_n is the remainder after n terms. The result can be interpreted in two ways:

(i)The value $f(a+h)$ of the function at a point may be approximated by a summation of the terms like $\frac{h^r}{r!}f^r(a)$ involving values of the function and its derivatives at some other point of the domain of definition, and

(ii)The value $f(a+h)$ of the function may be expanded in powers of h.

Here we present the application of Taylor's theorem in solving GLDAP evolution equation [34,35,36] at low-x which are already discussed elsewhere [37].

2.2. Taylor's Theorem and Structure Functions at Low-x:

The GLDAP evolution equations for the non-singlet and singlet quark structure functions have the standard forms [38]

$$\frac{\partial F_2^{NS}(x,t)}{\partial t}-\frac{A_f}{t}.\left[\{3+4\ln(1-x)\}F_2^{NS}(x,t)\right.$$

$$\left.+2\int_x^1\frac{dw}{1-w}\left\{(1+w^2)F_2^{NS}\left(\frac{x}{w},t\right)-2F_2^{NS}(x,t)\right\}\right]=0 \qquad (2.6)$$

and

$$\frac{\partial F_2^{S}(x,t)}{\partial t}-\frac{A_f}{t}.\left[\{3+4\ln(1-x)\}F_2^{S}(x,t)\right.$$

$$\left.+2\int_x^1\frac{dw}{1-w}\left\{(1+w^2)F_2^{S}\left(\frac{x}{w},t\right)+\frac{3}{2}N_f\left(w^2+(1-w)^2\right)G\left(\frac{x}{w},t\right)\right\}\right]=0, \qquad (2.7)$$

where, $t=\ln\left(\frac{Q^2}{\Lambda^2}\right)$ and $A_f=\frac{4}{(33-2N_f)}$, N_f being the number of flavours.

The F_2 structure functions measured in deep inelastic electro-production can be written in terms of singlet and non-singlet quark distribution functions as [38]

$$F_2^{ed} = \frac{5}{9} F_2^S \tag{2.8}$$

and

$$F_2^{ep} = \frac{3}{18} F_2^{NS} + \frac{5}{18} F_2^S . \tag{2.9}$$

Let us introduce the variable

$$u = 1 - w \Rightarrow w = 1 - u \tag{2.10}$$

and note that [39]

$$\frac{x}{w} = \frac{x}{1-u} = x \sum_{k=0}^{\infty} u^k . \tag{2.11}$$

Since $x < w < 1$, so $0 < u < 1 - x$, and hence the convergence criterion is satisfied. Using equation (2.11) we can rewrite $F_2^{NS}(x/w, t)$ as

$$F_2^{NS}(x/w, t) = F_2^{NS}\left(x + x\sum_{k=1}^{\infty} u^k, t\right)$$

$$= F_2^{NS}(x,t) + x\sum_{k=1}^{\infty} u^k \frac{\partial F_2^{NS}(x,t)}{\partial x} + \frac{1}{2}x^2\left(\sum_{k=1}^{\infty} u^k\right)^2 \frac{\partial^2 F_2^{NS}(x,t)}{\partial x^2} + \ldots\ldots\ldots,$$

which, covers the whole range of u, $0 < u < 1 - x$. Neglecting higher order terms $O(x^2)$, $F_2^{NS}(x/w, t)$ can then be approximated for low-x as,

$$F_2^{NS}\left(\frac{x}{w}, t\right) \approx F_2^{NS}(x,t) + x\sum_{k=1}^{\infty} u^k \frac{\partial F_2^{NS}(x,t)}{\partial x} . \tag{2.12}$$

Putting equations (2.10) and (2.12) in equation (2.6) and performing u-integrations, we have,

$$\frac{\partial F_2^{NS}(x,t)}{\partial t} - \frac{A_f}{t}\left[A(x)F_2^{NS}(x,t) + B(x)\frac{\partial F_2^{NS}(x,t)}{\partial x}\right] = 0 , \tag{2.13}$$

where,

$A(x) = 3 + 4\ln(1-x) - (1-x)(x+3)$ and $B(x) = x(1-x^2) - 2x\ln x$,

and we used the identity [39] $\sum_{k=1}^{\infty} \frac{u^k}{k} = \ln \frac{1}{1-u}$.

The general solution of (2.13) is [40] $F(u,v) = 0$, where, F is an arbitrary function and $u(x,t,F_2^{NS}) = C_1$ and $v(x,t,F_2^{NS}) = C_2$ form a solution of the equations

$$\frac{dx}{A_f B(x)} = \frac{dt}{-t} = \frac{dF_2^{NS}}{-A_f A(x) F_2^{NS}}. \tag{2.14}$$

Solving equation (2.14) one obtains

$$u(x,t,F_2^{NS}) = t.\exp\left[\frac{1}{A_f}\int\frac{dx}{B(x)}\right] \quad \text{and} \quad v(x,t,F_2^{NS}) = F_2^{NS}\exp\left[\int\frac{A(x)}{B(x)}dx\right].$$

It thus has no unique solution. The simplest possibility is that a linear combination of u and v is to satisfy, so that

$$A_{NS}u + B_{NS}v = 0 \tag{2.15}$$

where, A_{NS} and B_{NS} are arbitrary constants. Putting the values of u and v in equation (2.15) we obtain

$$F_2^{NS}(x,t) = -\frac{A_{NS}}{B_{NS}}.t.\exp\left[\int\left\{\frac{1}{A_f B(x)} - \frac{A(x)}{B(x)}\right\}dx\right].$$

Defining

$$F_2^{NS}(x.t_0) = -\frac{A_{NS}}{B_{NS}}.t_0.\exp\left[\int\left\{\frac{1}{A_f B(x)} - \frac{A(x)}{B(x)}\right\}dx\right],$$

one gets

$$F_2^{NS}(x,t) = F_2^{NS}(x,t_0).(t/t_0), \tag{2.16}$$

which gives the t-evolution of non-singlet structure function $F_2^S(x,t)$..

In order to solve equation (2.7), we need to relate singlet structure function $F_2^{NS}(x,t)$ with gluon distribution function $G(x,t)$. For low-x and high -Q^2, gluon is expected to be more dominant than the sea [41]. For simplicity, we therefore assume identical

t-dependence for both :

$$G(x,t) = KF_2^S(x,t), \tag{2.17}$$

where, K is a parameter to be determined from experiments. Putting equation (2.17) in equation (2.7) and following the same procedure as that for non-singlet case, we obtain for singlet structure function,

$$\frac{\partial F_2^S(x,t)}{\partial t} - \frac{A_f}{t}.\left[L(x)F_2^S(x,t) + M(x)\frac{\partial F_2^S(x,t)}{\partial x}\right] = 0, \tag{2.18}$$

where,

$$L(x) = 3 + 4\ln(1-x) - (1-x)(x+3) + \frac{1}{3}KN_f(1-x)(2-x+2x^2)$$

and

$$M(x) = x(1-x^2) - 2x\ln x + \frac{1}{2}KN_f\{-x(1-x).(5-4x+2x^2) - 2x\ln x\}.$$

The equation (2.18) can also be solved as before to get the solution,

$$F_2^S(x,t) = F_2^S(x,t_0)/(t/t_0), \tag{2.19}$$

where,

$$F_2^S(x,t_0) = -\frac{A_S}{B_S}.t_0.\exp\left[\int\left\{\frac{1}{A_f M(x)} - \frac{L(x)}{M(x)}\right\}dx\right].$$

Using equations (2.16) and (2.19) in equations (2.8) and (2.9), we get,

$$F_2^{ed}(x,t) = F_2^{ed}(x,t_0).(t/t_0) \tag{2.20}$$

and

$$F_2^{ep}(x,t) = F_2^{ep}(x,t_0).(t/t_0) \tag{2.21}$$

where, $F_2^{ed}(x,t_0) = \frac{5}{9}F_2^S(x,t_0)$ and $F_2^{ep}(x,t_0) = \frac{3}{18}F_2^{NS}(x,t_0) + \frac{5}{18}F_2^S(x,t_0)$.

Equations (2.20) and (2.21) will give t-evolution and proton structure functions. Again defining

$$F_2^{NS}(x_0,t) = -\frac{A_{NS}}{B_{NS}}.t.\exp.\left[\int\left\{\frac{1}{A_f B(x)} - \frac{A(x)}{B(x)}\right\}dx\right]_{t=t_0},$$

one obtains

$$F_2^{NS}(x,t) = F_2^{NS}(x_0,t)\exp\left[\int\left\{\frac{1}{A_f B(x)} - \frac{A(x)}{B(x)}\right\}dx\right]_{x=x_0}, \tag{2.22}$$

and similarly by defining

$$F_2^{S}(x_0,t) = -\frac{A_S}{B_S}.t.\exp\left[\left\{\frac{1}{A_f M(x)} - \frac{L(x)}{M(x)}\right\}dx\right]_{x=x_0},$$

we obtain

$$F_2^{S}(x,t) = F_2^{S}(x_0,t)\exp\left[\int_{x_0}^{x}\left\{\frac{1}{A_f M(x)} - \frac{L(x)}{M(x)}\right\}dx\right] \tag{2.23}$$

and

$$F_2^{ed}(x,t) = F_2^{ed}(x_0,t)\exp\left[\int_{x_0}^{x}\left\{\frac{1}{A_f M(x)} - \frac{L(x)}{M(x)}\right\}dx\right], \tag{2.24}$$

where,

$$F_2^{ed}(x_0,t) = \frac{5}{9}F_2^{S}(x_0,t).$$

Equation (2.24) will give x-evolution of deuteron structure function.

But the x-evolution of proton structure function like that of deuteron structure function is not possible by this methodology, because to extract the x-evolution of proton structure function we are to put equations (2.22) and (2.23) in equation (2.9). But as the function inside the integral sign of equations (2.22) and (2.23) are different, we need to separate the input functions $F_2^{NS}(x_0,t)$ and $F_2^{S}(x_0,t)$ from the data points to extract the x-evolutions of the proton structure function, which will contain large error.□

Chapter-3

GLUON DISTRIBUTION FUNCTION FROM STRUCTURE FUNCTION - A REVIEW

The measurement of the proton and the deuteron structure functions by Deep Inelastic scattering (DIS) processes in the low-x region where x is the Bjorken variable have opened a new era in parton density measurement [42]. It is important for understanding the inner structure of hadrons. In addition to these knowledge, it is also important to know the gluon distribution inside hadron at low-x because gluons are expected to be dominant in this region. Moreover gluon distributions are important inputs in many high-energy processes and also important for examination of Quantum Chromodynamics (QCD), the underlying dynamics of quarks and gluons. On the otherhand, gluon distribution can not be measured directly from experiment. It is therefore, important to measure gluon distribution $G(x,Q^2)$ indirectly from the proton as well as the deuteron structure functions $F_2(x,Q^2)$. A few numbers of papers have already been published [43,44,48,49,52,53] in this connection where several authors have presented their various methods to extract gluon distribution from quark structure function.

In Prytz method [43,44], gluon distributions are extracted from proton structure function data. Here use of leading order (LO) and next-to-leading order (NLO) has been done. In this method, Taylor expansion about $z = 1/2$ in GLDAP evolution equation has been used. In Bora and Choudhury method also, proton structure function data have been used to extract gluon distributions by using LO GLDAP evolution equation. But here, Taylor expansion about $z = 0$ in GLDAP evolution equation has been used. In Kotikov and Parente method also, proton structure function data have been used to extract gluon distributions, but they used NLO GLDAP evolution equation. Here they used standard input parametric equations of singlet quarks and gluons and solution of GLDAP evolution equation has been done by

standard moment method. Lastly, in Ellis, Kunszt and Levin method also gluon distributions have been extracted from proton structure function data. But here next-next-to-leading order (NNLO) GLDAP evolution equation has been used. Like Kotikov and Parente method, here also standard input parametric equations for structure functions has been used and solution of GLDAP evolution equation has been done by standard moment method.

3.1. Prytz Method:

K. Prytz [43,44] gives a method to obtain an approximate relation between the unintegrated gluon density and the F_2 scaling violations at low-x. The resulting formula can be used to determine the gluon density from the HERA data taken at low-x. It was shown in reference [45] that the gluon density at low-x can be obtained in a convenient way by analysing the longitudinal structure function. Here a similar method is applied using the Q^2 derivative of F_2 to obtain the gluon density to a good accuracy. The basic idea rests on the fact that the scaling violation of F_2 arises at low-x, from the gluon density alone and does not depend on the quark densities. At low-x, actually already at $x = 10^{-2}$, the quarks can be neglected in the GLDAP evolution equation and we have,

$$\frac{\partial F_2}{\partial \log Q^2} \simeq \frac{5\alpha_S}{9\pi} \int_0^{1-x} G\left(\frac{x}{1-z}, Q^2\right) P_{qg}(z)\, dz \tag{3.1}$$

for four flavours, where in lowest order

$$P_{qg}(z) = z^2 + (1-z)^2 . \tag{3.2}$$

When applying equation (3.1) to experimental data, the problem arises of determining the gluon distribution $G(x)$ over the complete x-range. At low-x, this problem can be avoided since the integral in equation (3.1) can then be performed approximately. For this purpose, the gluon distribution is expanded in the following way:

$$G\left(\frac{x}{1-z}\right) \simeq G(z=1/2) + (z-1/2)G'(z=1/2) + (z-1/2)^2 \frac{G''(z=1/2)}{2} .$$

This expression is then inserted in equation (3.1) and approximating the upper integration limit to 1, the second term will vanish in view of the symmetry of $P_{qg}(z)$ around z =1/2. The third term is expected to give a small contribution compared to the first and is neglected. As a result, one therefore obtains

$$\frac{\partial F_2(x)}{\partial \log Q^2} \simeq \frac{5\alpha_S}{9\pi} G(2x) \int_0^1 P_{qg}(z) dz \,. \tag{3.3}$$

For a numerical study, equation (3.3) is evaluated using the leading order expression equation (3.2) for $P_{qg}(z)$ to give

$$\frac{\partial F_2(x)}{\partial \log Q^2} \simeq \frac{5\alpha_S}{9\pi} \frac{2}{3} G(2x), \tag{3.4}$$

which is the main result of Prytz method at LO analysis.

Due to the large α_S^2 corrections to the F_2 scaling violations in the kinematical region of HERA [42], the approximate LO relation between the F_2 scaling violations and the gluon distributions at low-x need to be corrected. A new relation is presented in NLO and found to give reasonable agreement with the exact calculation. The gluon to quark splitting function K_g at NLO analysis is given by

$$K_g = \frac{\alpha_S}{4\pi} K_g^{(1)} + \left(\frac{\alpha_S}{4\pi}\right)^2 K_g^{(2)}.$$

Prytz used the formula derived by Floratos et. al. [46] which agrees with the independent calculation by Furmanski and Petronzio [47]. The first order contribution

$$\frac{\partial F_2^{(1)}(x)}{\partial \ln Q^2} = 2\sum_f e_i^2 \frac{\alpha_S}{4\pi} \int_x^1 G(x/z) K_g^{(1)}(z) dz$$

is equivalent to the LO calculation equation (3.4). The second order contribution is

$$\frac{\partial F_2^{(2)}(x)}{\partial \ln Q^2} = 2\sum_f e_i^2 \left(\frac{\alpha_s}{4\pi}\right)^2 \int_x^1 G(x/z) K_g^{(2)}(z) dz$$

$$\simeq 2\sum_f e_i^2 \left(\frac{\alpha_s}{4\pi}\right)^2 \left[\int_x^{0.5} G^{\exp}(x/2) K_g^{(2)}(z) dz + G(2x) \int_{0.5}^1 K_g^{(2)}(z) dz \right],$$

where, G^{exp} is the gluon distribution found from the complete QCD analysis of existing data. Now introducing the function $N(x,Q^2)$ for the first integral and evaluating the second integral, author obtained the total contribution for four flavours,

$$\frac{\partial F_2(x)}{\partial \ln Q^2} = 2\sum_{f+\bar{f}} e_i^2 \int_x^1 G(x/z)K_g(z)\,dz$$

$$\simeq G(2x).\frac{20}{9}.\frac{\alpha_S}{4\pi}\left[\frac{2}{3}+3.58.\frac{\alpha_S}{4\pi}\right]+\left(\frac{\alpha_S}{4\pi}\right)^2.\frac{20}{9}.N(x,Q^2)$$

in NLO analysis [44], where $N(x,Q^2)$ is given by

$$N(x,Q^2)=\int_x^0 G^{exp}(x/z,Q^2)P_g^{(2)}(z)\,dz\,,$$

where $P_g^{(2)}$ is a long and complicated function given in reference [44].

3.2. Bora and Choudhury Method:

Bora and Choudhury also present a method [48] to find the gluon distribution from the F_2 structure function and its scaling violation $\partial F_2/\partial \ln Q^2$ at low-x using Taylor expansion method. Here the LO GLDAP evolution equations are used to relate scaling violation with gluon distribution $G(x)$. They also used equation (3.1) at the beginning and expanded $G(x/(1-z),Q^2)$ using Taylor expansion about z = 0 taking only up to first order derivative in the expansion. While expanding they used first two terms in the expansion of the infinite series $x/(1-z)=x\sum_{k=0}^{\infty} z^k$ also. And using the fact that quark densities can be neglected and that the non-singlet contribution F_2^{NS} can be ignored safely at low-x, the GLDAP evolution equation becomes, for four flavours,

$$\frac{\partial F_2(x,Q^2)}{\partial \ln Q^2} = \frac{10\alpha_S}{9\pi}\int_x^1 dx' P_{qg}(x')(x/x').\,G(x/x',Q^2), \qquad (3.5)$$

where, $\alpha_S = \alpha_S(Q^2)$ is the strong coupling constant and the splitting function $P_{qg}(x')$ gives the probability of finding inside a gluon a quark with momentum fraction x' of the gluon. In LO, $P_{qg}(x')$ is given by

$$P_{qg}(x') = \{x'^2 + (1-x')^2\}/2 .$$

Equation (3.5) can be rearranged as

$$\frac{\partial F_2(x,Q^2)}{\partial \ln Q^2} = \frac{5\alpha_S}{9\pi}\int_x^1 dy . \frac{x}{y} . G(y,Q^2)\frac{1}{y^2} . [x^2 + (y-x)^2] . \qquad (3.6)$$

Substituting $y = x/(1-z)$, we can write the right hand side of equation (3.6) as

$$\frac{5\alpha_S}{9\pi}\int_0^{1-x} dz\, G(x/(1-z),Q^2)\,[(1-z)^2 + z^2] .$$

Now expanding $G(x/(1-z),Q^2)$ about $z = 0$ and retaining terms only up to the first derivative of $G(x)$ in the expansion, we get

$$\frac{\partial F_2(x,Q^2)}{\partial \ln Q^2} = \frac{5\alpha_S}{9\pi}\int_0^{1-x} dz \left[G(x) + z\,G(x) + z\,x\frac{d}{dz}G\left(\frac{x}{1-z}\right)\Big|_{z=0}\right][(1-z)^2 + z^2] .$$

Here in $G(x)$, the Q^2-dependence has been suppressed and they symbolize $G(x/(1-z),Q^2)$. After doing a simple algebra one gets,

$$\frac{\partial F_2(x,Q^2)}{\partial \ln Q^2} = \frac{5\alpha_S}{9\pi} A(x) . \left(G(x) + \frac{B(x)}{A(x)} . x . \frac{dG(x)}{dx} \right)$$

$$\simeq \frac{5\alpha_S}{9\pi}\frac{[A(x)+B(x)]^2}{A(x)+2B(x)} \times G\left(x + \frac{B(x)}{A(x)+B(x)} . x \right),$$

where,

$$A(x) = \frac{2(1-x)^3}{3} - (1-x)^2 + (1-x) \text{ and } B(x) = \frac{(1-x)^4}{2} - \frac{2(1-x)^3}{3} + \frac{(1-x)^2}{2} .$$

Finally,

$$G\left(x + \frac{B(x)}{A(x)+B(x)}x, Q^2 \right) \simeq \frac{9\pi}{5\alpha_S}\frac{A(x)+2B(x)}{[A(x)+B(x)]^2}\frac{\partial F_2(x,Q^2)}{\partial \ln Q^2} .$$

Using this approximate relation, they can find gluon distribution $G(x')$ at

$$x_1 = x + \frac{B(x)}{A(x)+B(x)} \cdot x$$

from the value of the derivative of F_2 with respect to Q^2 at x which is their main result. Of course, utilizing the asymptotic limit of $P_{qg}(x)$ for $x \to 0$ they also got the result,

$$G(x_1, Q^2) \simeq \frac{36\pi}{5\alpha_S} \frac{(2-x)}{[(1-x)(3-x)]^2} \frac{\partial F_2(x,Q^2)}{\partial \ln Q^2}.$$

3.3. Kotikov and Parente Method:

Kotikov and Parente presented a set of formula [49] to extract the gluon distribution from structure function F_2 and its derivative $\partial F_2 / \partial \ln Q^2$ at low-x in the NLO approximation. They began with the standard parametrizations of singlet quark $s(x,Q_0^2)$ and gluon $G(x,Q_0^2)$ parton distribution function at some Q_0^2 [50]. As the behaviour $p(x,Q^2)$~constant, $(p=(s,g))$ is not compatible with the GLDAP evolution equations, they considered more singular behaviour like $p(x,Q^2) \sim x^{-\delta_p(Q^2)}$ for Regge-like behaviour [4,49] and $p(x,Q^2) \sim \exp\left(0.5\sqrt{\delta_p(Q^2)\ln(1/x)}\right)$ for Double–logarithmical behaviour [49,51], where $\delta_s(Q^2) \neq \delta_g(Q^2)$. They then put these quark and gluon distributions in the GLDAP evolution equations and solved for gluon distribution by standard moment method. The method to arrive to the solution is based in the replacement of the Mellin convolution by ordinary products [52].

Assuming the Regge-like behaviour for the gluon distribution and $F_2(x,Q^2)$ at $x^{-\delta} >> 1$, $G(x,Q^2) = x^{-\delta}\tilde{G}(x,Q^2)$ and $F_2(x,Q^2) = x^{-\delta}\tilde{s}(x,Q^2)$, they obtained the following equation for the Q^2 derivative of F_2:

$$\frac{\partial F_2(x,Q^2)}{\partial \ln Q^2} = -\frac{1}{2} x^{-\delta} \sum_{p=s,g} \left(\gamma_{sp}^{1+\delta}(\alpha)\tilde{p}(0,Q^2) + \gamma_{sp}^{\delta}(\alpha) x\tilde{p}'(0,Q^2) + O(x^2)\right), \qquad (3.7)$$

where, $\gamma_{sp}^{\eta}(\alpha)$ are the combinations of the anomalous dimensions of Wilson operators $\gamma_{sp}^{\eta} = \alpha\gamma_{sp}^{(0),\eta} + \alpha^2\gamma_{sp}^{(1),\eta} + O(\alpha^3)$ and Wilson coefficients $\alpha B_2^{p,\eta} + O(\alpha^2)$ of the η moment:

$$\gamma_{ss}(\alpha) = \alpha\gamma_{ss}^{(0),\eta} + \alpha^2\left(\gamma_{ss}^{(1),\eta} + B_2^{g,\eta}\gamma_{gs}^{(0,\eta)} + 2\beta_0 B_2^{s,\eta}\right) + O(\alpha^3), \tag{3.8}$$

$$\gamma_{sg}^{\eta}(\alpha) = \frac{e}{f}\left[\alpha\gamma_{sg}^{(0),\eta} + \alpha^2\left(\gamma_{sg}^{(1),\eta} + B_2^{g,\eta}\left(2\beta_0 + \gamma_{gg}^{(0),\eta} - \gamma_{ss}^{(0),\eta}\right)\right)\right] + O(\alpha^3)$$

and

$$\tilde{p}(0,Q^2) \equiv \frac{d}{dx}\tilde{p}(x,Q^2) \quad \text{at} \quad x = 0,$$

where, $e = \sum_{i}^{f} e_i^2$ is the sum of square of quark charges. With accuracy of $O(x^{2-\delta})$, for equation (3.7) they got,

$$\frac{\partial F_2(x,Q^2)}{\partial \ln Q^2} = -\frac{1}{2}\left[\gamma_{sg}^{1+\delta}(\xi_{sg})^{-\delta} G\left(\frac{x}{\xi_{sg}},Q^2\right) + \gamma_{ss}^{1+\delta}F_2(x,Q^2) + \left(\gamma_{ss}^{\delta} - \gamma_{ss}^{1+\delta}\right)x^{1-\delta}.\tilde{s}'(x,Q^2) + O(x^{2-\delta})\right]$$

with $\xi_{sg} = \gamma_{sg}^{1+\delta} / \gamma_{sg}^{\delta}$. From equation (3.8), they obtained for gluon distribution,

$$G(x,Q^2) = -\frac{(\xi_{sg})^{\delta}}{1+\delta} \times \left[2.\frac{\partial F_2(x\xi_{sg},Q^2)}{\partial \ln Q^2} + \gamma_{ss}^{1+\delta}F_2(x\xi_{sg},Q^2)\right] + \left(\gamma_{ss}^{\delta} - \gamma_{ss}^{1+\delta}\right)x^{1-\delta}(\xi_{sg})^{-\delta}\tilde{s}'(x\xi_{sg},Q^2) + O(x^{2-\delta})\Big]. \tag{3.9}$$

Restricting the analysis to $O(x^{2-\delta}, \alpha x^{1-\delta})$, one can replace

$$\xi_{sg} \rightarrow \xi = \gamma_{sg}^{(0),1+\delta} / \gamma_{sg}^{(0),\delta}$$

and neglect the term $\sim \tilde{s}'(x\xi_{sg},Q^2)$ into equation (3.9), so that,

$$G(x,Q^2) = -\frac{\xi^{\delta}}{\gamma_{sg}^{1+\delta}}\left[2.\frac{\partial F_2(x\xi,Q^2)}{\partial \ln Q^2} + \gamma_{ss}^{1+\delta}F_2(x\xi,Q^2) + O(x^{2-\delta},\alpha x^{1-\delta})\right].$$

Using NLO approximation of $\gamma_{sp}^{1+\delta}$ we easily obtain the final result for $G(x,Q^2)$:

$$G(x,Q^2)=-\frac{2f}{\alpha e}\frac{\xi^{\delta}}{\gamma_{sg}^{(0),1+\delta}+\bar{\gamma}_{sg}^{(1),1+\delta}.\alpha}\left[\frac{\partial F_2(x\xi,Q^2)}{\partial \ln Q^2}+\frac{\alpha}{2}.\gamma_{ss}^{(0)1+\delta}F_2(x\xi,Q^2)\right.$$

$$\left.+O(\alpha,^2 x,^{2-\delta}\alpha x^{1-\delta})\right] \qquad (3.10)$$

and

$$G(x,Q^2)=-\frac{2f}{\alpha e}.\frac{1}{\gamma_{sg}^{(0),1+\delta}+\bar{\gamma}_{sg}^{(1),1+\delta}.\alpha}\left[\frac{\partial F_2(x,Q^2)}{\partial \ln Q^2}+\frac{\alpha}{2}\gamma_{ss}^{(0),1+\delta}F_2(x,Q^2)\right.$$

$$\left.+O(\alpha,^2 x^{1-\delta})\right] \qquad (3.11)$$

where, $\bar{\gamma}_{sg}^{(1),\eta}=\gamma_{sg}^{(1),\eta}+B_2^{g,\eta}(2\beta_0+\gamma_{gg}^{(0),\eta}-\gamma_{ss}^{(0),\eta})$.

In principle any equation from above formulae (3.10), (3.11) may be used, because there is a strong cancellation between the shifts in the arguments of the function F_2 and its derivative, and the shifts in the coefficients in front of them. The difference lies in the degree of accuracy one can reach with them, which depends on the x and Q^2 region of interest. For accurate values of $\delta = 0.5$,

$$G(x,Q^2)=\frac{0.62}{e\alpha(1+26.9\alpha)}\left[\frac{\partial F_2(0.3,Q^2)}{\partial \ln Q^2}+2.12\alpha F_2(0.3x,Q^2)+O(\alpha,^2 x,^{2-\delta}\alpha x^{1-\delta})\right]$$

and

$$G(x,Q^2)=\frac{1.14}{e\alpha(1+26.9\alpha)}\left[\frac{\partial F_2(x,Q^2)}{\partial \ln Q^2}+2.12\alpha F_2(x,Q^2)+O(\alpha,^2 x^{1-\delta})\right].$$

In obtaining the formulae, they neglected some higher order term $\sim\delta\,\tilde{s}(x\xi_{sq},Q^2)/\delta x$ where ξ_{sq} is the combinations of the anomalous dimensions of Wilson coefficients. Similarly assuming the Double-logarithmical behaviour for the gluon distribution and $F_2(x,Q^2)$, they obtained,

$$G(x,Q^2)=\frac{\exp\left(\frac{1}{2}\sqrt{\delta_g(Q^2)\ln\frac{1}{x}}\right)}{\left(2\pi\delta_g(Q^2)\ln\frac{1}{x}\right)^{\frac{1}{4}}}\tilde{G}(x,Q^2)$$

and

$$F_2(x,Q^2)=\frac{\exp\left(\frac{1}{2}\sqrt{\delta_s(Q^2)\ln\frac{1}{x}}\right)}{\left(2\pi\delta_s(Q^2)\ln\frac{1}{x}\right)^{\frac{1}{4}}}\,\tilde{s}(x,Q^2).$$

Then they obtained the following equation for the Q^2 derivative of the $F_2(x,Q^2)$,

$$\frac{\partial F_2(x,Q^2)}{\partial \ln Q^2}=-\frac{1}{2}\sum_{p=s,g}\frac{\exp\left(\frac{1}{2}\sqrt{\delta_p(Q^2)\ln\frac{1}{x}}\right)}{\left(2\pi\,\delta_p(Q^2)\ln\frac{1}{x}\right)^{\frac{1}{4}}}\times\left(\tilde{\gamma}^1_{sp}(\alpha)\tilde{p}(0,Q^2)+O(x')\right),$$

where, $\tilde{\gamma}^1_{sp}(\alpha)$ can be obtained from corresponding functions $\gamma^{1+\delta}_{sp}(\alpha)$ replacing the singular term $1/\delta$ at $\delta\to 0$ by $1/\tilde{\delta}$; that is,

$$\frac{1}{\delta}\xrightarrow{\delta\to 0}\frac{1}{\tilde{\delta}}=\sqrt{\frac{\ln\left(\frac{1}{x}\right)}{\delta_p(Q^2)}}-\frac{1}{4\delta_p(Q^2)}\left[1+\sum_{m=1}^{\infty}\frac{1\times 3\times\ldots\ldots\ldots\times(2m-1)}{\left(4\sqrt{\delta_p(Q^2)\ln\left(\frac{1}{x}\right)}\right)^m}\right]. \tag{3.12}$$

The singular term appears only in the NLO part of the anomalous dimension $\gamma^{(1),1+\delta}_{sp}$ in equation (3.8). The replacement equation (3.12) corresponds to the following transformation:

$$\gamma^{(1),1+\delta}_{sp}\equiv\hat{\gamma}^{(1),1}_{sp}\frac{1}{\delta}+\tilde{\gamma}^{(1),1+\delta}$$

and

$$\delta\to 0,\ \gamma^{(1),1}\equiv\hat{\gamma}^{(1),1}_{sp}\frac{1}{\tilde{\delta}}+\tilde{\gamma}_{sp}{}^{(1),1}, \tag{3.13}$$

where, $\hat{\gamma}^{(1),1}_{sp}$ and $\tilde{\gamma}^{(1),1+\delta}_{sp}$ are the co-efficients corresponding to singular and regular parts of $\gamma^{(1),1+\delta}_{sp}$ respectively. Repeating the analysis of the previous section step by step, using the replacement equation (3.13), we get,

$$G(x,Q^2)=\frac{3}{4e\alpha}\cdot\frac{1}{\left(1+26\alpha\left[1/\tilde{\delta}-41/13\right]\right)}\times\left[\frac{\partial F_2(x,Q^2)}{\partial\ln Q^2}+O(\alpha^2,x)\right].$$

Here also they neglected some higher order terms and replaced the singular term $1/\delta$ at $\delta \to 0$ by some non-singular term $1/\tilde{\delta}$.

3.4. Ellis, Kunszt and Levin Method:

A different method for the determination of $G(x,Q^2)$ at low values of x has been proposed by Ellis, Kunszt and Levin [53] based on the solution of GLDAP evolution equations in the moment space up to next-to-next to-leading order. In this method, the gluon momentum density and F_2 are assumed to behave as $x^{-\omega}$ where ω is a parameter the actual value of which must be extracted from the data. They can also estimate gluon distribution directly from the measurement of the $F_2(x,Q^2)$ structure function at HERA. The basic idea is that, the Q^2 derivative of F_2 is sensitive to the gluon distribution function [49].

The quantity Σ from the experimental data for F_2 is

$$\Sigma(x,Q^2) = \frac{F_2(x,Q^2)}{x\langle e^2 \rangle} \quad . \tag{3.14}$$

Knowledge of Σ as a function of x and Q^2 is the input which can be obtained from experiment. For four active flavours, $\langle e^2 \rangle = 5/18$. Let us consider only the DIS structure function F_2 which is given in terms of parton densities as

$$F_2(x,Q^2) = x\int_x^1 \frac{dz}{z}\{\langle e^2 \rangle\}\left[C^{FF}(z,Q^2)\Sigma(x/z,Q^2) + C^{FG}(x,Q^2)G(x/z,Q^2)\right]$$

$$-\frac{1}{6}C^{NS}(z,Q^2)\,\Delta_{NS}(x/z,Q^2) \tag{3.15}$$

with $\langle e^2 \rangle = \frac{4f_u + f_d}{f_d^2}$, where C denotes the co-efficient functions, f_u and f_d denote the number of up and down quarks respectively, and the non-singlet parton density Δ_{NS} is given in terms of the non-singlet combinations,

$$\Delta_{NS} = T_3 + \frac{1}{3}(T_8 - T_{15}) + \frac{1}{5}(T_{24} - T_{35})$$

$$\equiv \frac{2f_d}{f}\sum_{i=1}^{f_u} q_{u,i}^{+} - \frac{2f_u}{f}\sum_{i=1}^{f_d} q_{d,i}^{+}$$

where $f = f_u + f_d$. For an even number of flavours, $\langle e^2 \rangle = 5/18$ and

$\Delta_{NS} = \sum_{i=1}^{f/2}\left(q_{u,i}^{+} - q_{d,i}^{+}\right)$. From equation (3.15), for the lowest order in α_s we get

$F_2(x,Q^2) = x\langle e^2 \rangle \Sigma(x,Q^2)$, where the non-singlet contribution which gives a small contribution at low-x.

The lowest-order GLDAP equation for Σ reads

$$\frac{\partial \Sigma(x,Q^2)}{\partial \ln Q^2} = \frac{\alpha_s}{2\pi}\int_x^1 \frac{dz}{z}\left[P_0^{FF}(z)\Sigma(x/z) + P_0^{FG}(z)G(x/z)\right]. \qquad (3.16)$$

The information about the gluon is difficult to extract from this equation at normal x, because it involves a weighted integral over the quark and gluon distribution functions. In moment space, this means that we have to know the moments of Σ and $\partial\Sigma/\partial \ln Q^2$ for all values of ω. Taking moments of equation (3.16) we obtain

$$\frac{\partial \Sigma(\omega)}{\partial \ln Q^2} = \frac{\alpha_s}{2\pi}\left[P_0^{FF}(\omega)\Sigma(\omega) + P_0^{FG}(\omega)G(\omega)\right]. \qquad (3.17)$$

P_0^{FF} could be neglected in lowest order because $P_0^{FF}(0) = 0$. However the dominant value of ω is unlikely to be that small and furthermore this simplification does not occur in higher orders. Assuming a simple form for the gluon distribution,

$G(x) = A_G x^{-\omega_0}$ and $\Sigma(x) = A_\Sigma x^{-\omega_0}$, where $\omega_0 > 0$. Taking moments we get

$$G(\omega) = \frac{A_G}{\omega - \omega_0} \quad \text{and} \quad \Sigma(\omega) = \frac{A_\Sigma}{\omega - \omega_0}.$$

Now let us consider the simple form of equation (3.17) as

$$\frac{\partial \Sigma(\omega)}{\partial \ln Q^2} = \frac{\alpha_s}{2\pi}\left[P_0^{FF}(\omega_0)\Sigma(\omega) + P_0^{FG}(\omega_0)G(\omega)\right].$$

The value of ω_0 can be determined by the measured slope of F_2,

$$\omega_0 = \frac{\partial \ln \Sigma}{\partial \ln(1/x)}. \tag{3.18}$$

Therefore,

$$\frac{\partial \Sigma(x,Q^2)}{\partial \ln Q^2} = \frac{\alpha_s}{2\pi}\left[P_0^{FF}(\omega_0)\Sigma(x,Q^2) + P_0^{FG}(\omega_0)\, G(x,Q^2)\right]. \tag{3.19}$$

Since the GLDAP kernels are known as a function of ω, $G(x,Q^2)$ can be determined. The extension of the basic result to include higher order is straight forward but tedious. Here ω_0 is given by equation (3.18) and Σ is given by equation (3.14). Equation (3.19) is the basis of the method for determining $G(x,Q^2)$. And so ultimately we get for four flavours,

$$G(x,Q^2) = \frac{18/5}{P^{FG}(\omega_0)}\left[\frac{\partial F_2(x,Q^2)}{\partial \ln Q^2} - P^{FF}(\omega_0).F_2(x,Q^2)\right],$$

where, we replace $\Sigma(x,Q^2)$ by $F_2(x,Q^2)$ and the functions P have perturbative expansions

$$P^{FF}(\omega_0) \simeq \alpha_S P_0^{FF} + \alpha_S^2 P_1^{FF} + \alpha_S^3 P_2^{FF} + O(\alpha_S^4)$$

and

$$P^{FG}(\omega) \simeq \alpha_S P_0^{FG} + \alpha_S^2 P_1^{FG} + \alpha_S^3 P_2^{FG} + O(\alpha_S^4).$$

The coefficients P_i^{FF} and P_i^{FG} depend on the parameter ω_0 which are tabulated in reference [53] for a range of ω_0 values.□

Chapter-4

GLDAP EVOLUTION EQUATION AND GLUON DISTRIBUTION

In this chapter, we obtain t and x-evolutions of gluon distribution function at low-x from Gribov-Lipatov-Dokshitzer-Altarelli-Parisi (GLDAP) evolution equation. Comparison is made with the prediction of Balitskij-Kuraev-Fadin-Lipatov (BKFL) as well as Gribov-Levin-Ryskin (GLR) equations. We also make predictions for the HERA range. In a recent letter [54] the t-evolutions of non-singlet and singlet structure functions [38] have been reported. The same technique can be applied to the GLDAP equation [16] for the gluon distribution function to obtain t as well as x-evolution of gluon at low-x.

4.1. Theory:

The GLDAP evolution equation for the gluon distribution function has the standard form [38] as

$$\frac{\partial G(x,t)}{\partial t} - \frac{A_f}{t}\left\{\left(\frac{11}{12} - \frac{N_f}{18} + \ln(1-x)\right)G(x,t) + I_g\right\} = 0, \qquad (4.1)$$

where,

$$I_g = \int_x^1 d\omega\left[\frac{\omega\, G(x/\omega,t) - G(x,t)}{1-\omega} + \left(\omega(1-\omega) + \frac{1-\omega}{\omega}\right)G(x/\omega,t)\right.$$

$$\left. + \frac{2}{9}\left(\frac{1+(1-\omega)^2}{\omega}\right)F_2^s(x/\omega,t)\right],$$

$t = \ln(Q^2/\Lambda^2)$ and $A_f = \dfrac{36}{33-2N_f}$, N_f being the number of flavours.

For low-x and high-Q^2, gluon is expected to be more dominant than the sea [41]. For lower-Q^2 ($Q^2 \simeq \Lambda^2$), however, there is no such clearcut distinction between the two. For simplicity, we therefore, assume identical t-dependence for both ,

$$G(x,t) = KF_2^s(x,t),$$

where, K is a parameter to be determined from experiments. Then we get

$$I_g = \int_x^1 d\omega \left[\frac{\omega G(x/\omega,t) - G(x,t)}{1-\omega} + \left(\omega(1-\omega) + \frac{1-\omega}{\omega} \right) G(x/\omega,t) \right.$$

$$\left. + \frac{2}{9k} \left(\frac{1+(1-\omega)^2}{\omega} \right) G(x/\omega,t) \right]. \qquad (4.2)$$

Let us introduce the variable

$$u = 1-\omega \qquad (4.3)$$

and note that [39]

$$\frac{x}{1-u} = x\sum_{k=0}^{\infty} u^k . \qquad (4.4)$$

The series equation (4.4) is convergent for $|u| < 1$. Since $x<\omega<1$, so $0<u<1-x$ and hence the convergent criterion is satisfied. Using equation (4.4) we can rewrite $G(x/\omega,t)$ as [55] ,

$$G(x/\omega,t) = G\left(x + x\sum_{k=1}^{\infty} u^k, t \right)$$

$$= G(x,t) + x\sum_{k=1}^{\infty} u^k \frac{\partial G(x,t)}{\partial x} + \frac{1}{2} x^2 \left(\sum_{k=1}^{\infty} u^k \right)^2 \frac{\partial^2 G(x,t)}{\partial x^2} + \ldots\ldots, \qquad (4.5)$$

which covers the whole range of u, $0<u<1-x$. Neglecting higher order terms $O(x^2)$, $G(x/\omega,t)$ can then be approximated for low-x as

$$G(x/\omega,t) \simeq G(x,t) + x\sum_{k=1}^{\infty} u^k \frac{\partial G(x,t)}{\partial x}. \qquad (4.6)$$

Putting equations (4.3) and (4.6) in equation (4.2) and performing u – integrations, we obtain,

$$I_g = R(x)G(x,t) + S(x)\frac{\partial G(x,t)}{\partial x}, \tag{4.7}$$

where, we have used the identity $\sum_{k=1}^{\infty} \frac{u}{k} = \ln \frac{1}{1-u}$ [39], and where,

$$R(x) = -\left\{\left(1+\frac{2}{9K}\right)(1-x) + \left(-\frac{1}{2}+\frac{1}{9K}\right)(1-x)^2 + \frac{1}{3}(1-x)^3 + \left(1+\frac{4}{9K}\right)\ln x\right\}, \tag{4.8}$$

and

$$S(x) = x\left\{\left(1+\frac{4}{9K}\right)\frac{1}{4} + \left(2+\frac{4}{9K}\right)(1-x) + \frac{1}{9K}(1-x)^2 + \frac{1}{3}(1-x)^3 + \left(2+\frac{8}{9K}\right)\ln x - 1 - \frac{4}{9K}\right\}. \tag{4.9}$$

Using equation (4.7) in equation (4.1) we get,

$$\frac{\partial G(x,t)}{\partial t} - \frac{A_f}{t}\left\{\left(\frac{11}{12}-\frac{N_f}{8}\right) + \ln(1-x)G(x,t) + R(x)G(x,t) + S(x)\frac{\partial G(x,t)}{\partial x}\right\} = 0$$

which gives

$$\frac{\partial G(x,t)}{\partial t} - \frac{A_f}{t}\left\{P(x)G(x,t) + Q(x)\frac{\partial G(x,t)}{\partial x}\right\} = 0, \tag{4.10}$$

where,

$$\left.\begin{aligned} P(x) &= \left(\frac{11}{12}-\frac{N_f}{18}\right) + \ln(1-x) + R(x) \\ &\text{and} \\ Q(x) &= S(x). \end{aligned}\right\} \tag{4.11}$$

The general solution of equation (4.10) is [40]

$$F(U,V)=0, \tag{4.12}$$

where, F is an arbitrary function and $U(x,t,G)=C_1$ and $V(x,t,G)=C_2$ form a solution of the equations

$$\frac{dx}{A_f Q(x)}=\frac{dt}{-t}=\frac{dG}{-A_f P(x)G(x,t)}. \tag{4.13}$$

Solving equation (4.13) one obtains

$$U(x,t,G)=t.\exp\left[\frac{1}{A_f}\int\frac{dx}{Q(x)}\right]$$

and

$$V(x,t,G)=G(x,t)\exp\left[\int\frac{P(x)}{Q(x)}dx\right].$$

It thus has no unique solution. The simplest possibility is that a linear combination of U and V is to satisfy equation (4.12) so that

$$A_g U+B_g V=0, \tag{4.14}$$

where A_g and B_g are arbitrary constants. Putting the values of U and V in equation (4.14) we obtain,

$$G(x,t)=-\frac{A_g}{B_g}t\exp\left[\int\left\{\frac{1}{A_f Q(x)}-\frac{P(x)}{Q(x)}\right\}dx\right].$$

Defining

$$G(x,t_0)=-\frac{A_g}{B_g}t_0\exp\left[\int\left\{\frac{1}{A_f Q(x)}-\frac{P(x)}{Q(x)}\right\}dx\right],$$

one gets,

$$G(x,t)=G(x,t_0)(t/t_0) \tag{4.15}$$

which gives the t-evolution of gluon distribution function $G(x,t)$. Again defining

$$G(x_0,t) = -\frac{A_g}{B_g}\, t \exp\left[\int\left\{\frac{1}{A_f Q(x)} - \frac{P(x)}{Q(x)}\right\}dx\right]_{x=x},$$

one obtains,

$$G(x,t) = G(x_0,t)\exp\left[\int\left\{\frac{1}{A_f Q(x)} - \frac{P(x)}{Q(x)}\right\}dx\right], \tag{4.16}$$

which determines the $x-$evolution of gluon distribution function $G(x,t)$. We can perform the integration inside the exponential in the equation (4.16) with further approximation that $\ln(1-x)\to 0$ and $x\ln x \to 0$ for very low-x, $x\to 0$. Then we get from equation (4.11),

$$\left.\begin{aligned} P(x) &= \left(\frac{11}{12} - \frac{N_f}{18}\right) - \left(1+\frac{2}{9K}\right)(1-x) - \left(-\frac{1}{2}+\frac{1}{9K}\right)(1-2x) \\ &\quad - \frac{1}{3}(1-3x) - \left(1+\frac{4}{9K}\right)\ln x, \\ Q(x) &= \left(1+\frac{4}{9K}\right) + \left(2+\frac{4}{9K}\right)x + \left(\frac{x}{9K}+\frac{x}{3}\right) - \left(x+\frac{4}{9K}x\right), \end{aligned}\right\} \tag{4.17}$$

and

when we have neglected the square and higher terms of x. Putting the values of $P(x)$ and $Q(x)$ from equation (4.17) in equation (4.16) and performing the integrations analytically we get,

$$G(x,t) = G(x_0,t)\exp\left[-\frac{1}{b}(1+d+2e)(x-x_0)\right]\left(\frac{x}{x_0}\right)^{-(a/b)\ln a} \times \left\{\frac{(a+bx)^{\ln x}}{(a+bx_0)^{\ln x_0}}\right\}^{a/b}$$

$$\times\left(\frac{a+bx}{a+bx_0}\right)^{\left\{-1/b-(1/3-1/A_f+C_f-d-e)+a/b^2(1+d+2e)\right\}}, \tag{4.18}$$

where, $a = 1+\frac{4}{9K}$, $b = \frac{4}{3}+\frac{1}{9K}$, $c_f = \frac{11}{12}-\frac{N_f}{18}$, $d = 1+\frac{2}{9K}$ and $e = -\frac{1}{2}+\frac{1}{9K}$.

Instead of neglecting the higher order terms $O(x^2)$ from the equation (4.5) as is done in equation (4.6), let us retain the second term of Taylor expansion series (4.5) and neglect higher order terms $O(x^3)$. Then $G(x/\omega,t)$ can be approximated for low-x as [55],

$$G(x/\omega,t) \simeq G(x,t)+x\sum_{k=1}^{\infty}u^k\frac{G(x,t)}{x}+\frac{1}{2}x^2\left(\sum_{k=1}^{\infty}u^k\right)^2\frac{\partial^2 G(x,t)}{\partial x^2}. \qquad (4.19)$$

Putting equations (4.3) and (4.19) in equation (4.2) and performing $u-$integrations we obtain,

$$I_g = R(x)G(x,t)+S(x)\frac{\partial G(x,t)}{\partial x}+T(x)\frac{\partial^2 G(x,t)}{\partial x^2}, \qquad (4.20)$$

where, $R(x)$ and $S(x)$ are defined by equations (4.8) and (4.9) respectively and $T(x)$ is given by,

$$T(x)=\frac{1}{2}x^2\int_0^{1-x}\left(\sum_{k=1}^{\infty}u^k\right)^2\left(u(1-u)+\frac{u}{1-u}+\frac{1-u}{u}+\frac{2}{9K}\frac{1+u^2}{1-u}\right)du\,.$$

It does not need to calculate explicitly the value of $T(x)$ as a function of x for the reason which will be clear shortly. Using equation (4.20) in equation (4.1) we get

$$\frac{\partial G(x,t)}{\partial t}-\frac{A_f}{t}\left\{P(x)G(x,t)+Q(x)\frac{\partial G(x,t)}{\partial x}+T(x)\frac{\partial^2 G(x,t)}{\partial x^2}\right\}=0, \qquad (4.21)$$

where $P(x)$ and $Q(x)$ are defined by equation (4.11). The equation (4.21) is a second order partial differential equation which can be solved by Monge's method [40]. According to this method the solution of second order partial differential equation

$$R\,r + S\,s + T\,t = V \qquad (4.22)$$

can be obtained from the subsidiary equations

$$R\,dy^2 - S\,dx\,dy + T\,dx^2 = 0 \quad \text{and} \quad R\,dp\,dy + T\,dq\,dx - V\,dx\,dy = 0\,,$$

where, R,S,T,V are functions of x,y,z,p and q. Here z,p,q,r,s and t are defined as follows:

$$z=z(x,y),\quad p=\frac{\partial z}{\partial x},\quad q=\frac{\partial z}{\partial y},\quad r=\frac{\partial^2 z}{\partial x^2}=\frac{\partial p}{\partial x},\quad s=\frac{\partial^2 z}{\partial x\partial y}=\frac{\partial p}{\partial y}=\frac{\partial q}{\partial x}$$

and $t = \frac{\partial^2 z}{\partial y^2} = \frac{\partial q}{\partial y}$.

Comparing equation (4.21) with equation (4.22) we get, $R = A_f Y(x), S = 0, T = 0$ and

$$V = t.\frac{\partial G(x,t)}{\partial t} - A_f Q(x)\frac{\partial G(x,t)}{\partial x} - A_f P(x)G(x,t).$$

Substituting the values of R, S, T and V in subsidiary equations we obtain ultimately $V = 0$, which gives,

$$t.\frac{\partial G(x,t)}{\partial t} - A_f Q(x)\frac{\partial G(x,t)}{\partial x} - A_f P(x) G(x,t) = 0,$$

which is exactly the equation (4.10). This equation has been solved earlier and now it is clear that the introduction of the second order terms does not modify the solutions equation (4.15) or (4.16).

4.2. Result and Discussion:

We have presented our result qualitatively in Fig.4.1 and Fig.4.2. In Fig.4.1, the result of t or Q^2 – evolutions of $G(x,Q^2)$ from the equation (4.15) is given. We have taken arbitrary inputs $G(x,Q_0^2) = 1$, 2 and 3 for $x = x_1, x_2$ and x_3 respectively. Similarly in Fig.4.2, the results of x – evolutions of $G(x,Q^2)$ from the equation (4.16) (solid lines) and from the equation (4.18) (dashed lines) are presented. Integration in the equation (4.11) is computed numerically. We have taken arbitrary inputs $G(x_0,Q^2) = 10$ for $Q^2 = Q_1^2$ for both the sets. Different lines are due to different K – values, $K = 0.01$, 0.1, 1, 10 and 100 indicated in the Fig.4.2. For the dashed graphs, K – values are labelled as K' for convenience. It is clear from the figures that evolutions of gluon distribution functions $G(x,Q^2)$ depend upon inputs $G(x,Q_0^2)$ or $G(x_0,Q^2)$ and also upon K – values.

Eichen, Hinchliffe, Lane and Quigg (EHLQ) [56] began with input distribution inferred from experiment at $Q_0^2 = 5\ GeV^2$ and integrate the evolution equation

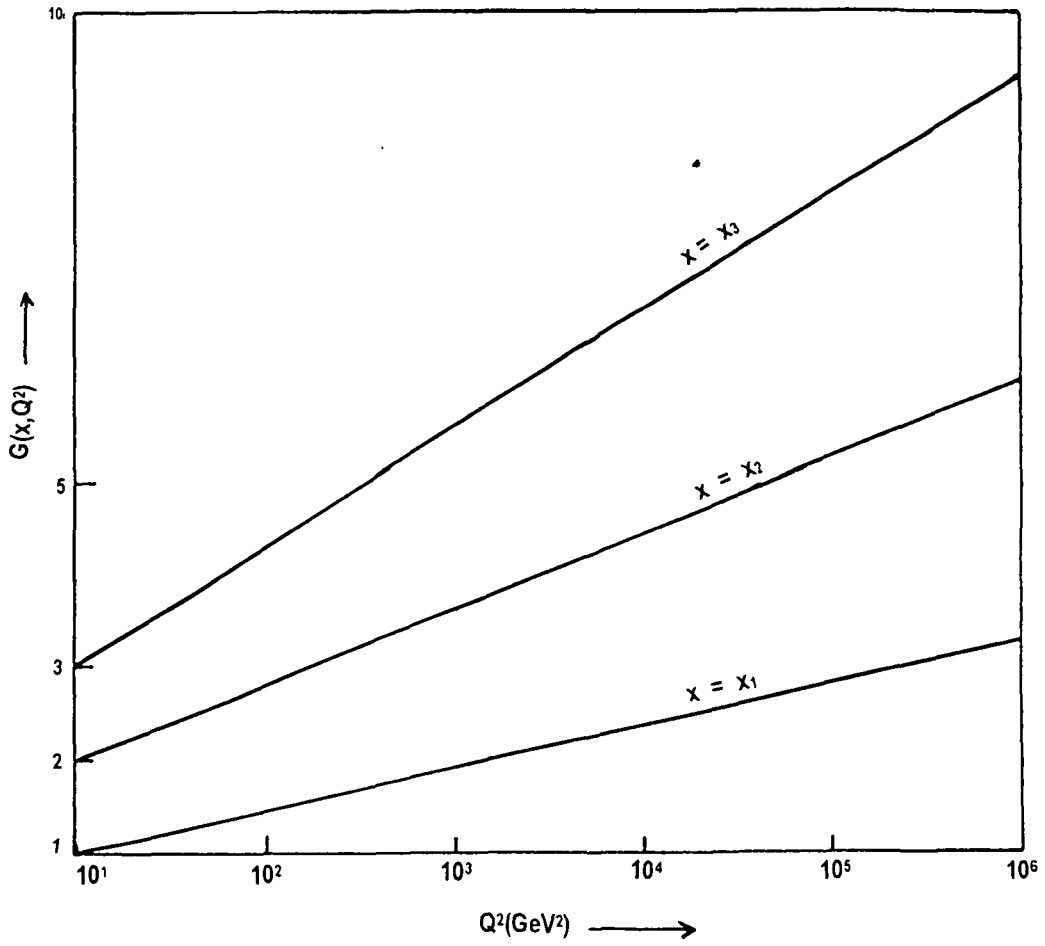

Fig.4.1: Q^2- evolutions of $G(x,Q^2)$ from equation (4.15). Arbitrary inputs $G(x,Q_0^2)$ = 1, 2 and 3 are taken for $x = x_1, x_2$ and x_3 respectively.

numerically. They started with the data of CDHS neutrino experiment [57] at CERN. Gluon distribution is determined indirectly and parametrized as

$$G\left(x,Q_0^2\right)=\left(2.62+9.17x\right)\left(1-x\right)^{5.9}$$

with $R=\sigma_L/\sigma_T=0.1$ and $\Lambda=200\,MeV$ at $Q_0^2=5\,GeV^2$. This is Set−1. Under the assumption that $R=\sigma_L/\sigma_T$ has the behaviour prescribed by QCD, gluon is parametrized as

$$G\left(x,Q^2\right)=\left(1.75+15.57\,x\right)\left(1-x\right)^{6\,03}$$

with $\Lambda=290\,MeV$ at $Q_0^2=5\,GeV^2$. This is Set-2. The calculated Q^2 – dependence of $G\left(x,Q^2\right)$ for Set-1 is shown in Fig. 4.3 (a) by dashed lines for x values $10^{-1}, 10^{-2}, 10^{-3}$ and 10^{-4} as indicated in the figure.

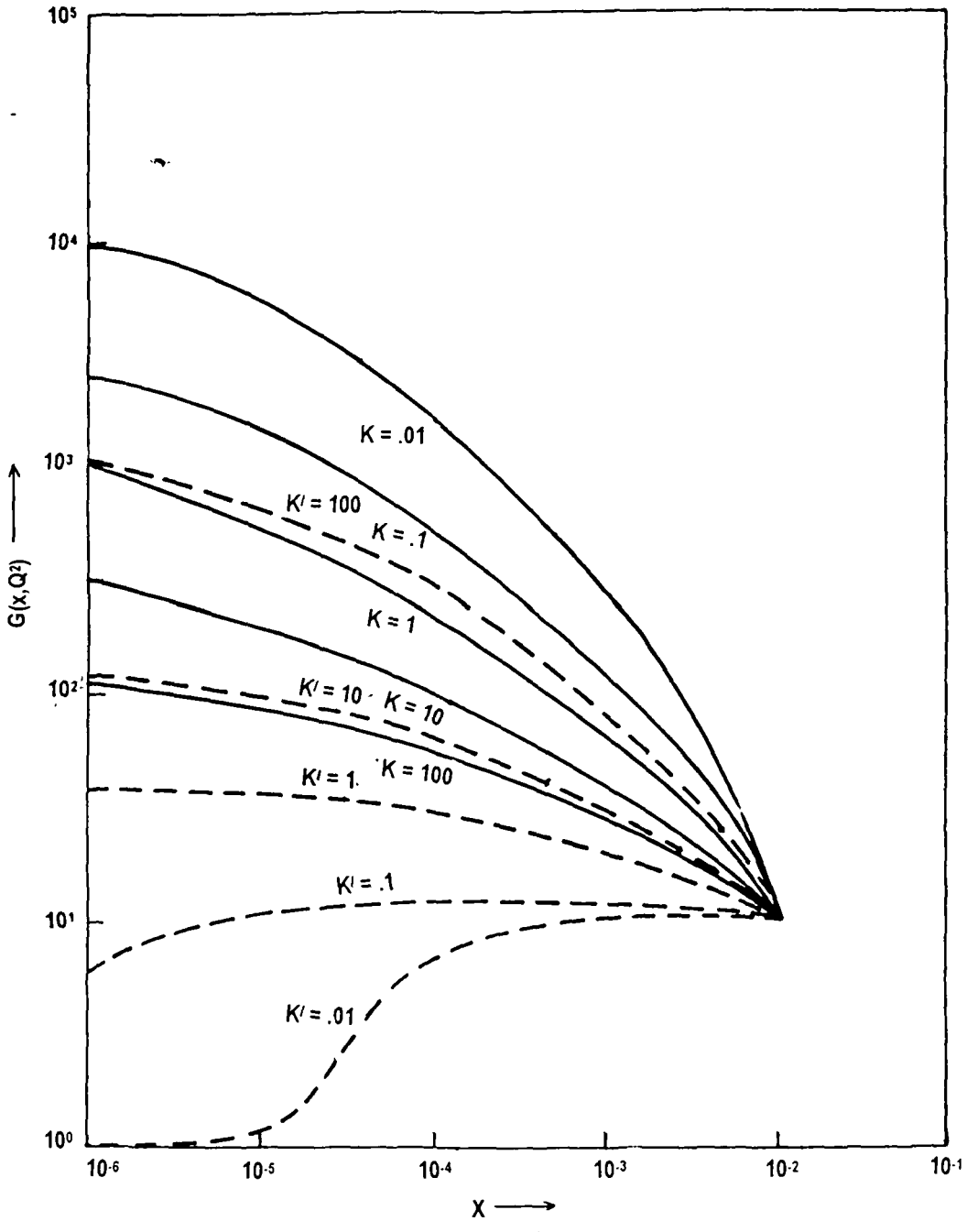

Fig.4.2: x - evolutions of $G(x,Q^2)$ from the equation (4.16) (solid lines) and (4.18) (dashed lines). Arbitrary input $G(x_0,Q^2) = 10$ for $Q^2 = Q_1^2$ is taken. K or K' = 0.01, 0.1, 1, 10 and 100.

The expected growth of the distributions at low-x is apparent. Our results from the equation (4.15) are given in the figure by solid lines for the same values of x. Inputs are taken from the corresponding values at $10\ GeV^2$ from the parametrization. The corresponding result for Set-2 is shown in Fig. 4.3 (b). Again to explore the uncertainties in low-x region EHLQ consider two modifications of Set-1 as follows:

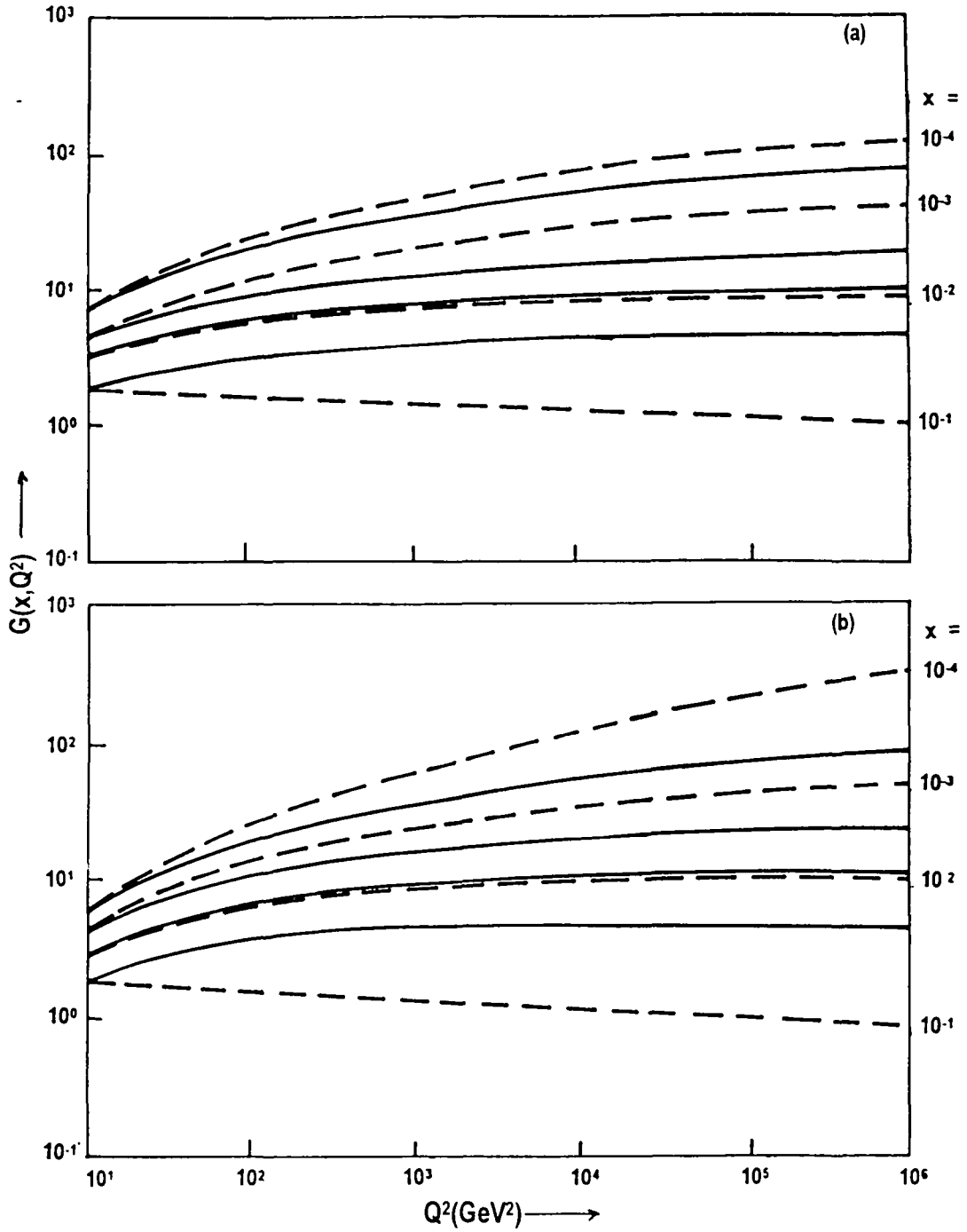

Fig.4.3(a) and Fig.4.3(b) Q^2 - evolutions of $G(x,Q^2)$ for EHLQ Set-1 and Set-2 respectively(dashed lines) for x = 10^{-1}, 10^{-2}, 10^{-3} and 10^{-4} Results from equation (4 15) (solid lines) are also given for same values of x Inputs are taken from the corresponding values at 10 GeV^2 from the parametrization

$$G\left(x,Q_0^2\right)=\left(2\,62+9.17\,x\right)\left(1-x\right)^{5\,9} \qquad \text{for} \qquad x>0.01,$$

and

$$G(x,Q_0^2) = (0.444x)^{-0.5} - 1.886 \\ (25.56x)^{0.5} \Big\} \quad \text{for } x < 0.01.$$

The results of these changes are presented in Fig. 4.4 (a) and Fig. 4.4 (b) for Set-1 (a) and Set-1 (b) respectively for $x = 10^{-2}, 10^{-3}$ and 10^{-4} along with our corresponding predictions. Diemoz, Ferroni, Longo and Martineli (DFLM) [58,59] also proceed in the same manner to parametrize the data from the neutrino experiments BEBC'85 [60], CCFRR'83 [61], CHARM'83 [62] and CDHS'83 [57] at $Q_0^2 = 10\ GeV^2$. For the set DFLM-2 they consider gluon function to be

$$G(x,Q^2) \sim (1-0.18x)(1-x)^{5.06},$$

with $\lambda_{\overline{MS}} = 300\ MeV$. Here the next to leading order QCD calculation is performed. The result is given in Fig. 4.5 for $x = 10^{-1}, 10^{-2}$, 10^{-3} and 10^{-4} by dashed lines Our results from the equation (4.15) is given by solid lines taking inputs as before.

The role of absorptive corrections in the low-x behaviour of deep inelastic gluon distribution functions $G(x,Q^2)$ is widely discussed now [63] due to the new generation of accelerators. Kim and Ryskin estimated [64] the non-linear absorption corrections with the parametrization used in semihard phenomenology [65]. As non-linear absorption effects are essentially at very low-x only [2], they decided to use the standard GLDAP evolution equation [16,66,67] in region of interest ($x>10^{-6}$, $Q^2<10^5\ GeV^2$), that is, $x>x_0(Q^2)$, where, $\ln x_0 = (1/12.7)\ln^2(Q^2/\Lambda^2)$. But in this case they are to add a new boundary condition

$$G(x,Q^2) = aQ^2 \qquad (A)$$

on line $x = x_0(Q^2)$, where, $a = G(x_0,Q^2)Q^2$, which is fixed by the initial condition

$$G(x) = A(1-x^3)x^{-\omega_0} \qquad (B)$$

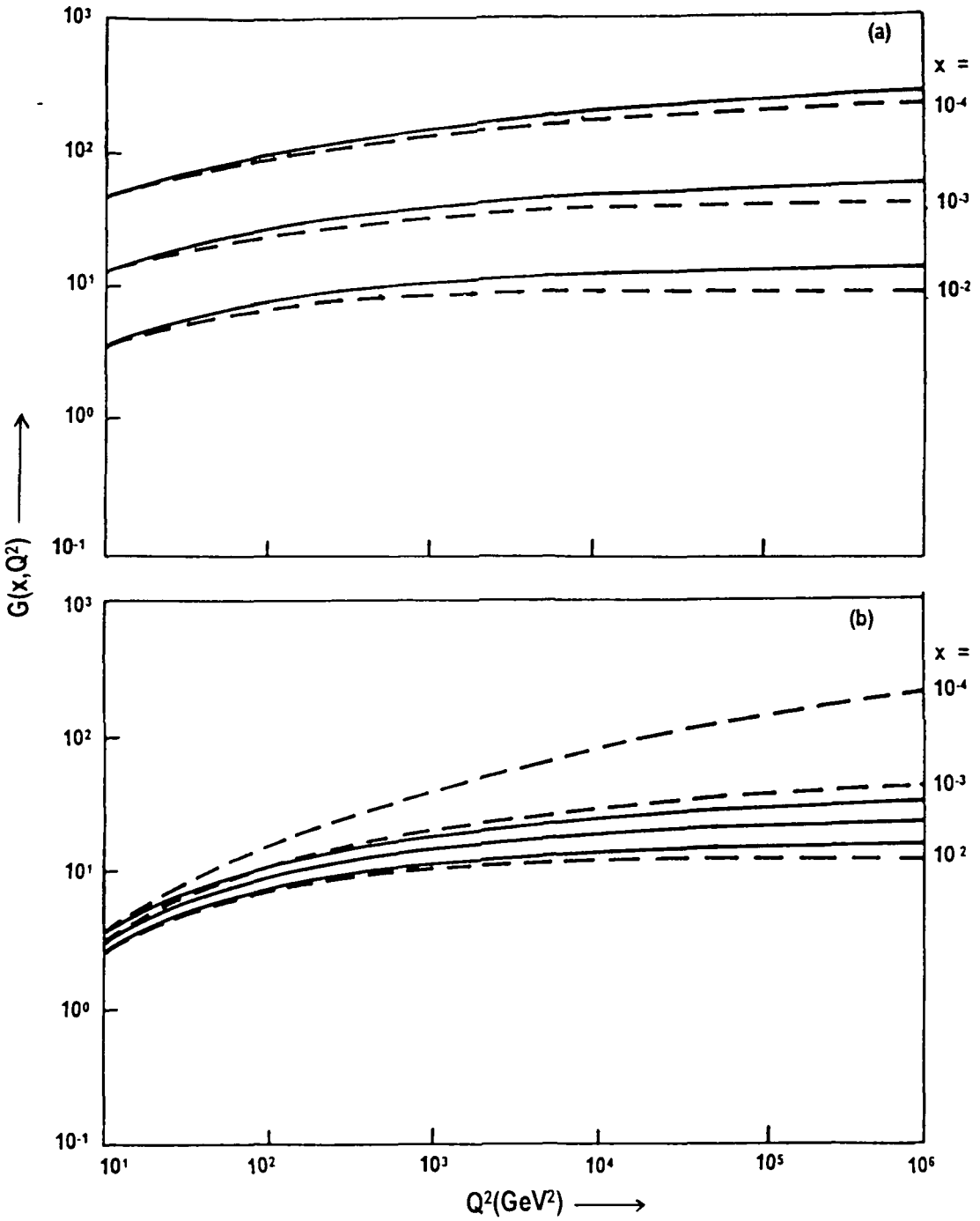

Fig.4.4(a) and Fig.4 4(b) Q^2 - evolutions of $G(x,Q^2)$ for EHLQ Set-1(a) and Set-1(b) respectively (dashed lines) for x = 10^{-1}, 10^{-2}, 10^{-3} and 10^{-4} along with the corresponding predictions (solid lines) from equation (4 15) as indicated in Fig 4 3(a) and Fig 4 3(b)

at $Q_S^2 = 4\ GeV^2$ The coefficient A is fixed by the normalization $\int G(x)dx = 0.55$ and $\omega_0 = (1/\pi)N_c\alpha_s(Q_S^2).4\ln 2$ corresponds to the QCD pomeron singularity given

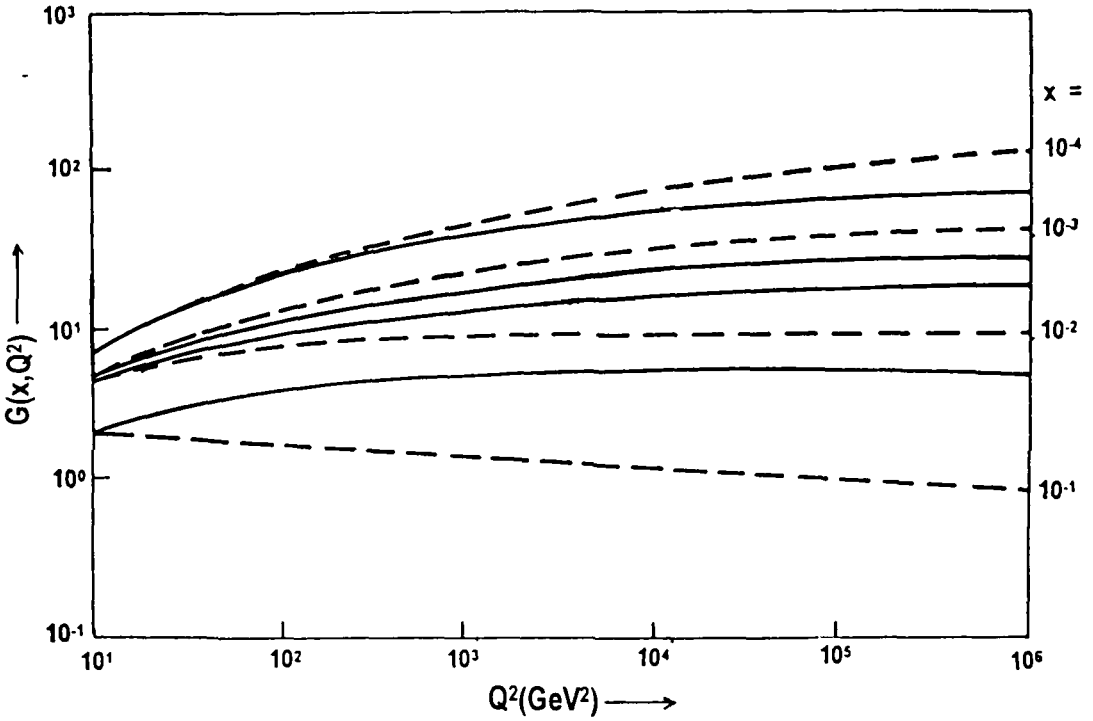

Fig.4.5 Q^2 - evolutions of $G(x,Q^2)$ for DFLM-2 (dashed lines) for x = 10^{-1}, 10^{-2}, 10^{-3} and 10^{-4} along with the DFLM-1 corresponding predictions (solid lines) from equation (4 15) as indicated in Fig 4 3(a) and Fig 4 3(b)

by the summation of leading-log contributions $\left(\alpha_s \ln\frac{1}{x}\right)^n$ [20], $N_c = 3$ be the number of colours. Absorption corrections reveal itself due to this new boundary condition. Kim and Ryskin obtained numerical solution of linear GLDAP evolution equation. The boundary condition corresponds to a strong correlation between gluons inside the proton. Gluons form groups in small Hot Spots [65,30] with radius $R_s \simeq 0.2\ F_m$ at $x = 1/3$. If gluons are distributed uniformly inside the proton. The screening would be smaller and non-linear effect reveals itself at lower-x. For this case $R_s \simeq 0.7\ F_m \simeq R_n$ at $x_0 = 0.0035$. In the Fig. 4.6(a), the x-dependence of gluon distribution functions $G\left(x,Q^2\right)$ at $Q^2 = 10, 100$ and $1000\ GeV^2$ is given by the curves 1, 4, 7; 2, 5, 8 and 3, 6, 9 respectively.

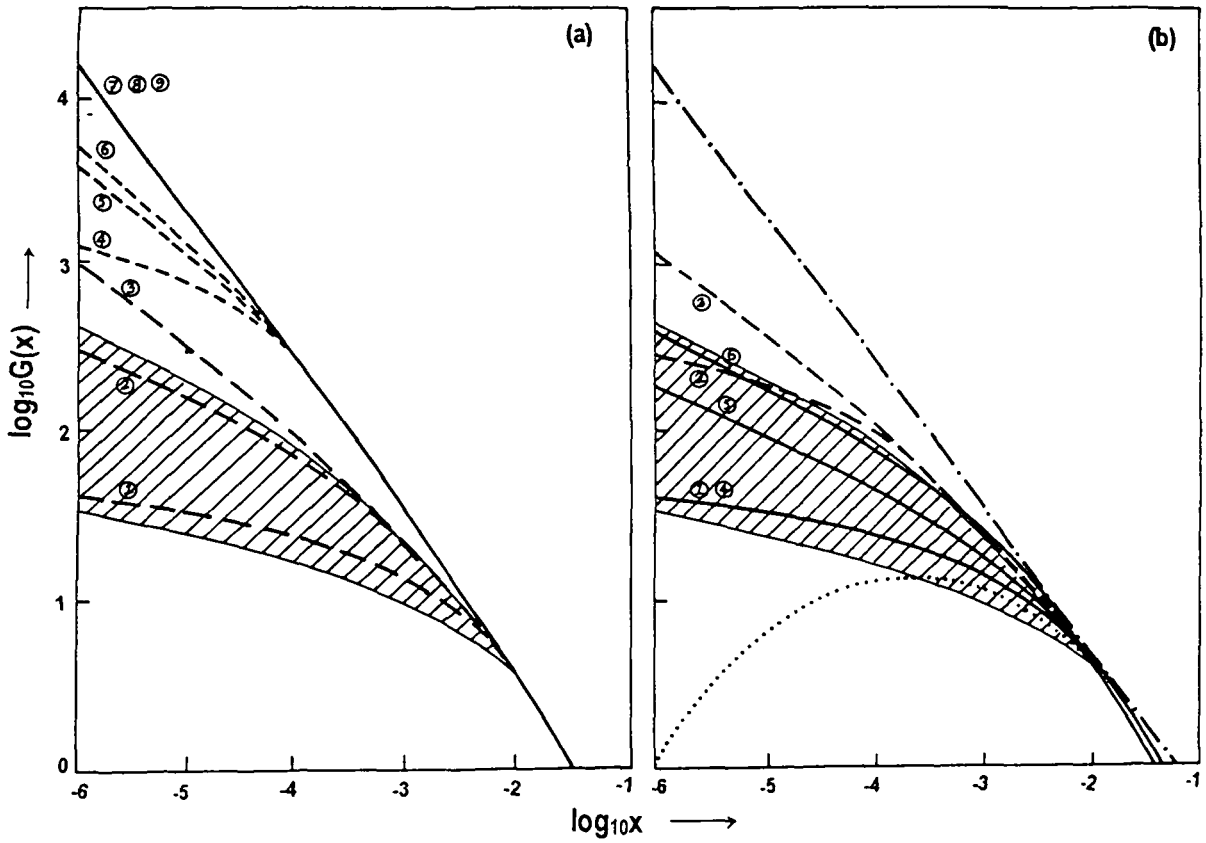

Fig.4.6(a) x - evolutions of $G(x,Q^2)$ at Q^2 = 10, 100 and 1000 GeV^2 are given by curves 1, 4, 7, 2, 5, 8 and 3, 6, 9 respectively Solid curves are GLDAP evolution, long-dashed curves take into account the absorption corrections through (A) for $R_s \simeq 0.2$ Fm, short dashed are the same for $R_s \simeq R_n$ The shaded area is the prediction from equation (4 16) with upper and lower boundaries corresponding to K = 1 and 100 respectively

Fig.4.6(b) Difference between GLDAP (solid curves) and GLR (dashed curves) equations. The curves 1, 4; 2, 5 and 3, 6 correspond to Q^2 = 10, 100 and 1000 GeV^2 respectively Initial conditions (A) and (B) are shown by dotted and dot-dashed curves respectively The shaded area is same as in Fig 4 6(a)

Solid curves are the ordinary linear GLDAP evolution equation; long dashed curves take into account the absorption corrections through the new boundary condition (A) for $R_s \sim 0.2\,F_m$. Short dashed is the same for $R_s \sim R_n$. Here $\Lambda = 200\,MeV$. In the Fig. 4.6(b) the difference between linear (solid curves) GLDAP and non-linear (dashed curves) GLR [2] evolution is given. The curves 1, 4; 2, 5 and 3, 6 correspond to $Q^2 = 10, 100$ and $1000\,GeV^2$ respectively. The new and old initial conditions (A) and (B) at $Q_s^2 = 4\,GeV^2$ are shown by dotted and dot-dashed curves respectively Here $\Lambda = 200\,MeV$. In both the figures, the dashed areas are our predictions from the equation (4.16) with upper and lower boundaries corresponding to $K = 1$ and 100

respectively. In both cases gluon distribution functions $G(x_0, Q^2)$ for linear GLDAP equation at $x_0 = 10^{-2}$ are taken as inputs; because, it is almost same for all curves.

In the leading $\log(1/x)$ approximation of QCD, it is expected that the gluon distribution will grow indefinitely as,

$$G(x,.Q^2) \simeq x^{-\lambda} \qquad (C)$$

in the low-x limit [68] with $\lambda \simeq 0.5$. This increase with decreasing x, will of course eventually be tamed by screening corrections which give rise to non-linear terms in the QCD evolution equations. The approximate framework is provided by the BKFL equation [8,69] with the addition of the non-linear shadowing term. This is known as GLR equation. The radius parameter R in the shadowing term characterises the area πR^2 in which the gluons are concentrated within the proton. We would expect R to be approximately equal to the radius of the proton that is $R \simeq 5\ GeV^{-1}$, although it has been argued that the gluons may be concentrated in Hot Spots within the proton. So, the results for $R \simeq 2\ GeV^{-1}$ are also shown. The non-linear integro-differential BKFL equation can now be solved numerically [68] with the analysis entirely confined to the low-x region $x < x_0$. It is informative to compare the above results with the gluon distributions to Set-$B\_$ of partons obtained in the Kwiecinski, Martin, Roberts and Stirling (KMRS) [70] global structure function analysis which attempted to incorporate both the BKFL and shadowing effects, albeit in an approximate manner. KMRS evolved the starting distributions up from $Q^2 = 4\ GeV^2$ using the next-to-leading order GLDAP equations. In Fig. 4.7 the continuous curves are the values of $G(x,Q^2)$ determined by solving the BKFL equation for $Q^2 = 100$ and $1000\ GeV^2$.

The dashed curves are $G(x,Q^2)$ of Set-$B\_$ of the KMRS next-to-leading order structure function analysis. In each case three curves are in descending order the solution with shadowing neglected, and the solutions with the shadowing term

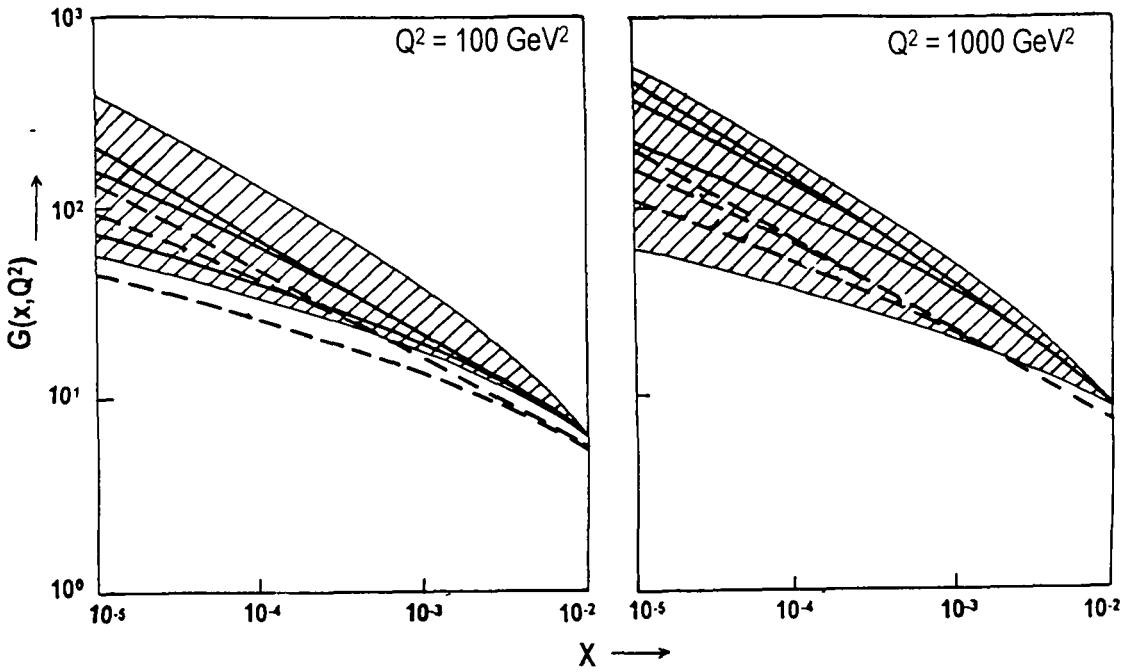

Fig.4.7 x - evolutions of $G(x,Q^2)$ of BKFL equation for Q^2 = 100 and 1000 GeV^2 (solid curves) The dashed curves are $G(x,Q^2)$ of KMRS Set-B_ In each case three curves in descending order are the solutions with shadowing neglected, with R = 5 GeV^{-1} and R = 2 GeV^{-1} respectively The shaded area is same as in Fig. 4 6(a)

included with $R = 5\ GeV^{-1}$ and $R = 2\ GeV^{-1}$ respectively. The shaded areas are our predictions described before. $G(x,Q^2)$ at $x = 10^{-2}$ for BKFL equation are taken as inputs. They are almost same for all the curves.

4.3. Conclusion:

In this chapter, we obtain t and x-evolutions of gluon distribution function at low-x from GLDAP evolution equation. Comparison is made with the prediction of BKFL as well as GLR equations. We also make predictions for the HERA range. It is clear from the figures that our results for $t-$evolutions of gluon distribution functions conform with those of EHLQ Set-1, EHLQ Set-2 and DFLM-2 parametrizations for $x<10^{-2}$, but do not conform for $x>10^{-2}$. But they conform excellently with Set-1(a) whereas differ badly with Set-1(b). The bands in all the figures gives our predictions for $x-$evolutions for $1<K<100$. Our predictions conform well with those of others It can be inferred from our predictions that screening correction at very low-x is more likely. To conclude, our simple approximate analytical solution of GLDAP evolution equation for structure function gives satisfactory predictions in HERA range. The

qualitative predictions of our results conform to those of several other authors. GLDAP evolution equation in present form thus stands as a viable alternative to BKFL and GLR predictions, at least in the x and Q^2 – range under study.□

Chapter-5

GLUON DISTRIBUTION FUNCTION FROM PROTON STRUCTURE FUNCTION

The measurements of proton structure function by Deep Inelastic Scattering (DIS) processes in the low-x region where x is the Bjorken variable have opened a new era in parton density measurements [42]. Gluon distribution can not be measured directly from experiments. It is therefore important to measure gluon distribution $G(x,Q^2)$ indirectly from the proton structure function $F_2(x,Q^2)$. A few number of papers have already been published [43-45,48,49,50,52,53] in this connection. Here we present an alternative method to relate $G(x,Q^2)$ with proton structure function and their derivatives with respect to $\ln Q^2$, $\partial F_2(x,Q^2)/\partial \ln Q^2$ and with respect to x, $\partial F_2(x,Q^2)/\partial x$ for fixed values of Q^2. Our method is more general with less approximation, simpler and mathematically more transparent.

5.1. Theory:

It is shown in the references [45,52] that the gluon distribution at low-x can be obtained by analysing the longitudinal structure function. Similarly it is also shown in the reference [48,49,53] that this distribution can be calculated from the proton structure function $F_2(x,Q^2)$ and their differential coefficient with respect to $\ln Q^2$, $\partial F_2(x,Q^2)/\partial \ln Q^2$. The basic idea lies on the fact that the scaling violation of $F_2(x,Q^2)$ arises, at low-x, from the gluon distribution alone and does not depend on the quark distribution. Then neglecting the quarks the leading order GLDAP evolution equation for four flavours [49] gives

$$\frac{\partial F_2(x,Q^2)}{\partial \ln Q^2} = \frac{5\alpha_s}{9\pi}\int_0^{1-x} G\left(\frac{x}{1-z},Q^2\right)P_{qg}(z)dz\,, \qquad (5.1)$$

where, the splitting function is

$$P_{qg}(z) = z^2 + (1-z)^2, \tag{5.2}$$

and, α_s is the strong coupling constant. Now,

$$\frac{x}{1-z} = x\sum_{k=0}^{\infty} z^k = x + x\sum_{k=1}^{\infty} z^k . \tag{5.3}$$

We have, $1-x>z>0 \Rightarrow |z|<1$ which implies that the expansion equation (5.3) is convergent. Now by the Taylor expansion [39] we get,

$$G\left(\frac{x}{1-z},Q^2\right) = G\left(x + x\sum_{k=1}^{\infty} z^k, Q^2\right)$$

$$= G(x,Q^2) + x\sum_{k=1}^{\infty} z^k \frac{\partial G(x,Q^2)}{\partial x} + \frac{1}{2}x^2\left(\sum_{k=1}^{\infty} z^k\right)^2 \frac{\partial^2 G(x,Q^2)}{\partial x^2} + O(x^3)$$

where, $O(x^3)$ are the higher order terms. Neglecting the terms containing x^2 and higher orders $O(x^3)$ for simplicity, we get,

$$G\left(\frac{x}{1-z},Q^2\right) = G\left(x + x\sum_{k=1}^{\infty} z^k, Q^2\right) \cong G(x,Q^2) + x\sum_{k=1}^{\infty} z^k \frac{\partial G(x,Q^2)}{\partial x}. \tag{5.4}$$

But as a matter of fact, we can not neglect the higher order terms, as these terms are not small in Regge-like behaviour [4,49] $G(x) \simeq x^{-\delta_p(Q^2)}$ or in Double-logarithmical behaviour [49,51] $G(x) \simeq \exp\left(0.5\sqrt{\delta_p(Q^2)\ln(1/x)}\right)$ for gluon at low-x. Here $\delta_p(Q^2)$ is a Q^2 – dependent parameter where $p = s$ (singlet quark) or g (gluon). On the otherhand, it has been shown that this Taylor expansion method is successfully applied in calculating Q^2 – evolution of proton structure functions [36] at low-x with reasonable phenomenological success. Bora and Choudhury [48] and also Prytz [43,44] has already applied Taylor expansion method to calculate gluon distributions from proton structure functions and scaling violations of them. But our method is more general and transparent with less approximation.

Putting equations (5.2) and (5.4) in equation (5.1) and performing z – integrations we get,

$$\frac{\partial F_2(x,Q^2)}{\partial \ln Q^2} = \frac{5\alpha_s}{9\pi}\left[A(x)G(x,Q^2) + B(x)\frac{\partial G(x,Q^2)}{\partial x}\right], \tag{5.5}$$

where,

$$A(x) = (1/3)(1-x)(2x^2 - x + 2)$$

and

$$B(x) = (1/3)x(1-x)(-2x^2 + 4x - 5) - x\ln x .$$

Here we used the identity [39] $\sum_{k=1}^{\infty}\frac{z^k}{k} = \ln\frac{1}{1-z}$. Recasting the equation (5.5) we get,

$$G(x,Q^2) + \frac{B(x)}{A(x)}.\frac{\partial G(x,Q^2)}{\partial x} = \frac{9\pi}{5\alpha_s.A(x)}.\frac{\partial F_2(x,Q^2)}{\partial \ln Q^2} \tag{5.6}$$

at constant $Q^2 = Q_0^2$, where, $G(x,Q^2) = G(x)$ and $\partial F_2(x,Q^2)/\partial \ln Q^2 = K(x)$.

And so, equation (5.6) gives,

$$G(x) + \frac{B(x)\partial G(x)}{A(x)\partial x} = \frac{9\pi K(x)}{5\alpha_s A(x)}. \tag{5.7}$$

Since the ratio $B(x)/A(x)$ is very small at low-x, $\lim_{x\to 0} B(x)/A(x) = 0$, the left hand side of equation (5.7) can be written as

$$G(x) + \frac{B(x)}{A(x)}.\frac{\partial G(x)}{\partial x} = G(x) + \frac{B(x)}{A(x)}.\frac{\partial G(x)}{\partial x} + \frac{1}{2}\left(\frac{B(x)}{A(x)}\right)^2.\frac{\partial^2 G(x)}{\partial x^2} + ... = G\left(x + \frac{B(x)}{A(x)}\right)$$

by Taylor expansion series [39]. Thus from equation (5.7) we get,

$$G\left(x + \frac{B(x)}{A(x)}\right) = \frac{9\pi}{5\alpha_s}.\frac{K(x)}{A(x)}. \tag{5.8}$$

The equation (5.8) is the relation between the gluon distribution $G(x',Q^2)$ at $x' = x + B(x)/A(x)$ and $\partial F_2(x,Q^2)/\partial \ln Q^2$ at x, at the fixed values of $Q^2 = Q_0^2$. This is our main result.

5.2. Results and Discussion:

We use HERA data taken by H1 and ZEUS collaborations from the Table-1 [71] and Table-2 [72] respectively. In these tables, the values of $\partial F_2(x,Q^2)/\partial \ln Q^2$ are listed for a range of $x-$values at $Q^2 = 20\,GeV^2$. Similarly we use parametrizations of the recent New Muon Collaboration (NMC) proton structure function data [73] from a 15- parameter function [73]. Here we calculate the values of $\partial F_2(x,Q^2)/\partial \ln Q^2$ at $Q^2 = 40\ GeV^2$. Moreover recent HERA data are also parametrized by H1 and ZEUS collaborations by some appropriate functions. In these cases also we calculate $\partial F_2(x,Q^2)/\partial \ln Q^2$ at $Q^2 = 20\ GeV^2$. From all these data or parametrizations we calculate the structure functions $F_2(x,Q^2)$ or scaling violations of structure functions with respect to $\ln Q^2$ and apply them in the equation (5.8) to calculate the gluon distribution functions $G(x',Q^2)$ at $x' = x + B(x)/A(x)$.

Table-1

The values of $\partial F_2(x,Q^2)/\partial \ln Q^2$ for different low values of x from HERA data given by H1 collaboration at $Q^2 = 20\ GeV^2$. $\sigma_{stat.}$ and σ_{syst} are statistical and systematic errors respectively.

x	$\partial F_2 / \ln Q^2$	σ_{stat}	σ_{syst}
0.000383	0.51	0.14	0.09
0.000562	0.65	0.18	0.10
0.000825	0.46	0.06	0.06
0.00133	0.28	0.06	0.11
0.00237	0.21	0.03	0.06
0.00421	0.20	0.03	0.03
0.0075	0.08	0.02	0.03
0.0133	0.06	0.02	0.02

Reference [71]: S. Aid et. al, H1 Collaboration, Phys. Lett. B 354 (1995) 494.

Table-2

The values of $\partial F_2(x,Q^2)/\partial \ln Q^2$ for different low values of x from HERA data given by ZEUS collaboration at $Q^2 = 20\ GeV^2$. σ_{stat} and σ_{syst} are statistical and systematic errors respectively.

x	$\partial F_2 / \ln Q^2$	σ_{stat}	σ_{syst}
0.00085	0.45	0.03	+0.05, -0.10
0.00155	0.30	0.03	+0.09, -0.30
0.00268	0.25	0.02	+0.07, -0.09
0.00465	0.23	0.03	+0.02, -0.05

Reference [72]: M. Dernck et. al., ZEUS collaboration, Phys. Lett. B 364 (1995) 576.

The 15-parameter function to describe the recent NMC proton structure function data is,

$$F_2(x,Q^2) = A(x)\left[\frac{\ln(Q^2/\Lambda^2)}{\ln(Q_0{}^2/\Lambda^2)}\right]^{B(x)}\cdot\left[1+\frac{C(x)}{Q^2}\right].$$

Here, $Q^2 = 20\ GeV^2$, $\Lambda = 0.250\ GeV$,

$$A(x) = x^{a_1}(1-x)^{a_2}\left\{a_3 + a_4(1-x) + a_5(1-x)^2 + a_6(1-x)^3 + a_7(1-x)^4\right\},$$

$$B(x) = b_1 + b_2 x + b_3/(x+b_4)$$

and

$$C(x) = c_1 x + c_2 x^2 + c_3 x^3 + c_4 x^4.$$

Table-3

15-parameters for $F_2^p(x,Q^2)$ and $F_2^d(x,Q^2)$.

Parameter	$F_2^p(x,Q^2)$			$F_2^d(x,Q^2)$		
	Middle Value	Upper Value	Lower Value	Middle Value	Upper Value	Lower Value
a_1	-0.02778	-0.05711	-0.01705	-0.4858	-0.04715	-0.02732
a_2	2.926	2.887	2.851	2.863	2.814	2.676
a_3	1.0362	0.998	0.8213	0.8367	0.7286	0.3966
a_4	-1.84	-1.758	-1.156	-2.532	-2.151	-0.608
a_5	8.123	7.89	6.836	9.145	8.662	4.946
a_6	-13.074	-12.696	-11.681	-12.504	-12.258	-7.994
a_7	6.215	5.992	5.645	5.473	5.452	3.686
b_1	0.285	0.247	0.325	-0.008	-0.048	0.141
b_2	-2.694	-2.611	-2.767	-2.227	-2.114	-2.464
b_3	0.0188	0.2043	0.0148	0.0551	0.0672	0.0299
b_4	0.0274	0.0307	0.0226	0.057	0.0677	0.0396
c_1	-1.413	-1.348	-1.542	-1.509	-1.57	-2.128
c_2	9.366	8.548	10.549	8.553	9.515	14.378
c_3	-37.79	-35.01	-40.81	-31.2	-34.94	-47.76
c_4	47.1	44.43	49.12	39.98	44.42	53.63

Reference [73]: M. Arneodo at. al., NMC,Phys. Lett. B 364 (1995) 107.

Table-4

Recent HERA data in parametrized by H1 collaboration as

$$F_2(x,Q^2) = \left[ax^b + cx^d\left(1 + e\sqrt{x}\right)\left(\ln Q + f\ln^2 Q^2\right)\right](1-x)g\,.$$

Parameter→	a	b	c	d	e	f	g
Value→	3.07	0.75	0.14	-0.19	-2.93	-0.05	3.65

Reference [74]: T. Ahmed et al, H1 collaboration, Nucl. Phys. B 439 (1995) 471.

Table-5

Recent HERA data is parametrized by ZEUS collaboration as

$F_2 = \left(1 - x^a\right)^b \left[c + d\, x^{\left(e + f \log_{10} Q^2\right)}\right]$ where, Q^2 – range is from $8.5\, GeV^2$ to $500\, GeV^2$.

a	b	c	d	e	f
2	4	0.35	0.017	-0.35	-0.16

Reference [75] : M. Derrick et al, ZEUS collaboration, DESY 94-143, (1994).

For our calculation, strong coupling constant α_s was taken from a next-to-leading order fit [76] to F_2 data which yields $\alpha_s = 0.180 \pm 0.008$ at $Q^2 = 50\, GeV^2$ corresponding to $\Lambda^{(4)}_{MS} = 0.263 + 0.042$ and $\alpha_s\left(M_z^2\right) = 0.113 \pm 0.005$. This value of α_s agrees with one given by Particle Data Group [77]. But in our practical calculations we neglect the errors of α_s and Λ which are rather small.

In the Fig.5.1, we calculate $G\left(x'\right)$ (equation (5.8)) for x' values which varies from 5.52×10^{-2} to 2.27×10^{-6} for highest and lowest values of x under consideration respectively. The gluon distribution increases from $\simeq$ 3.5 to 6.5 when x decreases from the highest to the lowest values under consideration. But gluon distribution decreases slightly (<1%) for a particular values of x when Q^2 increases from $40\, GeV^2$ to $100\, GeV^2$. We do not compare the result of NMC data with those of mainly HERA, because, their Q^2 and x - ranges are different.

In the Fig.5.2, the gluon distribution obtained by our method (equation (5.8)) from HERA data measured by H1 collaboration [71] is presented at $Q^2 = 20\, GeV^2$. The middle line is the result without considering any error in the data. The upper and lower lines are the results adding and subtracting algebraically the statistical and the systematic errors with the data respectively, and thereby calculating the gluon distributions. These two lines are symmetric about the middle lines and positive and negative errors are equal. The area bounded by these lines gives the result with

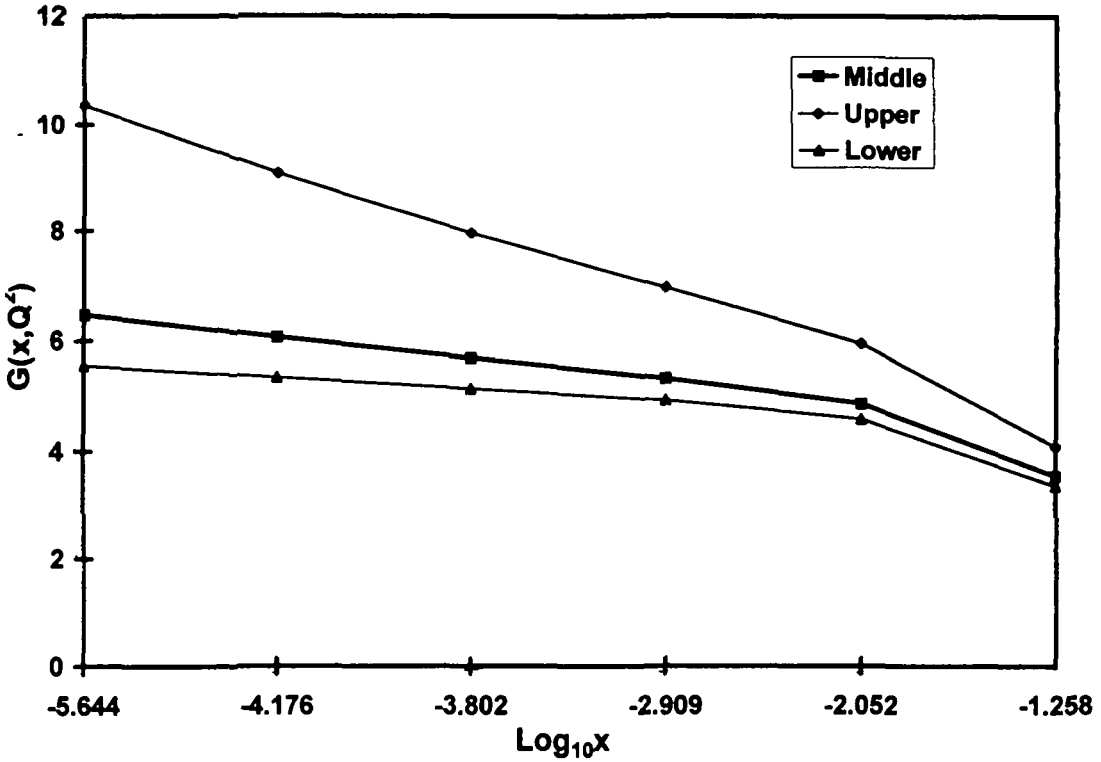

Fig.5.1 Gluon distribution obtained by our method (equation (5 8)) for NMC proton parametrization (15-parameter function -Table-3) at Q^2 = 40 GeV^2 The middle, upper and lower lines are the results (a)without considering any error, (b)adding algebraically the statistical and systematic errors and (c)subtracting algebraically the statistical and systematic errors respectively

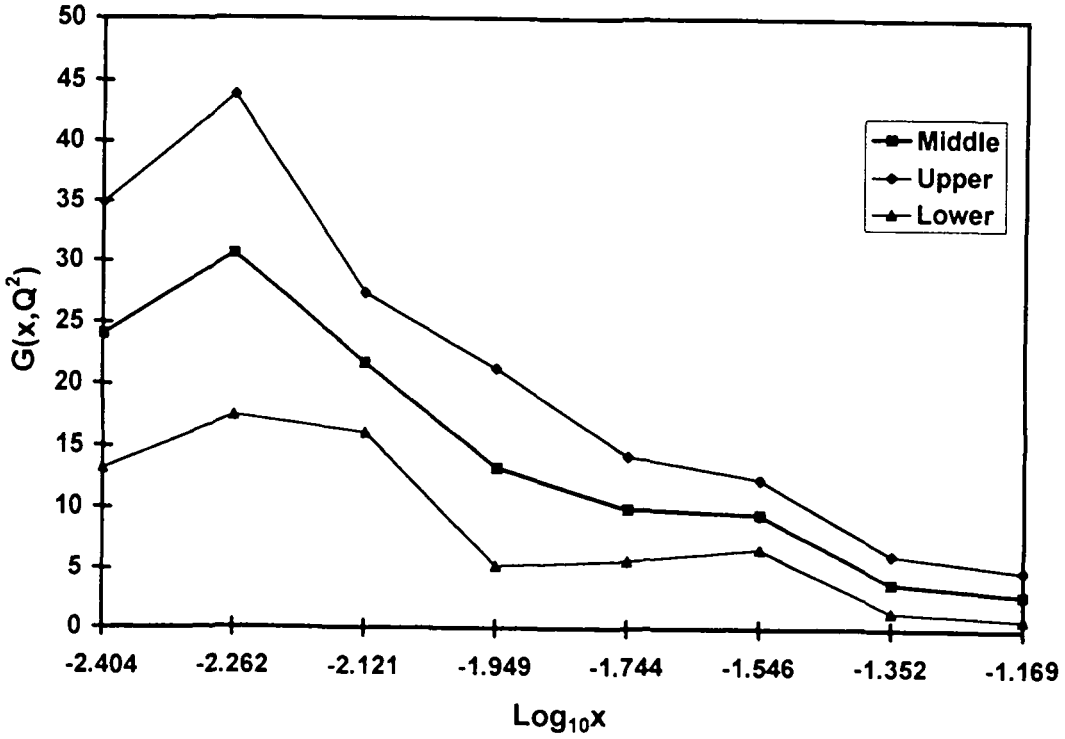

Fig.5.2 Same result as in Fig 5 1 (equation(5 8)) for HERA proton data by H1 collaboration (Table-1) at Q^2 = 20 GeV^2

maximum error. The x-values in the data ranges from the highest value 1.33×10^{-2} to the lowest value 3.83×10^{-4}. The corresponding x' values are 6.81×10^{-2} and 3.948×10^{-3} respectively, and also gluon distributions are $\simeq 3.0$ and $\simeq 24.0$ respectively for data without considering any error. Here also gluon distribution increases when x decreases except the lowest value when gluon distribution decreases. But the rate of increment for HERA data measured by H1 collaboration is much higher than that of NMC data.

In Fig.5.3 the same thing is presented for HERA data measured by ZEUS collaboration [72] at $Q^2 = 20\ GeV^2$.

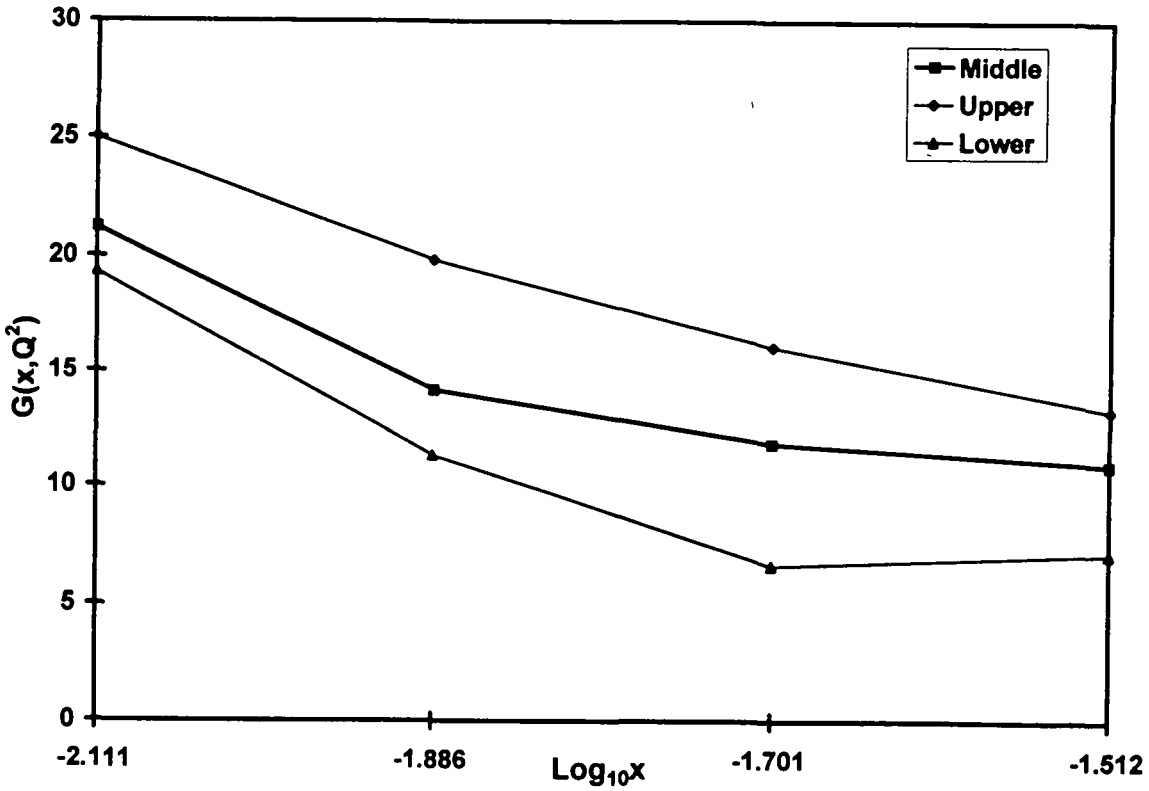

Fig.5.3 Same result as in Fig 5 1 (equation (5 8)) for HERA proton data by ZEUS collaboration (Table-2) at $Q^2 = 20\ GeV^2$

Here the x-values in the data ranges from the highest value 4.65×10^{-3} to the lowest value 8.5×10^{-4}. The corresponding x' values are 3.077×10^{-2} and 7.752×10^{-3} respectively and also gluon distributions are $\simeq 10.9$ and are $\simeq 21.2$ respectively for

data without considering any error. We see, in this case also, gluon distribution increases when x decreases. And the rate of increment is slightly higher to that of H1 collaboration in the x-range considered, but much higher than that of NMC data.

In the Fig.5.4 comparison of gluon distributions by our method (equation (5.8)) for HERA proton data by H1 and ZEUS parametrizations (Table-4 and Table-5 respectively) is presented at $Q^2 = 20\ GeV^2$.

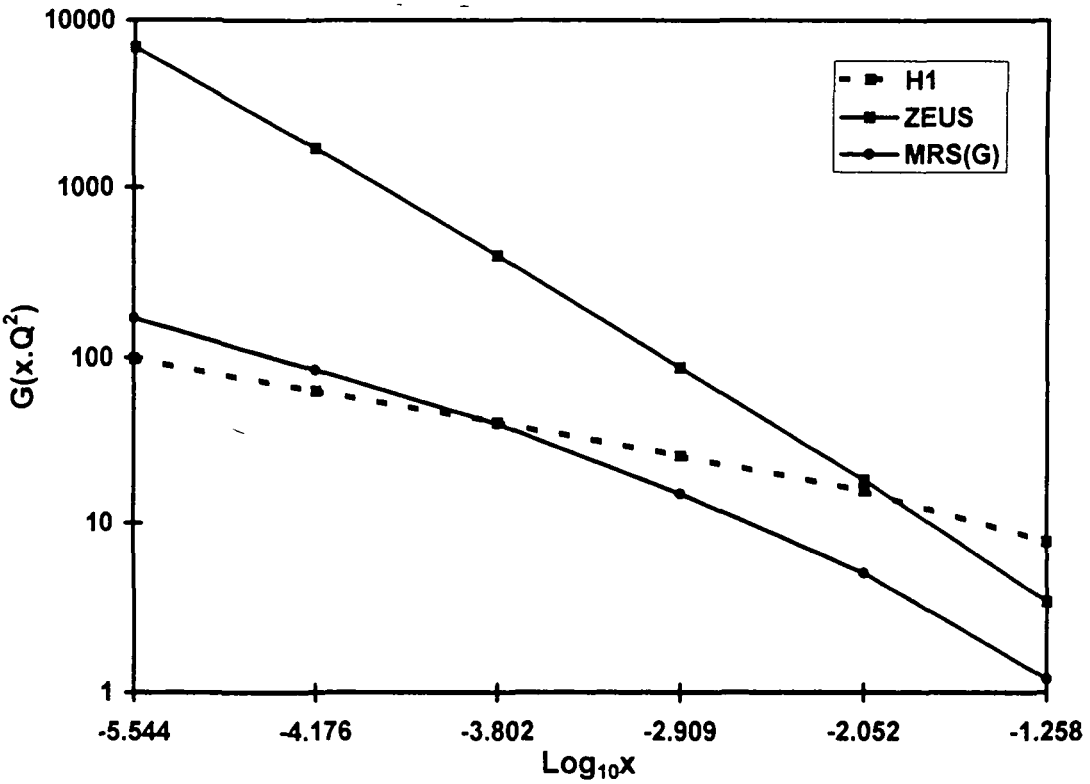

Fig.5.4 Comparison of gluon distributions by our method (Sarma and Medhi - equation (5.8)) for HERA proton data by H1 (dashed line) and ZEUS (solid line) parametrization (Table-4 and Table-5 respectively) with MRS(G) [50] input gluon distribution (thin solid lines with solid circles) at Q^2 = 20 GeV^2

The x range used by H1 collaboration is $10^{-4} < x < 1$ for Q^2 range $4\ GeV^2 < Q^2 < 2000\ GeV^2$. This parametrization also covers the F_2^p data from the NMC and BCDMS experiments. Similarly the x range used by ZEUS collaboration is up to small values $\simeq 10^{-4}$ for all values of Q^2 under consideration But it will also cover the high values of x from NMC collaboration. It is seen from the figure that as usual when x decreases gluon distribution increases, but in different rates.

In the Fig.5.5, comparison of gluon distribution from NMC proton data parametrization (Table-3) middle value only by our method (equation (5.8), line with solid diamonds), Bora and Choudhury method (line with solid squares), and Pryz method (line with solid triangles) at $Q^2 = 40\ GeV^2$ is presented.

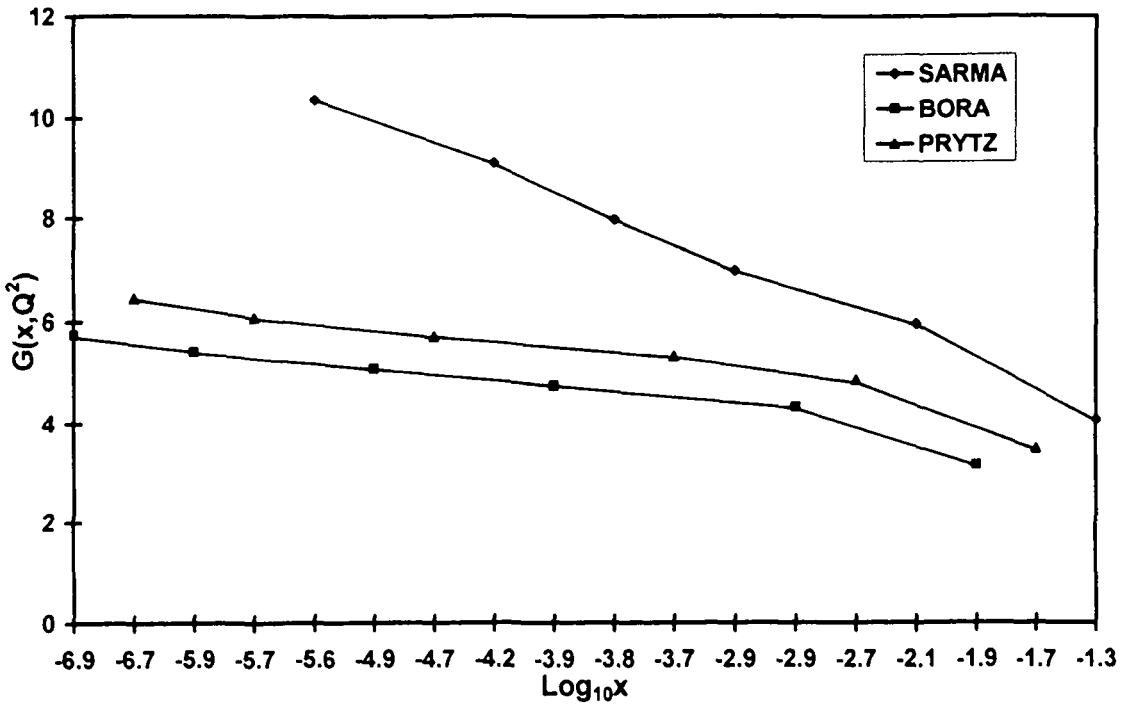

Fig.5.5 Same result as in Fig 5 4 for NMC proton parametrnzation (Table-3) middle value only by Sarma and Medhi (equation(5 8)), Bora and Choudhury [48] and Prytz [43,44] methods at $Q^2 = 40\ GeV^2$

If we apply proton structure functions and their scaling violations at a particular x-value, the calculated gluon distributions will be in different x-values for these different methods. They are $x' = x + B(x)/A(x)$ in our method, $x_1 = x + [B(x)/A(x) + B(x)].x$ in Bora and Choudhury method and $x_2 = 2x$ in Prytz method. Thus the shifting of the arguments in gluon distributions is appreciable in our method. For all the methods, gluon distribution increases when x decreases except for the last data point for which it decreases. But rate of increment is different for different methods. The values of gluon distributions are comparable but rate of increment is highest in our method and lowest in Bora and Choudhury method.

In Fig.5.6, the same thing as in Fig.5.5 is presented for HERA data middle value only measured by H1 collaboration (Table-1) at $Q^2 = 20\ GeV^2$.

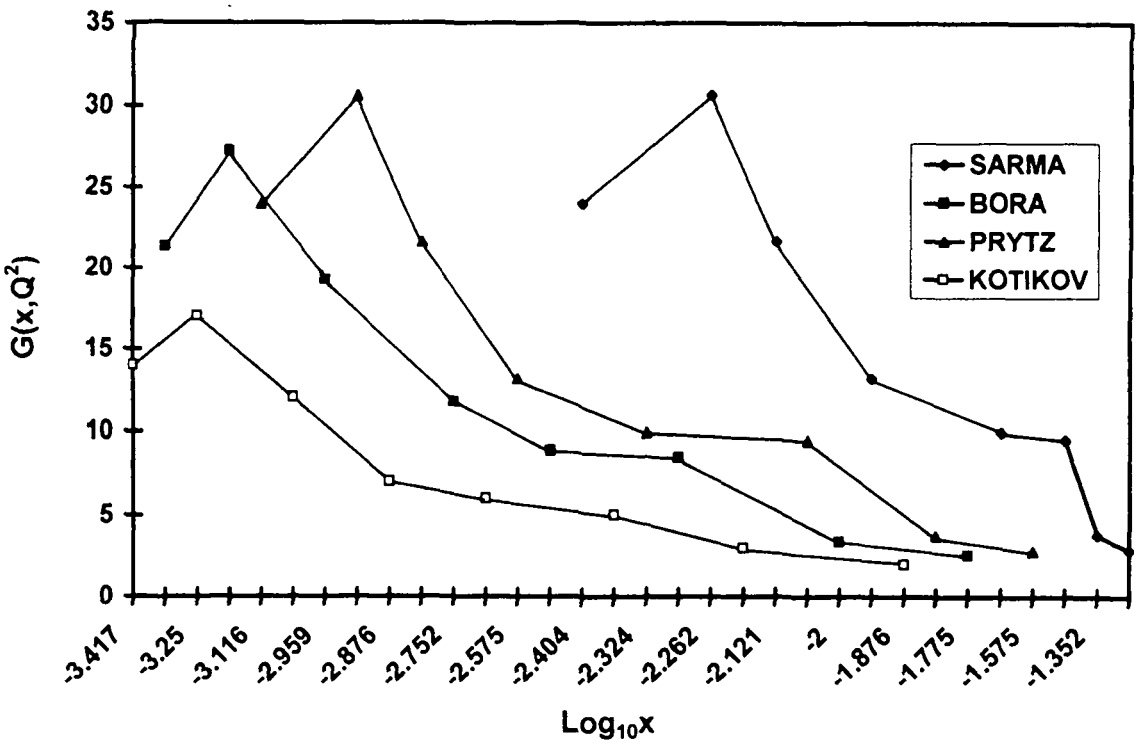

Fig.5.6: Same result as in Fig.5.5 for HERA proton data by H1 collaboration (Table-1) by various methods (Kotikov and Parente method) [49,52] at $Q^2 = 20\ GeV^2$.

Here results by an extra method, Kotikov and Parente method [49,52] are also included. The x- values under consideration are same as in Fig.5.2. But the arguments of the gluon distributions calculated are different for different methods as discussed earlier, except for Kotikov and Parente method for which the arguments do not change. Accordingly, for the highest and the lowest x values, x' values are 6.81×10^{-2} and 3.948×10^{-3}; x_1 values are 1.8×10^{-2} and 5.16×10^{-4} and x_2 values are 2.66×10^{-2} and 7.66×10^{-4} respectively. For all the methods gluon distribution increases when x decreases except for the last data point for which it decreases. But rate of increment is different for different methods. The values of gluon distributions are comparable but rate of increment is highest in our method and lowest in Kotikov and Parente method. It is intermediate in other two methods of which rate of Prytz method is slightly higher than that of Bora and Choudhury method.

In Fig.5.7 also, the same thing as in Fig.5.5 is presented for HERA data parametrization (Table- 4) measured by H1 collaboration [74] at $Q^2 = 20\,GeV^2$.

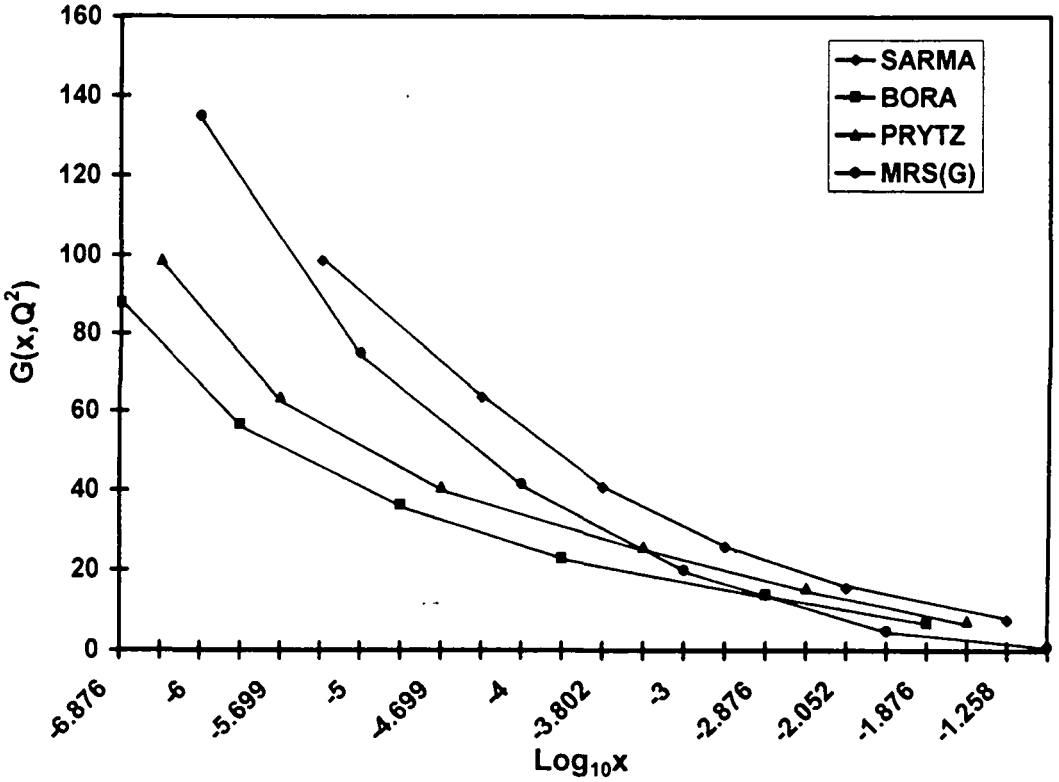

Fig.5.7: Same result as in Fig.5.5 for HERA proton parametrization by H1 collaboration (Table-4) by various methods at Q^2 = 20 GeV^2.

The x values under consideration are same as before in Fig.5.1. Accordingly shifted arguments of gluon distributions for different methods are exactly same as in Fig.5.5. When x decreases, gluon distribution increases for all the methods as usual, but with different rates for different methods as before. The growth rate is highest in our method and lowest in Bora and Choudhury method. In the same figure, we compare the result with Martin, Roberts, Stirling (MRS(G)) [50] input gluon distribution (solid line with solid circles) in the same Q^2 – value. MRS(G) distribution is close to our method.

In Fig.5.8, comparison of gluon distributions by various methods exactly same way as in Fig.5.6 is presented for HERA data middle value (Table–2) measured by ZEUS collaboration [72] at $Q^2 = 20\,GeV^2$.

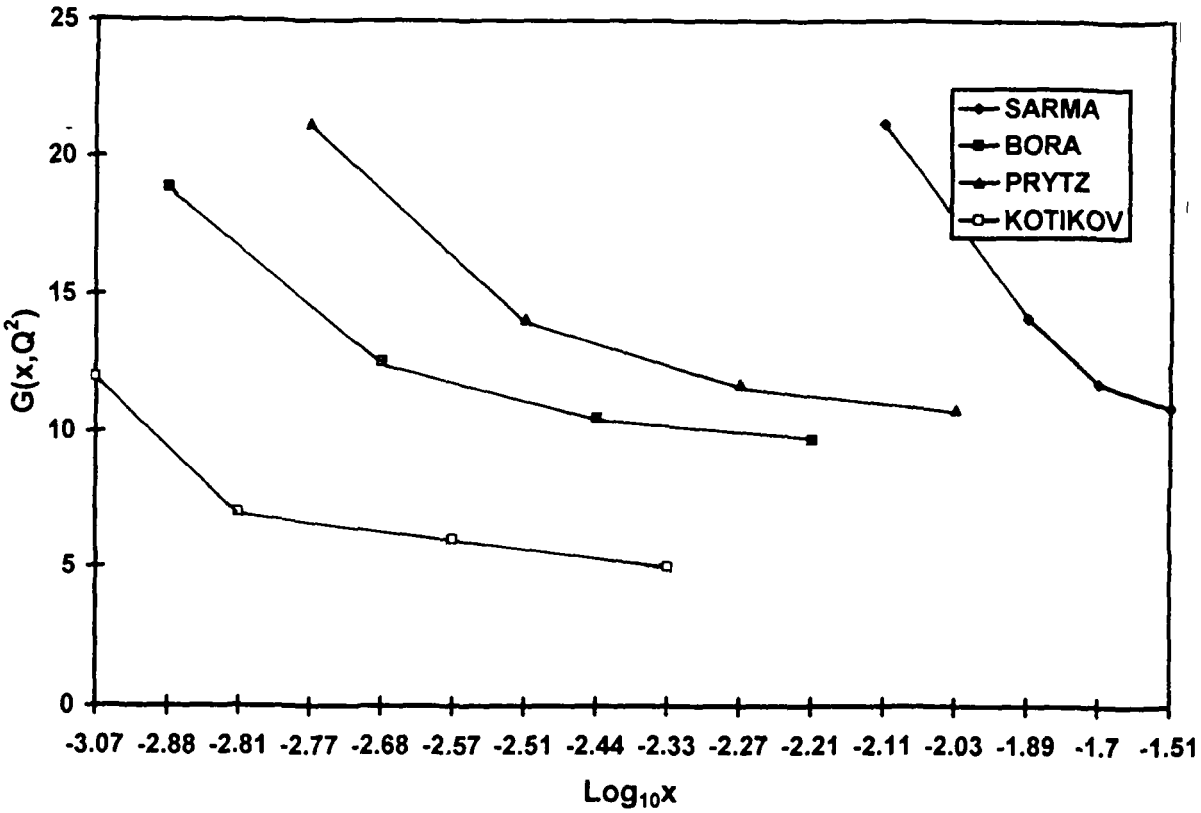

Fig.5.8: Same result as Fig.5.6 for proton data by ZEUS collaboration (Table-2) by various methods at Q^2 = 20 GeV^2.

The x-values under consideration is same as in Fig.5.3. But the arguments of the gluon distributions calculated are different for different methods as discussed earlier. Accordingly, for the highest and lowest x values x' values are 3.077×10^{-2} and 7.752×10^{-3}, x_1 values are 6.2×10^{-3} and 1.13×10^{-3}, and x_2 values are 9.3×10^{-3} and 1.7×10^{-3} respectively. The arguments of gluon distribution for Kotikov and Parente method are same as x-values under consideration. The gluon distribution increases when x decreases for all the methods as before, but the rate of increment is highest in our method and lowest in Kotikov ans Parente method. The rates are intermediate in other two methods of which rate of Prytz method is higher than that of Bora and Choudhury method.

In Fig.5.9, the same thing as Fig.5.7 is presented for HERA data prametrization (Table –5) measured by ZEUS collaboration [75] at $Q^2 = 20\ GeV^2$.

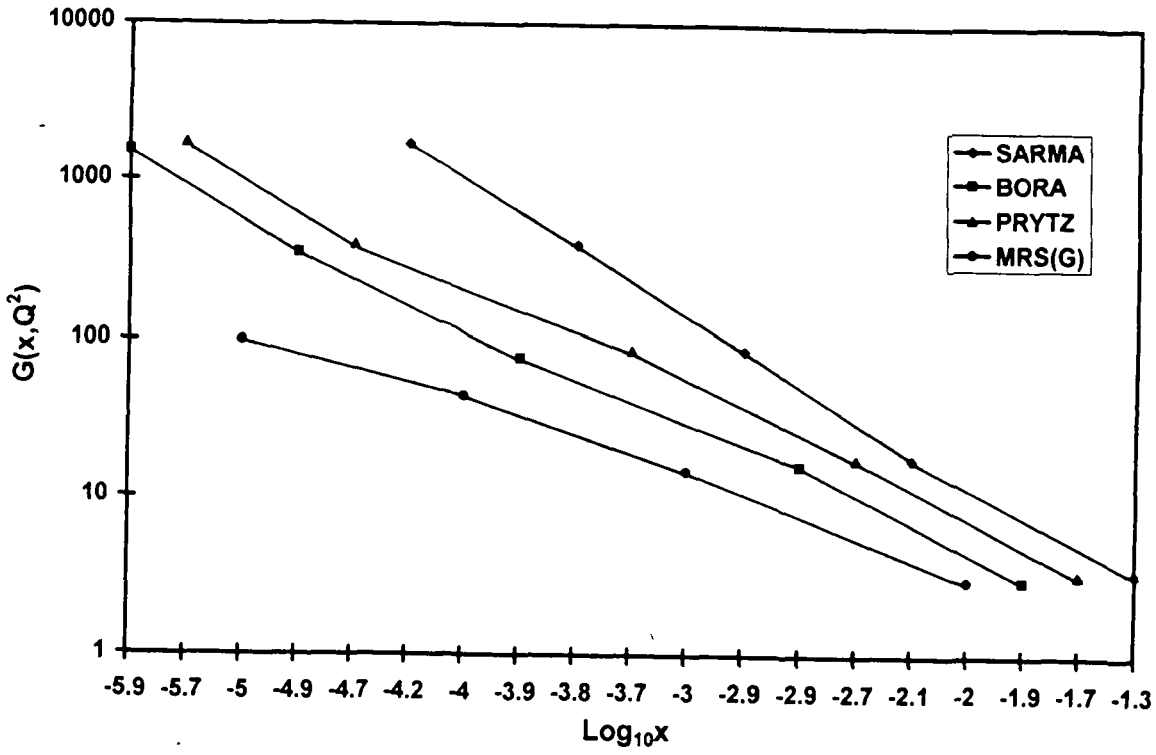

Fig.5.9: Same result as in Fig.5.7 for HERA proton parametrization by ZEUS collaboration (Table-5) by various methods at Q^2 = 20 GeV^2

The x values under consideration are same as before as in Fig.5.1 except the lowest x values which is 10^{-6} here instead of $\simeq 10^{-7}$ in the previous cases. Accordingly, the shifted arguments are also same as in Fig.5.5 with suitable modification for the lowest values. When x decreases gluon distribution increases as before with different rates. This is highest in our method and lowest in Bora and Choudhury method. In the same figure, we compare the result with MRS(G) [50] input gluon distribution in the same Q^2 – value. But it is far below than the gluon distribution calculated from ZEUS HERA data by other methods. It is because the rate of increment of HERA ZEUS data when x decreases is very high which makes the calculated gluon distributions also very high.

5.3 Conclusion:

In this chapter, we present an alternative method than other methods [43-45,48,49,52,53] to extract gluon distribution $G(x,Q^2)$ from the measurement of low–

x proton structure function $F_2(x,Q^2)$ and their differential coefficients $\partial F_2(x,Q^2)/\partial \ln Q^2$ with respect to $\ln Q^2$. For calculation of gluon distribution from proton structure function at low–x, we use HERA data measured by H1 [71] and ZEUS [72] collaborations, HERA data parametrizations presented by H1 [74] and ZEUS [75] collaborations and NMC data parametrizations [73]. Of course, the last parametrization includes SLAC [78] and BCDMS [79] low–x data also. In our method, gluon from NMC data [73] is appreciably small, it is almost one fifth of HERA data measured by H1 and ZEUS collaborations at $x \simeq 10^{-3}$. But if we compare with HERA data parametrizations, we will get slightly different result. In our method, gluon from NMC data parametrizations is almost one third than that of H1 and ZEUS HERA data parametrizations at $x \simeq 10^{-3}$. But it is almost one tenth of that of H1 parametrization and almost one thousandth of that of ZEUS parametrrization. In our method, gluon distributions calculated from direct HERA data measured by H1 and ZEUS collaborations up to $x \simeq 10^{-3}$ are almost in the same order. Gluon distribution from the HERA data parametrizations by H1 and ZEUS collaborations up to $x \simeq 10^{-3}$ are also of the same order to them and mutually are also same. But after $x \simeq 10^{-3}$ when x decreases the rate of increment of ZEUS parametrization is much higher than that of H1 and gluon distribution from the first parametrization becomes also hundred times of the second one at $x \simeq 10^{-7}$.

We compared our result with other methods, Bora and Choudhury, Prytz, Ktikov and Parente, and MRS(G) input gluon distribution. The general trend is that gluon distribution $G(x,Q^2)$ increases when x decreases. But the rate of increment of gluon distribution calculated by our method is in general higher than those of other methods. The result of Kotikov and Parente method are the lowest. The result of two other methods are the intermediate ones between these two methods of which the result of Prytz method is higher than that of Bora and Choudhury method. Results from our method are closed to those from Prytz method. This is because Bora and Choudhury method is a crude approximation as they include only one term of the infinite series $x/(1-z)$, whereas we include all the infinite terms. So the other terms enhance the

contribution in our method. In our method, the first order approximation in Taylor expansion of $G\left(x/(1-z),Q^2\right)$ is used; that is only terms having first order differentiation $\partial G\left(x,Q^2\right)/\partial x$ is used.□

Chapter-6

GLUON DISTRIBUTION FUNCTION FROM DEUTERON STRUCTURE FUNCTION

We present some simple methods to find gluon distribution from analysis of deuteron structure function data at moderately low-x. Here we use the leading order GLDAP evolution equation and New Muon Collaboratio (NMC) deuteron structure function data to extract gluon distribution. We also compare our results with those of other authors. Here we present two alternative methods to relate gluon distribution $G(x,Q^2)$ with deuteron $F_2(x,Q^2)$ structure function and their differential coefficients with respect to $\ln Q^2$ and x, that is, $\partial F_2(x,Q^2)/\partial \ln Q^2$ and $\partial F_2(x,Q^2)/\partial x$ for fixed values of Q^2. We report for the first time some methods to extract gluon distribution from deuteron structure function data. Our methods are simpler with less approximation and more transparent. Of course, there exist some established methods [80] for extracting gluon distribution from data based on global fits. In these methods, momentum distribution and other constraints [81] are used to get gluon distribution. But our methods are based on the direct solution of QCD evolution equation which may be some good alternatives.

6.1. Theory:

In the leading order analysis, deuteron structure function is directly related to the singlet structure function [38]. On the otherhand, the differential coefficient of singlet structure function $F_2^S(x,Q^2)$ with respect to $\ln Q^2$, that is, $\partial F_2^S(x,Q^2)/\partial \ln Q^2$ has a relation with singlet structure function itself as well as gluon distribution function [38]. Thus it is possible to calculate gluon distribution from singlet structure function or ultimately from deuteron structure function also. The leading order GLDAP evolution equation for singlet structure function [38] is given by

$$\frac{\partial F_2^S(x,t)}{\partial t} - \frac{A_f}{t}\left[\{3+4\ln(1-x)\}F_2^S(x,t)+2\int_0^{1-x}\frac{dz}{z}\{(z^2-2z+2)F_2^S(x/1-z,\,t)\right.$$

$$\left.-2F_2^S(x,t)\}+\frac{3}{2}N_f\int_0^{1-x}(2z^2-2z+1)G(x/1-z,\,t)\,dz\right]=0, \qquad (6.1)$$

where, $t=\ln(Q^2/\Lambda^2)$ and $A_f=4/(33-2N_f)$, N_f being the number of flavours and Λ is the QCD cut off parameter. Now,

$$\frac{1}{1-z} = x\sum_{k=0}^{\infty} z^k = x + x\sum_{k=1}^{\infty} z^k . \qquad (6.2)$$

We have, $1-x>z>0 \Rightarrow |z|<1$ which implies that the expansion equation (6.2) is convergent. Now by the Taylor expansion [39] we get,

$$F_2^S\left(\frac{x}{1-z},t\right) \simeq F_2^S(x,t)+x\sum_{k=1}^{\infty} z^k \frac{\partial F_2^S(x,t)}{\partial x} \qquad (6.3)$$

and

$$G_2^S\left(\frac{x}{1-z},t\right) \simeq G_2^S(x,t)+x\sum_{k=1}^{\infty} z^k \frac{\partial G_2^S(x,t)}{\partial x} \qquad (6.4)$$

neglecting the higher order terms.

But as a matter of fact, we cannot neglect the higher order terms for singlet structure function or gluon distribution function as they may have some contribution. On the otherhand, it has been shown that this Taylor expansion method is successfully applied in calculating Q^2-evolution [35,36] or x-evolution [34] of structure function with excellent phenomenological success. Some authors [43,44] again applied this method to extract gluon distribution from proton structure function. It was suggested that [34], one possible reason for success of this method may be due to the simplification of QCD processes at low-x for momentum constraints.

Putting equations (6.3) and (6.4) in equation (6.1) and performing z-integrations we get,

$$\frac{\partial F_2^S(x,t)}{\partial t} - \frac{A_f}{t}\left[A_S(x)F_2^S(x,t) + B_S(x)G(x,t) + C_S(x) + \frac{\partial F_2^S(x,t)}{\partial x}\right.$$

$$\left. + D_S(x)\frac{\partial G(x,t)}{\partial x}\right] = 0, \qquad (6.5)$$

where,

$$A_S(x) = 3 + 4\ln(1-x) + 2\{(1-x)(-2+(1-x)/2)\},$$

$$B_S(x) = (3/2)N_f\{(1-x)(x+(2/3)(1-x)^2)\},$$

$$C_S(x) = 2x\{\ln(1/x) + (1-x)(1-(1-x)/2)\}$$

and

$$D_S(x) = (3/2)N_f\{\ln(1/x) - (1-x)(1+(2/3)(1-x)^2)\}.$$

Now, we can have two methods to extract gluon distributions:

First Method:

At very low-x limit, $x \to 0$, the functions $A_S(x)$, $C_S(x)$ and $D_S(x)$ become vanished and $B_S(x) = N_f$. Equation (6.5) then becomes simplified and we get,

$$\frac{\partial F_2^S(x,t)}{\partial t} - \frac{A_f}{t}.N_f\,G(x,t) = 0$$

$$\Rightarrow G(x,t) = \frac{t}{A_f N_f}.\frac{\partial F_2^S(x,t)}{\partial t}. \qquad (6.6)$$

Equation (6.6) is a very simple relation between gluon distribution function with the differential coefficient of singlet structure function with respect to t.

Second Method:

Recasting equation (6.5) we get,

$$G(x,t)+\frac{D_S(x)}{B_S(x)}.\frac{\partial G(x,t)}{\partial x}$$

$$=\frac{1}{A_f B_S(x)}.t.\frac{\partial F_2^S(x,t)}{\partial t}-\frac{A_S(x)}{B_S(x)}.F_2^S(x,t)-\frac{C_S(x)}{B_S(x)}.\frac{\partial F_2^S(x,t)}{\partial x}. \qquad (6.7)$$

Now $D_S(x)/B_S(x)$ is very small at low-x, $\lim_{x\to 0} D_S(x)/B_S(x)=0$. So, applying the Taylor expansion series we can write ,

$$G(x,t)+\frac{D_S(x)}{B_S(x)}.\frac{\partial G(x,t)}{\partial x}=G\left(x+\frac{D_S(x)}{B_S(x)},t\right).$$

Thus equation (6.7) gives,

$$G(x,'t)=K_1(x).t.\frac{\partial F_2^S(x,t)}{\partial t}+K_2(x)\frac{\partial F_2^S(x,t)}{\partial x}+K_3(x)F_2^S(x,t), \qquad (6.8)$$

where,

$$x'=x+\frac{D_S(x)}{B_S(x)} \quad , \quad K_1(x)=\frac{1}{A_f B_S} \ , \ K_2(x)=\frac{C_S(x)}{B_S(x)} \text{ and } K_3(x)=-\frac{A_S(x)}{B_S(x)} .$$

Equation (6.8) is also a simple relation between gluon distribution function with the differential coefficients of singlet structure function with respect to t and x, and with singlet structure function itself. If we try to combine the last two terms of equation (6.8), let us take common $K_3(x)$ from both the terms and then they reduce to

$$K_3(x)\left[F_2^S(x,t)+\frac{K_2(x)}{K_3(x)}.\frac{\partial F_2^S(x,t)}{\partial x}\right].$$

But $K_2(x)/K_3(x)$ is not small at low-x and therefore these two terms can not be combined to one as in the case of gluon by applying Taylor expansion series.

The relation between deuteron and singlet structure function at leading order [38] is

$$F_2^d(x,t)=\frac{5}{9}F_2^S(x,t)\Rightarrow F_2^S(x,t)=\frac{9}{5}F_2^d(x,t). \qquad (6.9)$$

Then we get,

$$\frac{\partial F_2^S(x,t)}{\partial t}=\frac{9}{5}.\frac{\partial F_2^d(x,t)}{\partial t} \qquad (6.10)$$

and

$$\frac{\partial F_2^S(x,t)}{\partial x} = \frac{9}{5}.\frac{\partial F_2^d(x,t)}{\partial x}. \tag{6.11}$$

Putting equations (6.9), (6.10), and (6.11) in equations (6.6) and (6.8), we get respectively,

$$G(x,t) = \frac{9\,t}{5\,A_f N_f}.\frac{\partial F_2^d(x,t)}{\partial t} \tag{6.12}$$

and

$$G(x',t) = \frac{9}{5}\left[K_1(x).t.\frac{\partial F_2^d(x,t)}{\partial t} + K_2(x)\frac{\partial F_2^d(x,t)}{\partial x} + K_3(x)F_2^d(x,t)\right], \tag{6.13}$$

which are our main results. From these equations it is seen that if we have deuteron structure function and their differential coefficients with respect to t and x at any x for a fixed value of $t = t_0$, we can calculate gluon distribution function at x (first method) from equation (6.12) or at $x' = x + D_S(x)/B_S(x)$ (second method) from equation (6.13) as a leading order analysis.

For analysis of our result, we use NMC 15–parameter function [73,82] which parametrized their data for proton and deuteron structure functions for Q^2 – values from $0.5\,GeV^2$ to $75\,GeV^2$ and low-x values from 0.002 to 0.6. This parametrization can also well describe the SLAC [78] and BCDMS [79] data, and Fermilab [83] low-x data. The function used to describe proton as well as deuteron data is given by,

$$F_2(x,Q^2) = A(x)\left[\frac{\ln(Q^2/\Lambda^2)}{\ln(Q_0^2/\Lambda^2)}\right]^{B(x)}.\left[1+\frac{C(x)}{Q^2}\right]. \tag{6.14}$$

Here,

$Q_0^2 = 20\,GeV^2$, $\Lambda = 0.250\ GeV$,

$A(x) = x^{a_1}(1-x)^{a_2}\{a_3 + a_4(1-x) + a_5(1-x)^2 + a_6(1-x)^3 + a_7(1-x)^4\}$,

$B(x) = b_1 + b_2 x + b_3/(x+b_4)$

and

$$C(x) = c_1 x + c_2 x^2 + c_3 x^3 + c_4 x^4,$$

where, a_1, a_2, a_3, a_4, a_5, a_6, a_7, b_1, b_2, b_3, b_4, c_1, c_2, c_3 and c_4 are the 15–parameters used to fit the data. Actually two different sets of these parameters are used to describe proton and deuteron structure functions in the same equation (equation (6.14)). Thus for the respective sets of parameters, equation (6.14) gives the deuteron structure function as

$$F_2^d(x,t) = A(x).\left[\frac{t}{t_0}\right]^{B(x)}.\left[1+\frac{e^{-t}}{\Lambda^2}.C(x)\right], \tag{6.15}$$

where, $t = \ln\left(Q^2/\Lambda^2\right)$ and $t_0 = \ln\left(Q_0^{\,2}/\Lambda^2\right)$. Differentiating $F_2^d(x,t)$ with respect to t and x, we get respectively,

$$\frac{\partial F_2^d(x,t)}{\partial t} = \left(\frac{B(x)}{t}-1\right)F_2^d(x,t) + A(x)\left(\frac{t}{t_0}\right)^{B(x)} \tag{6.16}$$

and

$$\frac{\partial F_2^d(x,t)}{\partial x} = \left[\left(\frac{t}{t_0}\right).\frac{\partial A(x)}{\partial x} + A(x)\left(\frac{t}{t_0}\right)^{B(x)}.\ln\left(\frac{t}{t_0}\right).\frac{\partial B(x)}{\partial x}\right]$$

$$\times\left[1+\frac{e^{-t}}{\Lambda^2}.C(x)\right] + A(x)\left(\frac{t}{t_0}\right)^{B(x)}.\left[\frac{e^{-t}}{\Lambda^2}.\frac{\partial C(x)}{\partial x}\right], \tag{6.17}$$

where,

$$\frac{\partial A(x)}{\partial x} = \left(\frac{a_1}{x}-\frac{a_2}{1-x}\right)A(x) - x^{a_1}(1-x)^{a_2}.\left\{a_4 + 2a_5(1-x) + 3a_6(1-x)^2 + 4a_7(1-x)^3\right\},$$

$$\frac{\partial B(x)}{\partial x} = b_2 - \frac{b_3}{(x+b_4)^2}$$

and

$$\frac{\partial C(x)}{\partial x} = c_1 + 2c_2 x + 3c_3 x^2 + 4c_4 x^3.$$

Now putting equations (6.15), (6.16) and (6.17) in equations (6.12) and (6.13), we can easily calculate gluon distributions at x (first method) or $x' = x + D_S(x)/B_S(x)$ (second method) respectively.

6.2. Result and Discussion:

The NMC 15–parameter function [73,82] parametrizes the NMC data for Q^2 – values from 0.5 GeV^2 to 75 GeV^2 and low-x values from 0.002 to 0.6 which also well describes the SLAC [78], BCDMS [79] and Fermilab [83] low-x data. As the data range of x we use is moderately low, we will restrict our analysis values from10 GeV^2 to 60 GeV^2 and low-x values from 0.1 to 0.001. We can not extend our analysis to HERA low-x region [42] due to lack of deuteron F_2 structure function data in that region.

In Fig.6.1(a) and Fig.6.1(b) gluon distributions obtained by our first method (equation (6.12)) from NMC deuteron parametrization from the 15–parameter function are represented at $Q^2 = 10\ GeV^2$ and 60 GeV^2 respectively. The middle lines are the results without considering the error. The upper and the lower lines are the results with parameter values by adding and subtracting the statistical and systematic errors with the middle values respectively. It has been seen that the middle lines almost coincide with the upper ones. We calculate gluon distributions for x-values from 10^{-1} to 10^{-3} for both $Q^2 = 10\ GeV^2$ and $Q^2 = 60\ GeV^2$. In both the cases, $G(x,Q^2)$ values increases when x decreases as expected, but $G(x,Q^2)$ is higher in $Q^2 = 60\ GeV^2$ than in $Q^2 = 10\ GeV^2$ for same x, especially in lower-x side. Moreover, rate of increment of $G(x,Q^2)$ is very high from $x = 10^{-1}$ to 10^{-2}. But the rate decreases to some extent to lower-x region.

Exactly in the similar way, in Fig.6.2(a) and Fig.6.2(b) gluon distribution obtained by our second method (equation (6.13))from NMC deuteron parametrization from the 15 – parameter function are presented at $Q^2 = 10\ GeV^2$ and 60 GeV^2 respectively.

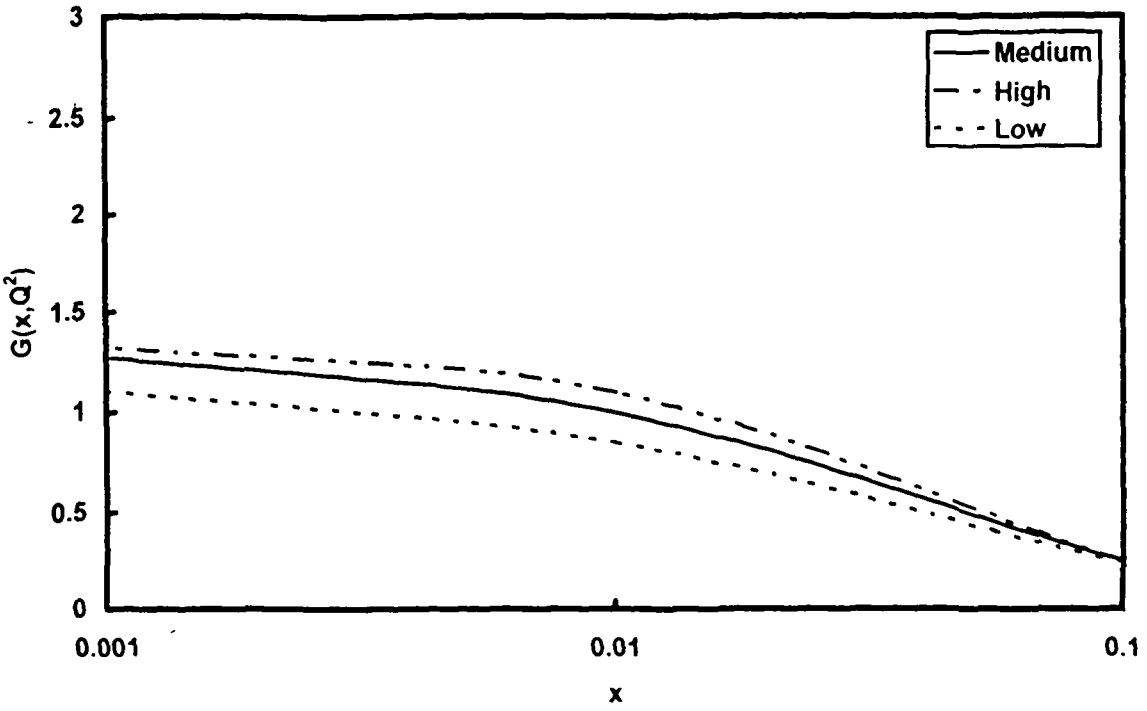

Fig.6.1(a) Gluon distributions obtained by our first method (equation (6 12)) from NMC deuteron parametrization from the 15-parameter function at Q^2 = 10 GeV^2 The middle line is the result without considering the error The upper and lower lines are the results with parameter values by adding and subtracting the statistical and systematic errors with the middle values respectively

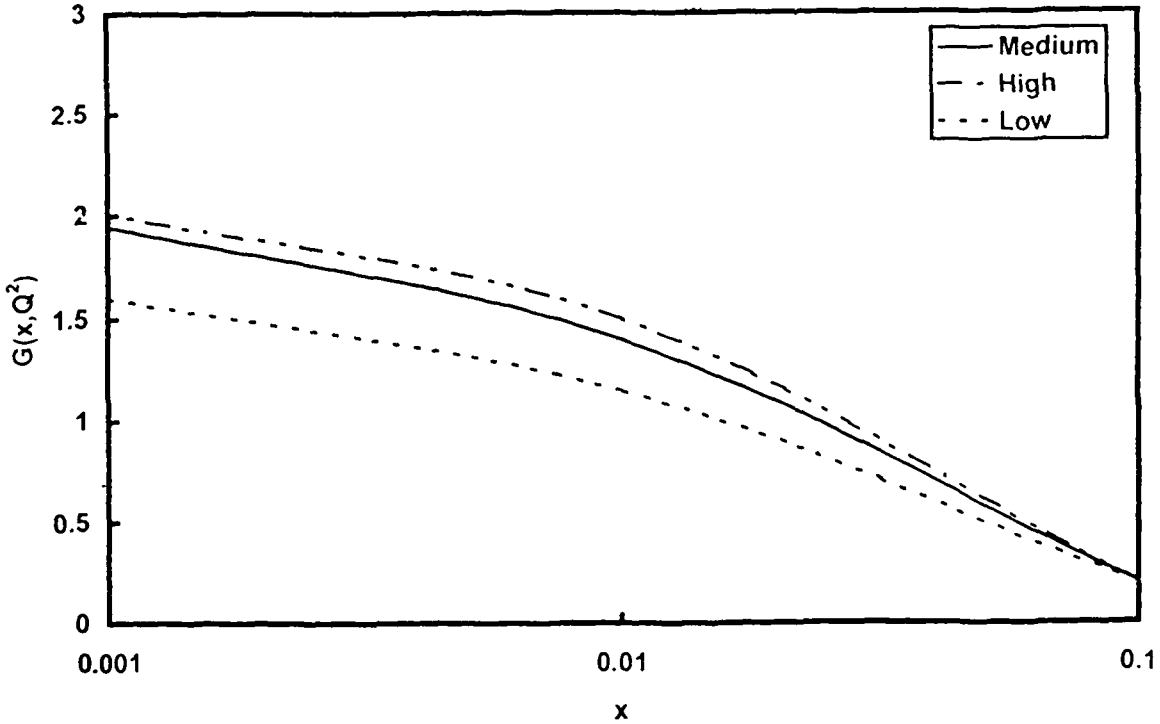

Fig.6.1(b) Gluon distributions obtained by our first method (equation (6 12)) from NMC deuteron parametrization from the 15- parameter function at Q^2 = 60 GeV^2 The middle line is the result without considering the error The upper and lower lines are the results with parameter values by adding and subtracting the statistical and systematic errors with the middle values respectively

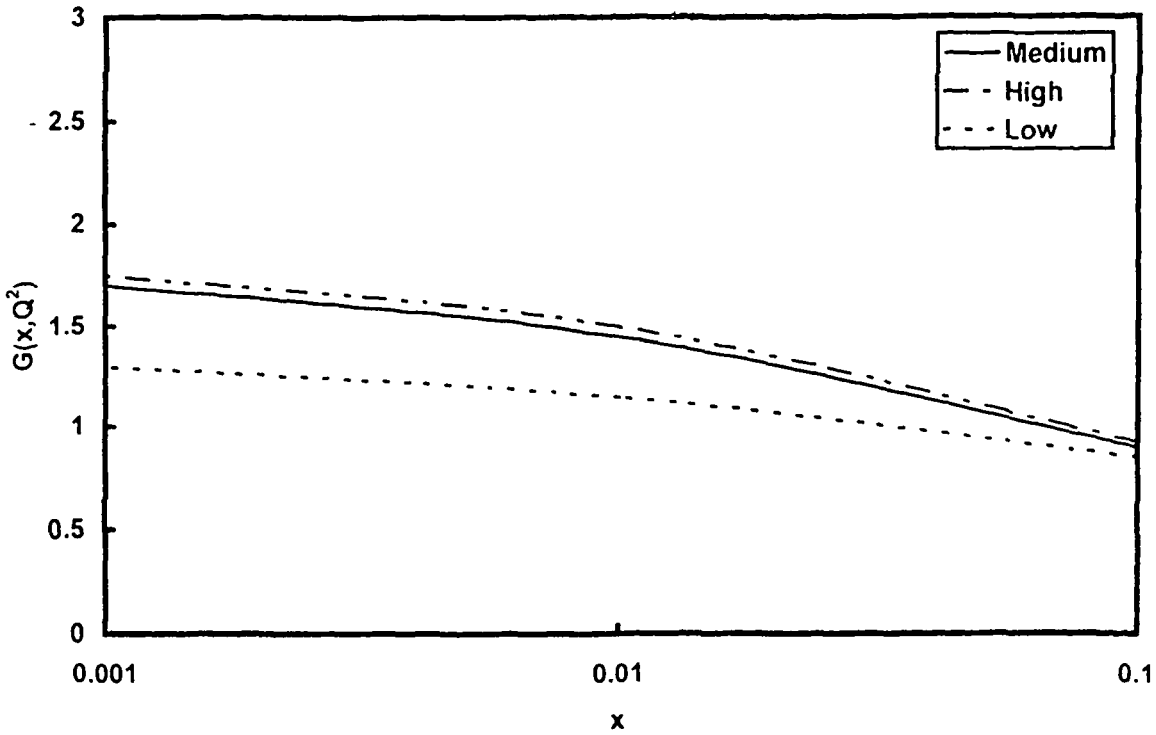

Fig.6.2(a) Same result as in Fig 6 1(a) by our second method (equation (6 13))

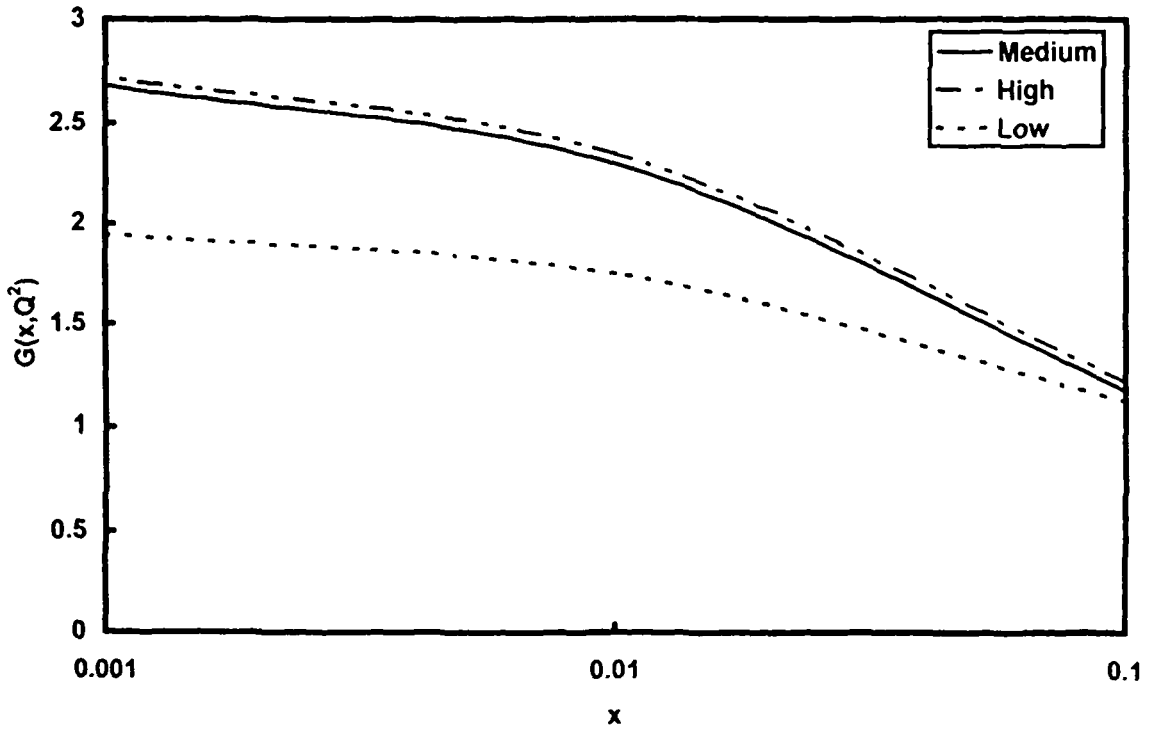

Fig.6.2(b) Same as in Fig 6 1(b) by our second method (equation (6 13))

All discussion are exactly same as for Fig.6.1(a) and Fig.6.1(b) respectively. But overall values of $G(x,Q^2)$ are higher in second method than in first one for any value of x. For example, $G(x,Q^2)$ medium values are almost 20% and 25% higher in second method than in first method for $Q^2 = 10\ GeV^2$ and $Q^2 = 60\ GeV^2$ respectively at $x = 10^{-3}$. This is because in our first method, we apply very low-x approximation and neglected $A_S(x)$, $C_S(x)$ and $D_S(x)$ in equation (6.5) as they are vanishingly small at very low-x to obtain equation (6.6) and then equation (6.12). On the otherhand, in our second method, we do not apply such approximation and automatically the contributions from these functions have been included in equation (6.13).

In Fig.6.3, comparison of gluon distributions obtained by Bora and Choudhury method (BC), Prytz method , our first method (SM 1st) and our second method (SM 2nd) is presented for middle values only for $Q^2 = 60\ GeV^2$.

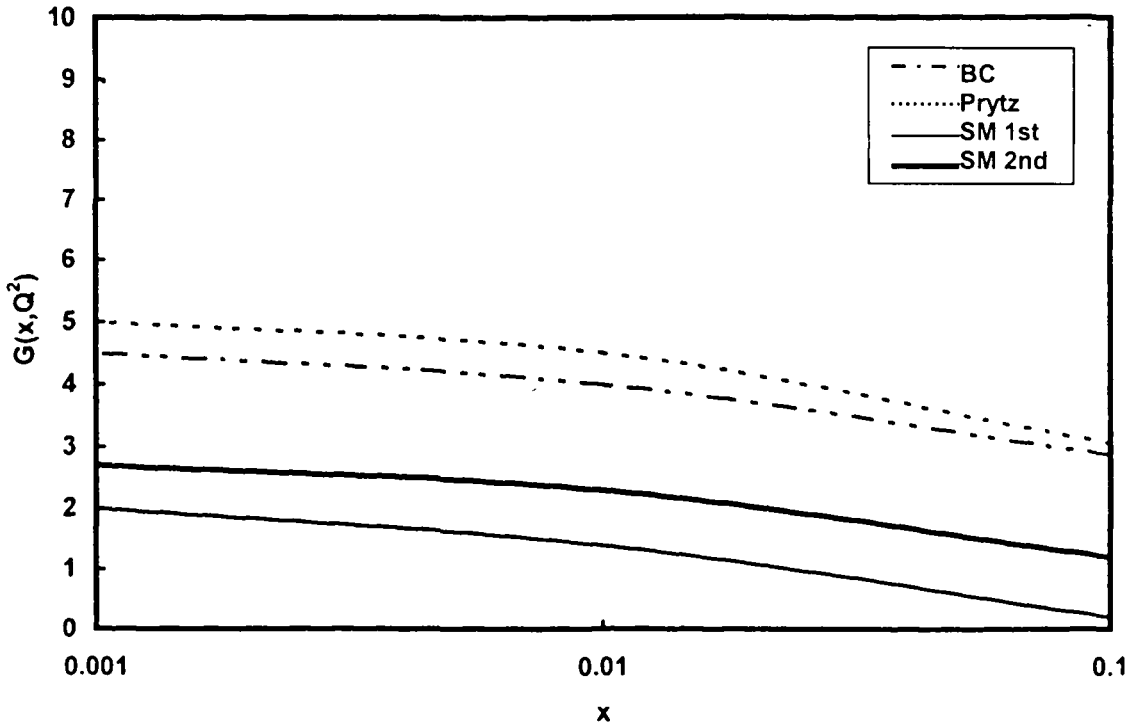

Fig.6.3: Comparison of gluon distributions obtained by Bora and Choudhury method (BC), Prytz method, our first method (SM 1st) and our second method (SM 2nd) for middle values only at $Q^2 = 60\ GeV^2$.

Values are higher for the result of other authors with proton structure function data than of ours with deuteron structure function data. This is actually due to the fact that the scaling violations of deuteron structure functions $F_2^d(x,Q^2)$ with respect to $\ln Q^2$ are themselves considerably less than those of HERA proton data due to H1 [71] and ZEUS [72,84] collaborations and these scaling violations are directly proportional to gluon distributions in the formulas used by Bora and Choudhury and Prytz to calculate gluon distributions. These HERA proton data covers x- values up to at least $\simeq 10^{-4}$ in comparison with those of NMC data which covers up to $\simeq 10^{-3}$ only. Gluon distribution increases as x decreases due to all the authors as expected from QCD analysis. Moreover, gluon distribution by our first method is lowest and Prytz method is the highest for a particular low-x.

6.3. Conclusion:

In this chapter, we present for the first time a method to extract gluon distribution from the measurement of moderately low-x deuteron structure functions and their differential coefficient with respect to $\ln Q^2$ and x. Here we use leading order GLDAP evolution equation to relate gluon distribution function with moderately low-x structure function or differential coefficient. In our analysis, we use only NMC deuteron data parametrization by a 15- parameter function. We find gluon distribution from deuteron also increases when x decreases as in the case of proton as usual. We can not compare our result of NMC data with other because low-x deuteron data is not sufficiently available. Moreover, no other work to calculate gluon distribution function from deuteron data has been so far reported. But we compare our result with gluon distributions due to Bora and Choudhury and Prytz calculated from low-x proton data. We see that our result is to some extent less, as differential coefficient of deuteron structure function with respect to $\ln Q^2$ is much less than of proton structure function.□

Chapter-7

REGGE BEHAVIOUR AND GLUON DISTRIBUTION FUNCTION

In this chapter, we present a method to find the gluon distribution function from proton structure function data at low-x assuming the Regge behaviour of gluon distribution function at this limit. We use the leading order GLDAP evolution equation in our analysis and compare our result with those of other authors. We also discuss the limitations of Taylor expansion method in extracting gluon distribution from quark structure function used by those authors.

7.1. Theory:

The gluon distribution at low-x can be obtained by analysing the longitudinal structure function [45,52]. Similarly it is also shown that, this distribution can be calculated from the proton structure function and its scaling violation [43,44]. Moreover, in reference [84] we see that, it is also possible to calculate gluon distribution from deuteron structure function and its scaling violation. The basic idea lies on the fact that the scaling violation of quark structure function arises at low-x from the gluon distribution alone and does not depend on the quark distribution. Neglecting the quark, GLDAP evolution equation for four flavour [43,44] gives,

$$\frac{\partial F_2(x,Q^2)}{\partial \ln Q^2} = \frac{5\alpha_s}{9\pi}\int_0^{1-x} G\left(\frac{x}{(1-x)},Q^2\right)P_{qg}(z)dz \ , \qquad (7.1)$$

where the leading order splitting function is

$$P_{qg}(z) = z^2 + (1-z)^2$$

and α_s is the strong coupling constant. Now let $1-z = y \Rightarrow dz = -dy$. Again $z = 0 \Rightarrow 0 \Rightarrow y = 1$ and $z = 1-x \Rightarrow y = x$. Therefore equation (7.1) gives,

$$\frac{\partial F_2(x,Q^2)}{\partial \ln Q^2} = \frac{5\alpha_s}{9\pi}\int_x^1 G(x/z,Q^2).(2z^2-2z+1)\,dz\ . \qquad (7.2)$$

Now, let us consider the Regge behaviour of gluon distribution [4],

$$G(x,Q^2) = C.x^{-\lambda(Q^2)}, \qquad (7.3)$$

where, C is a constant and $\lambda(Q^2)$ is the intercept. The Regge behaviour of the structure function $F_2(x)$ in the large$-Q^2$ region reflects itself in the low-x behaviour of the quark and the antiquark distributions. Thus the Regge behaviour of the sea quark and antiquark distribution for low-x is given by $q_{sea}(x) \sim x^{-\alpha_P}$ corresponds to a pomeron exchange of intercept $\alpha_P = 1$. But the valence quark distribution for low-x given by $q_{val}(x) \sim x^{-\alpha_R}$ corresponds to a reggeon exchange of intercept $\alpha_R = 1/2$. Since the same processes lead to gluon and sea quarks distributions in the nucleon, we expect $G(x) \simeq 1/x$. The x-dependence of the proton densities given above is aften assumed at moderate - Q^2.

Applying equation (7.3) in equation (7.2) we get,

$$\frac{\partial F_2(x,Q^2)}{\partial \ln Q^2} = \frac{5\alpha_S}{9\pi}.C.\int_0^1 x^{-\lambda(Q^2)}.z^{\lambda(Q^2)}.(2z^2-2z+1)\,dz\ . \qquad (7.4)$$

For fixed Q^2, let $K(x) = \partial F_2(x,Q^2)/\partial \ln Q^2$ and $A = 5\alpha_s/(9\pi)$. Thus equation (7.4) gives,

$$K(x) = A.C.x^{-\lambda(Q^2)}\int_x^1 (2z^{\lambda+2} - 2z^{\lambda+1} + z^{\lambda})\,dz\ . \qquad (7.5)$$

Taking logarithm and rearranging the terms, equation (7.5) gives

$$\lambda = \frac{1}{\ln x}\left[\ln\left\{\frac{2}{\lambda+3}\left(1-x^{\lambda+3}\right)-\frac{2}{\lambda+2}\left(1-x^{\lambda+2}\right)+\frac{1}{\lambda+1}\left(1-x^{\lambda+1}\right)\right\}\right]$$

$$-\frac{1}{\ln x}\left[\ln\left\{\frac{K(x)}{(A.C)}\right\}\right] \tag{7.6}$$

$$\Rightarrow \lambda - \phi(\lambda) = 0, \tag{7.7}$$

where, $\lambda \equiv \lambda(Q^2)$ and $\phi(\lambda)$ represents the right hand side of equation (7.6). Now equation (7.7) has been solved numerically using iteration method [85] to calculate the values of $\lambda(Q^2)$ for different x-values for a fixed value of Q^2. Scaling violation of structure function $K(x) = \partial F_2(x,Q^2)/\partial \ln Q^2$ and strong coupling constant at leading order α_s are experimental inputs. C is the only free parameter in our calculation. After calculation of $\lambda(Q^2)$, we can calculate $G(x,Q^2)$ from equation (7.3) for different values of the free parameter C and compare our result with those due to other authors.

Now, let us discuss the limitation of Taylor expansion method in this regards. Applying Taylor expansion in equation (7.1) we get

$$G\left(\frac{x}{1-z},Q^2\right) = G\left(x + x\sum_{k=1}^{\infty} z^k, Q^2\right)$$

$$= G\left(x, Q^2 + x\sum_{k=1}^{\infty} z^k \frac{\partial G(x,Q^2)}{\partial x}\right) + \frac{1}{2}x^2\left(\sum_{k=1}^{\infty} z^k\right)^2 \frac{\partial^2 G(x,Q^2)}{\partial x^2} + O(x^3), \tag{7.8}$$

where, $O(x^3)$ are the higher order terms. Here we have $1-x > z > 0 \Rightarrow |z| < 1$, which implies that $x/(1-z) = x\sum_{k=0}^{\infty} z^k$ is convergent. In the previous methods, either the terms beyond second order [43,44] or beyond first order [48,84] derivatives of x are neglected in the expansion series equation (7.8). But in actual practice, this type of simplification is may not be possible because the contributions from the higher order terms can not be neglected due to the singular behaviour of gluon distribution.

There are some other methods also which are not based on Taylor expansion. Kotikov and Parente presented [49] a set of formulae to extract gluon distribution from quark structure function and its scaling violation at low-x in the next-to-leading order approximation. A different method for the determination of gluon distribution at low values of x has been proposed by Ellis, Kunszt and Levin [53] based on the solution of GLDAP evolution equations in the moment space up to next-to-next-to leading order.

7.2. Result and Discussion:

We use HERA data taken by H1 [71] and ZEUS [72] collaborations where the values of $\partial F_2(x,Q^2)/\partial \ln Q^2$ are listed for a range of x values at $Q^2 = 20\ GeV^2$. The recent HERA data is parametrized by H1 [74] and ZEUS [75] collaborations by some appropriate functions and we calculate $\partial F_2(x,Q^2)/\partial \ln Q^2$ at $Q^2 = 20\ GeV^2$ for those functions also. We also use parametrizations of the recent New Muon Collaboration (NMC) [73,82] proton structure function data from a 15- parameter function from which also we calculate $\partial F_2(x,Q^2)/\partial \ln Q^2$ at $40\ GeV^2$. Now we apply the values of $\partial F_2(x,Q^2)/\partial \ln Q^2$ in equation (7.7) to calculate λ numerically by iteration method [85] and hence gluon distribution function $G(x,Q^2)$ for $C = 1$ and $C = 100$. For our calculation, strong coupling constant α_s was taken from a next-to-leading order fit [76] to F_2 data which yield $\alpha_s = 0.180 \pm 0.008$ at $Q^2 = 50\ GeV^2$ corresponding to $\Lambda^{(4)}_{\overline{MS}} = 0.263 \pm 0.042\ GeV$. This value of α_s agrees with one given by Particle Data Group [77]. But in our practical calculations, we neglect the errors of α_s and Λ, which are rather small. We compare our result with those of other authors discussed in the theory as well as with the recent MRST global fit [80].

In Fig.7.1(a) – Fig.7.1(d), we present gluon distributions $G(x)$ for different low-x values from NMC proton data parametrization [73,82] at $Q^2 = 40, 60, 80$ and $100\ GeV^2$ respectively for $C = 1$ and $C = 100$.

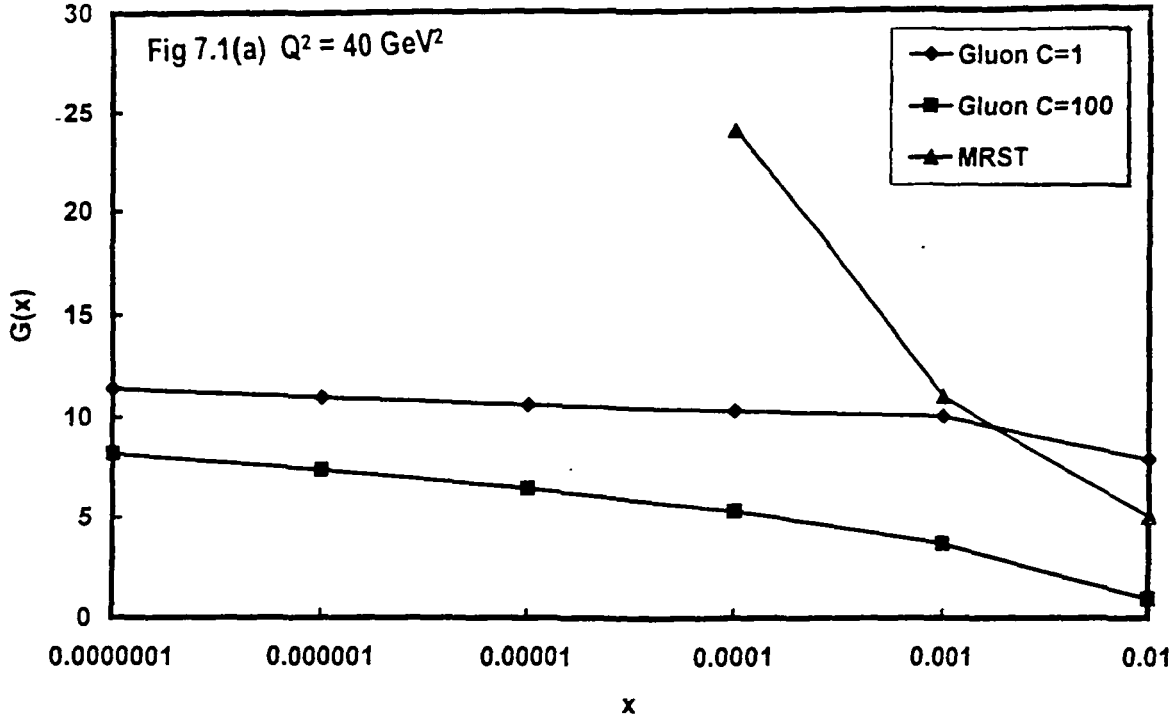

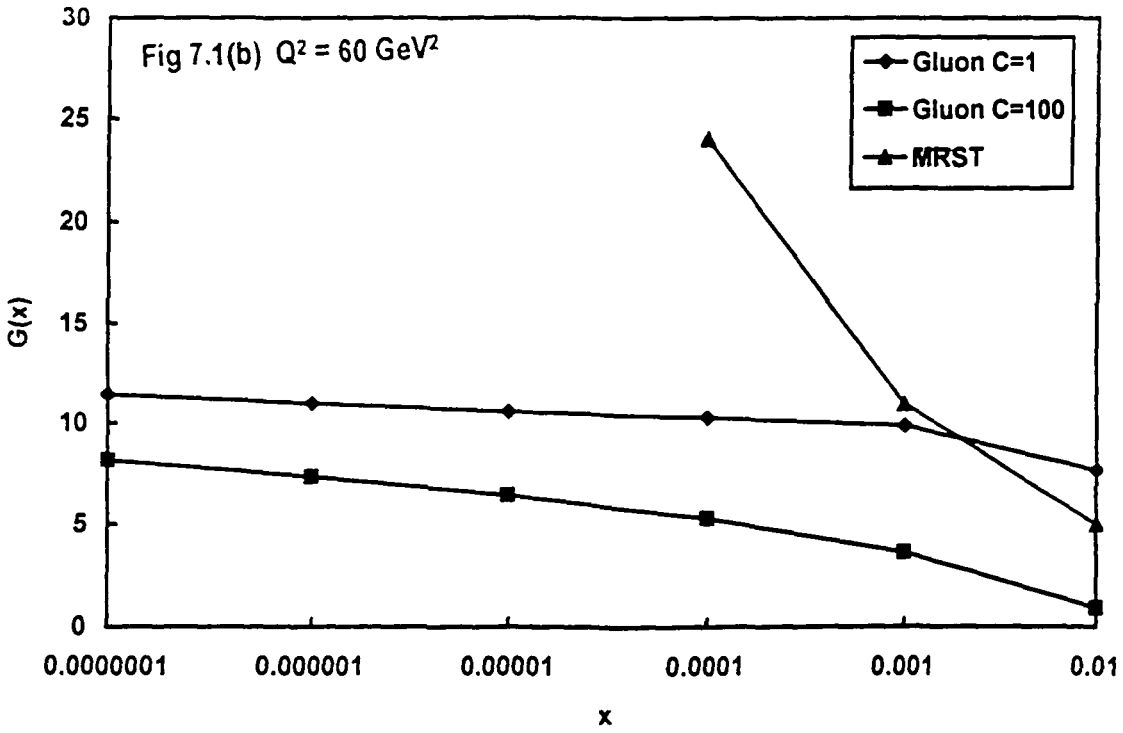

From the figures, it is seen that results are almost same for all Q^2 values and $G(x)$ slowly increase when x decreases logarithmically. We also present the MRST global

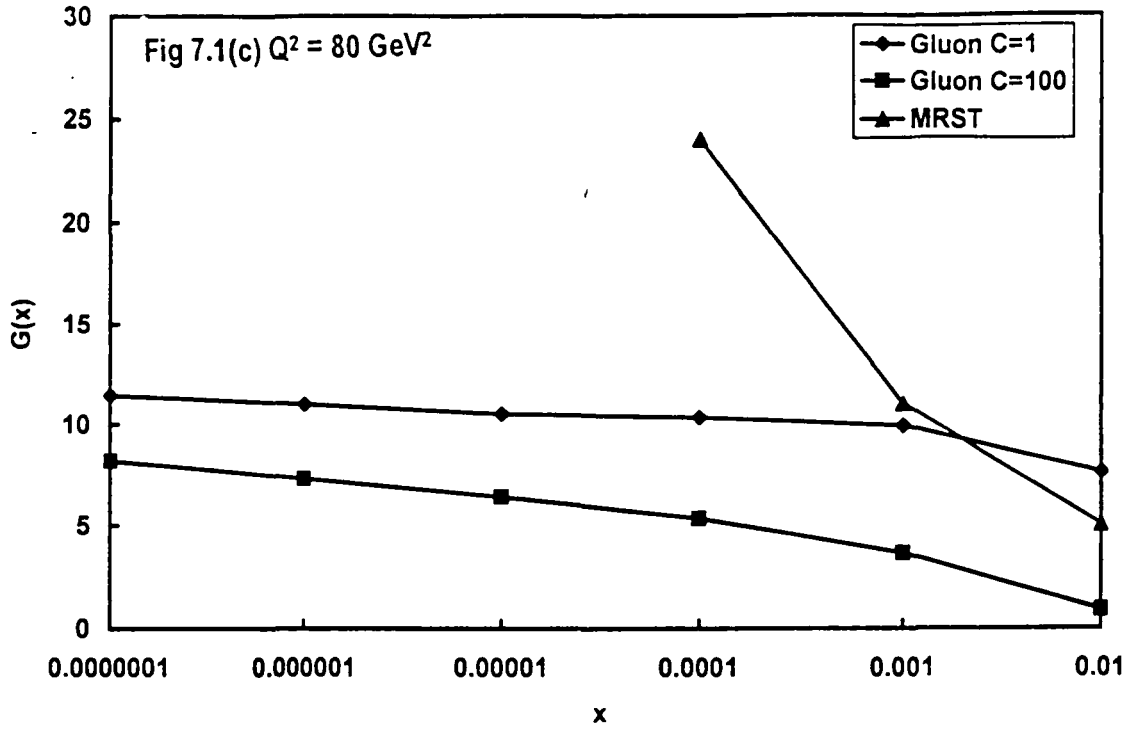

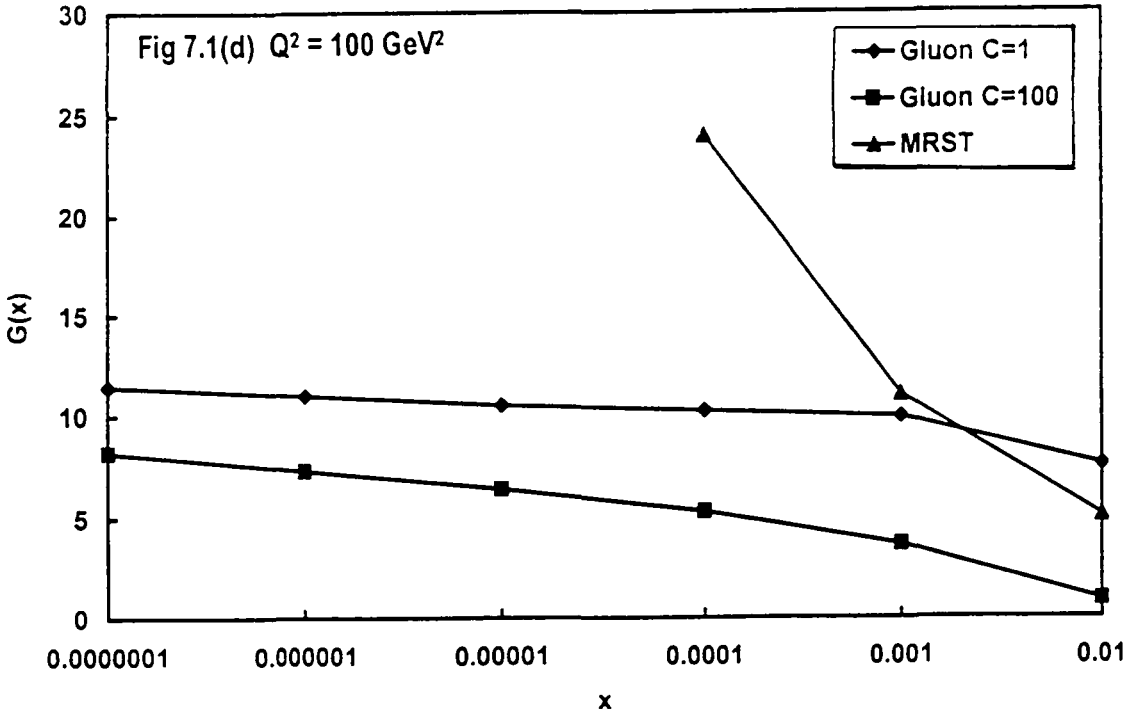

Fig.7.1(a) - Fig.7.1(d): Gluon distribution G(x) by our method from NMC proton parametrization [73,82] at Q^2 = 40, 60 and 100 GeV^2 respectively with C = 1 and C = 100. In the same figures we include a global fit by MRST [80].

fit [80] result, but its rate of increment is much higher. The values of $G(x)$ are higher for $C = 1$ than those for $C = 100$ for a particular value of low-x.

In Fig.7.2(a) and Fig.7.2(b), we present the gluon distributions $G(x)$ for different

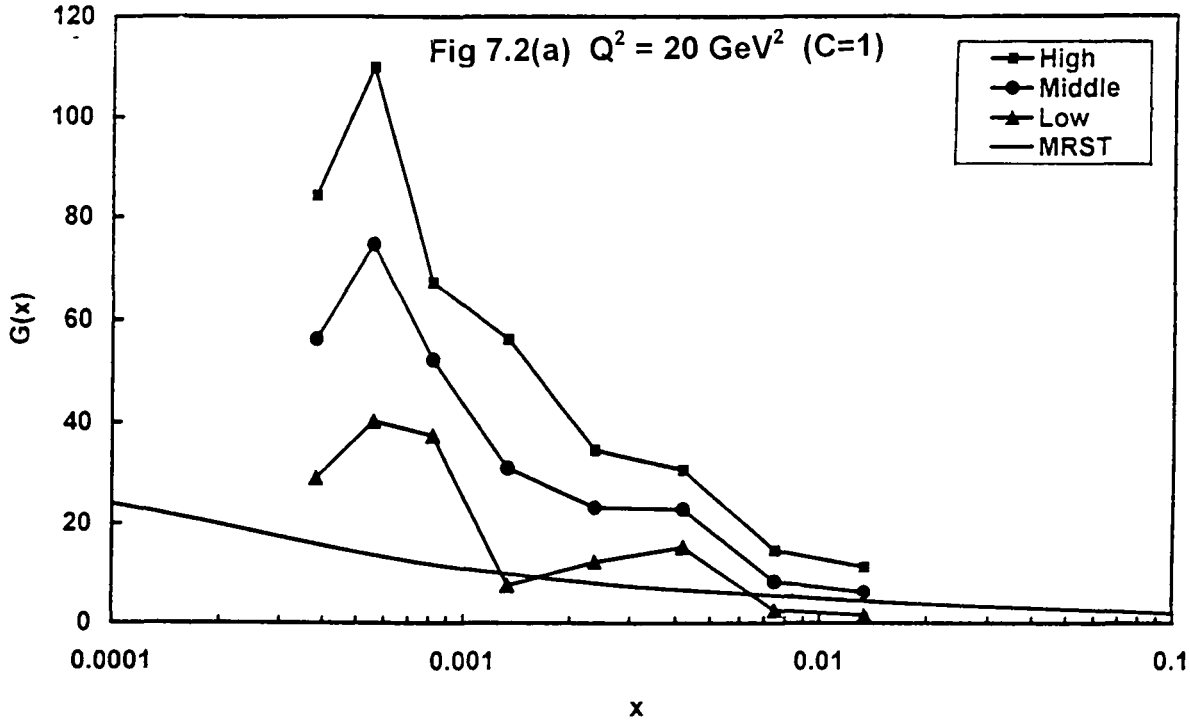

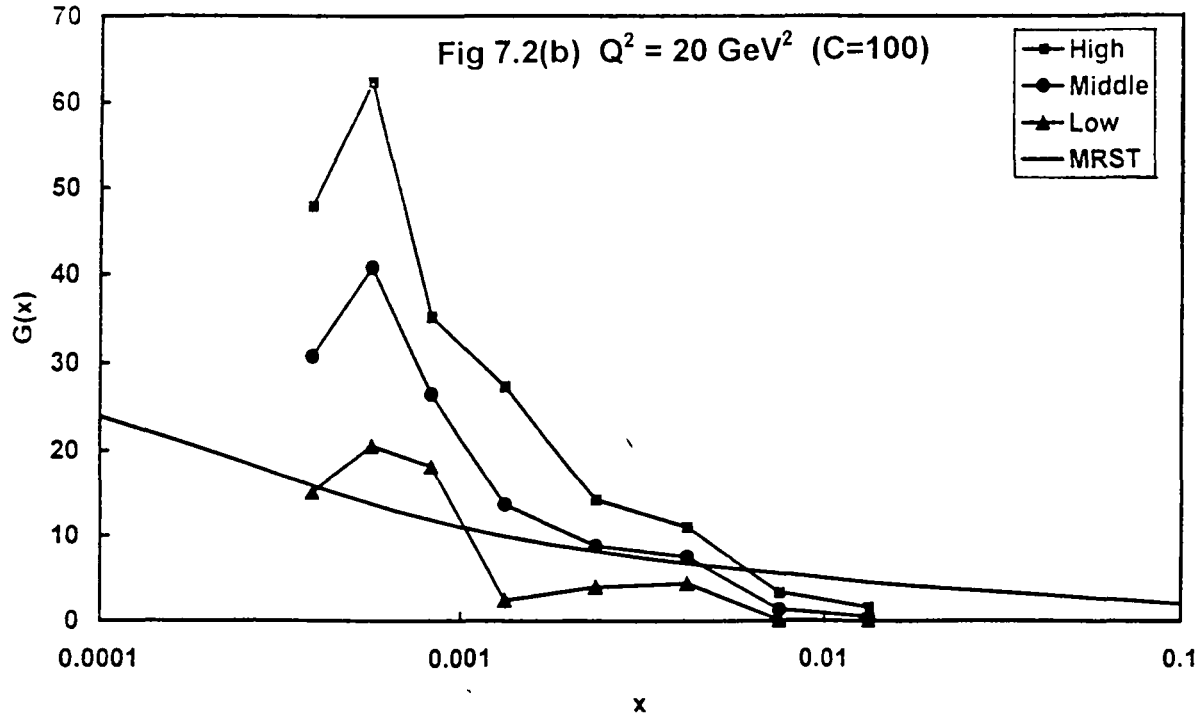

Fig.7.2(a) - Fig.7.2(b) Gluon distribution G(x) by our method from H1 HERA proton data [71] at Q^2 = 20 GeV^2 with C = 1 and C = 100 respectively Here we present the results for the data (i)without considering the error (middle), (ii)adding algebraically statistical and systematic errors (high) and (iii)subtracting algebraically statistical and systematic errors (low) In the same figures we include a global fit by MRST [80]

low-x values from H1 HERA proton data [71] at $Q^2 = 20\,GeV^2$ for $C = 1$ and $C = 100$ respectively. The middle line in each figure is the result without considering any error in the data. The upper and lower lines are the results with data adding and subtracting systematic and statistical errors with the middle values respectively. As usual, gluon distribution $G(x)$ increases when x decreases, but the whole system of lines in the graphs shifts towards the lower $G(x)$ values when we change from $C = 1$ to $C = 100$. In the same graphs, we also present the $G(x)$ values for MRST global fit [80] which is also increasing towards low-x values, but with somewhat lesser rate. But for $C = 100$ our $G(x)$ values come in the range of this fit.

In Fig.7.3, we present gluon distributions $G(x)$ for H1 HERA proton parametrization [74] at $Q^2 = 20\,GeV^2$ for different low-x values for $C = 1$ and $C = 100$ respectively

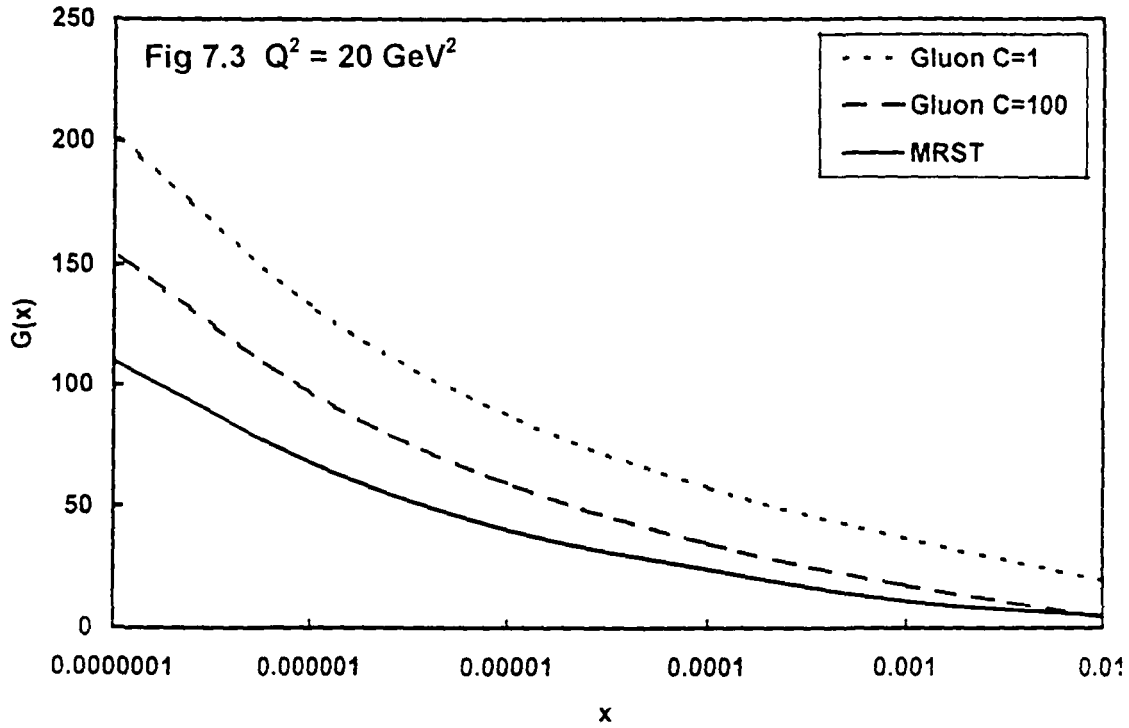

Fig.7.3 Gluon distribution G(x) by our method from H1 HERA proton data parametrization [74]] at Q^2 = 20 GeV² with C = 1 and C = 100 In the same figures we include a global fit by MRST [80]

Gluon distribution $G(x)$ increases when x decreases, but the line in the graph shifts towards the lower $G(x)$ values when we change from $C = 1$ to $C = 100$. In the same

figure, we present $G(x)$ values for MRST global fit [80] which also increases towards low-x values with somewhat lesser rate. But for $C = 100$ our $G(x)$ values are closer to this fit.

In Fig.7.4(a) and Fig.7.4(b), we present gluon distributions $G(x)$ for ZEUS HERA proton data [72] at $Q^2 = 20\ GeV^2$ for different low-x values for $C = 1$ and $C = 100$ respectively. The descriptions and the results are same as H1 HERA data [71] depicted in Fig.7.2(a) and Fig.7.2(b) respectively.

In Fig.7.5, we present gluon distributions $G(x)$ for ZEUS HERA proton parametrization [72] at $Q^2 = 20\ GeV^2$ for different low-x values for $C = 1$ and $C = 100$. The descriptions and the results are same as H1 HERA parametrization [74] depicted in Fig.7.3.

In Fig.7.6, we present the values of λ (Lambda) for H1 HERA proton data [71] for low, middle and high values of them at $Q^2 = 20\ GeV^2$ for different low-x values for $C = 1$ and $C = 100$. For $C = 1$, all the graphs are almost parallel and λ - values tend to $\simeq 0.5$ at low-x. For $C = 100$, for all the graphs, λ -values tend to $\simeq 0.0$ from some negative values at low-x.

In Fig.7.7, we present the λ -values for ZEUS HERA proton data [72] in the same way as in Fig.7.6. For $C = 1$, for all the graphs, λ -values tend to $\simeq 0.5$, as we approach lower-x from some slightly higher values in comparatively higher x. On the other hand, for $C = 100$, for all the graphs, λ -values tend to $\simeq -0.1$, as we approach lower x from some slightly lower negative values in comparatively higher x.

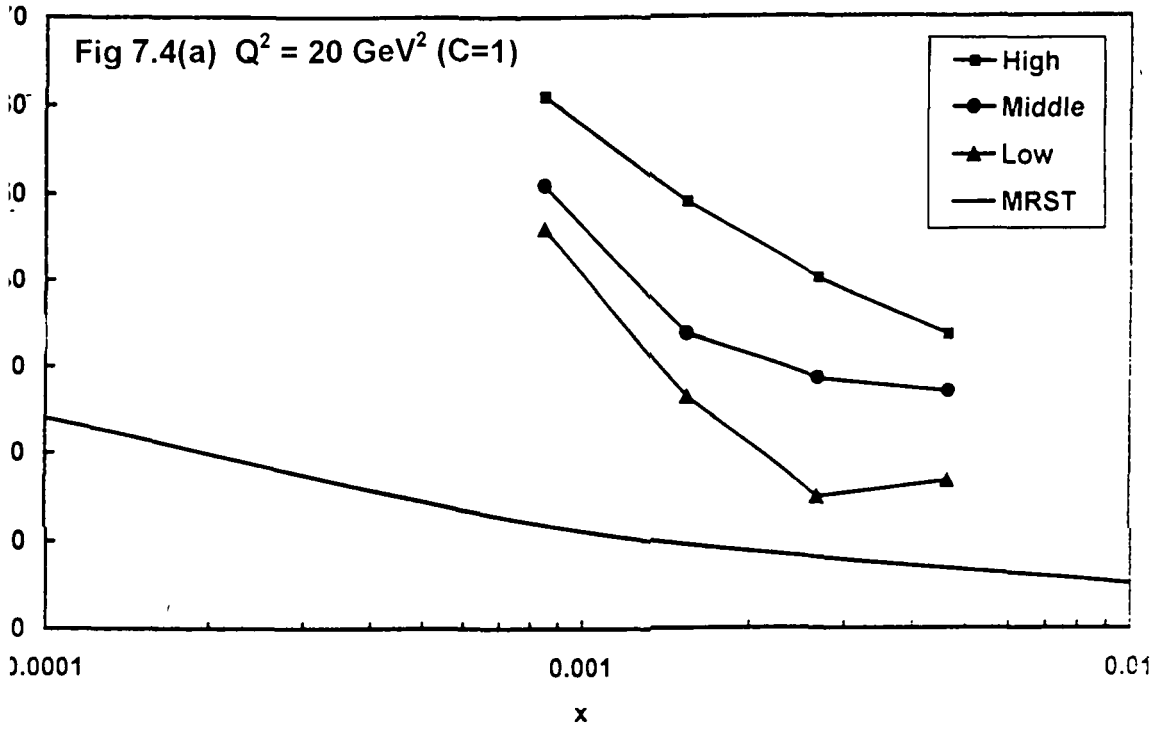

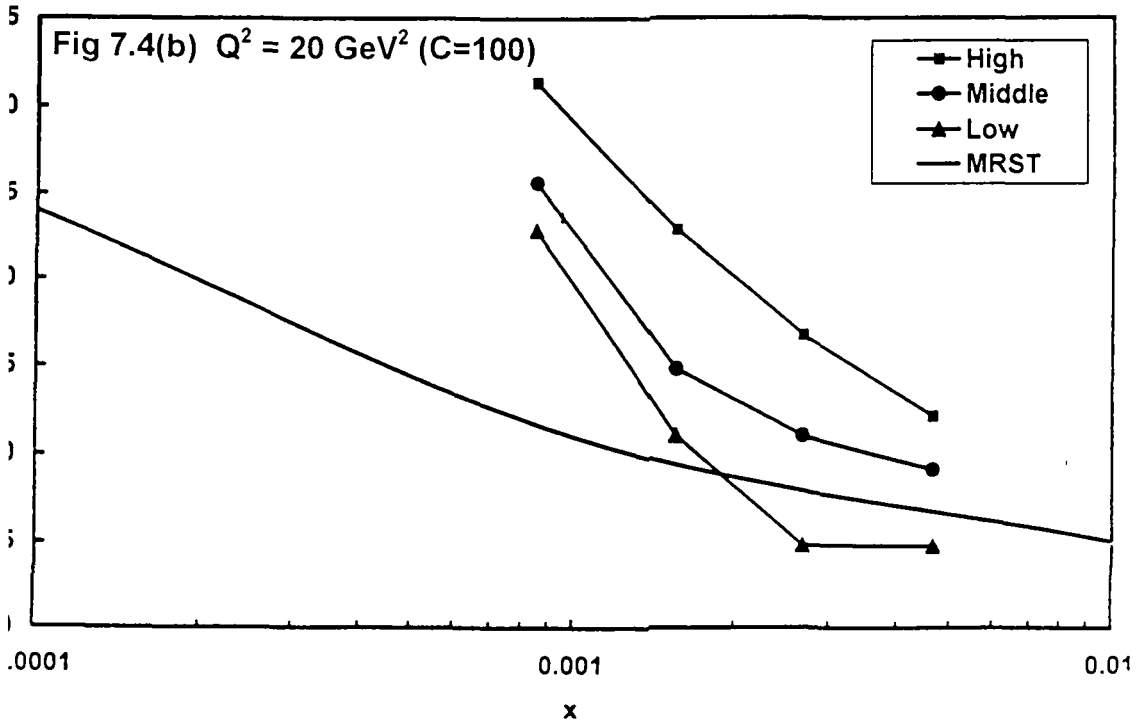

Fig.7.4(a) - Fig.7.4(b): Same results as in Fig.7.2(a) - 7.2(b) respectively from ZEUS HERA proton data [72] at Q^2 = 20 GeV^2

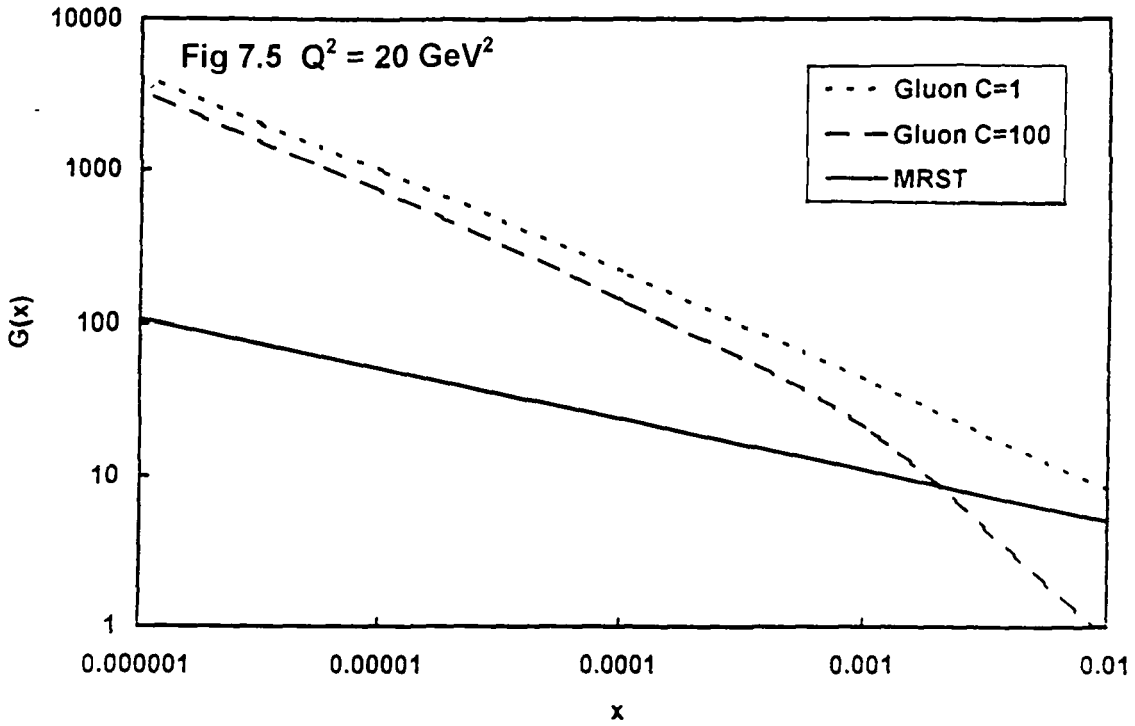

Fig.7.5 Same results in Fig 7 3 from ZEUS HERA proton data parametrization [72] at Q^2 = 20 GeV^2

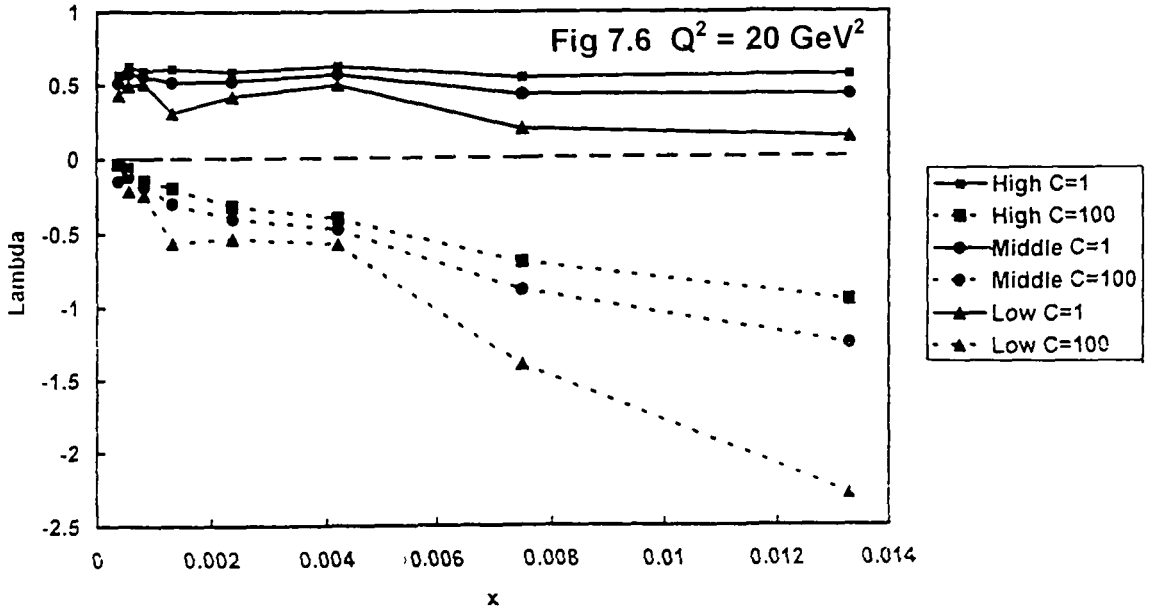

Fig.7.6 λ - values by our method from H1 HERA proton data [71] at Q^2 = 20 GeV^2 with C = 1 and C = 100 Here we present the results for the data (i)without considering the error (middle), (ii)adding algebraically statistical and systematic errors (high) and (iii)substracting algebraically statistical and systematic errors (low)

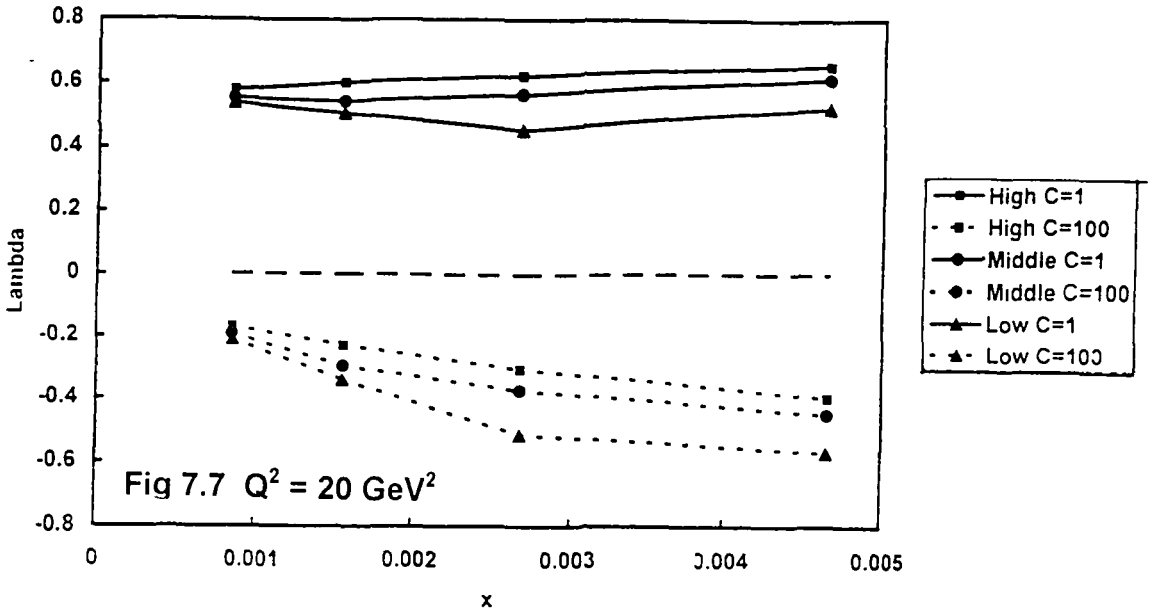

Fig.7.7 Same results as in Fig 7 6 from ZEUS HERA proton data [72] at Q^2 = 20 GeV^2

In Fig.7.8, we compare our results for HERA H1 data (middle value only) [71] at $Q^2 = 20\ GeV^2$ for $C = 1$ and $C = 100$ with those of Bora and Choudhury [48] and

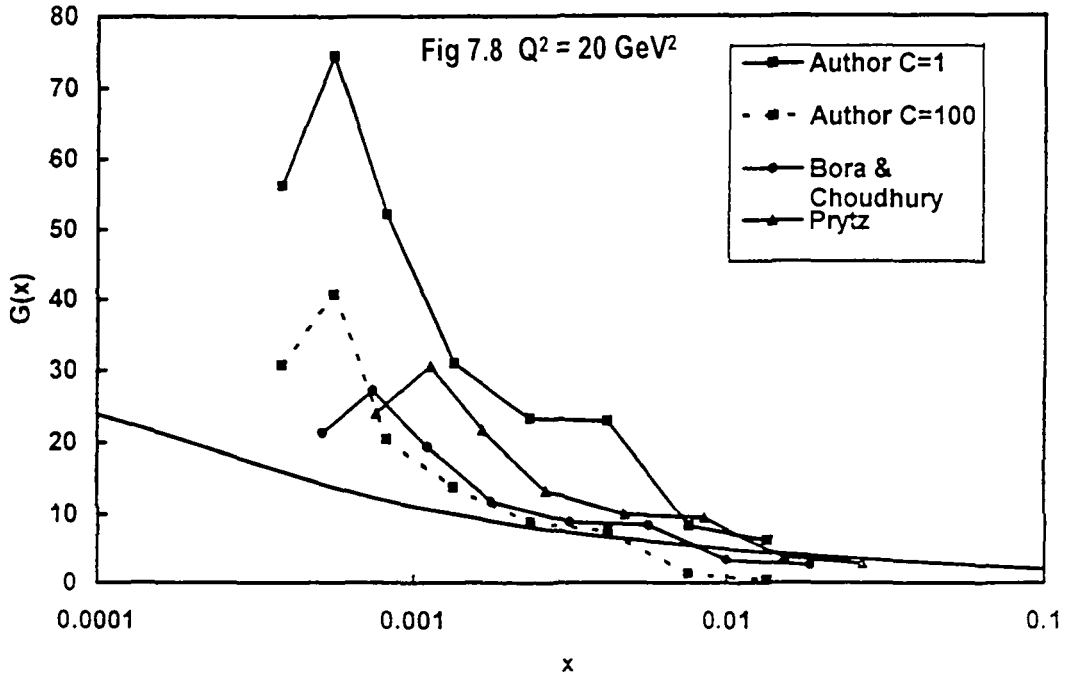

Fig.7.8 Comparison of gluon distribution G(x) from H1 HERA proton data [71] for middle values only by our method for C = 1 and C = 100 at Q^2 = 20 GeV^2 with those by other methods due to Bora and Choudhury [48] and Prytz [43,44] In the same figures, we include a global fit MRST [80]

Prytz [43,44] In the same figure, we also present the result for MRST global fit [80] For all the cases, gluon distribution $G(x)$ increases when x decreases, but with different rates The rates of increment in our result for $C = 1$ is highest and in MRST is lowest But our result with $C = 100$ is very close with that of Bora and Choudhury, and also inside the range of MRST

Lastly, we include a simple FORTRAN programme for calculation of λ from the scaling violation of structure function given in Programme-1

Programme-1

```
C       GLUON DISTRIBUTION FROM SCALING VIOLATION OF PROTON DATA
05      REAL Y, K, X, A, PHIX1, PHIX2, PHIX3, PHIX, P, AB, G
10      PRINT*, "Y=?"
15      READ*, Y
20      PRINT*, "K=?"
25      READ*, K
30      PRINT*, "C=?"
35      READ*, C
40      X= 3
45      ALPH= 118
50      PI=3 1416
55      A=(5 *ALPH)/(9 *PI)
56      PHIX1=2 /(X+3 )*(1 -y**(X+3 ))-2 /(X+2 )*(1 -Y**(X+2 ))
57      PHIX2=1 /(X+1 )*(1 -Y**(X+1 ))
58      PHIX3=ALOG(K/(A*C))
60      PHIX=1 /ALOG(Y)*(ALOG(PHIX1+PHIX2)-PHIX3)
65      P=X-PHIX
70      AB=ABS(P)
75      G=C*(Y**(-PHIX))
80      IF (AB  LT  00000001) THEN
                PRINT*, C, Y, PHIX, G
        GOTO 10
        ELSE
                X=PHIX
        ENDIF
        GOTO 56
85      END
```

7.3. Conclusion:

In this method, we present an alternative method than other methods to extract gluon distribution $G(x,Q^2)$ from the scaling violation of proton structure function $\partial F_2(x)/\partial \ln Q^2$ at low-x. We compare our result with those of other methods due to Bora and Choudhury [48] and Prytz [43,44] and with a global fit due to MRST [80]. Gluon distribution will increase as usual when x decreases with different rates for the different values of the parameter $C = 1$ and $C = 100$. But our graph with $C = 100$ is very close to that due to Bora and Choudhury and the global fit due to MRST. We discussed the limitation of Taylor expansion method [85] in calculating gluon distribution from scaling violation of structure function at low-x. Prytz in both leading order [43] and next-to-leading order [44], and Bora and Choudhury in leading order [48] used this method to extract gluon distribution from scaling violation of structure function at low-x in a slightly different way. But all the authors neglected the higher order terms in the Taylor expansion series which is not a very good approximation for a singular behaviour of gluon distribution at low-x, because the contributions from the higher order terms in the series are not negligible. Sarma and Medhi [84] used this method in some improved way with less number of approximation, yet this basic approximation of neglecting higher order terms in the expansion series could not be avoided. On the other hand, in Kotikov and Parente method [49,52] also, authors approximated their result by neglecting some higher order terms. Moreover, their method is to some extent complicated. Again Ellis, Kunszt and Levin method [53] is also not much developed than other methods. In the present method, of course, we use a free parameter C, yet the other ambiguities due to the approximation of the Taylor expansion series can be avoided. Moreover, our method is very simple one and the computer programme can calculate gluon distribution immediately when we put the value of scaling violation from experiment. □

Chapter-8

CONCLUSION

In Chapter-1, we present a brief introduction of the problem. Gluon distribution function at low-x is important for understanding of inner structure of hadrons and for examination of Quantum Chromodynamics (QCD), the underlying dynamics of quarks and gluons. Moreover, gluons are expected to be dominant in the low-x region. In addition to that, gluon distributions are important inputs in many high energy processes. On the otherhand, gluon distribution cannot be measured directly from experiment. It is therefore, important to measure gluon distribution function indirectly from quark structure function. In this chapter, we discuss about structure of matter, deep inelastic scattering, structure function, low-x physics, evolution equations and screening corrections.

In Chapter-2, we discuss about the Taylor expansion method. Here we discuss the Taylor's theorem and application of it in determination of t and x evolution of structure function at low-x.

In Chapter-3, we discuss briefly the various methods to extract the gluon distribution function from quark structure function due to other authors. Accordingly, here, we discuss about Bora and Choudhury method, Kotikov and Prente method, and Ellis, Kunszt and Levin method. We also discuss about the differences and limitations of these methods.

In the Chapter-4, we discuss briefly about the t and x evolutions of gluon structure function at low-x. We consider the leading order GLDAP evolution equation for gluon distribution function and extract gluon distribution by solving it by applying Taylor expansion method. We compare our methods with some standard parametrizations and make predictions for the HERA range.

In Chapter-5, we discuss briefly about the gluon distribution function at low-x from proton structure function. Here we present an alternative method than other methods to extract gluon distribution from proton structure function. Here HERA data measured by H1 and ZEUS collaborations are used and we compare our results with those of other methods.

In Chapter-6, we discuss briefly about the gluon distribution function at low-x from deuteron structure function. Here we present for the first time a method to extract gluon distribution from deuteron structure function. We use NMC deuteron data parametrization by a 15-parameter function and compare our result with those of other methods.

In Chapter-7, we discuss briefly about the Regge behaviour of structure function and gluon distribution at low-x. Here we present an alternative method to extract gluon distribution method in this regard. We also compare our results with those of other methods and global fits.

In all the result from other methods as well as global fits, it is seen that gluon distribution function increases when x decreases and Q^2 increases for fixed values of Q^2 and x respectively. But the rates are different in different methods. It is observed that the results from our methods also generally comparable with those of other methods and they can easily be considered as some viable alternative to other methods. On the otherhand, our methods are mathematically more simpler with less number of approximations.

In extracting gluon distribution function from quark structure function, we use here only leading order GLDAP evolution equation. But we can extend it to next-to-leading or higher orders as subsequent works. Moreover, we are mostly restricted up to the term containing the first order derivations of the Taylor expansion series we used. We can try to include the terms containing higher order derivatives for lesser approximation. We neglected contributions from quarks in obtaining gluon

distribution function from proton structure function as well as by using Regge behaviour. But we can test the result by including the contribution from quarks also. Lastly, we may try to apply Taylor expansion method in longitudinal structure function and thereby extract gluon distribution function from it.□

REFERENCE

[1] E. M. Levin and M. G. Ryskin: Phys. Rep. 189 (1990) 267.

[2] L. V. Gribov, E. M. Levin and M. G. Ryskin: Phys. Rep. 100 (1983)1; E. M. Levin: "Orsay lectures on Low-x Deep Inelastic Scattering," LPTHE preprint, Orsay 91/02 (1991).

[3] P. V. Landshoff and J. C. Polkinghorne: Phys. Rep. 5 (1972) 1.

[4] P. D. B. Collins: "An Introduction to Regge Theory and High Energy Physics", Cambridge Univ. Press, Cambridge (1977).

[5] G. V. Frolov, V. N. Gribov and L. N. Lipatov: Phys. Lett. B 31 (1970) 34.

[6] A. R. White: Nucl. Phys. B 159 (1979) 77.

[7] J. Bartels: Nucl. Phys. B 151 (1979) 293; Acta Phys. Polon. B 11 (1980) 281.

[8] Ya. Ya. Balitskij and L. N. Lipatov: Yad. Fiz. 28 (1978) 1597; Sov. J. Nucl. Phys. 28 (1978) 822.

[9] J. B. Bronzan and R. L. Sugar: Phys. Rev. D 17 (1978) 585.

[10] L. N. Lipatov and L. Szymanowski: Warsaw INR report I B J / 11 / UW / 80 (1980).

[11] E. M. Levin and M. G. Ryskin: Talk presented at the "Topical Workshop on the Small-x Behaviour of Deep Inelastic Scattering Structure Functions in QCD", DESY, Humburg, May 1990, Nucl. Phys. B (Proc. Suppl.) 18 C (1990) 92.

[12] T. Jaroszewicz: Acta Phys. Polon. B 11(1980) 965; Phys. Lett. B 116 (1982) 291.

[13] L. N. Lipatov: in "Perturbative QCD" (World Scientific) ed. A. H. Mueller (1989) 411; L. N. Lipatov: Yad. Fiz. 23 (1976) 642; Sov. J. Phys. 23 (1976) 338.

[14] H. Cheng and T. T. Wu: Phys. Rev. Lett. 24 (1969) 1456.

[15] M. Foissart: Phys. Rev. 123 (1961) 1053; A. Martin: Z. Phys. C 15 (1982) 185.

[16] G. Altarelli and G. Parisi: Nucl. Phys. B 126 (1977) 298.

[17] Yu. L. Dokshitzer, D. I. Dyakonov and S. I. Troyan: Phys. Rep. 58 (1980) 265.

[18] G. Altarelli: Phys. Rep. 81 (1982) 1.

[19] E. Reya: Phys. Rep. 69 (1981) 195.

[20] E. A. Kuraev, L.N. Lipatov and V. S. Fadin: Zh. Eh. Eksp. Teor. Fiz. 72 (1977) 373; Sov. Phys. JETP 45 (1977) 199.

[21] M. Ciafaloni: Nucl. Phys. B 296 (1988) 49.

[22] S. Catani, F. Fiorani and G. Marchesini: Phys. Lett. B 234 (1990) 339; Nucl. Phys. B 336 (1990) 18.

[23] J. Kwiecinski: Z. Phys. C 29 (1985) 561.

[24] J. L. Cardy: Phys. Lett. B 53 (1974) 355; Nucl. Phys. B 93 (1975) 525.

[25] L. N. Lipatov: Sov. JETP 63 (1986) 904.

[26] J. Collins and J. Kwiecinski: Nucl. Phys. B 316 (1989) 307.

[27] J. Kwiecinski: Z. Phys. C 29 (1985) 147.

[28] M. Krawczyk: Talk presented at the "Topical Workshop on the Small-x Behaviour of Deep Inelastic Scattering Structure Function *in QCD*", DESY, Hamburg, May 1990, Nucl. Phys. B *(Proc. Suppl.)* 18 C (1990) 64; K. Charchula and M. Krawczyk: DEYS Preprint 90-122.

[29] G. Marchesini and B. R. Webber: Nucl. Phys. B 349 (1991) 617.

[30] A. H. Mueller and J. Qiu: Nucl. Phys. B 268 (1986) 427.

[31] L. V. Gribov, E. M. Levin and M. G. Ryskin: Nucl. Phys. B 188 (1981) 155; Sov. Phys. JETP 53 (1981) 1113.

[32] S. C. Malik, S. Arora: "Mathematical Analysis", Wiley Eastern Ltd. (1995).

[33] R. K. Ghosh, K. C. Maity: "An Introduction to Analysis of Differential Calculus", Part-I, Books and Allied (P) Ltd., Cacutta, India, (1998).

[34] J. K. Sarma, D. K. Choudhury, G. K. Medhi: Phys. Lett. B 403 (1997) 139.

[35] D. K. Choudhury and A. Saikia: Pramana- J. Phys. 29 (1987) 385; 33 (1989) 359; 34 (1990) 85; 38 (1992) 313.

[36] D. K. Choudhury and J. K. Sarma, Praman-J. Phys. 38 (1992) 481; 39 (1992) 273.

[37] D. K. Choudhury, G. K. Medhi and J. K. Sarma: Gau. Univ. J. Sc. (1998) 39-53.

[38] L. F. Abbot, W. B. Atwood and R. M. Barnett: Phys. Rev. D 22 (1980) 582.

[39] I. S. Granshteyn and I. M. Ryzhik: "Tables of Integrals, Series and Products," ed. Alen Jeffrey, Academic Press, New York (1970).

[40] I. Sneddon: "Elements of Partial Differential Equations," Mc. Graw Hill, New York (1957).

[41] F. J. Yudurain: "Quantum Chromodynamics," Sringer-Verlag, NewYork (1983).

[42] W. Buchmuller and G. Ingleman: eds., Proc. Workshop "Physics at HERA," Hamburg (1991).

[43] K. Prytz : Phys. Lett. B 311 (1993) 286.

[44] K. Prytz : Phys. Lett. B 332 (1994) 393.

[45] A. M. Copper-Sarkar et. al. : Z. Phys. C 39 (1988) 281.

[46] E. G. Floratos et. al. : Nucl. Phys. B 192 (1981) 417.

[47] W. Furmanski and R. Petronzio: Phys. Lett. B 97 (1980) 437.

[48] K. Bora and D. K. Choudhury: Phys. Lett. B 354 (1995) 151.

[49] A. V. Kotikov and G. Parente : Phys. Lett. B 379 (1996) 195.

[50] A. D. Martin, W. J. Stirling and R. G. Roberts: Phys. Lett. B 354 (1995) 155.

[51] R. D. Ball and S. Forte: Phys. Lett. B 335 (1994) 77; B 336 (1994) 77.

[52] A.V. Kotikov: Phys. Rev. D 49 (1994) 5746.

[53] R. K. Ellis, Z. Kunszt and E. M. Levin: Nucl. Phys. B 420 (1994) 517.

[54] J. K. Sarma and B. Das, Phys. Lett. B 126 (1993) 323.

[55] L. A. Pipes and L. R. Harvill: "Applied Mathematics for Engineers and Physicists", Mc Graw-Hill Book Company, New York (1970).

[56] E. Eichten, Z. Hinchliffe, K. Lane and C. Quigg: Rev. Mod. Phys. 56 (1984) 579.

[57] H. Aramowicz et. al.: CDHS'83, Z. Phys. C 17 (1983) 283.

[58] M. Diemoz, F. Ferroni, E. Longo and G. Martinelli: Z. Phys. C 39 (1988) 21.

[59] M. Diemoz, F. Ferroni and E. Long: Phys. Rep. 130 (1986) 293.

[60] D. Alasia et. al. : BEBC'85, Z. Phys. C 28 (1985) 321.

[61] D. Mac Farlane et. al. : CCFRR'83, Fermilab-Pub. 83, 108, Exp. (1983).

[62] F. Bergsma et. al. : CHARM'83, Phys. Lett. B123 (1983) 269.

[63] A. Ali and J. Bartels: eds., Proceeding of the "DESY Topical Meeting in the Small-x Behaviour of Deep Inelastic Structure Function in QCD", 1990, North Holland (1991).

[64] V. T. Kim and M. G. Ryskin: DEYS 91-064, June, (1991).

[65] E. M. Levin and M. G. Ryskin: Phys. Rep. 189 (1990) 267.

[66] V. N. Gribov and L. N. Lipatov: Sov. J. Nucl. Phys. 15 (1972) 438.

[67] Yu. L. Dokshitzer: Sov. Phys. JETP 46 (1977) 641.

[68] J. Kwiecinski, A. D. Martin and P. J. Sutton: Durham Preprint, DTP/ 91/92, April, (1991).

[69] S. Catani, F. Fiorani, G. Marchesini and G. Oriani : Cavendish Lab. Preprint, HEP-90-24 (1990).

[70] J. Kwiecinski, A. D. Martin, R. G. Roberts and W. J. Stirling: KMRS, Phys. Rev. D 42 (1990) 3645.

[71] S. Aid et. al.: H1 Collaboration, Phys. Lett. B 354 (1995) 494.

[72] M. Derrick et. al. : ZEUS Collaboration, Phys. Lett. B 364 (1995) 576.

[73] M. Arneodo et. al., NMC, Phys. Lett. B 364 (1995) 107.

[74] T. Ahmed et. al.: H1 Collaboration, Nucl. Phys. B 439 (1995) 471.

[75] M. Derrick et. al. : ZEUS Collaboration, DEYS 94-143, August (1994).

[76] M. Virchaux and A. Milsztajn: Phys. Lett. B 274 (1992) 221.

[77] L. Montanet et. al. : Particle Data Group, Phys. Rev. (1994)1173.

[78] L. W. Whitlow et. al.: Phys. Lett. B 282 (1992) 475.

[79] A. C. Benvenuti et. al. : BCDMS Collaboration, Phys. Lett. B 233 (1989) 485.

[80] A. D. Martin et. al. : hep-ph 9803445 (1998).

[81] F. Halzen and A. D. Martin: "Quarks and Lepton, An Introductory Course in Modern Particle Physics", John Wiley and Sons, New York (1990).

[82] M. Arneodo et. al. : NMC, Phys. Lett. B 483 (1997) 3.

[83] A. V. Kotikov; Ph. D. Thesis, Harvard University (1995).

[84] J. K. Sarma and G. K. Medhi: T U / THEP-1 / 98 (1998).

[85] J. B. Scarborough, "Numerical Mathematical Analysis", John Hopkins Press, Baltimore (1996).□

PUBLICATION AND PRESENTATION

Publications:

1. Taylor expansion method and gluon distribution from structure function data at low-x: the leading order analysis, J. of Assam Sc. Soc. 41 (2000) 54- 69.
   Co-author: J. K. Sarma.

2. Regge behaviour of structure function and gluon distribution at low-x in leading order, Euro. Phys. J. C 16 (2000) 481- 487.
   Co-author: J. K. Sarma.

3. Regge behaviour of structure function and gluon distribution at low-x in leading order, Proc. Annual Tech. Session, Assam Sc. Soc., Guwahati, India, February 23, 1999 (1999)1- 21.
   Co-author: J. K. Sarma.

4. t and x-Evolution of gluon structure functions at low-x, Gauhati Univ. J. of Sc., Golden Jubilee Vol. (1998) 39 - 53.
   Co-authors: J. K. Sarma and D. K. Choudhury.

5. x-Distribution of deuteron structure function at low-x, Phys. Lett. B 403 (1997) 139-144.
   Co-authors: J. K. Sarma and D. K. Choudhury.

6. The gluon distribution $G(x,Q^2)$ as a function of $dF_2(x,Q^2)/d\ln Q^2$ at low-x; the leading order analysis, Proc. of 8th Manipur Sc. Cong., Imphal, India, February 26 to 29, 1997 (1997).
   Co-author: J. K. Sarma.

Presentations:

1. Regge behaviour of structure function and gluon distribution at low-x in leading order, Annual Tech. Session, Assam Sc. Soc., Guwahati, India, February 23, 1999.

ADDENDA

Journal of Asssam Science Society, Vol.41 No 1, March 2000 pp 54 69

Taylor Expansion Method and Gluon Distribution from Structure Function Data at Low-x : the Leading Order Analysis

J. K. Sarma[1]

Department of Physics, Tezpur University, Napaam, Tezpur-784028, Assam, India

and

G. K. Medhi

Department of Physics, Birjhora Mahavidyalaya, Bongaingaon - 783380, Assam, India

ABSTRACT

We present a method to find the gluon distribution from proton and deuteron structure function data at low-x. Here we use the leading order (LO) Altarelli-Parisi (AP) evolution equation to relate the gluon distribution with the structure functions and the scaling violations of them extracted by various collaborations from recent low-x data. We also analyse other methods and compare our results with them.

Key Words: *Gluon distribution; low-x physics, Q C D Taylor expansion method*

INTRODUCTION

The measurements of the proton and the deuteron structure functions by Deep Inelastic Scattering (DIS) processes in the low-x region where x is the Bjorken variable have opened a new era in parton density measurements (Buchmuller and Inglelman, 1991) It is important for understanding the inner structure of hadrons In addition to these knowledge, it is also important to know the gluon distribution inside hadron at low-x because gluons are expected to be dominant in this region. On the otherhand, gluon distribution can not be measured directly from experiments. It is, therefore, important to measure directly from experiments It is, therefore, important to measure gluon distribution G (x, Q^2) indirectly from the proton as well as the deuteron structure functions F_2 (x, Q^2) A few number of papers have already

E-mail : [1] jks@ agnigarh. tezu.ernet.in.

been published [Copper-Sarkar, 1988, Sarma and Medhi(*in press*)] in this connection Here we present an alternative method to relate G (x, Q^2) with proton and deuteron structure functions and their derivatives with respect to $\ln Q^2\ \partial F_2(x, Q^2) / \partial \ln Q^2$ and with respect to $x\ \partial F_2(x, Q^2) / \partial x$ for fixed values of Q^2 Our method is more general with less approximation, simpler and more transparent

THEORY

Gluon Distribution from the Proton

It is shown (Copper-Sarkar, 1988) that the gluon distribution at low-x can be obtained by analysing the longitudinal structure function. Similarly it is also shown by Prytz (1993), Kotikov and Parente (1996) that this distribution can be calculated from the proton structure function $F_2(x, Q^2)$ and their differential coefficient with respect to $\ln Q^2\ \partial F_2(x, Q^2) / \partial \ln Q^2$. The basic idea lies on the fact that the scaling violation of $F_2(x, Q^2)$ arise, at low-x, from the gluon distribution alone and does not depend on the quark distribution Then neglecting the quarks the LO AP evolution equation for four flavours (Prytz, 1993, 1994) gives

$$\frac{\partial F_2(x, Q^2)}{\partial \ln Q^2} = \frac{5\alpha_s}{9\pi} \int_0^x G\left(\frac{x}{1-z}, Q^2\right) P_{qg}(z)dz \tag{1}$$

where in LO, the splitting function

$$P_{qg}(z) = \tfrac{1}{2}[z^2 + (1 - z)^2] \tag{2}$$

and α_s is the strong coupling constant Now

$$\frac{x}{1-z} = x \sum_{k=0}^{\infty} z^k = x + x \sum_{k=1}^{\infty} z^k \tag{3}$$

We have, $1 - x > z > 0 \Rightarrow |z| < 1$ which implies that the expansion (3) is convergent. Now by the Taylor expansion (Grandshteyn and Ryzhik, 1965)

$$G\left(\frac{x}{1-z}, Q^2\right) = G\left(x + x \sum_{k=1}^{\infty} z^k, Q^2\right) = G(x, Q^2) + x \sum_{k=1}^{\infty} z^k \frac{\partial G(x, Q^2)}{\partial x}$$

$$+ \frac{1}{2}x^2 \left(\sum_{k=1}^{\infty} z^k\right)^2 \frac{\partial^2 G(x, Q^2)}{\partial x^2} + O(x^3), \tag{4}$$

where $O(x^1)$ are the higher order terms Neglecting the terms containing x^2 and higher orders $O(x^1)$ for simplicity, we get

$$G(\frac{x}{1-z}, Q^2) = G(x + x \sum_{k=1}^{\infty} z^k \simeq G(x, Q^2) + x \sum_{k=1}^{\infty} z^k \frac{\partial G(x, Q^2)}{\partial x} \quad (5)$$

But as a matter of fact, we can not neglect the higher order terms as these terms are not small in Regge-like behaviour (Kotikov and Parente, 1996, Collins, 1977) $G(x) \sim x^{\delta_p}(Q^2)$ or in Double-Logarithmical behaviour (Kotikov and Parente, 1996, Ball and Forte, 1994) $G(x) \sim \exp(0.5\sqrt{\delta_p(Q^2)\ln(1/x)})$ for gluon at low-x Here $\delta_p(Q^2)$ is a Q^2 - dependent parameter where p = s (singlet quark) or g(gluon) On the otherhand, it has been shown that this Taylor expansion method is successfully applied in calculating Q^2 - evolution of proton structure function (Choudhury and Sarma, 1992, Sarma and Das, 1993) at low-x with reasonable phenomenological success It was a natural improvement of an earlier analysis at intermediate-x (Choudhury and Saikia, 1989) This approximation neglecting higher order terms in Taylor expansion is also applied recently (Sarma et al , 1997) in calculating x-evolution of deuteron structure function with excellent phenomenological success The authors suggested that one possible reason for the success of this method at low-x is that traditionally the AP evolution equations provide a means of calculating the manner in which parton distributions change at fixed x as Q^2 varies This change comes about because of the various types of parton branching emission processes and the x-distributions are modified as the initial momentum is shared among the various daughter partons However, the exact rate of modifications of x distributions at fixed Q^2 cannot be obtained from the AP equations since it depends not only on the initial x but also on the rates of change of parton distributions with respect to x $\partial^n I / \partial x^n$ (n = 1 to ∞), upto infinite order Physically this implies that at high x the parton has a large momentum fraction at its disposal and as a result radiates partons including gluons in innumerable ways, some of them involving complicated QCD mechanisms However for low-x many of the radiation processes will cease to occur due to momentum constraints and the x-evolutions get simplified It is then possible to visualize a situation in which the modification of the x-distribution simply depends on its initial value and its first derivative Bora and Choudhury (1995) and also Prytz (1993, 1994) has already applied Taylor expansion method to calculated gluon distributions from structure functions and scaling violations of them But our mathod is more general and transperent with less approximation than other two methods mentioned above which will be discussed later on

Putting equations (2) and (5) in equation (1) and performing z-integrations we get

$$\frac{\partial I_2(x, Q^2)}{\partial \ln Q^2} = \frac{5\alpha_s}{9\pi} [A(x)\, G(x, Q^2) + B(x) \frac{\partial G(x, Q^2)}{dx}] \quad (6)$$

where, $A(x) = (1/3)(1 - x)(2x^2 - x + 2)$ (7)

and $B(x) = (1/3)x(1 - x)(-2x^2 + 4x - 5) - x\ln x$ (8)

Recasting the equation (6), we get

$$G(x, Q^2) + \frac{B(x)}{A(x)} \frac{\partial G(x, Q^2)}{\partial x} = \frac{9\pi}{5\alpha_s A(x)} \frac{\partial F_2(x, Q^2)}{\partial \ln Q^2} \tag{9}$$

At constant $Q^2 = Q_0^2$, $G(x, Q^2) = G(x)$ and $\partial F_2(x, Q^2) / \partial \ln Q^2 = K(x)$ and so, equation (9) gives

$$G(x) + \frac{B(x)}{A(x)} \frac{\partial G(x)}{\partial x} = \frac{9\pi}{5\alpha_s} \frac{K(x)}{A(x)} \tag{10}$$

Since the ratio $B(x) / A(x)$ is very small at low-x, $\lim_{x \to 0} B(x) / A(x) = 0$, the left hand side of equation (10) can be written as

$$G(x) + \frac{B(x)}{A(x)} \frac{\partial G(x)}{\partial x} = G(x) + \frac{B(x)}{A(x)} \frac{\partial G(x)}{\partial x} + \frac{1}{2} \left(\frac{B(x)}{A(x)}\right)^2 \frac{\partial G(x)}{\partial x^2} + \cdots$$
$$= G\left(x + \frac{B(x)}{A(x)}\right)$$

by Taylor expansion series. Thus from equation (10), we get

$$G\left(x + \frac{B(x)}{A(x)}\right) = \frac{9\pi}{5\alpha_s} \frac{K(x)}{A(x)} \tag{11}$$

The equation (11) is the relation between the gluon distribution $G(x', Q^2)$ at $x' = x + B(x) / A(x)$ and $\partial F_2(x, Q^2) / \partial \ln Q^2$ at x at the fixed value of $Q^2 = Q_0^2$. This is one of our main results.

GLUON DISTRIBUTION FROM THE DEUTERON

In the LO analysis deuteron structure function is directly related to singlet structure function (Sarma et al., 1997). On the otherhand, the differential coefficient of siglet structure function F_2^S with respect to $\ln Q^2$ $\partial F_2 / \partial \ln Q^2$ has a relation with singlet structure function itself as well as gluon distribution function from AP evolution equation (Altarelli and Parisi, 1997; Dokshitzer, 1977). Thus, it is possible to calculate gluon distribution from singlet structure function or ultimate deuteron structure functtion also. No author has uptill now reported a method to calculate gluon distribution from deuteron in the literature. The LO AP evolution equation for singlet structure function is given by

$$\frac{\partial F_2^S(x,t)}{\partial t} - \frac{\Lambda_s}{t}\{[3 + 4\ln(1 - x)]F_2^S(x, t) + 2\int \frac{dz}{z}[z^2 - 2z + 2)F_2^S\left(\frac{x}{1 - z}, t\right)$$
$$- 2F_2^S(x, t)\} + (3/2)N_f\int(2z^2 - 2z + 1)G\left(\frac{x}{1 - z}, t\right)dz = 0 \tag{12}$$

where, $t = \ln(Q^2 / \Lambda^2)$ and $\Lambda_f = 4/(33 - 2N_f)$, N_f being the number of flavour and Λ is the QCD cut off parameter

Applying the same method of Taylor expansion as in the case of proton we get here also,

$$\Gamma_2^s\left(\frac{x}{1-z}, t\right) = \Gamma_2^s\left(x + x\sum_{k=1}^{\infty} z^k, t\right)$$

$$\simeq F_2^s(x, t) + x\sum_{k=1}^{\infty} z^k \frac{\partial \Gamma_2^s(x, t)}{\partial x} \qquad (13)$$

$$\text{and } G_2^s\left(\frac{x}{1-z}, t\right) = G_2^s\left(x + x\sum_{k=1}^{\infty} z^k, t\right)$$

$$\simeq G_2^s(x, t) + x\sum_{k=1}^{\infty} z^k \frac{\partial G_2^s(x, t)}{\partial x} \qquad (14)$$

neglecting the higher order terms as before

Putting equations (13) and (14) in equation (12) and performing z-integrations as in the case of proton, we get

$$\frac{\partial \Gamma_2^s(x, t)}{\partial t} - \frac{\Lambda_f}{t}\left[A_s(x)\Gamma_2^s(x, t) + B_s(x)G(x, t) + C_s(x)\frac{\partial \Gamma_2^s(x, t)}{\partial x} + D_s(x)\frac{\partial G(x, t)}{\partial x}\right] = 0 \qquad (15)$$

$$\left.\begin{aligned} \text{where, } A_s(x) &= 3 + 4\ln(1 - x) + 2\{(1 - x)(-2 + (1 - x)/2)\}, \\ B_s(x) &= (3/2)N_f\{(1 - x)(x + (2/3)(1 - x)^2)\}, \\ C_s(x) &= 2x\{\ln(1/x) + (1 - x)(1 - (1 - x)/2)\}, \\ \text{and } D_s(x) &= (3/2)N_f\{\ln(1/x) - (1 - x)(1 + (2/3)(1 - x)^2)\} \end{aligned}\right\} \qquad (16)$$

Recasting equation (15) we get,

$$G(x,t) + \frac{D_s(x)}{B_s(x)}\frac{\partial G(x, t)}{\partial x} = \frac{1}{A_f B_s(x)}\, t\, \frac{\partial \Gamma_2^s(x, t)}{\partial t} - \frac{A_s(x)}{B_s(x)}\Gamma_2^s(x, t) - \frac{C_s(x)}{B_s(x)}\frac{\partial \Gamma_2^s(x, t)}{\partial x} \qquad (17)$$

Now D_s/B_s is very small at low-x, $\lim_{x \to 0} D_s/B_s = 0$ So, applying the Taylor expansion series as before we can write

$$G(x,\ t) + \frac{D_1(x)}{B_1(x)} \frac{\partial G(x,\ t)}{\partial x} = G(x + \frac{D_1(x)}{B_1(x)})$$

Thus equation (17) gives

$$G(x'',\ t) = K_1(x)\, t \frac{\partial F_2^N(x,\ t)}{\partial t} + K_2 \frac{\partial F_2^N(x,\ t)}{\partial x} + K_3 F_2^N(x,\ t) \tag{18}$$

$$\left.\begin{aligned} \text{where, } x'' &= x + \frac{D_1(x)}{B_1(x)}, \\ K_1(x) &= \frac{1}{A_1 B_1}, \\ K_2(x) &= -\frac{C_1(x)}{B_1(x)} \\ \text{and } K_3(x) &= -\frac{A_1(x)}{B_1(x)} \end{aligned}\right\} \tag{19}$$

If we try to combine the last two terms of equation (18) let us take common $K_3(x)$ from both the terms which reduce to

$$K_3(x)[F_2^N(x,\ t) + \frac{K_2(x)}{K_3(x)} \frac{\partial F_2^N(x,\ t)}{\partial x}]$$

But $K_2(x) / K_3(x)$ is noty small at low-x and therefore these two terms can not be combined to one as in the case of gluon by applying Taylor expansion series

The relation between deuteron and singlet structure functions at LO is

$$F_2^D(x,\ t) = (5/9)\ F_2^N(x,\ t) \Rightarrow F_2^N(x,\ t) = (9/5)\ F_2^D(x,\ t) \tag{20}$$

Then we get,

$$\frac{\partial F_2^N(x,\ t)}{\partial t} = \frac{9}{5} \frac{\partial F_2^D(x,\ t)}{\partial t} \tag{21}$$

and

$$\frac{\partial F_2^N(x,\ t)}{\partial x} = \frac{9}{5} \frac{\partial F_2^D(x,\ t)}{\partial x} \tag{22}$$

Putting equations (20), (21) and (22) in equation (18) we get ultimately

$$G(x'',\ t) = \frac{9}{5}\ [K_1(x) t \frac{\partial F_2^D(x,\ t)}{\partial t} + K_2 \frac{\partial F_2^D(x,\ t)}{\partial x} + K_3 F_2^D(x,\ t)] \tag{23}$$

which is one of our main results. From this equation it is seen that if we have deuteron structure function and its differential coefficients with respect to $\ln Q^2$ and x at any x for a fixed value of $Q^2 = Q_0^2$, we can calculate the gluon distribution function at $x'' = x + D_1(x)/B_1(x)$ from equation (23) as a LO analysis.

RESULTS AND DISCUSSION

We use HERA data taken by H1 and ZEUS collaborations from ref. Aid, S., H1 collaboration (1995) and ref. Derrick, M., ZEUS collaboration (1995) respectively. In these tables the values of $\partial F_2(x, Q^2) / \partial \ln Q^2$ are listed for a range of x values at $Q^2 = 20$ GeV^2. Similarly we use parametrizations of the recent New Muon Collaboration (NMC) proton and deuteron structure function data (Arneodo, M., NMC 1995; 1997) from a 15-parameter function given in ref. Arneodo, M., NMC (1995). Here we calculate the values of $\partial F_2(x, Q^2) / \partial \ln Q^2$ at $Q^2 = 40$ GeV^2. From all these data or parametrizations we calculate the structure functions $F_2(x, Q^2)$ or scaling violations of structure functions with respect to $\ln Q^2$ and apply them in the equation (11) and equation (23) to calculate the gluon distribution functions $G(x', Q^2)$ or $G(x'',Q^2)$, where $x' = x + B(x) / A(x)$ and $x'' = x + D_s(x) / B_s(x)$ from proton and deuteron structure functions respectively.

For our calculation, strong coupling constant α_s was taken from a NLO fit (Virchaux and Milsztajn 1992) to F_2 data which yields $\alpha_s = 0.180 \pm 0.008$ at $Q^2 = 50$ GeV^2 coresponding to $\Lambda^{(4)}_{MS} = 0.263 + 0.042$ GeV and $\alpha_s (M_z^2) = 0.113 \pm 0.005$. This value of α_s agrees with one given by Particle Data Group (PDG)(Montanet, 1994). But in our practical calculations we neglect the errors of α_s and Λ which are rather small.

In the Fig. 1. the gluon distribution obtained by our method (equation (23)) for the deuteron paramerization (Arneodo, 1995, 1997) from a 15-parameter function (Arneodo, 1995) is presented at $Q^2 = 40$ GeV^2. The middle line is the result without considering any error. The upper and the lower lines are the results with paramter values by adding and substracting the statistical and systematic errors with the middle values respectively. It has been seen that the middle line almost coincides with the upper line. The area between these lines are the result with full errors. The NMC at first parametrized their data from proton and deuteron for Q^2 values from 0.5 GeV^2 to 75 GeV^2 and low-x values from 0.006 to 0.9 (Arneodo, 1995) by a 15-parameter function (Arneodo, 1995). This parametrization can also well describe the SLAC and BCDMS (Benvenuti, 1989) data. The recent NMC data (Arneodo, 1997) has been extended for low-x values from 0.002 to 0.6; but in that case also the same parametrization fits well with SLAC and BCDMS data. We calculate F_2^d and $\partial F_2^d / \partial \ln Q^2$ for x values 10^{-2} to 10^{-7} for the equation (23) which gives G(x") for x" values from 5.52×10^{-2} to 2.27×10^{-6} . We obtain our result for Q^2 values from 40 GeV^2 to 100 GeV^2. It is seen that the gluon distribution increases from $\simeq$ 1.0 to $\simeq$ 2.0 when x decreases from higher to lowest values in our consideration; but deuteron gluon distribution is almost three times smaller than proton gluon distribution from NMC data. Moreover deuteron gluon distribution increases slightly (almost 15%) for a particular value of x when Q^2 increases from 40 GeV^2 to 100 GeV^2. We can not compare our result of NMC data with others because sufficient low-x deuteron data is not avialable. Moreover, no other author has tried to calculate gluon distribution from deuteron structure function and so, we can also compare our result with those of others.

In the Fig. 2, the same result is presented for NMC proton parametrization from the same references as for deuteron. Here also we use the same 15-parameter function (Arneodo, 1995) with different parameters which also describe SLAC and BCDMS data in addition to the recent NMC data (Arneodo, 1997) exactly same as before at 40 GeV^2. The Q^2 and x-ranges of our calculations are also same. We calculate G(x')(equation (11)) for x' values which varies from 5.52×10^{-2} to 2.27×10^{-6} for highest and lowest values of x under consideration respectively. The gluon distribution increases from $\simeq 3.5$ to $\simeq 6.5$ when x decreases from the highest to lowest values under consideration. But proton gluon distribution decreases slightly (< 1%) for a particular values of x when Q^2 increases from 40 GeV^2 to 100 GeV^2. We do not compare the results of NMC data with those of mainly HERA because their Q^2 and x-ranges are different.

In the Fig. 3, the gluon distribution obtained by our method (equation (11)) from HERA data measured by H1 collaboration (Aid, H1, 1995) is presented at $Q^2 = 20$ GeV^2. The middle line is the result without considering any error in the data. The upper and the lower lines are the results adding and subtracting algebrically the statistical and systematic errors with the data respectively and thereby calculating the gluon distributions. These two lines are symmetric about the middle lines and positive and negative errors are equal. The area bounded by these lines gives the result with maximum error. The x-values in the data ranges from the highest value 1.33×10^{-2} to the lowest value 3.83×10^{-4}. The corresponding x' values are 6.81×10^{-2} and 3.948×10^{-3} respectively, and also gluon distributions are also $\simeq 3.0$ and $\simeq 24.0$ respectively for data without considering any error. Here also gluon distribution increases when x decreases except the lowest value when gluon distribution decreases. But the rate of increament for HERA data measured by H1 collaboration is much higher than that of NMC data.

In the Fig. 4, the same thing is presented for HERA data measured by ZEUS collaboration (Derrick, ZEUS, 1995) at $Q^2 = 20$ GeV^2. Here the x-values in the data ranges from the highest value 4.65×10^{-3} to the lowest value 8.5×10^{-4}. The corresponding x' values are 3.077×10^{-2} and 7.752×10^{-4} respectively, and also gluon distribution $\simeq 10.9$ and $\simeq 21.2$ respectively for data without considering any error. We see, in this case also, gluon distribution increases when x decreases. And the rate of increament is slightly higher to that of H1 collaboration in the x range considered; but much higher than that of NMC data.

In the Fig. 5, comparison of gluon distributions by our method (Sarma, equation (11)), Bora and Choudhury Method (Bora), Prytz method (Prytz) and Kotikov and Parente method (Kotikov) is presented for HERA data middle value only measured by H1 collaboration at $Q^2 = 20$ GeV^2. The x values under consideration is same as in Fig. 3. But the arguments of the gluon distributions calculated are different for different methods except for Kotikov and Parente's method for which the arguments do not change, they are the same x values under consideration. Accordingly for the highest and the lowest x values, x' values are 6.81×10^{-2} and 3.948×10^{-4} respectively. For all the methods gluon distribution increases when x decreases

except for the last data point for which it decreases But rate of increament is different for different methods The values of gluon distributions are comparable but rate of increament is highest in our method and lowest in Kotikov and Parente's method It is intermediate in other two mentods of which rate of Prytz's method is slightly higher than that of Bora and Choudhury's method

In the Fig 6, comparison of gluon distributions by various methods exactly same way as in Fig 5 is presented for HERA data middle value measured by ZEUS collaboration (Derrick, ZEUS 1995) at $Q^2 = 20$ GeV^2 The x values under consideration is same as in Fig 4 But the arguments of the gluon distributions calculated are different for different methods as discussed earlier Accordingly, for the highest and the lowest x values x' values are $3\ 077 \times 10^2$ and $7\ 752 \times 10^3$ respectively The arguments of gluon distribution for Kotikov and Parente's method are same as x values under consideration, i e they do not change The gluon distribution increases when x decreases for all the methods as before, but the rate of increasement is highest in our method and lowest in Kotikov and Parente's method The rates are intermediate in other two methods of which rate at Prytz s method is higher than that of Bora and Choudhury's method

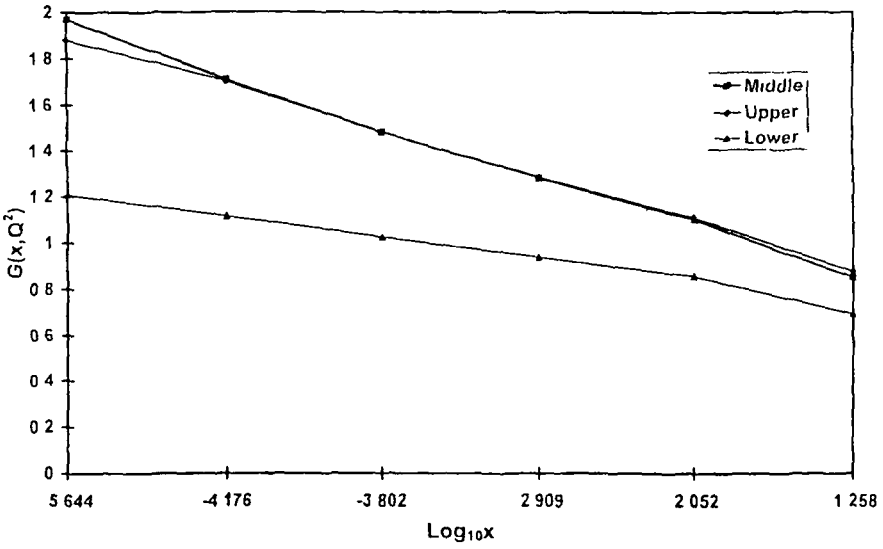

Fig. 1 : The gluon distribution obtained by our method for the NMC deuteron parametrization (15 - parameter function, Table-3) at $Q^2 = 40$ GeV^2 The (i) middle, (ii) upper and (iii) lower lines are the results (a) without considering any error, (b) adding algebrically the statistical and systematic errors and (c) substracting algebrically the statistical and systematic errors respectively

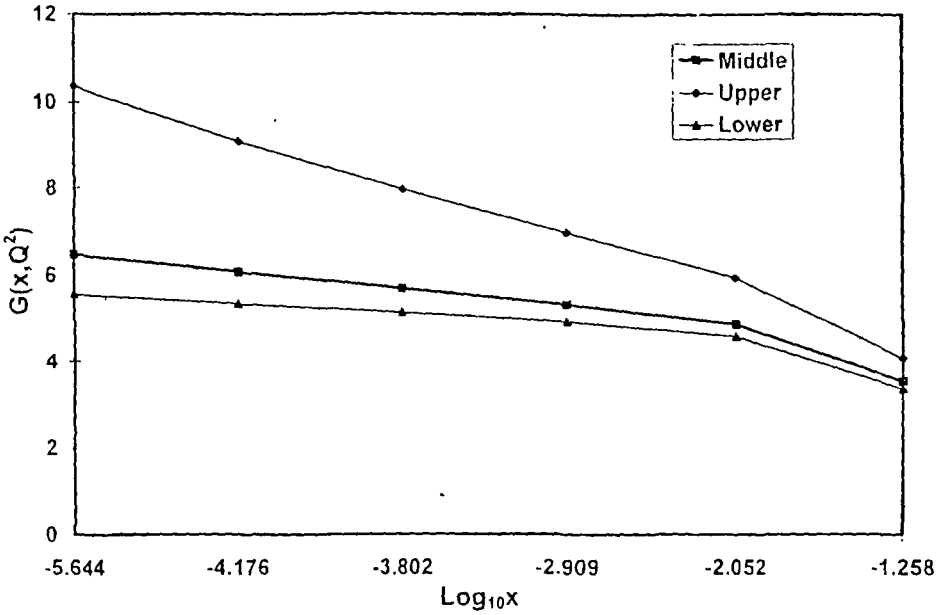

Fig. 2 : Same result as in Fig.1 (equation-11) for NMC proton parametrization at Q^2 = 40 GeV^2.

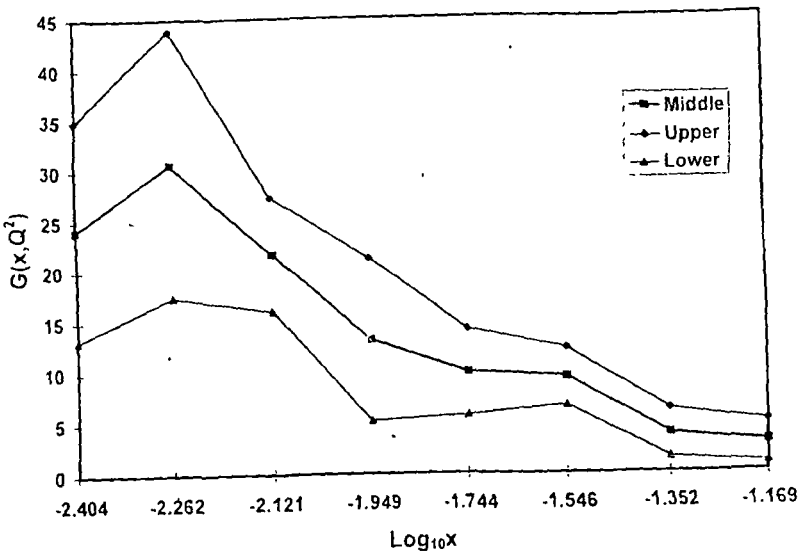

Fig. 3 : Same result as in Fig.1 (equation-11) for HERA proton data by H1 collaboration at Q^2 = 20GeV^2.

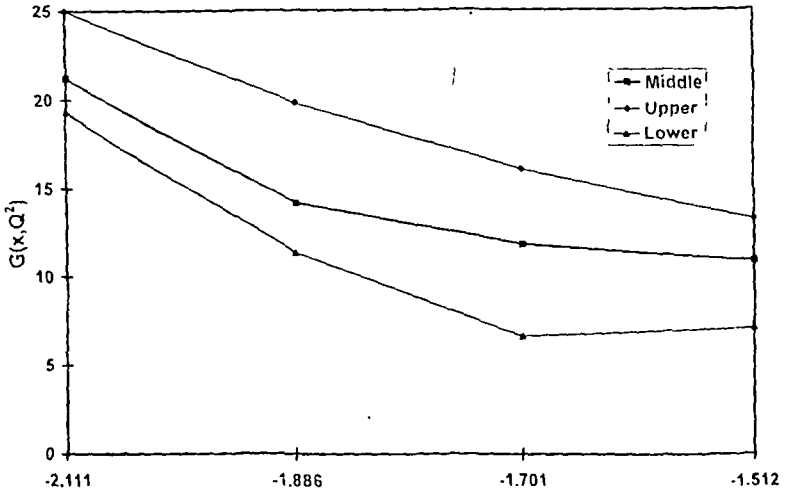

Fig. 4 : Same result as in Fig.1 (equation-11) for HERA proton data by ZEUS collaboration at $Q^2 = 20GeV^2$.

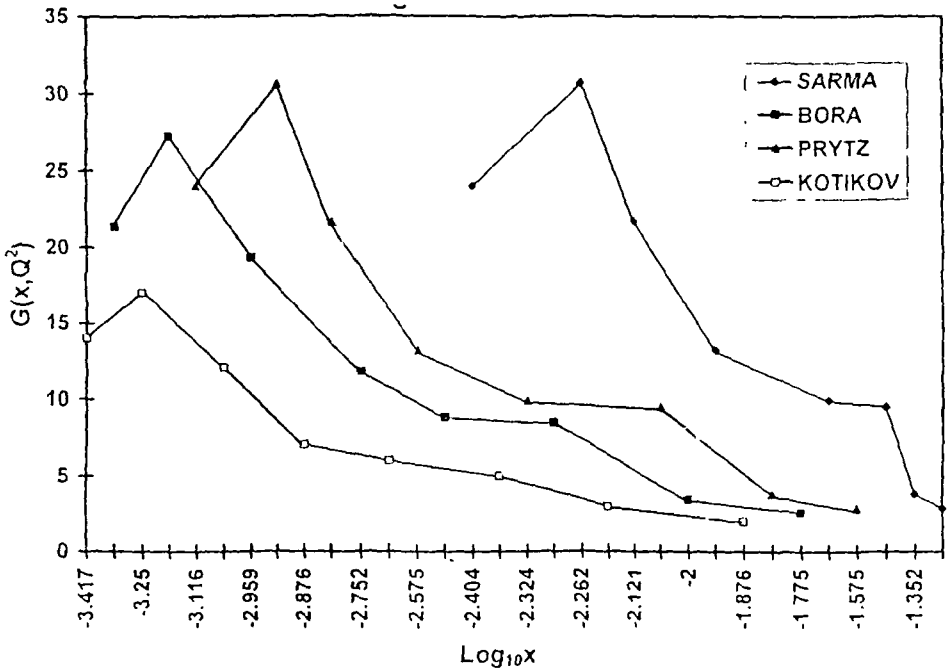

Fig. 5 : Comparison of gluon distributions for HERA proton data by H1 collaboration by various methods at $Q^2 = 20GeV^2$.

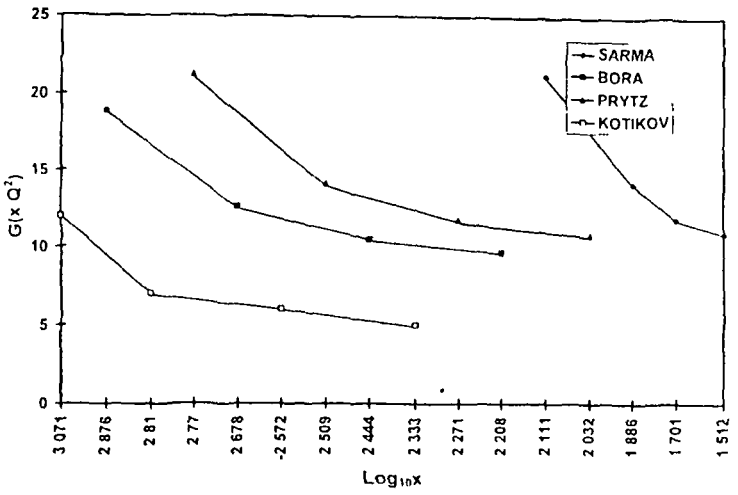

Fig. 6 : Same result as in Fig 5 for proton data by ZEUS collaboration by various methods at $Q^2 = 20GeV^2$

SUMMARY AND CONCLUSION

In this article we present an alternative method than other methods (Copper Sarkar 1988) to extract gluon distribution $G(x, Q^2)$ from the measurement of low-x proton and deuteron structure functions $F_2(x, Q^2)$ and their differential coefficients $\partial F_2(x, Q^2) / \partial \ln Q^2$ and $\partial F_2(x, Q^2) / \partial x$ with respect to $\ln Q^2$ and x respectively Here we report for the first time a method to find gluon distribution from deuteron structure function $F_2^d(x, Q^2)$ at low-x Here we use the LO AP evolution equation (Altarelli and Parisi, 1997) to relate gluon distribution function with low-x structure function or their differential coefficients We compare our results with other methods also In Bora and Choudhury's method (Bora and Choudhury, 1995) to extract gluon distribution $G(x, Q^2)$ authors expanded $G(x / (1 - z), Q^2)$ using Taylor expansion about $z = 0$ taking only upto first order derivative in the expansion While expanding they used only first two terms in the expansion of the infinite series $x / (1 - z) = x \sum_{k=0}^{\infty} z^k$ also But this approximation is very crude Similarly in Prytz's method (Prytz 1993, 1994) author expanded $G(x / (1 - z), Q^2)$ using the whole infinite series $x / (1 - z)$ which is more general than the previous method Of course, we also take first two terms in Taylor expansion series $G(x / (1 - z), Q^2)$ upto the first order derivative of $G(x, Q^2)$ with respect to x On the otherhand in Kotikov and Parente's method (Kotiko and Parente, 1996), authors assumed some recent parametrizations for singlet quarks and gluon, put them in AP evolution equation and solved for gluon distribution by standard moment method in NLO But here also authors approximated

their solution by neglecting some higher order terms and differential coefficient of singlet gluon $\partial S/\partial x$ with respect to x Moreover, here the solving process by moment method is also a bit complicated Again Ellis, Kunszt and Levin's method (Ellis et al , 1994) is also not much developed than other methods Like Kotikov and Parente's method here also the authors assumed some behaviour for F_2 and gluon momentum density with some unkonwn parameter and solved AP equations in moment space, of course, in NNLO analysis But here NNLO kernals are also parameter dependent Moreover, this mehtod covers the x-range lower than HERA rance and so we become do not serious to include the result of this method in our analysis In calculating the gluon distribution from deuteron at low-x we use only NMC deuteron data parametrization (Arneodo, 1995) by a 15-parameter function and find that it is also increasing when x decreasing as in the case of proton as usual But it is seen that the value of gluon distribution from deuteron is much less than that from proton data, almost one third in case of NMC data and still smaller in other data like HERA etc A possible interpretation is that gluon distribution $G(x, Q^2)$ is actually small in deuteron It is seen that in our theory (equation (23)) gluon distribution depends upon deuteron structure function $F_2^d(x, t)$, $(t = \ln (Q^2 / \Lambda^2)$ and its derivatives with respect to t and x The structure function and its derivatives for deuteron are small (Arneodo, 1995, 1997) due to which ultimately gluon distributions from deuteron are small Moreover, dependence of the gluon distribution on Q^2 is very small at low-x In a particular low-x gluon distributiondecreases very slightly when Q^2 increases The 15-parameter function not only describes the NMC data but also SLAC and BCDMS (Benvenuti, 1989) data and so our calculation automatically includes these two types of experiments

For calculation of gluon distribution from proton structure function at low-x we use HERA data measured by H1 (Aid, H1, 1995) and ZEUS (Derrick, ZEUS 1995) collaborations and NMC data parametrization (Arneodo, 1995) In our method gluon from NMC data (Virchaux and Milsztajn, 1992) is appreciably small, it is almost one fifth of HERA data measured by H1 and ZEUS collaborations at $x \simeq 10^{-4}$

In our method, gluon distributions calculated from direct HERA data measured by H1 and ZEUS collaborations upto $x \simeq 10^{-2}$ are almost in the same order Gluon distributions from the HERA data parametrizations by H1 and ZEUS collaborations upto $x \simeq 10^{-4}$ are also of the same order to them and are mutually are also same But after $x \simeq 10^{-4}$ when x decreases the rate of increament of ZEUS parametrization is much higher than that of H1 and gluon distribution from the first parametrization becomes also hundred times of the second one at $x \simeq 10^{-7}$

We compare our results with other methods by Bora and Choudhury, Pritz and Kotikov and Parente The general trend is that gluon distribution $G(x, Q^2)$ increases when x decreases But the rate of increment of gluon distribution calculated by our method is in general higher than those of other methods The result of Kotikov and Parente s method are the lowest The

results of two other methods are the intermediate ones between these two methods of which the result of Prytz's method is higher than that of Bora and Choudhury's method Results from our method are closed to those from Prytz's method This is because Bora and Choudhury's method is a crude approximation as they include only one term of the infinite series $x / (1 - z)$ whereas we include all the infinite terms So the other terms enhance the contribution in our method In our method, the first order approximation in Taylor expansion of $G(x / (1 - z), Q^2)$ is used, i e only terms having first order differentiation $\partial G(x, Q^2) / \partial x$ is used Scope is still there to include higher order terms of the Taylor expansion series and we have the plan to do so in the subsequent work We did a preliminary work in this regard including the second order differential coefficient $\partial^2 G(x, Q^2) / \partial x^2$ but it seems that this does not contribute in a significant way Moreover, this is only a LO analysis To have a better result we must include NLO and the subsequent terms in perturbative QCD Work is going on in this regard Lastly, in extracting gluon distribution from scaling violation of structure function, we assume that at low-x scaling violation arises entirely from gluon distribution only and there is no contribution from quarks Of course at low-x this is a very good approximation But small contribution from quarks still there and we plan to examine this point also in our latter work

ACKNOWLEDGEMENT

We are very much grateful to Professor (Dr) Y V G S Murthi for providing necessary facilities in Physics Department of IIT, Guwahati where most of the work was done We are also grateful to Professor (Dr) R S Bhalerao of TIFR Mumbai for sending to us useful preprints and reprints and Professor (Dr) R Ramachandran of Mathscience, Chennai and Professor (Dr) D K Choudhury of Gauhati University for useful discussions

REFERENCES

1 Aid, S et al, H_1 Collaboration (1995) The Gluon Density of the Proton at Low-x from QCD Analysis of F_2, Phys Lett B 354 494

2 Altarelli, G and Parisi, G (1997) Asymptotic Freedom in Parton Language, Nucl Phys B 12 298

3 Arneodo, M, NMC (1995) Measurement of the Proton and the Deuteron Structure Functions, F_2^p and F_2^d, Phys Lett B 364 107

4 Arneodo, M, NMC (1997) Measurement of the Proton and Deuteron Structure Functions, F_2^p and F_2^d and of the Ratio σ_L / σ_T Nucl Phys B 483 3

5 Ball, R D and Forte, S (1994) Double Asymptotic Scaling at HERA, Phys Lett B 335 77, B 336 77

6 Benvenuti, A C , BCDMS Collaboration (1989), (1990) A High Statistics Measurement of the Proton Structure Functions F_2 (x, Q^2) and R from Deep Inelastic Muon Scatting at High Q^2 Phys Lett B 23 485, B 27 592

7 Bora, Kalpana and Choudhury, D K (1995) Finding the Gluon Distribution of the Proton at Low-x from F_2, Phys Lett B 354 151

8 Buchmuller, W and Ingelman, G [eds] (1991) Proc Workshop 'Physics at HLRA, Hamburg

9 Choudhury, D K and Saikia, A (1989) An Improved Approximate Solution of Altarelli-Parisi Equation , Pramana-J, Phys 33 359

10 Choudhury, D K and Sarma, J K (1992) Perturbative and Non-perturbative Evolutions of Structure Function at Low-x , Pramana-J Phys 38 481

11 Collins, P D B (1977) An Introduction to Regge Theory and High Energy Physics Cambridge University Press, Cambridge

12 Copper-Sarkar, A M et al , (1988) Measurement of the Longitudinal Structure Function and the Small-x Gluon Density of the Proton, Z phys C-39 281

13 Derrick, M , ZEUS Collaboration (1995) Phys Lett B 364 576

14 Dokshitzer, Y I (1977) Calculation of Structure Function of Deep Inelastic Structure and $e^+ e^-$ Anhilation by Perturbative Theory in Quantum Chromodynamics , Sov Phys JETP 46 641

15 Ellis R K , Kunszt, Z and Levin, E M (1994) The Evolution of Proton Distributions at Small-x, Nucl Phys B 420 517

16 Grandshteyn, I S and Ryzhik I M (1965) 'Tables of Integrals, Series and Products [ed] Jeffery, A Accademic Press New York

17 Kotikov, A V and Parente, G (1996) The Gluon Distribution as a Function of F_2 and $dF_2 / d\ln Q^2$ at Small-x The Next-to-Leading Analysis , Phys Lett B 379 195

18 Montanet L , (1994) Particle Data Group (PDG), Phys Rev D 50 1173

19 Prytz, K (1993) Approximate Determination of the Gluon Density at Low-x from the F_2 Scaling Violations, Phys Lett V 311 286

20 Prytz K (1994) An Approximate Next-to-Leading Order Relation Between the Low-x F_2 Scalling Violations and the Gluon Density, Phys Lett B 332 393

21 Sarma, J K and Das, B (1993) t-Evolutions of Structure Function at Low-x Phys Lett B 304 323

22 Sarma J K , Choudhury, D K and Medhi, G K (1997) -x-Distribution of Deuteron Structure Function at Low-x Phys Lett B 403 139

23 Sarma, J K and Medhi, G K (in press) Regge Behaviour of Structure Function and Gluon Distribution at Low-x Euro Phys J C

24 Virchaux, M and Milsztajn (1992) A Measurement of α_s and of Higher Twists from a QCD Analysis of High Statistics F_2 Data on Hydrogen and Deuterium Targets Phys Lett B 274 221

Eur Phys J C 16, 481–487 (2000)
Digital Object Identifier (DOI) 10.1007/s100520000384

THE EUROPEAN PHYSICAL JOURNAL C

Regge behaviour of structure function and gluon distribution at low-x in leading order

J K Sarma[1] [a], G K Medhi[2]

[1] Physics Department, Tezpur University, Napaam, Tezpur-784 028, Assam, India
[2] Physics Department, Birjhora Mahavidyalaya, Bongaigaon-783 380, Assam, India

Received 2 January 2000 / Revised version 23 February 2000 /
Published online 6 July 2000 – © Springer-Verlag 2000

Abstract We present a method to find the gluon distribution from the F_2 proton structure function data at low-x assuming the Regge behaviour of the gluon distribution function at this limit We use the leading order (LO) Altarelli–Parisi (AP) evolution equation in our analysis and compare our result with those of other authors We also discuss the limitations of the Taylor expansion method in extracting the gluon distribution from the F_2 structure function used by those authors

1 Introduction

The measurements of the F_2 (proton and deuteron) structure functions by deep inelastic scattering (DIS) processes in the low-x region, where x is the Bjorken variable have opened a new era in parton density measurements [1] It is important for understanding the inner structure of hadrons and ultimately of matter It is also important to know the gluon distribution inside a hadron at low-x because gluons are expected to be dominant in this region On the otherhand, the gluon distribution cannot be measured directly from experiments It is, therefore, important to measure the gluon distribution $G(x, Q^2)$ indirectly from the proton as well as the deuteron structure functions $F_2(x, Q^2)$ Here the representation for the gluon distribution $G(x) = xg(x)$ is used, where $g(x)$ is the gluon density

A few papers have already been published [2–9] in this connection Here we present an alternative method to extract $G(x, Q^2)$ from the scaling violations of $F_2(x, Q^2)$ with respect to $\ln Q^2$, i e $\partial F_2(x, Q^2)/\partial \ln Q^2$ Our method is mathematically more transparent and simpler than those of other authors

2 Theory

It is shown in [2,8] that the gluon distribution $G(x)$ at low-x can be obtained by analysing the longitudinal structure function Similarly it is also shown in [3–7] that this distribution can be calculated from the F_2 proton structure function and its scaling violation Moreover, in [9] we see that it is also possible to calculate the gluon distribution from the F_2 deuteron structure function and its scaling violation The basic idea relies on the fact that the scaling violation of the F_2 structure function arises at low-x from the gluon distribution alone and does not depend on the quark distribution As a demonstration of this fact, the scaling violation of the sea quark distribution as a function of x has been illustrated in [3] Here as in Figs 1a,b the scaling violation of the sea quark distribution using the KMRS B_- and B_0 parametrizations [10] are demonstrated, respectively At low-x, actually already at $x = 10^{-2}$, the quarks can be neglected in the AP evolution for the number of flavours of $n_f = 4$

Neglecting the quark the AP evolution equation for four flavours [3,4] gives

$$\frac{\partial F_2(x, Q^2)}{\partial \ln Q^2} = \frac{5\alpha_s}{9\pi} \int_0^{1-x} G(x/(1-z), Q^2) P_{qq}(z) \mathrm{d}z \quad (1)$$

where the LO splitting function is

$$P_{qq}(z) = z^2 + (1 - z^2), \quad (2)$$

and α_s is the strong coupling constant

Now, let $1 - z = y \Rightarrow \mathrm{d}z = -\mathrm{d}y$ Again $z = 0 \Rightarrow y = 1$ and $z = 1 - x \Rightarrow y = x$ Therefore (1) gives

$$\frac{\partial F_2(x\ Q^2)}{\partial \ln Q^2} = \frac{5\alpha_s}{9\pi} \int_x^1 G(x/z, Q^2)(2z^2 - 2z + 1) \mathrm{d}z \quad (3)$$

Now, let us consider the Regge behaviour of the gluon distribution [11]

$$G(x, Q^2) = C x^{-\lambda(Q^2)} \quad (4)$$

where C is a constant and $\lambda(Q^2)$ is the intercept The Regge behaviour of the structure function in the large-Q^2 region reflects itself in the small-x behaviour of the

[a] e-mail jks@agnigarh tezu ernet in

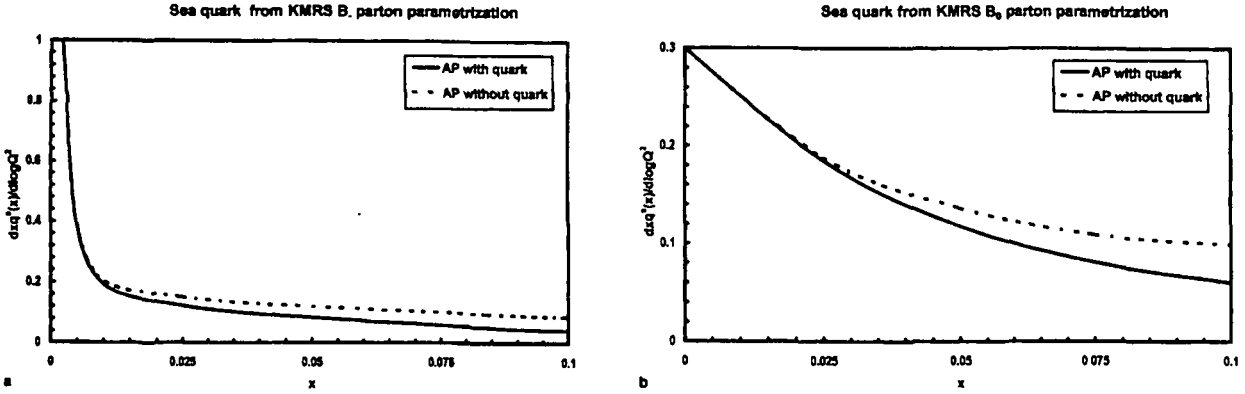

Fig. 1a,b. Scaling violations of sea quark distributions using the KMRS B_- and B_0 parametrizations [10] respectively as in [3]. The solid lines were obtained using the complete AP equations and the dashed lines were obtained neglecting quark distributions.

quark and the antiquark distributions. Thus the Regge behaviour of the sea quark and antiquark distribution for small-x is given by $q_{\rm sea}(x) \sim x^{-\alpha_P}$ corresponding to a pomeron exchange of intercept α_P=1. But the valence quark distribution for small-x given by $q_{\rm val}(x) \sim x^{-\alpha_R}$ corresponds to a reggeon exchange of intercept $\alpha_R = 1/2$. Since the same processes lead to gluon and sea quark distributions in the nucleon, we expect $G(x) \sim 1/x$. The x-dependence of the parton densities given above is often assumed at moderate-Q^2.

Applying (4) in (3) we get

$$\frac{\partial F_2(x,Q^2)}{\partial \ln Q^2} = \frac{5\alpha_s}{9\pi} C \int_x^1 x^{-\lambda(Q^2)} z^{\lambda(Q^2)} (2z^2 - 2z + 1) \mathrm{d}z. \quad (5)$$

For fixed-Q^2, let $K(x) = \partial F_2(x,Q^2)/\partial \ln Q^2$ and $A = 5\alpha_s/(9\pi)$. Thus (5) gives

$$K(x) = ACx^{-\lambda(Q^2)} \int_x^1 (2z^{\lambda+2} - 2z^{\lambda+1} + z^{\lambda}) \mathrm{d}z. \quad (6)$$

Taking the logarithm and rearranging the terms (6) gives

$$\lambda = \frac{1}{\ln x}\left[\ln\left\{\frac{2}{\lambda+3}(1-x^{\lambda+3}) - \frac{2}{\lambda+2}(1-x^{\lambda+2}) + \frac{1}{\lambda+1}(1-x^{\lambda+1})\right\}\right] - \frac{1}{\ln x}\left[\ln\{K(x)/(AC)\}\right], \quad (7)$$

$$\Rightarrow \lambda - \Phi(\lambda) = 0, \quad (8)$$

where $\lambda \equiv \lambda(Q^2)$ and $\Phi(\lambda)$ represents the right hand side of (7). Now, (8) has been solved numerically using the iteration method [12] to calculate the values of $\lambda(Q^2)$ for different x-values for a fixed value of Q. A simple computer programme for this iteration method is given in Appendix A. Scaling violation of the F_2 structure function, i.e. $K(x) = \partial F_2(x,Q^2)/\partial \ln Q^2$, and the strong coupling constant at LO α_s are experimental inputs. C is the only free parameter in our calculation. After the calculation of $\lambda(Q^2)$ we can calculate $G(x,Q^2)$ from (4) for different values of the free parameter C and compare our results with those due to other authors.

Now, let us discuss the methods due to other authors. Prytz reported a method to obtain an approximate relation between the unintegrated gluon density and the scaling violations of the quark structure function at low-x at leading order (LO) [3] as well as at next-to-leading order (NLO) [4]. He expanded $G(x/(1-z))$ of (1) using the Taylor expansion formula at $z = 1/2$ to obtain the expression [3]

$$G\left(\frac{x}{1-z}\right) \approx G\left(z=\frac{1}{2}\right) + \left(z-\frac{1}{2}\right) G'\left(z=\frac{1}{2}\right) + \left(z-\frac{1}{2}\right)^2 \frac{G''\left(z=\frac{1}{2}\right)}{2}, \quad (9)$$

taking the derivative up to second order. This expression is then inserted in (1) and after integration one gets

$$\frac{\partial F_2(x)}{\partial \ln Q^2} \approx \frac{5\alpha_s}{9\pi}\frac{2}{3} G(2x) \quad (10)$$

for fixed-Q^2, which is the main result for the LO [3] analysis. Using a similar method he obtained the formula for the NLO [4] analysis,

$$\frac{\partial F_2(x)}{\partial \ln Q^2} \approx G(2x)\frac{20}{9}\frac{\alpha_s}{4\pi}\left[\frac{2}{3} + \frac{\alpha_s}{4\pi} 3.58\right] + \left(\frac{\alpha_s}{4\pi}\right)^2 \frac{20}{9} N(x,Q^2), \quad (11)$$

where $N(x,Q^2)$ is given in [4].

Bora and Choudhury also presented a method [5] to find the gluon distribution from the F_2 proton structure function and its scaling violation at low-x using the Taylor expansion method. They also expanded $G(x/(1-z),Q^2)$ of (1) using the Taylor expansion method about $z = 0$ taking only the derivative up to first order in the expansion. While expanding they used only the first two terms

in the infinite expansion series $x/(1-z) = x\sum_{k=0}^{\infty} z^k$ to get an expression This expression is then inserted in (1) and after integration one gets

$$G(x_1, Q^2) \simeq \frac{9\pi}{5\alpha_s} \frac{A(x) + 2B(x)}{[A(x) + B(x)]^2} \frac{\partial F_2(x, Q^2)}{\partial \ln Q^2}, \quad (12)$$

at

$$x_1 = x + \frac{B(x)}{A(x) + B(x)} x$$

Sarma and Medhi also obtained a method [9] to find the gluon distribution from the F_2 proton and deuteron structure functions and their scaling violations at low-x They also expanded $G(x/(1-z), Q^2)$ of (1) by using the Taylor expansion method taking only the derivative up to first order in the expansion But unlike Bora and Choudhury method they considered the whole series $x/(1-z) = x\sum_{k=0}^{\infty} z^k$ to get the expression

$$G\left(\frac{x}{1-z}, Q^2\right) = G\left(x + x\sum_{k=1}^{\infty} z^k, Q^2\right) = G(x, Q^2) + x\sum_{k=1}^{\infty} z^k \frac{\partial G(x, Q^2)}{\partial x} \quad (13)$$

Using this relation in (1) and then integrating one obtains for the proton

$$G(x_p, t) = \frac{9\pi}{5\alpha_s} \frac{1}{A(x)} \frac{\partial F_2^p(x, t)}{\partial t} \quad (14)$$

and for the deuteron

$$G(x_d, t) = \frac{9}{5}\left[K_1(x) t \frac{\partial F_2^d(x, t)}{\partial t} + K_2 \frac{\partial F_2^d(x, t)}{\partial x} + K_3 F_2^d(x, t)\right], \quad (15)$$

where $x_p = x + B(x)/A(x)$ $x_d = x + D(x)/C(x)$ and $t = \ln(Q^2/\Lambda^2)$, Λ being the QCD cut-off parameter Here $A(x), B(x), C(x), D(x), K_1(x), K_2(x)$ and $K_3(x)$ are some functions of x mentioned in [9]

Now, let us discuss the limitation of the Taylor expansion method in this regard Applying the Taylor expansion [12] for the gluon distribution function in (1), we get

$$G\left(\frac{x}{1-z}, Q^2\right) = G\left(x + x\sum_{k=1}^{\infty} z^k, Q^2\right) = G(x, Q^2) + x\sum_{k=1}^{\infty} z^k \frac{\partial G(x, Q^2)}{\partial x} + \frac{1}{2}x^2\left(\sum_{k=1}^{\infty} z^k\right)^2 \frac{\partial^2 G(x, Q^2)}{\partial x^2} + O(x^3), \quad (16)$$

where $O(x^3)$ are the higher order terms Here we have $1 - x < z < 0 \Rightarrow |z| < 1$ which implies that $x/(1-z) = x\sum_{k=0}^{\infty} z^k$ is convergent In the previous methods either the terms beyond second order [3,4] or beyond first order derivatives [5,9] of x are neglected in the expansion series (16) But in actual practice this type of simplification is not possible because the contributions from the higher order terms cannot be neglected due to the singular behaviour of the gluon distribution

There are some other methods also which are not based on the Taylor expansion method Kotikov and Parente presented [7] a set of formulae to extract the gluon distribution function from the F_2 structure function and its scaling violation at small-x in the NLO approximation They considered for singlet quark and gluon parton distributions $p(x, Q^2) \approx x^{-\delta_i(Q^2)}$ for a Regge-like behaviour and $p(x\ Q^2) \approx \exp(0\,5(\delta_p(Q^2)\ln(1/x))^{1/2})$ for double-logarithmical behaviour [6] where $p \equiv s\ g$ and $\delta_s(Q^2) \neq \delta_g(Q^2)$ Then they put these distributions in the AP equations and solved for the gluon distribution by the standard moment method Now for Regge-like behaviour the gluon distribution becomes

$$g(x, Q^2) = \frac{1\ 14}{e\alpha(1 + 26\ 9\alpha)}\left[\frac{\partial F_2(x\ Q^2)}{\partial \ln Q^2} + 2\ 12\alpha F_2(x\ Q^2) + O(\alpha^2\ x^{1-\delta}\right] \quad (17)$$

for $\delta = 0\,5$ and the number of flavours $f = 4$ Again for double-logarithmical behaviour the gluon distribution becomes

$$g(x, Q^2) = \frac{3}{4e\alpha} \frac{1}{(1 + 26\alpha[1/\delta - 41/13])} \times \left[\frac{\partial F_2(x, Q^2)}{\partial \ln Q^2} + O(\alpha^2 x)\right] \quad (18)$$

A different method for the determination of the gluon distribution at small values of x has been proposed by Ellis Kunszt and Levin [6] based on the solution of the AP evolution equations in the moment space up to next-to-next-to-leading order (NNLO) In this method the quark and gluon momentum densities are assumed to behave as x^{-w_0} where w_0 is a parameter the actual value of which must be extracted from the data Here the gluon momentum density for four flavours is

$$xg(x, Q^2) = \frac{18/5}{P^{FG}(w_0)} \times \left[\frac{\partial F_2(x\ Q^2)}{\partial \ln Q^2} - P^{FF}(w_0) F_2(x\ Q^2)\right] \quad (19)$$

The evolution kernels P^{FF} and P^{FG} calculated in the $\overline{\text{MS}}$ scheme are expanded up to third order in α_s

3 Results and discussion

We use HERA data taken by the H1 [13] and ZEUS [14] collaborations where the values of $\partial F_2(x, Q^2)/\partial \ln Q^2$ are listed for a range of x values at $Q^2 = 20\,\text{GeV}^2$ The recent HERA data are parametrized by the H1 [15] and

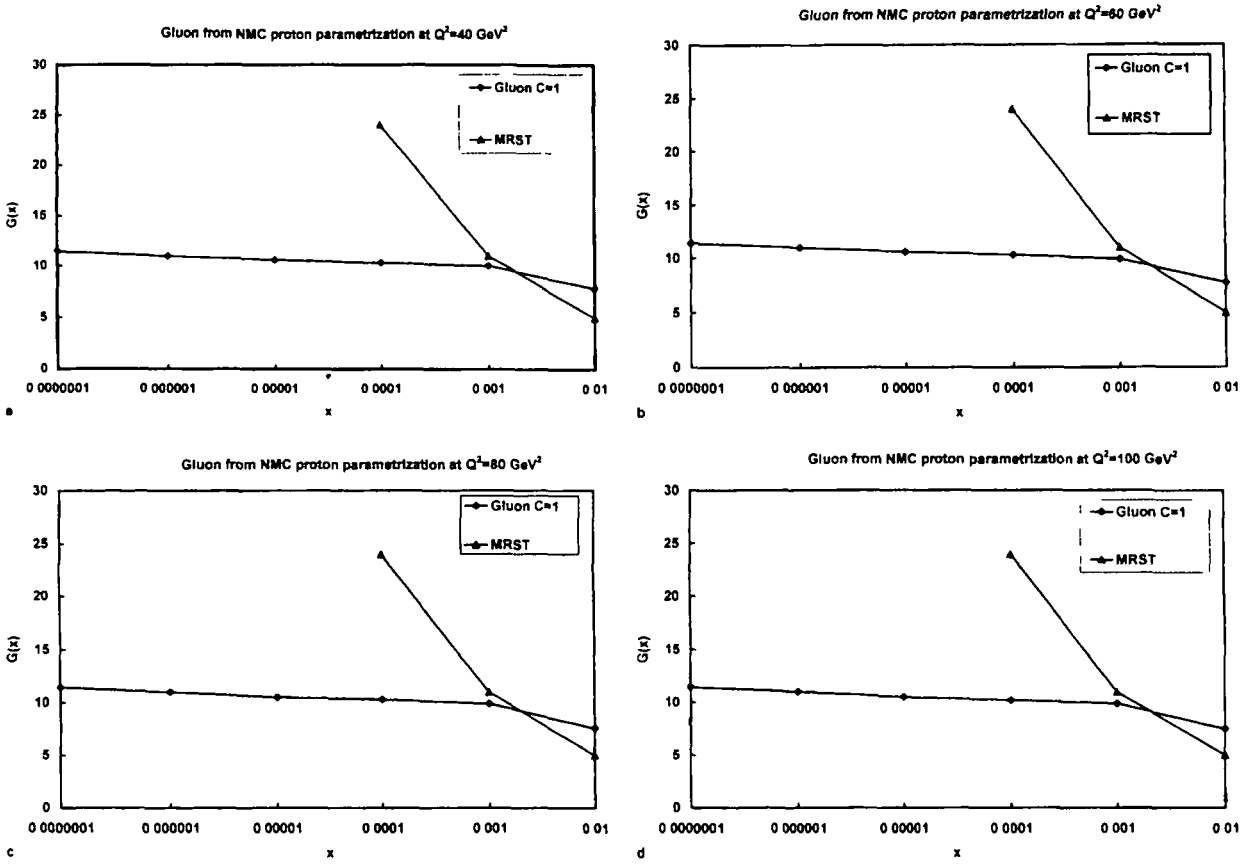

Fig. 2a,b. Gluon distribution $G(x)$ by our method from the NMC proton parametrization [17,18] at $Q^2 = 40, 60, 80$ and $100\,\mathrm{GeV}^2$ respectively with $C = 1$ In the same figure we include a global fit by MRST [21]

ZEUS [16] collaborations by some appropriate functions and we calculate $\partial F_2(x\ Q^2)/\partial \ln Q^2$ at $Q^2 = 20\,\mathrm{GeV}^2$ for those functions also We also use the parametrizations of the recent New Muon Collaboration (NMC) [17,18] F_2 proton structure function data from a 15-parameter function from which also we calculate $\partial F_2(x, Q^2)/\partial \ln Q^2$ at $40\,\mathrm{GeV}^2$ Now we apply the values of $\partial F_2(x, Q^2)/\partial \ln Q^2$ in (8) to calculate λ numerically by the iteration method [6] and hence the gluon distribution function $G(x, Q^2)$ for $C = 1$ We do not consider higher values of C, say $C = 100$, because in this case the neglect of the valence quark distribution $xq_{\mathrm{val}} \sim x^{1/2}$ is not so correct as the λ-value is close to -1/2 in quite a broad range of x Moreover, in this case we obtain $xg \sim x^{1/2}$ and $xq_{\mathrm{val}} \sim x^{1/2}$ Then also we get $xq_{\mathrm{sea}} \sim x^{1/2}$ Otherwise it should not be neglected in (1) Then it is easy to obtain $F_2 \sim x^{1/2}$ which contradicts the experimental data For our calculation the strong coupling constant α_s was taken from a NLO fit [19] to the F_2 data yielding $\alpha_s = 0\ 180 \pm 0\ 008$ at $Q^2 = 50\,\mathrm{GeV}^2$ corresponding to $\Lambda^{(4)}_{\overline{\mathrm{MS}}} = 0\ 263 \pm 0\ 042\,\mathrm{GeV}$ and $\alpha_s(M_{z^2}) = 0\ 113 \pm 0\ 005$ This value of α_s agrees with the one given by the Particle Data Group (PDG) [20] But in our practical calculations we neglect the errors of α_s and Λ which are rather small

We compare our result with the results of other authors discussed in the theory as well as the recent MRST global fit [21]

In Figs 2a–d we present the gluon distributions $G(x)$ for different low-x values from the NMC proton data parametrization [17,18] at $Q^2 = 40, 60, 80$ and $100\,\mathrm{GeV}^2$ respectively From the figures it is seen that the results are almost the same for all Q^2-values and $G(x)$ is slowly increasing when x decreases logarithmically We also present the MRST global fit [21] result, but its rate of increment is much higher

In Fig 3 we present the gluon distributions $G(x)$ for different low-x values from the H1 HERA proton data [13] at $Q^2 = 20\,\mathrm{GeV}^2$ The middle line is the result without considering any error in the data The upper and lower lines are the results with data adding and subtracting systematic and statistical errors with the middle values, respectively As usual the gluon distribution $G(x)$ increases when x decreases In the same graph we also present the $G(x)$ values for the MRST global fit [21] which is also increasing towards low-x values but with a somewhat smaller rate

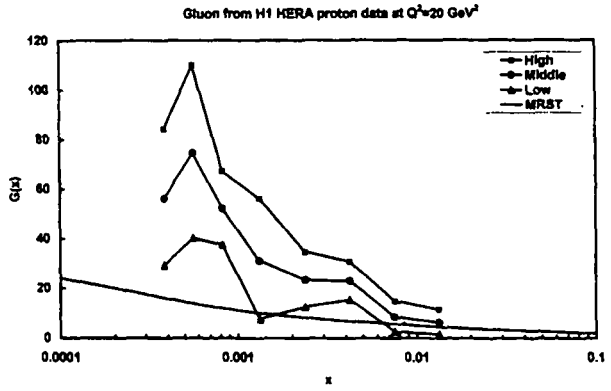

Fig. 3. Gluon distribution $G(x)$ by our method from the H1 HERA proton data [13] at $Q^2 = 20\,\mathrm{GeV}^2$ with $C = 1$. Here we present the results for the data (i) without considering the error (middle), (ii) adding algebrically statistical and systematic errors (high) and (iii) substracting algebrically statistical and systematic errors (low). In the same figures we include a global fit by MRST [21].

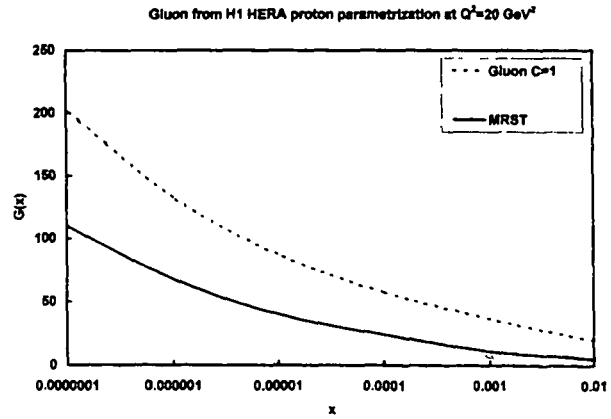

Fig. 4. Gluon distribution $G(x)$ by our method from the H1 HERA proton data parametrization [15] at $Q^2 = 20\,\mathrm{GeV}^2$ with $C = 1$. In the same figures we include a global fit by MRST [21].

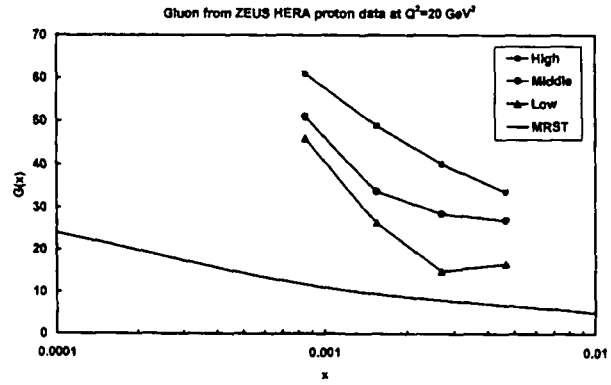

Fig. 5. Same result as in Fig. 3 from the ZEUS HERA proton data [14] at $Q^2 = 20\,\mathrm{GeV}^2$.

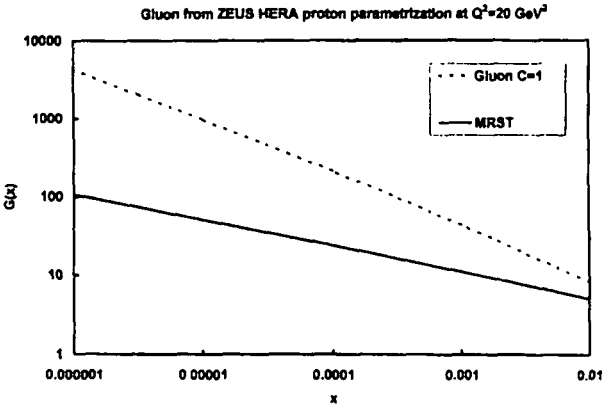

Fig. 6. Same result as in Fig. 4 from the ZEUS HERA proton data parametrization [16] at $Q^2 = 20\,\mathrm{GeV}^2$.

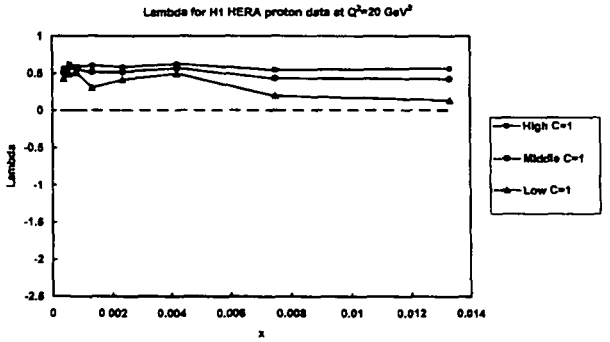

Fig. 7. λ-values by our method from the H1 HERA proton data [13] at $Q^2 = 20\,\mathrm{GeV}^2$ with $C = 1$. Here we present the results for the data (i) without considering the error (middle), (ii) adding algebrically statistical and systematic errors (high) and (iii) subtracting algebraically statistical and systematic errors (low).

In Fig. 4 we present the gluon distributions $G(x)$ for the H1 HERA proton parametrization [15] at $Q^2 = 20\,\mathrm{GeV}^2$ for different low-x values. The gluon distribution $G(x)$ is increasing when x is decreasing. In the same graph we present the $G(x)$ values for the MRST global fit [21], which is also increasing towards low-x values with a somewhat smaller rate.

In Fig. 5 we present the gluon distribution $G(x)$ ZEUS HERA proton data [14] at $Q^2 = 20\,\mathrm{GeV}^2$ for different low-x values. The descriptions and the results are the same as the H1 HERA data [13] depicted in Fig. 3.

In Fig. 6 we present the gluon distributions $G(x)$ for the ZEUS HERA proton parametrization [16] at $Q^2 = 20\,\mathrm{GeV}^2$ for different low-x values. The descriptions and the results are the same as the H1 HERA parametrization [15] depicted in Fig. 4.

In Fig. 7 we present the value of λ (Lambda) for the H1 HERA proton data [13] for low, middle and high values at $Q^2 = 20\,\mathrm{GeV}^2$ for different low-x values. All the graphs are almost parallel and the λ-values tend to ~ 0.5 at lower-x. That is, the parameter λ has a small dependence on x and

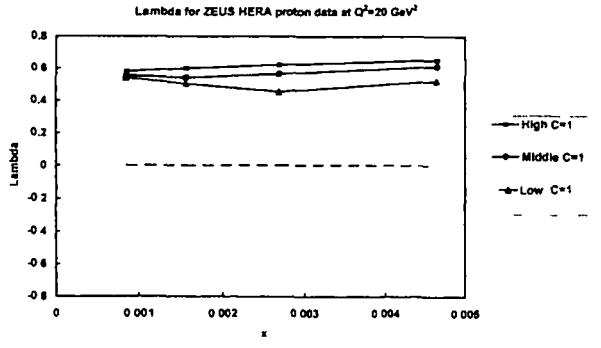

Fig. 8. Same result as in Fig 7 from the ZEUS HERA proton data [14] at $Q^2 = 20\,\mathrm{GeV}^2$

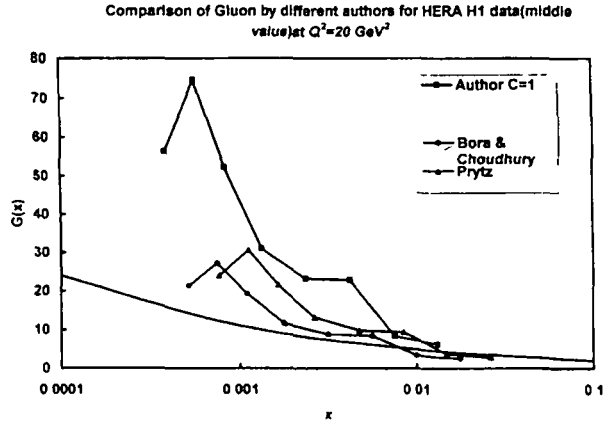

Fig. 9. Comparison of gluon distribution $G(x)$ from the H1 HERA proton data [13] by our method for $C = 1$ with those by other methods due to Bora and Choudhury [5] and Prytz [3] In the same figure, we include a global fit by MRST [21]

Q^2 This behaviour is in good agreement with experimental data [22], fits [21,23] and with the double-logarithmical semi-analytical analysis [24–26]

In Fig 8, we present the λ-values for the ZEUS HERA proton data [14] in the same way as in Fig 7 and the analysis is also the same For all the graphs λ values tend to $\sim 0\,5$ as we approach a lower-x from some higher values of x

In Fig 9, we compare our results for the HERA H1 data (middle value only) [13] at $Q^2 = 20\,\mathrm{GeV}^2$ with those of Bora and Choudhury [5] and Prytz [3] In the same figure, we also present the result for the MRST global fit [21] For all cases the gluon distribution $G(x)$ is increasing when x is decreasing but with different rates The rates of increment in our result is highest and in MRST is lowest

4 Summary and conclusion

In this paper we present an alternative method [2–9] to extract the gluon distribution $G(x, Q^2)$ from the scaling violation of the F_2 proton structure function $\partial F_2(x)/\partial \ln Q^2$ at low-x We compare our result with those of other methods due to Bora and Choudhury [5] and Prytz [3], and with a global fit due to MRST [21] The gluon distribution will increase as usual when x decreases

We discussed the limitations of the Taylor expansion method [12] in calculating the gluon distribution from the scaling violation of the F_2 structure function at low-x Prytz in both LO [3] and NLO [4] and Bora and Choudhury in LO [5] used this method to extract the gluon distribution from the scaling violation of the F_2 structure function at low-x in a slightly different way But all the authors neglected the higher order terms in the Taylor expansion series, which is not a good approximation for the singular behaviour of the gluon distribution at low-x, because the contributions from the higher order terms in the series are not negligible Sarma and Medhi [9] used this method in some improved way with a better approximation, yet the basic approximation of neglecting higher order terms in the expansion series could not be avoided On the other hand in the Kotikov and Parente method [7,8] also these authors approximated their results by neglecting some higher order terms Moreover, their method is to some extent complicated The Ellis, Kunszt and Levin method [6] neither has been more developed than other methods Though their analysis is up to NNLO, the kernels are parameter dependent and the x-ranges are lower than the HERA region In the present method of course we use a free parameter C, yet the other ambiguities due to the approximation of the Taylor expansion series can be avoided Moreover, our method is very simple and the computer programme can calculate the gluon distribution immediately when we put in the value of the scaling violation from experiment

We can use this method by assuming a double-logarithmical behaviour [7] of the gluon distribution at low-x also The present procedure is a LO analysis only But there is a possibility to extend this method to NLO or higher to have more accurate results

Acknowledgements One of us (JKS) is very grateful to Professor Dr R Ramachandran for providing the necessary facilities in IMSC, Chennai where most of the work was done He is also grateful to DST, New Delhi, for a SERC visiting fellowship in IMSC, Chennai and UGC, New Delhi, for financial assistance in the form of a minor research project

Appendix

A simple FORTRAN programme for the calculation of λ from the scaling violation of the structure function is given here

```
C     GLUON DISTRIBUTION FROM SCALING VIOLATION OF PROTON DATA
05    REAL Y, K, C, X, A, PHIX1, PHIX2, PHIX3, PHIX, P, AB, G
10    PRINT*, "Y=?"
15    READ*, Y
20    PRINT*, "K=?"
25    READ*, K
30    PRINT*, "C=?"
35    READ*, C
40    X=3
45    ALPH=.118
50    PI=3.1416
55    A=(5.*ALPH)/(9.*PI)
56    PHIX1=2./(X+3.)*(1.-Y**(X+3.))-2./(X+2.)*(1.-Y**(X+2.))
57    PHIX2=1./(X+1.)*(1.-Y**(X+1.))
58    PHIX3=ALOG(K/(A*C))
60    PHIX=1./ALOG(Y)*(ALOG(PHIX1+PHIX2)-PHIX3)
65    P=X-PHIX
70    AB=ABS(P)
75    G=C*(Y**(-PHIX))
80    IF (AB .LT. .00000001) THEN
            PRINT*, C, Y, PHIX, G
      GOTO 10
      ELSE
            X=PHIX
      ENDIF
      GOTO 56
85    END
```

References

1 See for example, Proceedings Workshop "Physics at HERA", edited by W Buchmuller, G Inglelman Hamburg (1991)
2 A M Copper-Sarkar et al , Z Phys C **39**, 281 (1988)
3 K Prytz, Phys Lett B **311**, 286 (1993)
4 K Prytz, Phys Lett B **332**, 393 (1994)
5 Kalpana Bora, D K Choudhury, Phys Lett B **354** 151 (1995)
6 R K Ellis, Z Kunszt, E M Levin, Nucl Phys B **420**, 517 (1994)
7 A V Kotikov, G Parente, Phys Lett B **379**, 195 (1996)
8 A V Kotikov, Phys Rev D **49**, 5746 (1994)
9 J K Sarma, G K Medhi, TU/THEP-1/98 (1998)
10 J Kwiecinski, A D Martin, R G Roberts, W J Stirling, Phys Rev D **42**, 3645 (1990)
11 P D B Collins, An introduction to Regge theory and high-energy physics (Cambridge University Press, Cambridge 1977)
12 J B Scarborough, Numerical mathematical analysis (John Hopkins Press, Baltimore 1996)
13 S Aid et al , H1 collaboration, Phys Lett B **354**, 494 (1995)
14 M Derrick et al , ZEUS collaboration, Phys Lett B **364**, 576 (1995)
15 T Ahmed et al , H1 collaboration, Nucl Phys B **439** 471 (1995)
16 M Derrick et al , ZEUS collaboration, DESY 94-143 August(1994)
17 M Arneodo et al , NMC, Phys Lett B **364**, 107 (1995)
18 M Arneodo et al , NMC, Nucl Phys B **483**, 3 (1997)
19 M Virchaux, A Milsztajn, Phys Lett B **274** 221 (1992)
20 L Montanet et al , Particle Data Group (PDG), Phys Rev D **50**, 1173 (1994)
21 A D Martin et al , DTP/98/10, RAL-tr-98-029, hep-ph/9803445 (1998)
22 S Aid et al , H1 collaboration, Nucl Phys B **470**, 3 (1996)
23 M Gluck, E Reya A Vogt, Eur Phys J C **5**, 461 (1998)
24 R D Ball, S Forte, Phys Lett B **336**, 77 (1994)
25 L Mankiewcz, A Saalfeld, T Weigl Phys Lett B **393** 175 (1997)
26 A V Kotikov, G Parente, Nucl Phys B **549** 242 (1999)

Proceedings of the Annual Technical Session,
Assam Science Society, 1999

REGGE BEHAVIOUR OF STRUCTURE FUNCTION AND GLUON DISTRIBUTION AT LOW-X IN LEADING ORDER

J. K. Sarma* and G. K. Medhi**

Abstract

We present a method to find the gluon distribution from F_2 proton structure function data at low-x assuming the Regge behaviour of gluon distribution function at this limit. We use the leading order (LO) Altarelli-Parisi (AP) evolution equation in our analysis and compare our result with those of other authors. We also discuss the limitations of Taylor expansion method in extracting gluon distribution from F_2 structure function use by those authors

Key words : Altarelli Parisi evolution equation, Bjorken variable, gluon distribution.

1. INTRODUCTION

The measurements of the quark (proton and the deuteron) structure functions by Deep Inelastic Scattering (DIS) processes in the low-x region where x is the Bjorken variable have opened a new era in parton density measurements [1]. It is important for understanding the inner structure of hadrons and ultimately of matter. It is also important to know the gluon distribution inside hadron at low-x because gluons are expected to be dominant in this region. On the other hand, gluon distribution can not be measured directly from experiments. It is, therefore, important to measure gluon distribution $G(x, Q^2)$. indirectly from the proton as well as the deuteron structure functions $F_2(x, Q^2)$

A few number of papers have already been published [2-9] in this connection. Here we present an alternative method to extract $G(x, Q^2)$ from scaling violations of $F_2(x, Q^2)$ with respect to lnQ^2 $\partial F_2(x,Q^2)/\partial lnQ^2$. Our method is mathematically more transparent and simpler than those of other authors

2. THEORY

It is shown in the ref. [2,8] that the gluon distribution at low-x can be obtained by analysing the longitudinal structure function. Similarly it is also shown in the ref. [3-7] that this distribution can be calculated from the proton structure function and its scaling violation Moreover in ref. [9] we see that it is also possible to calculate gluon distribution from deuteron structure function and its scaling violation. The basic idea lies on the fact that the scaling violation of quark structure function arises at low-x from the gluon distribution alone

*Physics Department, Tezpur University, Nappam, Tezpur - 784 028, Assam, India
**Physics Department, Birjhora Mahavidyalaya, Bongaigaon - 783 380, Assam. India

and does not depend on the quark distribution. Neglecting the quark the AP evolution equation for four flavours [3,4] gives

$$\frac{\partial F_2(x,Q^2)}{\partial \ln Q^2} = \frac{5\alpha_s}{9\pi} \int_0^{1-x} G(x/(1-x),\ Q^2).P_{qg}(z)\,dz \tag{1}$$

where the LO splitting function is

$$Pqg\ (z) = z^2 + (1 - z^2) \tag{2}$$

and α_s is the strong coupling coristant.

Now, let $1 - z = y \Rightarrow dz = -dy$. Again $z = 0 \Rightarrow y = 1$ and $z = 1 - x \Rightarrow y = x$. Therefore eq. (1) gives

$$\frac{\partial F_2(x,\ Q^2)}{\partial \ln Q^2} = \frac{5\alpha_s}{9\pi} \int_x^1 G(x/z,\ Q^2).\,(2z^2 - 2z + 1)\,dz. \tag{3}$$

Now, let us consider the Regge behaviour of gluon distribution [10]

$$G(x,\ Q^2) = C.x^{\lambda(Q^2)} \tag{4}$$

where C is a constant and $\lambda\,(Q^2)$ is the intercept. The Regge behaviour of the structure function $F_2(x)$ in the large-Q^2 region reflects itself in the small-x behaviour of the quark and the antiquark distributions. Thus the Regge behaviour of the sea quark and antiquark distributions for small-x is given by $q_{sea}\,(x) \sim x^{-\alpha p}$ corresponds to a pomeron exchange of intercept $\alpha p = 1$. But the valence quark distribution for small-x given by $q_{val}\,(x) \sim x^{-\alpha R}$ corresponds to a reggeon exchange of intercept $\alpha_R = 1/2$. Since the same processes lead to gluon and sea quarks distributions in the nucleon, we expect $G(x) \sim 1/x$. The x-dependence of the parton densities given above are often assumed at moderate-Q^2.

Applying eq.(4) in eq. (3) we get

$$\frac{\partial F_2(x,\ Q^2)}{\partial \ln Q^2} = \frac{5\alpha_s}{9\pi}.C. \int_x^1 x^{-\lambda(Q^2)}.z^{\lambda(Q^2)}.\,(2z^2 - 2z + 1)\,dz \tag{5}$$

For fixed Q^2 let $K(x) = \partial F^2\,(x,\ Q^2) / \partial \ln Q^2$ and $A = 5\alpha_s / (9\pi)$. Thus eq. (5) gives

$$K(x) = A.C.x^{-\lambda(Q^2)} \int_x^1 (2z^{\lambda+2} - 2z^{\lambda+1} + z^{\lambda})\,dz. \tag{6}$$

Taking logarithm and rearranging the terms eq. (6) gives

$$\lambda = \frac{1}{\ln x}\left[\ln\left\{\frac{2}{\lambda+3}\,(1 - x^{\lambda+3}) - \frac{2}{\lambda+2}\,(1 - x^{\lambda+2}) + \frac{1}{\lambda+1}\,(1 - x^{\lambda+1})\right\}\right]$$

$$- \frac{1}{\ln x}\,[\ln\,\{K\,(x)/(A.C)\}] \tag{7}$$

$$\Rightarrow \lambda - \Phi(\lambda) = 0 \tag{8}$$

where $\lambda \equiv \lambda\,(Q^2)$ and $\Phi\,(\lambda)$ represents the right hand side of eq. (7). Now, eq. (8) has been solved numerically using iteration method [11] to compute the values of $\lambda\,(Q^2)$ for different

x-values for a fixed value of Q. Scaling violation of structure function $K(x) = \partial F_2(x, Q^2)/\partial \ln Q^2$ and strong coupling constant at LO α_s are experimental inputs in our computations. C is the only free parameter in our computation. After computation of $\lambda(Q^2)$ we can compute $G(x, Q^2)$ from eq. (4) for different values of the free parameter C and compare our results with those due to other authors.

Now, let us discuss the methods due to other authors. Prytz reported a method to obtain an approximate relation between the unitegrated gluon density and scaling violations of quark structure function at low-x at leading order (LO) [3] as well as at next-to-leading order (NLO) [4]. He expanded $G(x/(1-z))$ of eq. (1) using Taylor expansion at $z = 1/2$ to obtain the expression [3]

$$G\left(\frac{x}{1-z}\right) \approx G\left(z = \frac{1}{2}\right) + \left(z - \frac{1}{2}\right) G'\left(z = \frac{1}{2}\right) + \left(z - \frac{1}{2}\right)^2 \frac{G''\left(x = \frac{1}{2}\right)}{2} \qquad (9)$$

taking upto second order derivative. This expression is then inserted in eq. (1) and after interation one gets

$$\frac{\partial F_2(x)}{\partial \ln Q^2} \approx \frac{5\alpha_s}{9\pi} \cdot \frac{2}{3} \cdot G(2x) \qquad (10)$$

for fixed Q^2 which is the main result for LO[3] analysis. Using a similar method he obtained the formula for NLO[4] analysis

$$\frac{\partial F_2(x)}{\partial \ln Q^2} \approx G(2x) \cdot \frac{20}{9} \cdot \frac{\alpha_s}{4\pi} \left[\frac{2}{3} + \frac{\alpha_s}{4\pi} \cdot 3.58\right] + \left(\frac{\alpha_s}{4\pi}\right)^2 \cdot \frac{20}{9} \cdot N(x, Q^2) \qquad (11)$$

where $N(x,Q^2)$ is given in ref. [4].

Bora and Choudhury also presented a method[5] to find the gluon distribution from the quark structure function and its scaling violation at low-x using Taylor expansion method. They also expanded $G(x/(1 - z), Q^2)$ of eq. (1) using Taylor expansion method about $z = 0$ taking only upto first order derivative in the expansion. While expanding they used only first two terms in the infinite expansion series $x/(1 - z) = x\sum_{k=0}^{\infty} z^k$ to get an expression. This expression is then inserted in eq (1) and after integration one gets

$$G(x_1, Q^2) \sim \frac{9\pi}{5\alpha_s} \cdot \frac{A(x) + 2B(x)}{[A(x) + B(x)]^2} \cdot \frac{\partial F_2(x, Q^2)}{\partial \ln Q^2} \qquad (12)$$

at

$$x_1 = x + \frac{B(x)}{A(x) + B(x)} \cdot x$$

Sarma and Medhi also obtained a method [9] to find the gluon distribution from proton and deuteron structure functions and their scaling violations at low-x. They also expanded $G(x/(1 - z), Q^2)$ of eq. (1) by using Taylor expansion method taking only upto first order derivative in the expansion. But unlike the Bora and Choudhury method, they considered the whole series $x/(1 - z) = x \sum_{k=0}^{\infty} z^k$ to get the expresion

$$G\left(\frac{x}{1-z},\ Q^2\right) = G\left(x + x\sum_{k=1}^{\infty} z^k,\ Q^2\right) = G(x,\ Q^2) + x\sum_{k=1}^{\infty} z^k\ \frac{\partial G\ (x,\ Q^2)}{\partial x} \quad . \qquad (13)$$

Using this relation in eq. (1) and then integrating one obtains for proton

$$G\ (x_p,\ t) = \frac{9\pi}{5\alpha_s} \cdot \frac{1}{A(x)} \cdot \frac{\partial F^p{}_2\ (x,\ t)}{\partial t} \qquad (14)$$

and for deuteron

$$G\ (x_d,\ t) = \frac{9}{5}\ \left[K_1(x)t\ \frac{\partial F^d{}_2\ (x,\ t)}{\partial t} + K_2\ \frac{\partial F^d{}_2\ (x,\ t)}{\partial x} + K_3\ F^d{}_2\ (x,\ t)\right], \qquad (15)$$

where $x_p = x + B(x) / A(x)$, $x_d = x + D(x)/C(x)$ and $t = ln(Q^2/\Lambda^2)$, Λ being the QCD cut off parameter. Here $A(x)$, $B(x)$, $C(x)$, $D(x)$, $K_1(x)$, $K_2(x)$ and $K_3\ (x)$ are some functions of x mentioned in ref. [9].

Now, let us discuss the limitation of Taylor expansion method in this regard. Applying Taylor expansion [11] in eq. (1), we get

$$G\left(\frac{x}{1-z},\ Q^2\right) = G\left(x + x\sum_{k=1}^{\infty} z^k,\ Q^2\right) = G(x,\ Q^2) + x\sum_{k=1}^{\infty} z^k \frac{\partial G\ (x,\ Q^2)}{\partial x}$$

$$+\frac{1}{2}\ x^2\ \left(\sum_{k=1}^{\infty} z^k\right)^2\ \frac{\partial^2 G\ (x,\ Q^2)}{\partial x^2}\ +\ O(x^3), \qquad (16)$$

where $O(x^3)$ are the higher order terms. Here we have $1 - x < z < 0 \Rightarrow |z| < 1$ which implies that $x\ /(1 - z) = x\ \sum_{k=0}^{\infty} z^k$ is convergent. In the previous methods, either the terms beyond second order [3,4] or beyond first order [5,9] derivatives of x are neglected in the expansion series eq. (17). But in actual practice, this type of simplification is not possible because the contributions from the higher order terms can not be neglected due to the singular behaviour of gluon distribution.

There are some other methods also which are not based on Taylor expansion method. Kotikov and Parente presented [7] a set of formulae to extract gluon distribution function from quark structure function and its scaling violation at small-x in the NLO approximation. They considered for singlet quark and gluon parton distributions $p(x,\ Q^2) \approx x^{-\delta_p}\ (Q^2)$ for Regge-like behaviour and $p(x,\ Q^2) \approx \exp\ (0.5\sqrt{\delta_p(Q^2)\ ln(1/x)})$ for Double-logarithmical behaviour [6] where $p \equiv s,\ g$ and $\delta_s(Q^2) \neq \delta_g\ (Q^2)$. Then they put these distributions in AP equations and solved for gluon distribution by standard moment method. Now for Regge-like behaviour, gluon distribution becomes

$$g(x,\ Q^2) = \frac{1.14}{e\alpha(1\ +\ 26.9\alpha)}\ \left[\frac{\partial F_2(x,\ Q^2)}{\partial lnQ^2}\ +\ 2.12\alpha F_2(x,\ Q^2)\ +\ O(\alpha^2,\ x^{1-\delta})\right] . \qquad (17)$$

for $\delta = 0.5$ and number of flavour $f = 4$. Again for Double-logarithmical behaviour gluon distribution becomes,

$$g(x, Q^2) = \frac{3}{4e\alpha} \quad \frac{1}{(1 + 26\alpha\,[1/\delta - 41/13])}$$

$$\left[\frac{\partial F_2(x, Q^2)}{\partial \ln Q^2} + O(\alpha^2 x) \right] \tag{18}$$

A different method for the determination of gluon distribution at small values of x has been proposed by Ellis, Kunszt and Levin[6] based on the solution of AP evolution equations in the moment space upto next-to-next-to leading order (NNLO) In this method quark and gluon momentum densities are assumed to behave as x^{-w_0} where w_0 is a parameter the actual value of which must be extracted from the data Here gluon momentum density for four flavour is

$$xg(x, Q^2) = \frac{18/5}{P^{FG}(w_0)} \left[\frac{\partial F_2(x, Q^2)}{\partial \ln Q^2} - P^{FF}(w_0)\, F_2(x, Q^2) \right] \tag{19}$$

The evolution kernels P^{FF} and P^{FG} calculated in $\overline{MS}$ scheme are expanded upto third order in α_s

3. RESULTS AND DISCUSSIONS

We use HERA data taken by H1[12] and ZEUS[13] collaborations where the values of $\partial F_2(x, Q^2)/\partial \ln Q^2$ are listed for a range of x values at $Q^2 = 20GeV^2$ The recent HERA data are parametrized by H1[14] and ZEUS[15] collaborations by some appropriate functions and we calculate $\partial F_2(x,Q^2)/\partial \ln Q^2$ at $Q^2 = 20GeV^2$ for those functions also We also use parametrizations of the recent New Muon Collaboration (NMC) [16, 17] proton structure function data from a 15-parameter function from which also we calculate $\partial F_2(x,Q^2)/\partial \ln Q^2$ at $40GeV^2$ Now we apply the values of $\partial F_2(x,Q^2)/\partial \ln Q^2$ in eq (8) to compute λ numerically by iteration method[6] and hence gluon distribution function $G(x,Q^2)$ for C = 1 and C = 100 For our calculations strong coupling constant α_s was taken from a NLO fit[18] to F_2 data which yield α_s = 0 180 ± 0 008 at Q^2 $50GeV^2$ corresponding to $\Lambda^{(4)}_{\overline{MS}}$ = 0 263 ± 0 042GeV and $\alpha_s(M_z^2)$ = 0 113 ± 0 005 This value of α_s agrees with the one given by Particle Data Group (PDG)[19] But in our practical calculations we neglected the errors of α_s and A which are rather small

We compare our result with the results of other authors discussed in the theory as well as the recent MRST global fit[20]

In Fig 1(a)-Fig 1(d) we present gluon distributions G(x) for different low-x values from NMC proton data parametrization [16,17] at Q^2 = 40, 60, 80 and $100GeV^2$ respectively for C=1 and C=100 From the figures it is seen that results are almost same for all Q^2 values and G(x) are slowly increasing when x decreases logarithmically We also present the MRST global fit[20] result, but its rate of increment is much higher The values of G(x) are higher for C=1 than those for C=100 for a particular value of low-x

In Fig 2(a) and Fig 2(b) we present the gluon distributions g(x) for different low x values from H1 HERA proton data[12] at $Q^2 = 20GeV^2$ for C=1 and C=100 respectively The middle line in each figure is the result without considering any error in the data The upper and lower lines are the result with data adding and subtracting systematic and statistical errors with the middle values respectively As usual gluon distribution G(x) increases when x decreases but the whole system of lines in the graphs shifts towards the lower G(x) values when we change from C=1 to C=100 In the same graphs we also present the G(x) values for MRST global fit[20] which is also increasing towards low-x values but with somewhat lesser rate But for C=100 our G(x) values come in the range of this fit

In Fig 3 we present the gluon distributions G(x) for H1 HERA proton parametrization[14] at $Q^2 = 20GeV^2$ for different low-x values for C=1 and C=100 respectively Gluon distribution G(x) is increasing when x is decreasing, but the line in the graph shifts towards the lower G(x) values when we change from C=1 to C=100 In the same graph we present the G(x) values for MRST global fit[20] which is also increasing towards low-x values with somewhat lesser rate But for C=100 our G(x) values are closer to this fit

In Fig 4(a) and Fig 4(b) we present the gluon distributions G(x) ZEUS HERA proton data[13] at $Q^2 = 20GeV^2$ for different low-x values for C=1 and C=100 respectively The descriptions and the results are same as H1 HERA data[12] depicted in Fig 2(a) and Fig 2(b) respectively

In Fig 5 we present the gluon distributions G(x) for ZEUS HERA proton parametrization[15] at $Q^2 = 20GeV^2$ for different low-x values for C=1 and C=100 The descriptions and the results are same as H1 HERA parametrization[14] depicted in Fig 3

In Fig 6 we present the value of λ (Lambda) for H1 HERA proton data[12] for low, middle and high values of them at $Q^2 = 20GeV^2$ for different low-x values for C=1 and C=100 For C=1, all the graphs are almost parallel and λ-values tend to ~ 0 5 at low-x For C=100 for all the graphs λ-values tend to ~ 0 0 from some negative values at low x

In Fig 7, we present the λ-values for ZEUS HERA proton data[13] in the same way as in Fig 6 For C=1, for all the graphs λ-values tend to ~ 0 5 as we approach lower x from some slightly higher values in comparatively higher-x On the other hand for C=100, for all the graphs λ-values tend to ~ - 0 1 as we approach lower-x from some slightly lower negative values in comparatively higher-x

If Fig 8, we compare our results for Hera H1 data (middle value only) [12] at $Q^2 = 20GeV^2$ for C=1 and C=100 with those of Bora and Choudhury [5] and Prytz[3] In the same Fig we also present the result for MRST global fit[20] For all the cases gluon distribution G(x) is increasing when x is decreasing but with different rates The rates of increment in our result for C=1 is highest and in MRST, lowest But our result with C=100 is very close with that of Bora and Choudhury and also inside the range of MRST

4. SUMMARY AND CONCLUSION

In this method we present an alternative method to extract gluon distribution $G(x,Q^2)$ from the scaling violation of proton structure function $\partial F_2(x)/\partial lnQ^2$ at low-x We compare our result with those of other methods due to Bora and Choudhury[5] and Prytz[3], and with a global fit due to MRST[20] Gluon distribution will increase as usual when x decreases with different rates for the different values of the parameter C=1 nd C=100 But our graph with C=100 is very close to that due to Bora and Choudhury and the global fit due to MRST

We discussed the limitations of Taylor expansion method[11] in calculating gluon distribution from scaling violation of structure function at low-x Prytz in both LO[3] and NLO[4] and Bora and Choudhury in LO[5] used this method to extract gluon distribution from scaling violation of structure function at low-x in a slightly different way But all these authors neglected the higher order terms in the Taylor expansion series which is not a good approximation for a singular behaviour of gluon distribution at low-x because the contributions from the higher order terms in the series are not negligible Sarma and Medhi [9] used this method in an improved way with less number of approximations, yet the basic approximation of neglecting higher order terms in the expansion series could not be avoided On the other hand in Kotikov and Parente method [7,8] also the authors approximated their results by neglecting some higher order terms Moreover their method is to some extent complicated Again Ellis, Kunszt and Levin method[6] is also not more developed than other methods Though their analysis is upto NNLO, the kernels are parameter dependent and its x-ranges are lower than HERA region In the present method of course we use a free parameter C, yet the other ambiguities due to the approximation of the Taylor expansion series can be avoided. Moreover our method is a very simple one

We can use this method by assuming the Double-logarithmical behaviour[7] of gluon distribution at low-x also The present procedure is an LO analysis only But there is possibility to extend this method to NLO or higher to have more accurate results

ACKNOWLEDGEMENT

One of us (JKS) is very much grateful to Professor Dr R Ramachandran for providing necessary facilities in IMSC, Chennai where most of the work was done. He is also grateful to DST, New Delhi for a SERC visiting fellowship in IMSC, Chennai

Fig.1(a) : from NMC proton parametrization at $Q^2 = 40GeV^2$

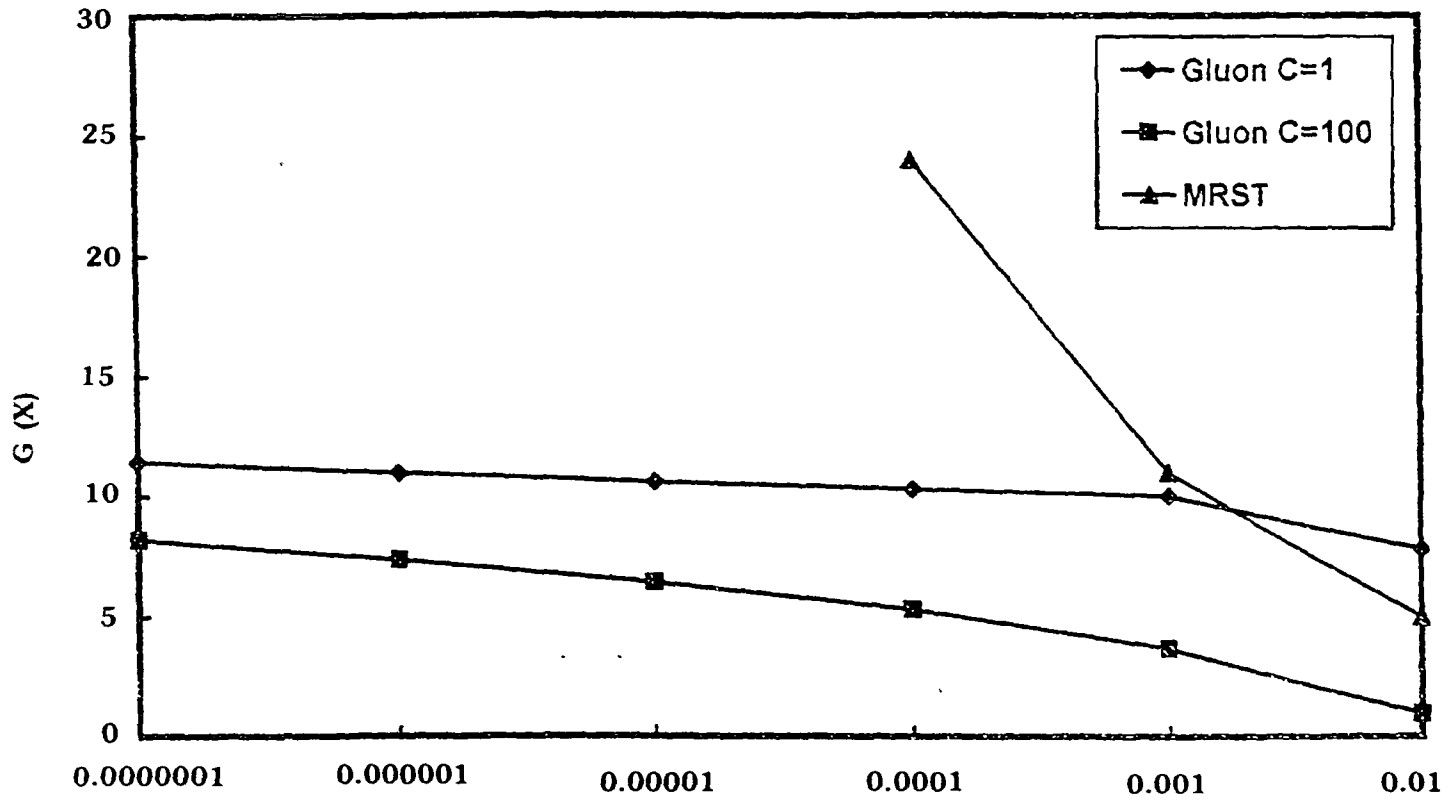

Fig.1(a) : Gluon distribution G(x) by our method from NMC proton parametrization[16] 17] at $Q^2 = 40, 60, 80$ and $100GeV^2$ respectively with C=1 and C=100 In the same figure we include a global fit by MRST[20]

Fig.1(b) : Gluon from NMC proton parametrization at $Q^2 = 60GeV^2$

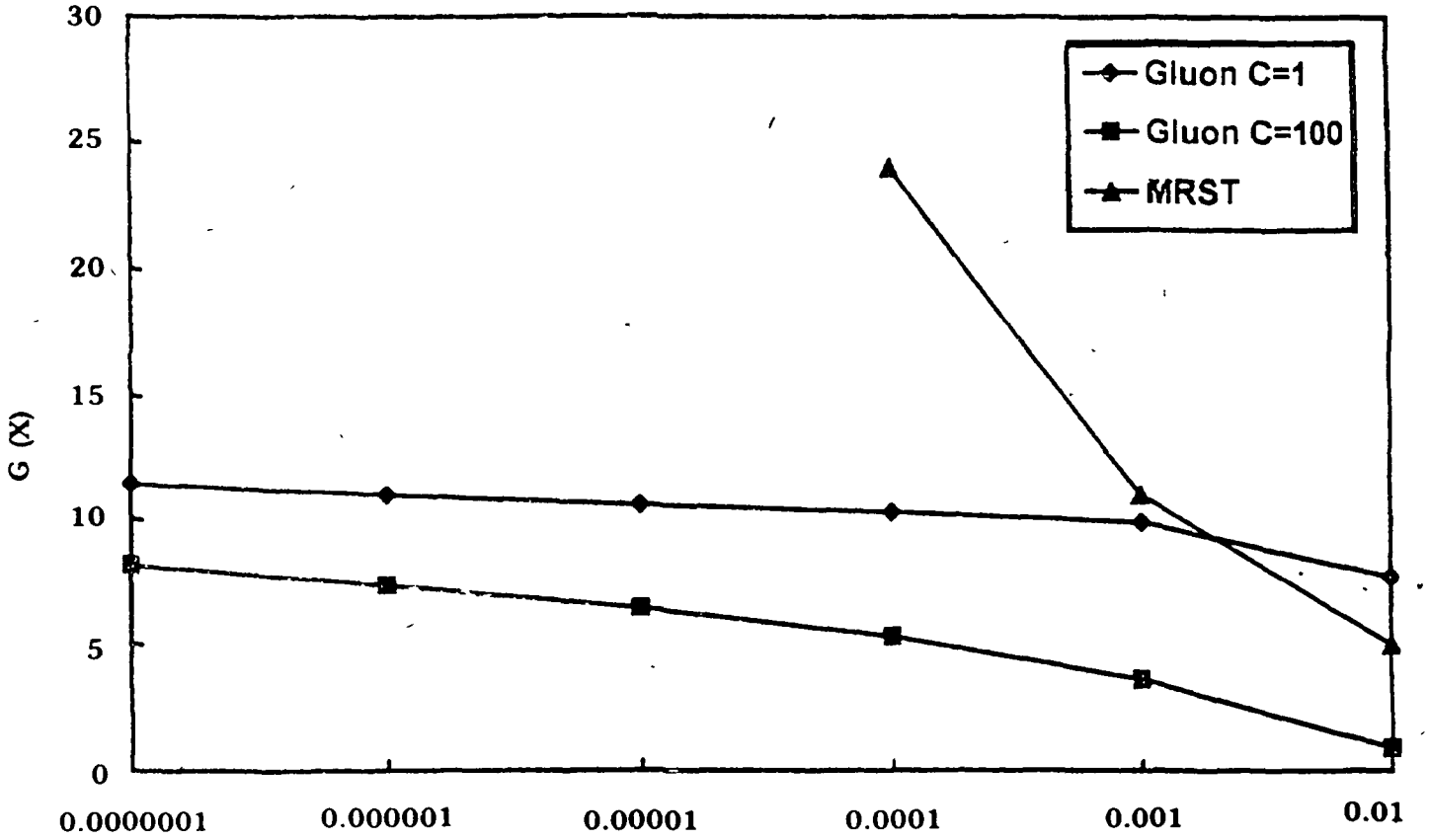

Fig.1(b) : Gluon distribution G(x) by our method from NMC proton parametrization[16] 17] at Q^2 = 40, 60, 80 and $100GeV^2$ respectively with C= 1 and C=100 In the same figure we include a global fit by MRST[20]

Fig.1(c) : Gluon from NMC proton parametrization at $Q^2 = 80GeV^2$

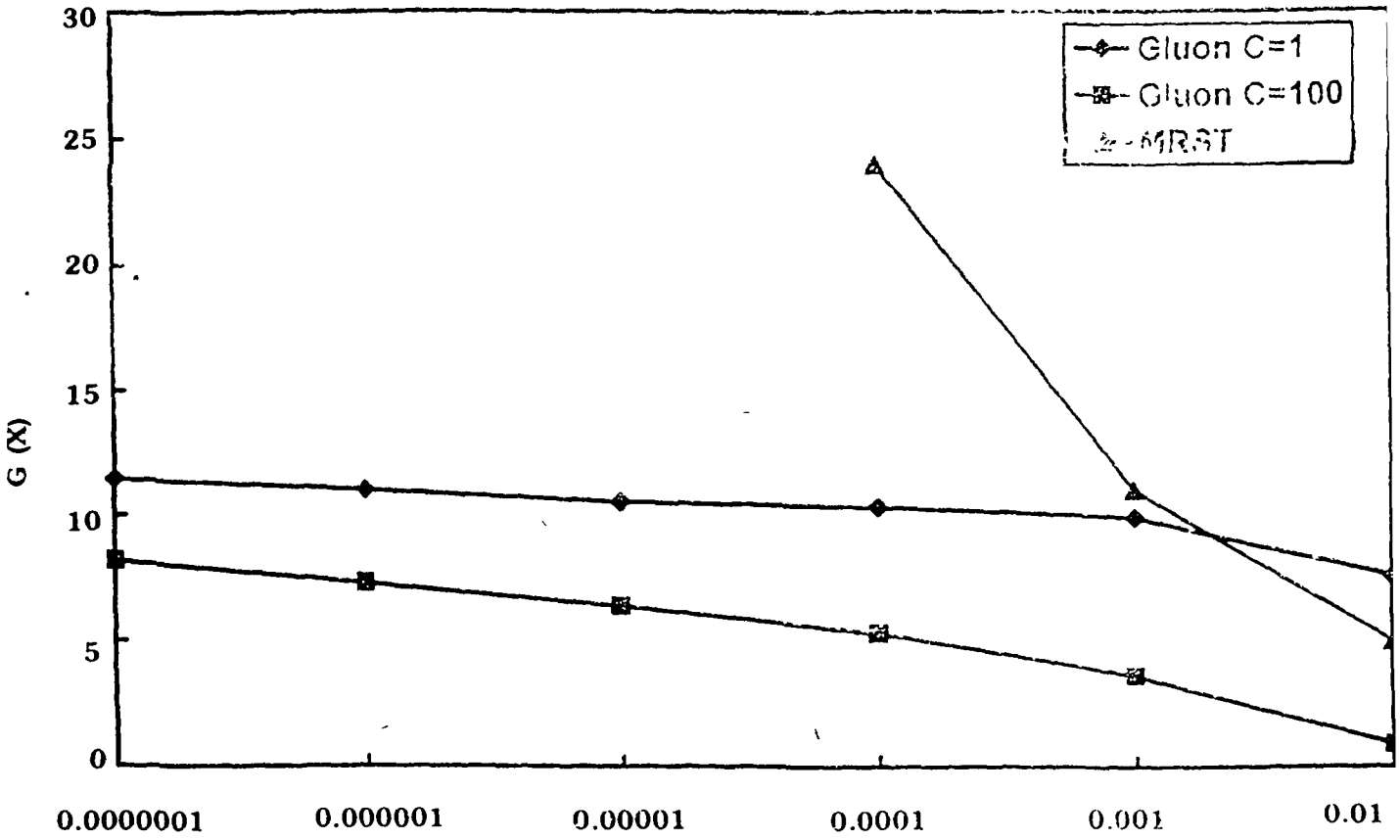

Fig.1(c) : Gluon distribution G(x) by our method from NMC proton parametrization[16] 17] at $Q^2 = 40$ 60, 80 and $100GeV^2$ respectively with C=1 and C=100 In the same figure we include a global fit by MRST[20].

Fig.1(d) : Gluon from NMC proton parametrization at Q^2 = 100 GeV^2

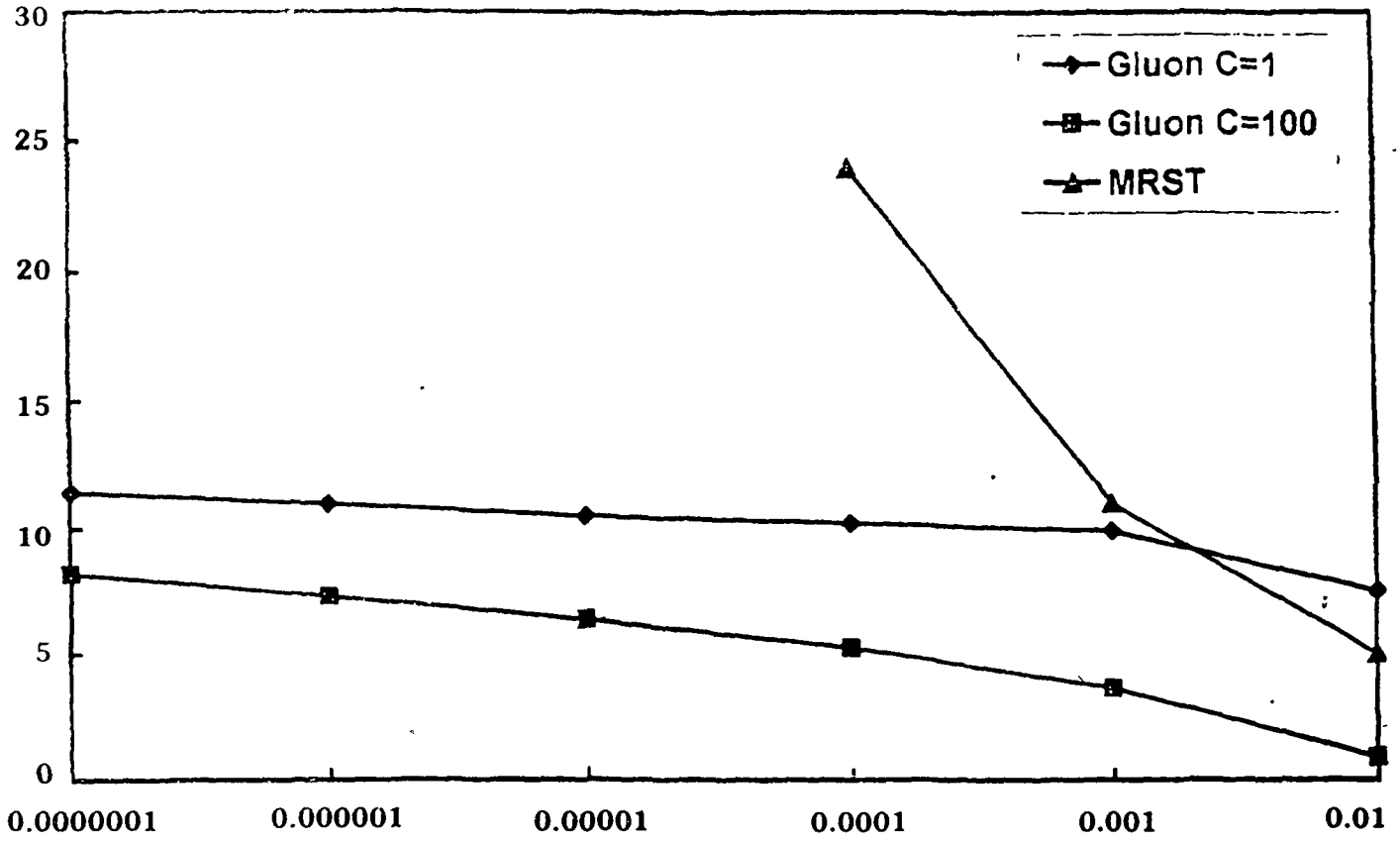

Fig.1(d) : Gluon distribution G(x) by our method from NMC proton parametrization[16] 17] at Q^2 = 40, 60, 80 and 100GeV^2 *respectively with C=1 and C=100 In the same figure we include a global fit by MRST[20]*

Fig.2 (a) : Gluon from H1 HERA proton data at $Q^2 = 20\ GeV^2$ (C=1)

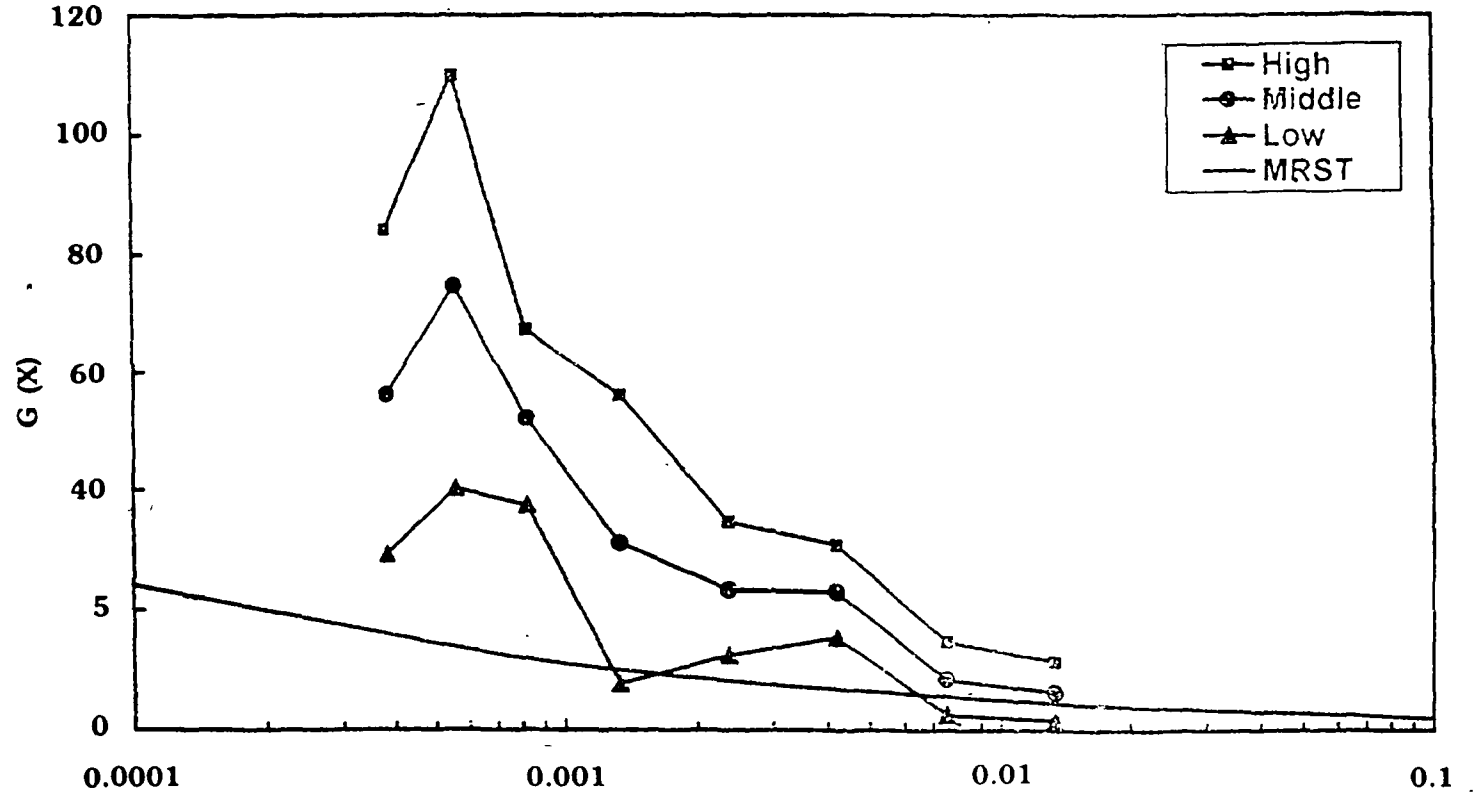

Fig.2(a) : Gluon distribution G(x) by our method from H1 HERA proton data[12] at $Q^2 = 20GeV^2$ with C=1 and C=100 respectively Here we present the results for the data (i) without considering the error (middle), (ii) adding algebrically statistical and systematic errors (high) and (iii) substracting algebrically statistical and systematic errors(low) In the same figure we include a global fit by MRST[20].

Fig.2 (b) : Gluon from H1 HERA proton data at Q^2 = 20 GeV^2 (C=100)

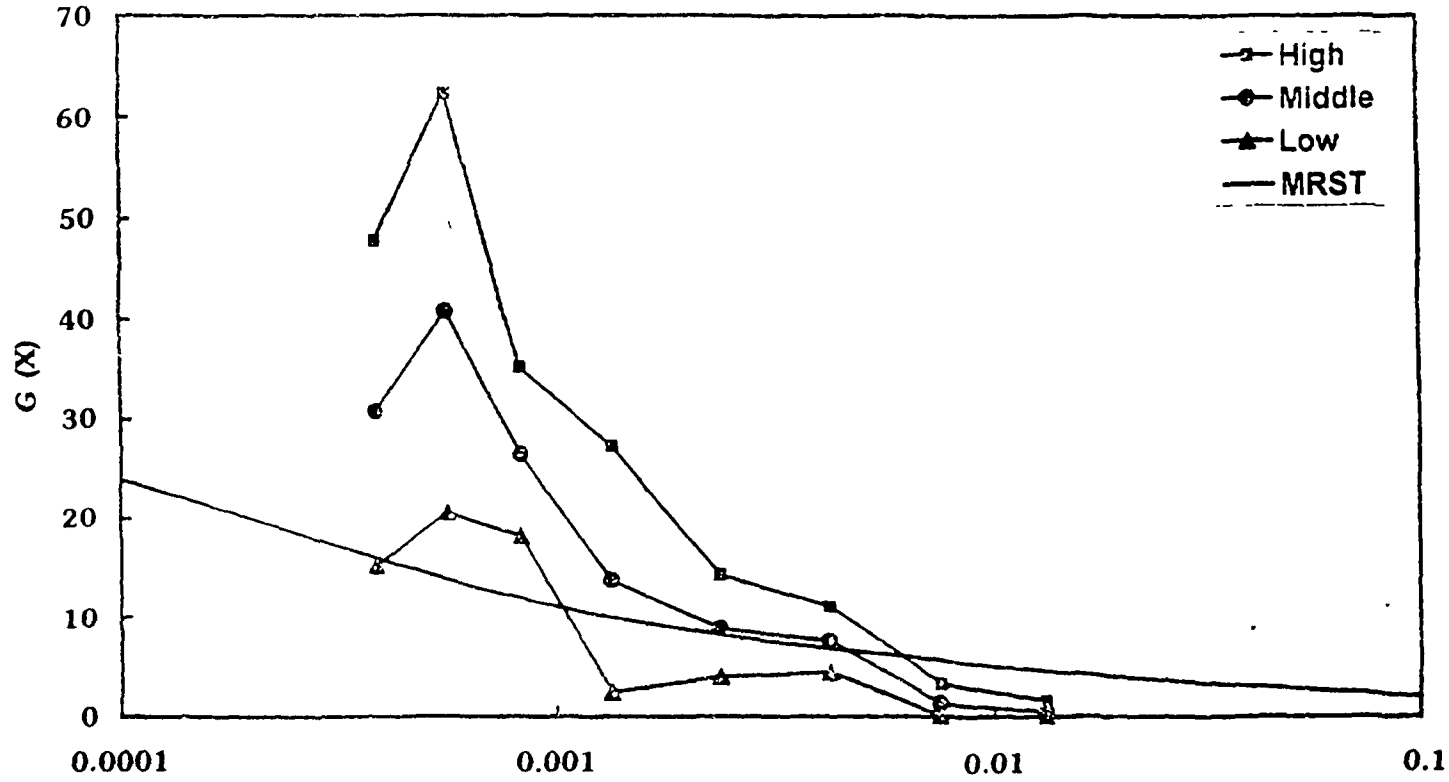

Fig.2(b) : Gluon distribution G(x) by our method from H1 HERA proton data[12] at Q^2 = 20GeV^2 with C=1 and C=100 respectively Here we present the results for the data (i) without considering the error (middle), (ii) adding algebrically statistical and systematic errors (high) and (iii) substracting algebrically statistical and systematic errors(low) In the same figure we include a global fit by MRST[20]

Fig.3 : Gluon from H1 HERA proton parametrization at $Q^2 = 20\ GeV^2$

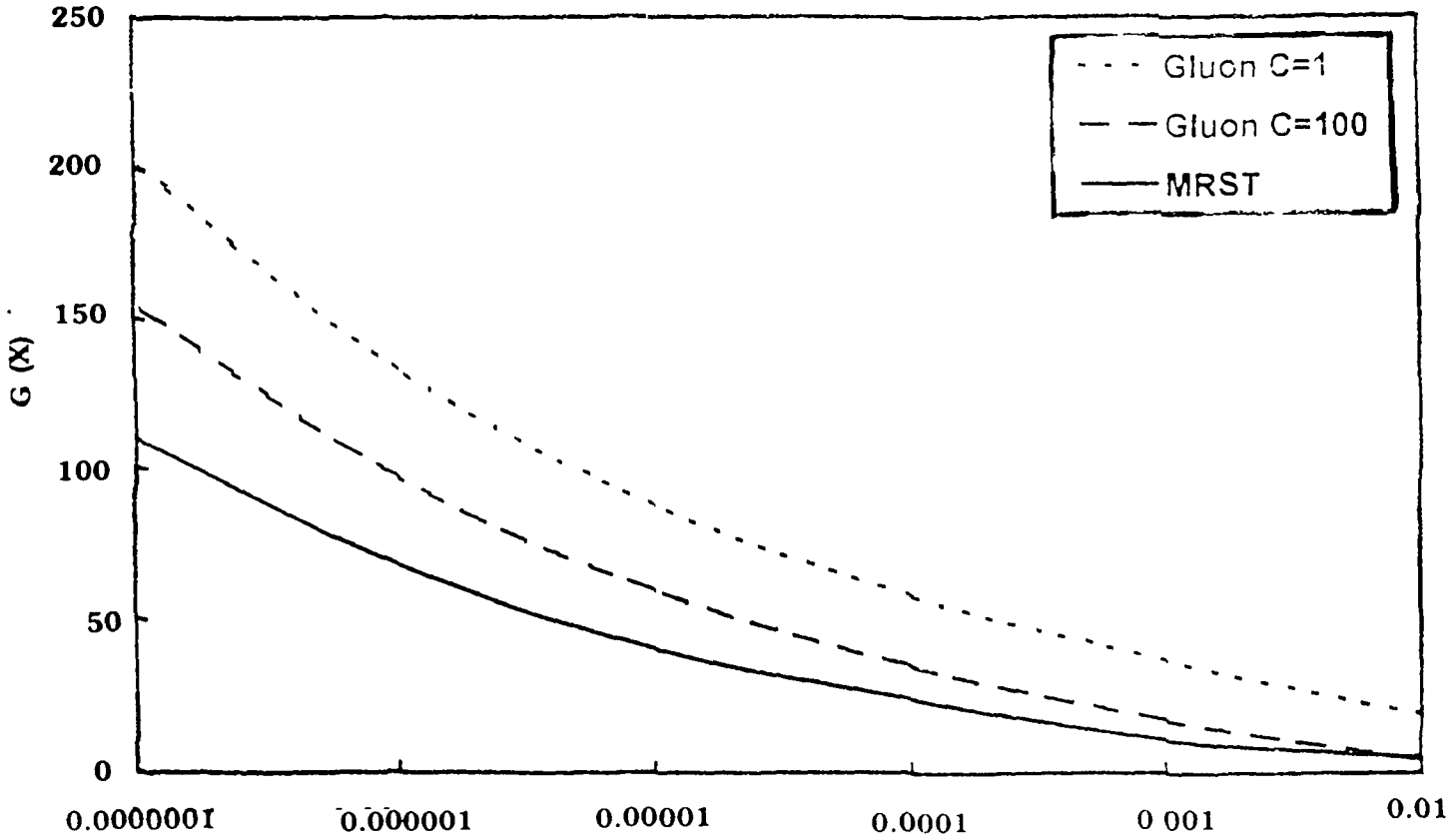

Fig.3 : Gluon distribution G(x) by our method from H1 HERA proton data parametrization[14] at $Q^2 = 20GeV^2$ with C=1 and C=100 In the same figure we include a global fit by MRST[20]

Fig.4(a) : Gluon from ZEUS HERA proton data at Q^2 = 20 GeV^2 (C=1)

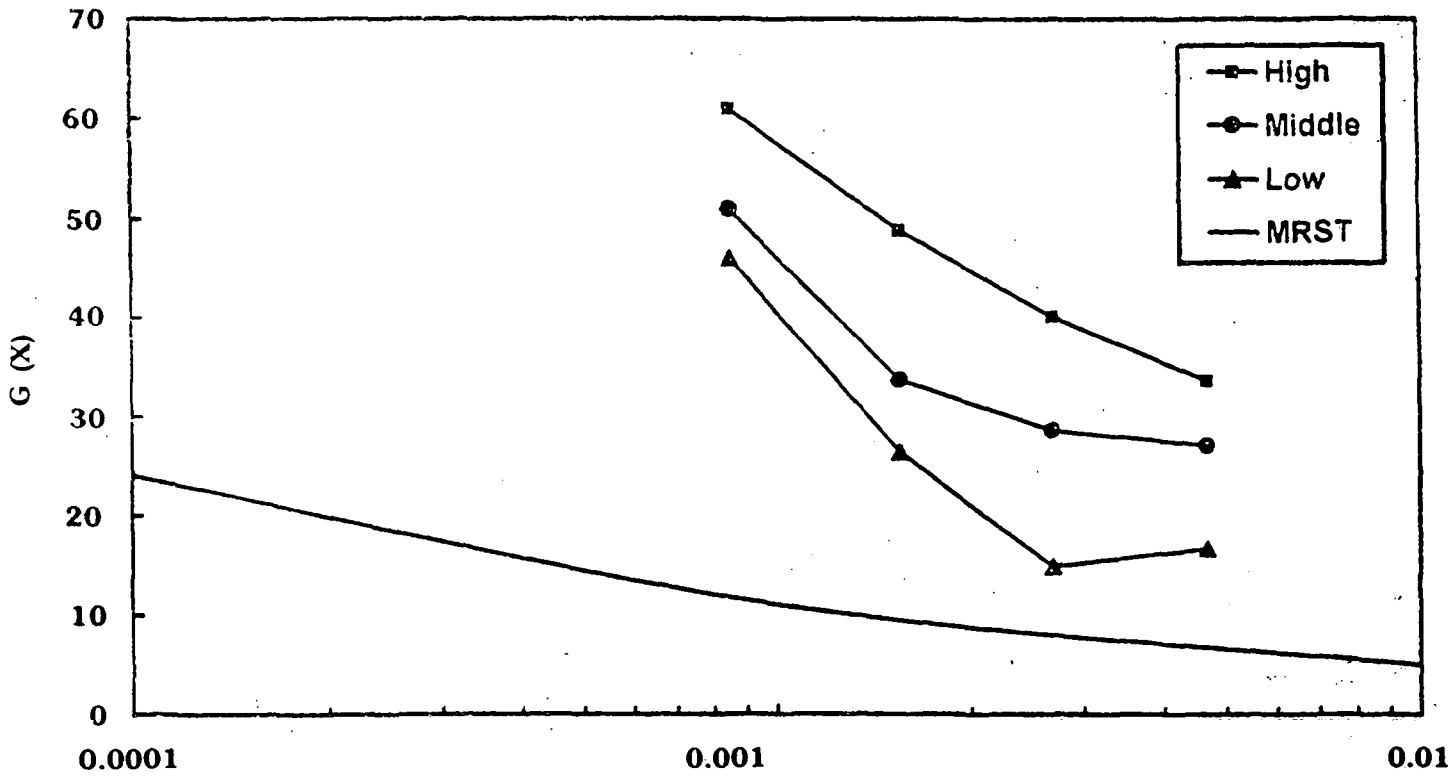

Fig.4(a) : Same result as in Fig.2(a)-2(b) respectively from ZEUS HERA proton data[13] at Q^2 = 20GeV^2.

Fig.4(b) : Gluon from ZEUS HERA proton data at Q^2 = 20 GeV^2 (C=100)

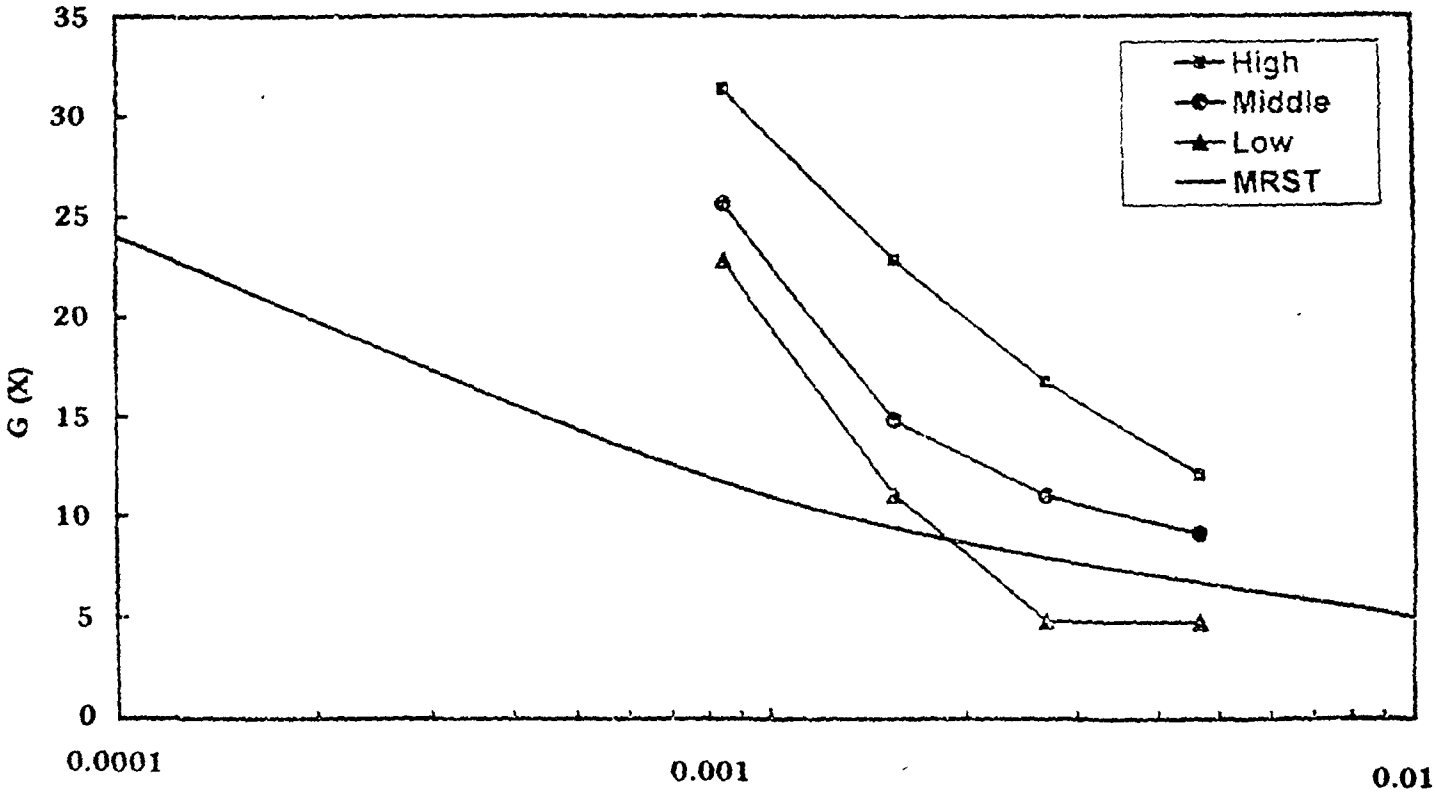

Fig.4(b) : Same result as in Fig 2(a)-2(b) respectively from ZEUS HERA proton data[13] at Q^2 = 20GeV^2

Fig.5 : Gluon from ZEUS HERA proton parametrization at Q^2 = 20 GeV^2

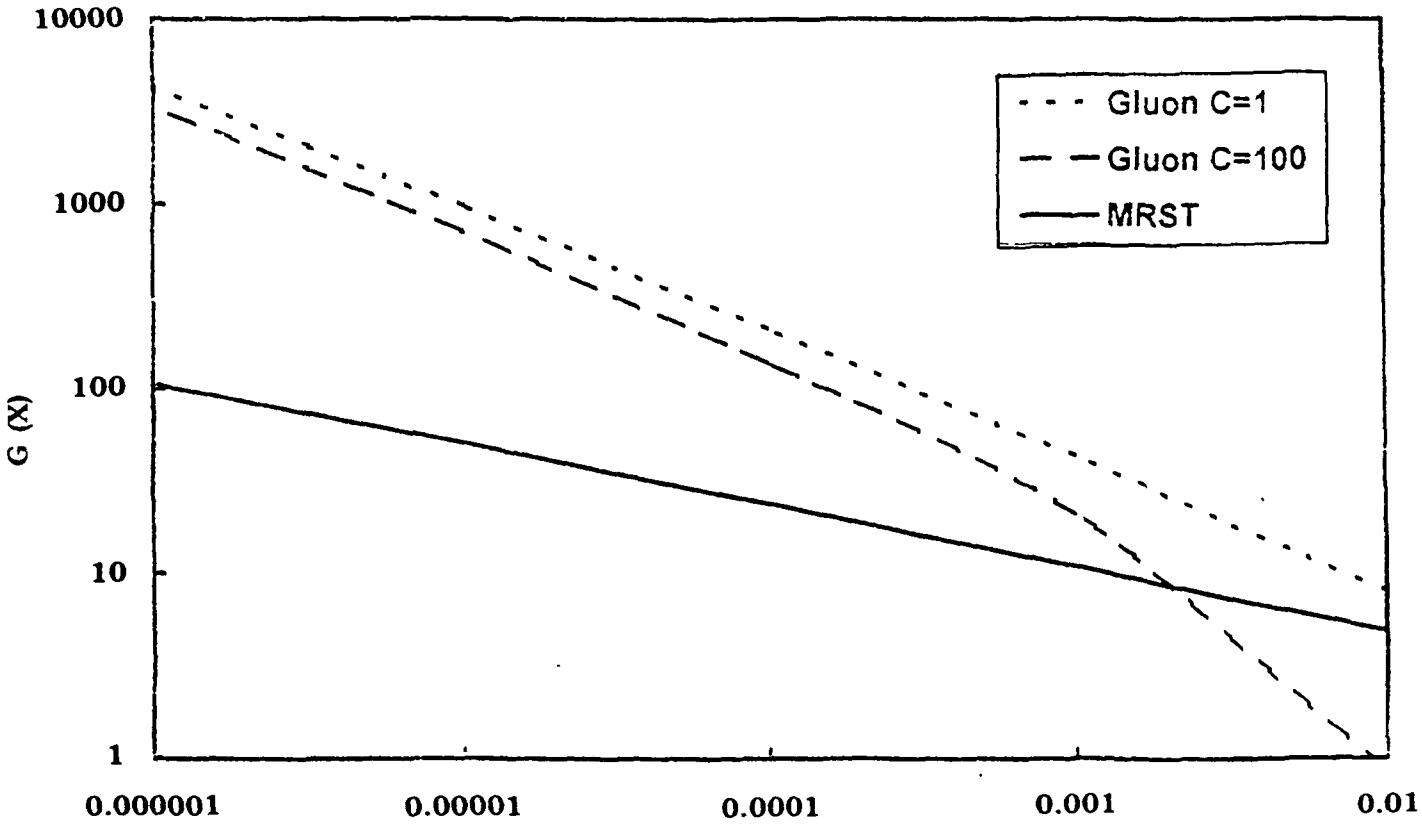

Fig.5 : Same result as in Fig 3 from ZEUS HERA proton data parametrization[15] at Q^2 = 20GeV^2

Fig.6 : Lambda for H1 HERA proton data at Q^2 = 20 GeV^2

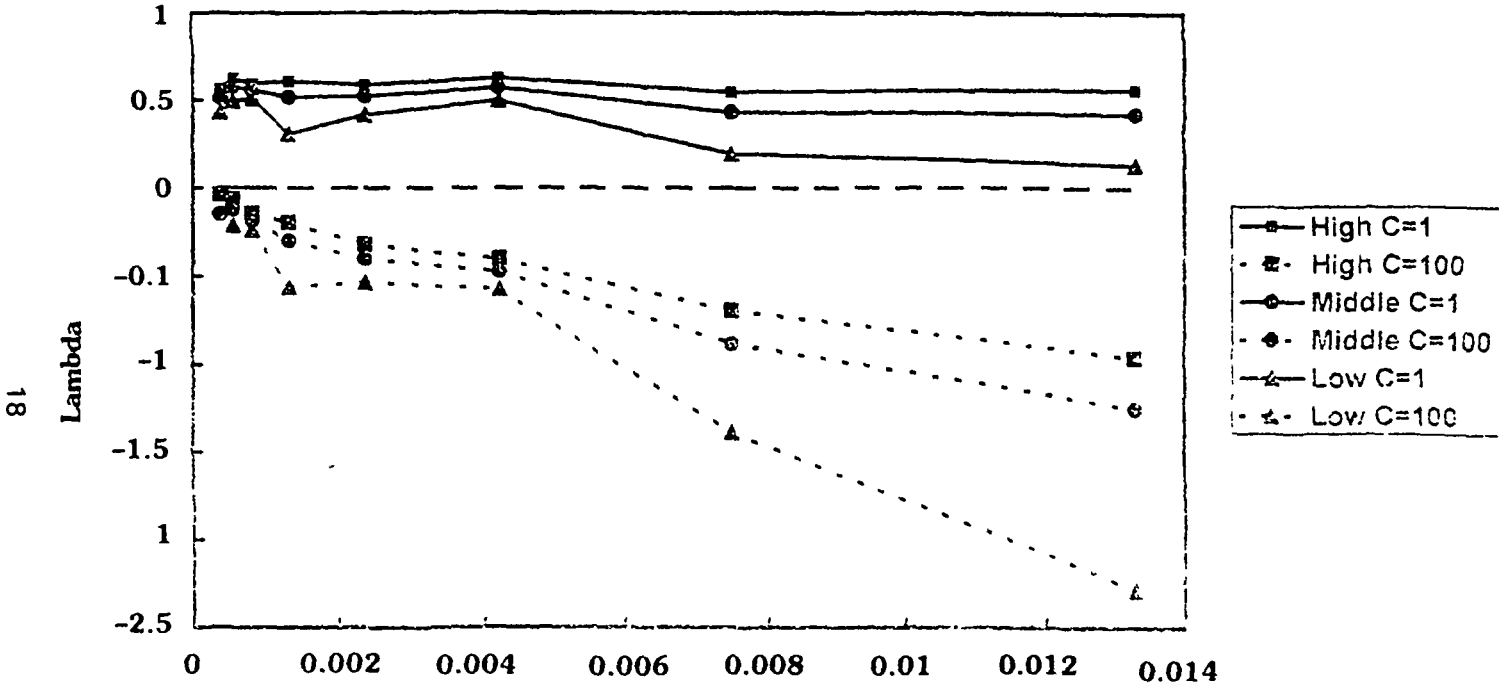

Fig.6 : λ-values by our method from H1 HERA proton data[12] at Q^2 = 20GeV^2 with C=1 and C=100 Here we present the results for the data (i) without considering the error(middle), (ii) adding algebrically statistical and systematic errors (high) and (iii) substracting algebrically statistical and systematic errors (low)

Fig.7 : Lambda for ZEUS HERA proton data at Q^2 = 20 GeV^2

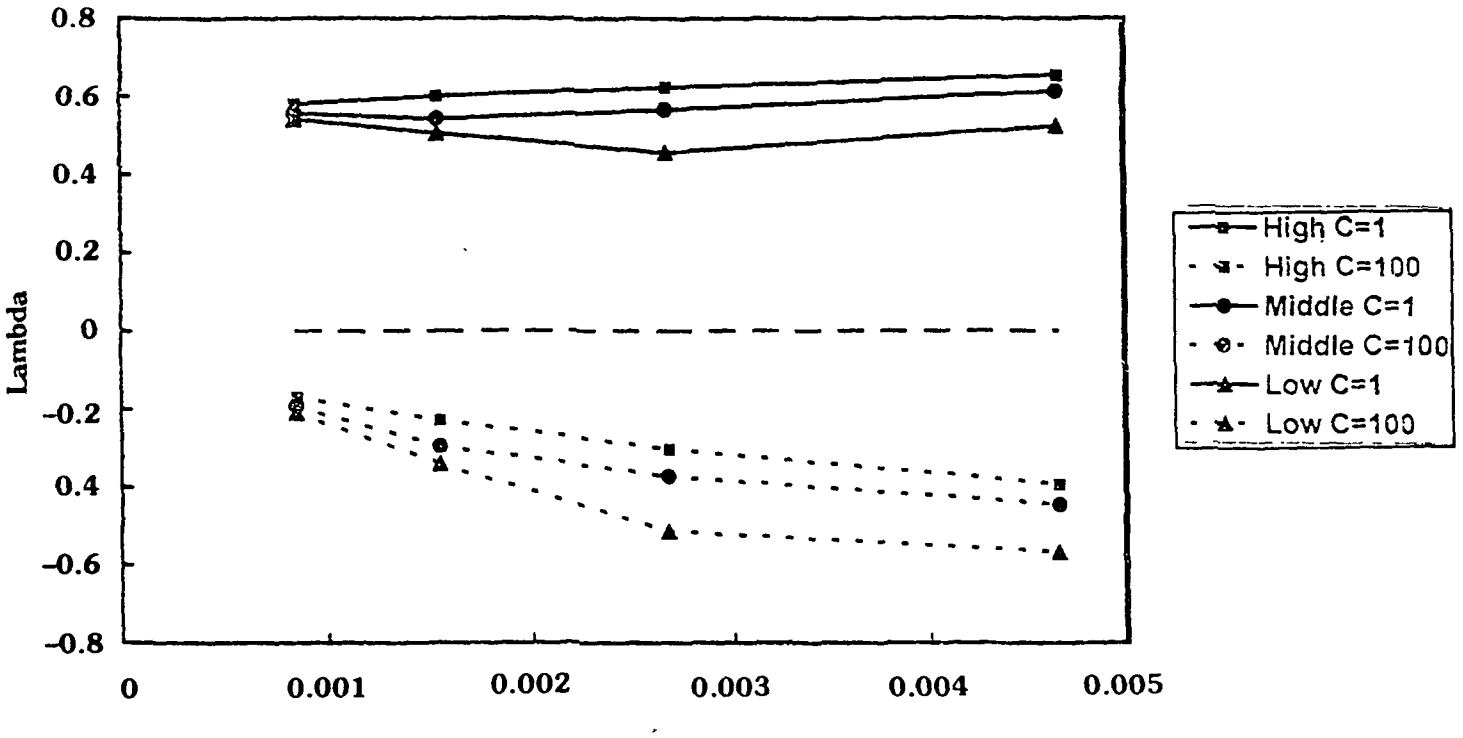

Fig.7 : Same result as in Fig 6 from ZEUS HERA proton data[13] at Q^2 = 20GeV^2

Fig.8 : Comparison of Gluon by different authors for HERA H1 data (middle value) at Q^2 = 20 GeV^2

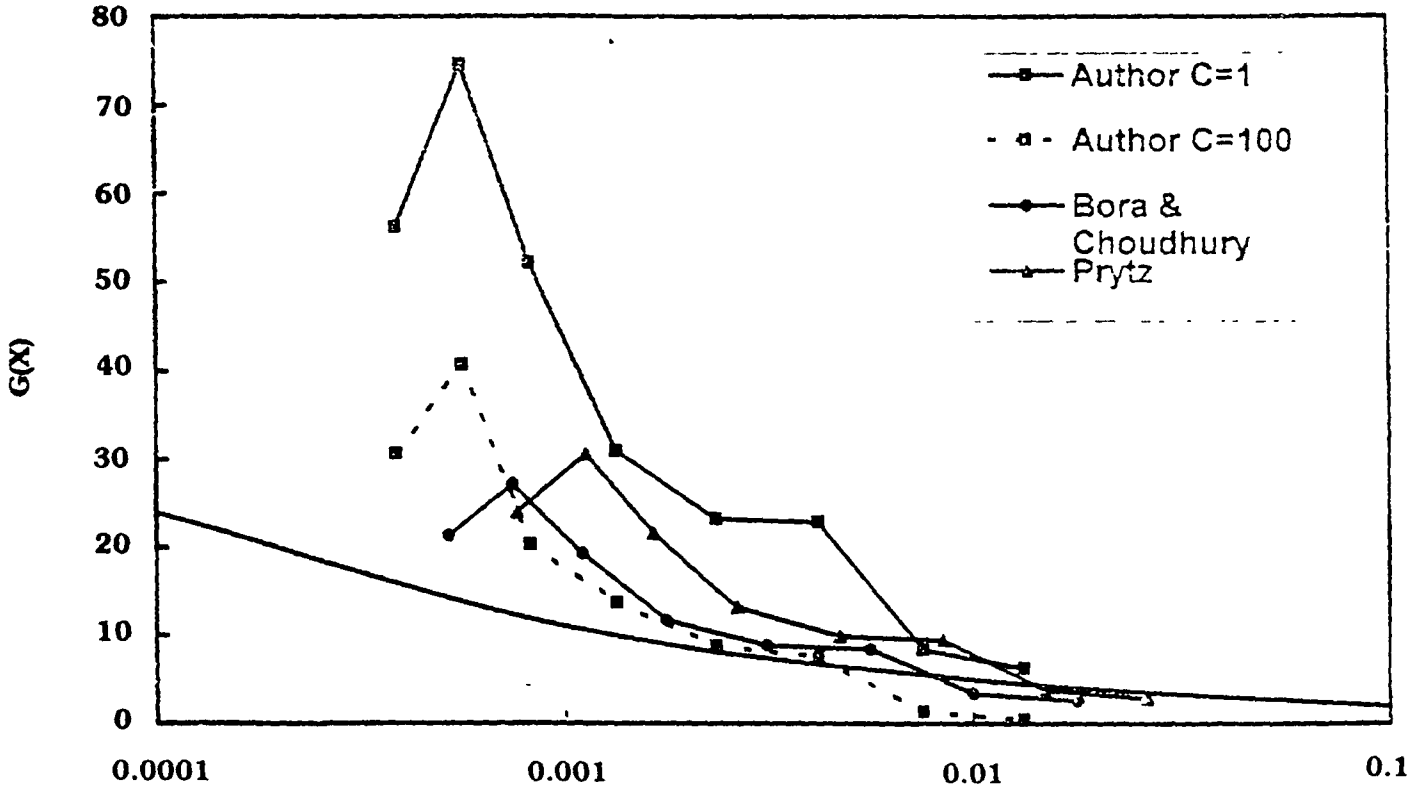

Fig.8 : Comparison of gluon distribution G(x) from H1 HERA proton data[12] by our method for C=1 and C=100 with those by other methods due to Bora and Choudhury[5] and Prytz[3] In the same figure, we include a global fit by MRST[20]

REFERENCES

[1] See for example, W Buchmuller and G Inglelman, eds , *Proc Workshop 'Physics at HERA'*, Hamburg (1991)

[2] A M Copper Sarkar *et al* , *Z Phys* C39 (1988) 281

[3] K Prytz, *Phys Lett* B311 (1993)286

[4] K Prytz, *Phys Lett* B332 (1994)393

[5] Kalpana Bora and D K Choudhury, *Phys Lett* B354 (1995)151

[6] R K Ellis, Z Kunszt and E M Levin, *Nucl Phys* B420 (1994) 517

[7] A V Kotikov, G Parente, *Phys Lett* B379 (1996) 195

[8] A V Kotikov, *Phys Rev* D49 (1994) 5746

[9] J K Sarma and G K Medhi, TU/THEP-198 (1998)

[10] P K B Collins, 'An Introduction to Regge Theory and High-Energy Physics', Cambridge University Press, Cambridge (1977)

[11] J B Scarborough Numerical Mathematical Analysis, John Hopkins Press, Baltimore (1996)

[12] S Aid *et al* , H1 collaboration, *Phys Lett* B354(1995)494

[13] M Derrick *et al* , ZEUS collaboration, *Phys Lett* B364(1994)576

[14] T Ahmed *et al* , H1 collaboration, *Nucl Phys* B439(1995)471

[15] M Derrick *et al* , ZEUS collaboration, *DESY* 94-143, August, (1994)

[16] M Arneodo *et al* , NMC, *Phys Lett* B364(1997)107

[17] M Arneodo *et al* , NMC, *Nucl Phys* B483(1997)3

[18] M Virchaux and A Milsztajan, *Phys Lett* B274(1992)221

[19] L Motanet *et al* , Particle Data Group (PDG), *Phys Rev* D50(1994)1173

[20] A D Martin *et al* , DTP/98/10, RAL tr-98 029, hep-ph/9803445(1998)

Gau. Univ. J. Sc., Golden Jubilee Volume (1998) pp.39–53

t and x-evolutions of gluon structure functions at low-x

D.K. CHOUDHURY, *G.K. MEDHI and **J.K. SARMA†
Department of Physics, Gauhati University, Guwahati 781014
*Department of Physics, Birjhora Mahavidyalaya, Bongaigaon
**Department of Electronics Science, Gauhati University, Guwahati 781014

Abstract. We obtain x and t-evolutions of gluon structure function at low-x from Altarelli-Parisi equation. Comparison is made with the prediction of Lipatov as well as GLR equations. We also make predictions for the HERA range.

Keywords. Structure function, Altarelli-Parisi equations, low-x.

1. In a recent letter [J.K. Sarma and B. Das, 1993] the t-evolutions of non-singlet and singlet structure functions [L.F. Abbot, W.B. Atwood and R.N. Barnett, 1980] have been reported. The same technique can be applied to the Altarelli-Parisi (AP) equation [G. Altarelli and G. Parisi, 1977] for the gluon structure function to obtain t as well as x-evolution of gluon at low-x.

The AP equation for the gluon structure function has the standard form [L.F. Abbot, W.B. Atwood and R.N. Barnett, 1980]

$$\frac{\partial G(x,t)}{\partial t} - \frac{A_f}{t}\left\{\left(\frac{11}{12} - \frac{N_f}{18} + \ln(1-x)\right) G(x,t) + Ig\right\} = 0, \tag{1}$$

where

$$I_g = \int_x^1 dw \left[\frac{wG(x/w,t) - G(x,t)}{1-w} + \left(w(1-w) + \frac{1-w}{w}\right) G(x/w,t) + \frac{2}{9}\left(\frac{1+(1-w)^2}{w}\right) F_2^s(x/w,t)\right], \tag{2}$$

$t = \ln(Q^2/\Lambda^2)$,

$$A_f = \frac{36}{33 - 2N_f},$$

N_f being the number of flavour.

†*Present address:* Department of Physics, Tezpur University, Tezpur 784025

For small-x and high-Q^2, gluon is expected to be more dominant than the sea [F.J. Yadurain, 1983]. For lower-$Q^2(Q^2 \approx \Lambda^2)$, however, there is no such clear cut distinction between the two. For simplicity, we therefore, assume identical t-dependence for both:

$$G(x,t) = KF_2^{\gamma}(x,t), \tag{3}$$

where, K is a parameter to be determined from experiments. This results in

$$I_{q} = \int_x^1 dw \left[\frac{wG(x/w,t) - G(x,t)}{1-w} + \left(w(1-w) + \frac{1-w}{w}\right) G(x/w,t) + \frac{2}{9k}\left(\frac{1+(1-w)^2}{w}\right) G(x/w,t)\right]. \tag{4}$$

Let us introduce the variable

$$u = 1 - w \tag{5}$$

and note that [I.S. Granshteyn and I.M. Ryzhik, 1965]

$$\frac{x}{1-u} = x\sum_{k=0}^{\infty} u^k \tag{6}$$

The series (6) is convergent for $|u| < 1$. Since $x < w < 1$, so $0 < u < 1 - x$ and hence the convergence criterion is satisfied. Using (6) we can rewrite $G(x/w,t)$ as [L.A. Pipes and L.R. Harvill, 1970]

$$G(x/w,t) = G\left(x + x\sum_{k=1}^{\infty} u^k, t\right) = G(x,t) + x\sum_{k=1}^{\infty} u^k \frac{\partial G(x,t)}{\partial x} + \frac{1}{2}x^2\left(\sum_{k=1}^{\infty} u^k\right)^2 \frac{\partial^2 G(xt)}{\partial x^2} + \ldots, \tag{7}$$

which covers the whole range of u, $0 < u < 1 - x$. Neglecting higher order terms $o(x^2)$, $G(x/w,t)$ can then be approximated for small-x as

$$G(x/w,t) \approx G(x,t) + x\sum_{k=1}^{\infty} u^k \frac{\partial G(x,t)}{\partial x}. \tag{8}$$

Putting (5) and (8) in (4) and performing u-integrations we obtain

$$I_q = R(x)G(x,t) + S(x)\frac{\partial G(x,t)}{\partial x}, \tag{9}$$

where we have used the identity [I.S. Granshteyn and I.M. Ryzhik, 1965]

$$\sum_{k=1}^{\infty} \frac{u}{k} = \ln\frac{1}{1-u}, \tag{10}$$

and where,

$$R(x) = -\left\{\left(1+\frac{2}{9K}\right)(1-x)+\left(-\frac{1}{2}+\frac{1}{9K}\right)(1-x)^2+\frac{1}{3}(1-x)^3 + \left(1+\frac{4}{9K}\right)\ln x\right\}, \tag{11}$$

$$S(x) = x\left\{\left(1+\frac{4}{9K}\right)\frac{1}{4}+\left(2+\frac{4}{9K}\right)(1-x)+\frac{1}{9K}(1-x)^2+\frac{1}{3}(1-x)^3 + \left(2+\frac{8}{9K}\right)\ln x - 1 - \frac{4}{9K}\right\} \tag{12}$$

Using (9) in (1) we get,

$$\frac{\partial G(x,t)}{\partial t} - \frac{A_f}{t}\left\{\left(\frac{11}{12}-\frac{N_f}{8}\right)+\ln(1-x)G(x,t) + R(x)G(x,t)+S(x)\frac{\partial G(x,t)}{\partial x}\right\} = 0,$$

which gives,

$$\frac{\partial G(x,t)}{\partial t} - \frac{A_f}{t}\left\{P(x)G(x,t)+Q(x)\frac{\partial G(x,t)}{\partial x}\right\} = 0, \tag{13}$$

where,

$$\left.\begin{aligned} P(x) &= \left(\tfrac{11}{12}-\tfrac{N_f}{18}\right)+\ln(1-x)+R(x), \\ Q(x) &= S(x) \end{aligned}\right\} \tag{14}$$

The general solution of (13) is [I. Sneddon, 1957]

$$F(U,V) = 0, \tag{15}$$

where, F is an arbitrary function and

$$\left.\begin{aligned} U(x,t,G) &= C_1 \\ V(x,t,G) &= C_2 \end{aligned}\right\} \tag{16}$$

form a solution of the equations

$$\frac{dx}{A_f Q(x)} = \frac{dt}{-t} = \frac{dG}{-A_f P(x) G(x,t)}. \tag{17}$$

Solving (17) one obtains,

$$U(x,t,G) = t\exp\left[\frac{1}{A_f}\int\frac{dx}{Q(x)}\right]. \tag{18}$$

and ,

$$V(x,t,G) = G(x,t)\exp\left[\int\frac{P(x)}{Q(x)}dx\right]. \tag{19}$$

It thus has no unique solution. The simplest possibility is that a linear combination of U and V is to satisfy (15) so that

$$A_q U + B_q \bar{B} = 0, \tag{20}$$

where A_g and B_q are arbitrary constants Putting the values of U and V in (20) we obtain

$$G(x,t) = -\frac{A_g}{B_q} t \exp\left[\int \left\{\frac{1}{A_f Q(x)} - \frac{P(x)}{Q(x)}\right\} dx\right]. \tag{21}$$

2(a). Defining,

$$G(x,t_0) = -\frac{A_q}{B_g} t_0 \exp\left[\int \left\{\frac{1}{A_f Q(x)} - \frac{P(x)}{Q(x)}\right\} dx\right], \tag{22}$$

One gets,

$$G(x,t) = G(x,t_0)(t/t_0), \tag{23}$$

which gives the t-evolution of gluon structure function $G(x,t)$.

2(b). Again defining,

$$G(x_0,t) = -\frac{A_g}{B_g} t \exp\left[\int \left\{\frac{1}{A_f Q(x)} - \frac{P(x)}{Q(x)}\right\} dx\right]_{x=x_0}, \tag{24}$$

one obtains,

$$G(x,t) = G(x_0,t) \exp\left[\int \left\{\frac{1}{A_f Q(x)} - \frac{P(x)}{Q(x)}\right\} dx\right]. \tag{25}$$

which determines the x-evolution of gluon structure function $G(x,t)$

3. We can perform the integration inside the exponential in the equation (25) with further approximation that $\ln(1-x) \to 0$ and $x \ln x \to 0$ for very small-x, $x \to 0$ Then we get from (14),

$$\left.\begin{aligned} P(x) &= \left(\tfrac{11}{12} - \tfrac{N_f}{18}\right) - \left(1 + \tfrac{2}{9K}\right)(1-x) - \left(-\tfrac{1}{2} + \tfrac{1}{9K}\right)(1-2x) \\ &\quad -\tfrac{1}{3}(1-3x) - \left(1 + \tfrac{4}{9K}\right) \ln x, \\ \text{and } Q(x) &= \left(1 + \tfrac{4}{9K}\right) + \left(2 + \tfrac{4}{9K}\right) x + \left(\tfrac{x}{9K} + \tfrac{x}{3}\right) - \left(x + \tfrac{4}{9K} x\right), \end{aligned}\right\} \tag{26}$$

when we have neglected the square and higher terms of x.

Putting the values of $P(x)$ and $Q(x)$ from (26) in (25) and performing the integrations analytically we get,

$$G(x,t) = G(x_0,t) \exp\left[-\frac{1}{b}(1+d+2e)(x-x_0)\right] \left(\frac{x}{x_0}\right)^{-\frac{a}{b}\ln a} \times \left\{\frac{(a+bx)^{\ln x}}{(a+bx_0)^{\ln x_0}}\right\}^{\frac{a}{b^2}(1+d+2e)}$$
$$\times \left(\frac{a+bx}{a+bx_0}\right)^{\left\{-\frac{1}{b} - \left(\frac{1}{3} - \frac{1}{4_f} + C_f - d - e\right) + \frac{a}{b^2}(1+d+2e)\right\}}, \tag{27}$$

where,

$$\left.\begin{aligned} a &= 1+\tfrac{4}{9K}, \\ b &= \tfrac{4}{3}+\tfrac{1}{9K}, \\ C_f &= \tfrac{11}{12}-\tfrac{N_f}{18}, \\ d &= 1+\tfrac{2}{9K}, \\ \text{and} \quad e &= -\tfrac{1}{2}+\tfrac{1}{9K}. \end{aligned}\right\} \tag{28}$$

4. Instead of neglecting the higher order terms $o(x^2)$ from the equation (7) as is done in (8), let us retain the second order terms of Taylor expansion series (7) and neglect higher order terms $o(x^3)$; $G(x/w,t)$ can then be approximated for small-x as [L.A. Pipes and L.R. Harvill, 1970]

$$G(x/w,t) \simeq G(x,t) + x\sum_{k=1}^{\infty} u^k \frac{G(x,t)}{x} + \frac{1}{2}x^2\left(\sum_{k=1}^{\infty} u^k\right)^2 \frac{\partial^2 G(x,t)}{\partial x^2}. \tag{29}$$

Putting (5) and (29) in (4) and performing u-integrations we obtain,

$$I_{\mu} = R(x)G(x,t) + S(x)\frac{\partial G(x,t)}{\partial x} + T(x)\frac{\partial^2 G(x,t)}{\partial x^2}, \tag{30}$$

where $R(x)$ and $S(x)$ are defined by equations (11) and (12) respectively and $T(x)$ is given by,

$$\begin{aligned} T(x) &= \frac{1}{2}x^2\int_0^{1-r}\left(\sum_{k=1}^{\infty} u^k\right)^2\left(u(1-u)+\frac{u}{1-u}+\frac{1-u}{u}\right. \\ &\qquad \left.+\frac{2}{9K}\frac{1+u^2}{1-u}\right)du. \end{aligned} \tag{31}$$

It does not need to calculate explicitly the value of $T(x)$ as a function of x for the reason which will be clear shortly. Using (30) in (1) we get,

$$\begin{aligned} \frac{\partial G(x,t)}{\partial t} - \frac{A_f}{t}\left\{P(x)G(x,t) + Q(x)\frac{\partial G(x,t)}{\partial x}\right. \\ \left. +T(x)\frac{\partial^2 G(x,t)}{\partial x^2}\right\} &= 0, \end{aligned} \tag{32}$$

where $P(x)$ and $Q(x)$ are defined by equation (14).

The equation (32) is a second order partial differential equation which can be solved by Monge's method [I. Sneddon, 1957]. According to this method the solution of second order partial differential equation

$$Rr + Ss + Tt = V \tag{33}$$

can be obtained from the subsidiary equations

$$\left.\begin{aligned} Rdy^2 - Sdxdy + Tdx^2 &= 0 \\ \text{and} \quad Rdpdy + Tdqdx - Vdxdy &= 0, \end{aligned}\right\} \tag{34}$$

where R, S, T, V are functions of x, y, z, p and q. Here z, p, q, r, s and t are defined as follows:

$$Z = z(x,y), \quad p = \frac{\partial z}{\partial x}, \quad q = \frac{\partial z}{\partial y}, \quad r = \frac{\partial^2 z}{\partial x^2} = \frac{\partial p}{\partial x},$$
$$S = \frac{\partial^2 z}{\partial x \partial y} = \frac{\partial p}{\partial y} = \frac{\partial q}{\partial x}, \quad t = \frac{\partial^2 z}{\partial y^2}, = \frac{\partial q}{\partial y}.$$

Comparing equation (32) with (33) we get,

$$\left.\begin{aligned} R &= A_f Y(x), \\ S &= 0, \\ T &= 0, \\ V &= t\tfrac{\partial G(x\,t)}{\partial t} - A_f Q(x)\tfrac{\partial G(x,t)}{\partial x} - A_f P(x)G(x,t). \end{aligned}\right\} \tag{35}$$

Substituting the values of R, S, T and V in subsidiary equations we obtain ultimately $V = 0$, which gives

$$t\frac{\partial G(x,t)}{\partial t} - A_f Q(x)\frac{\partial G(x,t)}{\partial x} - A_f P(x)G(x,t) = 0,$$

which is exactly the equation (13). This equation is solved earlier and now it is clear that the introduction of the second order terms does not modify the solutions (23) or (25).

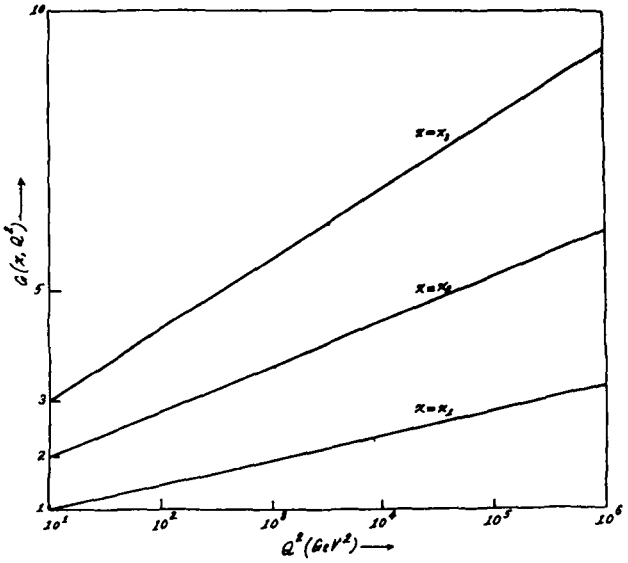

Fig. 1. Q^2-evolutions of $G(x, Q^2)$ from the equation (23). Arbitrary inputs $G(x, Q^2) = 1, 2$ and 3 are taken for $x = x_1, x_2$ and x_3 respectively.

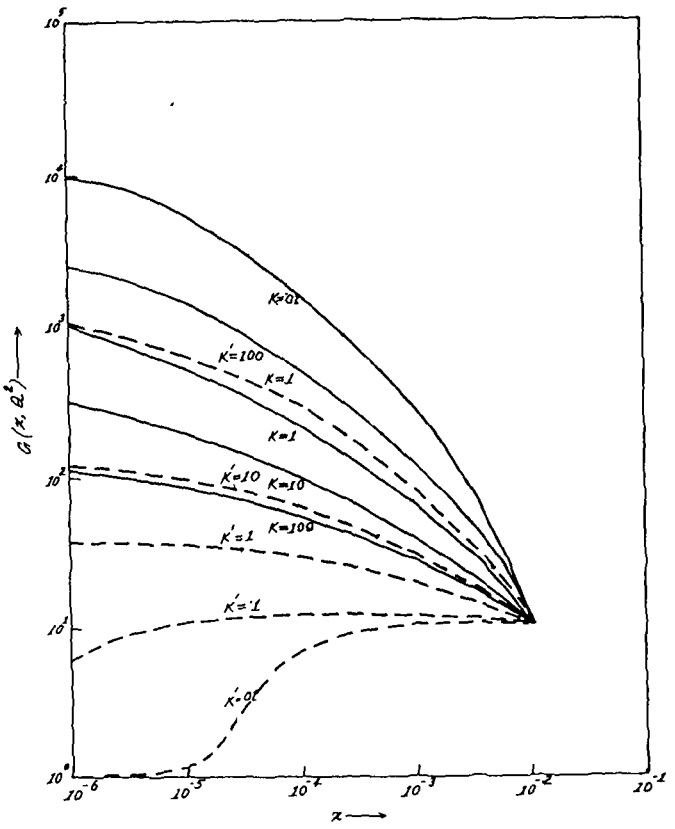

Fig. 2. x-evolutions of $G(x,Q^2)$ from the equation (25) (solid lines) and from equation (27) (dashed lines). Arbitrary inputs $G(x_0,Q^2)=10$ for $Q^2=Q_1^2$ is taken. K or K' = 0.01, 0.1, 1, 10 and 100.

5. We have presented our results qualitatively in Fig. 1 and Fig. 2. In Fig. 1 the result of t or Q^2-evolutions of $G(x,Q^2)$ from the equation (23) is given. We have taken arbitrary inputs $G(x,Q_0^2)=1,2$ and 3 for $x=x_1,x_2$ and x_3 respectively Similarly in Fig. 2 the results of x-evolutions of $G(x,Q^2)$ from the equation (25) (solid lines) and from the equations (27) (dashed lines) are presented. Integration in the equation (25) is computed numerically. We have taken arbitrary inputs $G(x_0,Q^2)=10$ for $Q^2=Q_1^2$ for both the sets. Different lines are due to different K-values, $K=0.01$, 0.1, 1, 10 and 100 indicated in the Fig. 2 for the dashed graphs, K-values are labelled as K' for convenience It is clear from the figures that evolutions of gluon structure functions $G(x,Q^2)$ depend upon inputs $G(x,Q_0^2)$ or $G(x_0,Q^2)$ and also upon K-values. Moreover, AP and GLAP or $G(x,Q^2)$, $xG(x,Q^2)$, $g(x,Q^2)$ and $xq(x,Q^2)$ are equivalent here.

EHLQ [E. Eichten, Z. Hinchliffe, K. Lane and C. Quigg, 1984] begin with input distributions inferred from experiment at $Q_0^2=5\text{GeV}^2$ and integrate the evolution

equation numerically. They started with the data of CDHS neutrino experiment [H. Abramowicz et al. 1983] at CERN. Gluon distribution is determined indirectly and parametrized as

$$xG(x, Q_0^2) = (2.62 + 9.17x)(1 - x)^{5.9},$$

with $R = \sigma_L/\sigma_T = 0.1$ and $\Lambda = 200$MeV at $Q_0^2 = 5\text{GeV}^2$. This is set-1. Under the assumption that $R = \sigma_L/\sigma_T$ has the behaviour prescribed by QCD, gluon is parametrized as

$$xG(x, Q_0^2) = (1.75 + 15.57x)(1 - x)^{6.03},$$

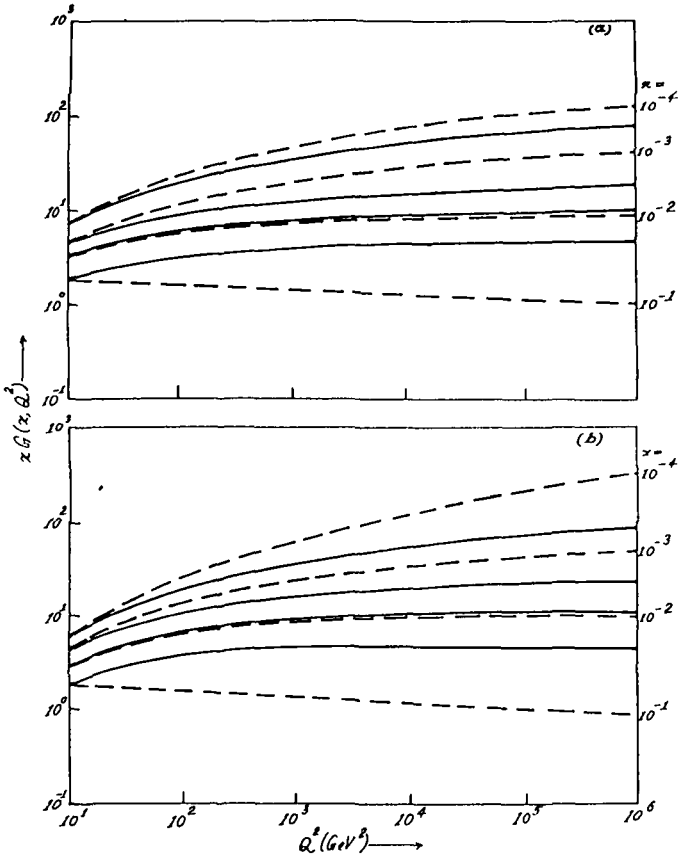

Fig. 3(a) and **Fig. 3(b).** Q^2-evolutions of $xG(x, Q^2)$ for EHLQ Set-1 and Set-2 respectively (dashed lines) for $x = 10^{-1}, 10^{-2}, 10^{-3}$ and 10^{-4}. Results from equation (23) (solid lines) are also given for same values of x. Inputs are taken from the corresponding values at $10Gev^2$ from the parametrization.

with $\Lambda = 290$ MeV at $Q_0^2 = 5\text{GeV}^2$. This is set-2. The calculated Q^2 dependence of $xG(x, Q^2)$ for set-1 is shown in Fig. 3(a) by dashed lines for x values $10^{-1}, 10^{-2}, 10^{-3}$

and 10^{-4} as indicated in the figure. The expected growth of the distributions at small-x is apparent. Our results from the equation (23) are given in the figure by solid lines for the same values of x. Inputs are taken from the corresponding values at 10GeV^2 from the parametrization. The corresponding result for set-2 is shown in Fig. 3(b). Again to explore the uncertainties in the small-x region EHLQ consider two modifications of set-1 as follows:

$$xG(x,Q_0^2) = (2.62+9.17x)(1-x)^{5.9}, \quad x > 0.01,$$

and

$$xG(x,Q_0^2) = \begin{cases} (0.444x^{-0.5} - 1.886 & \text{(a)} \\ 25.56x^{0.5}, & \text{(b)} \end{cases}$$

for $x < 0.01$.

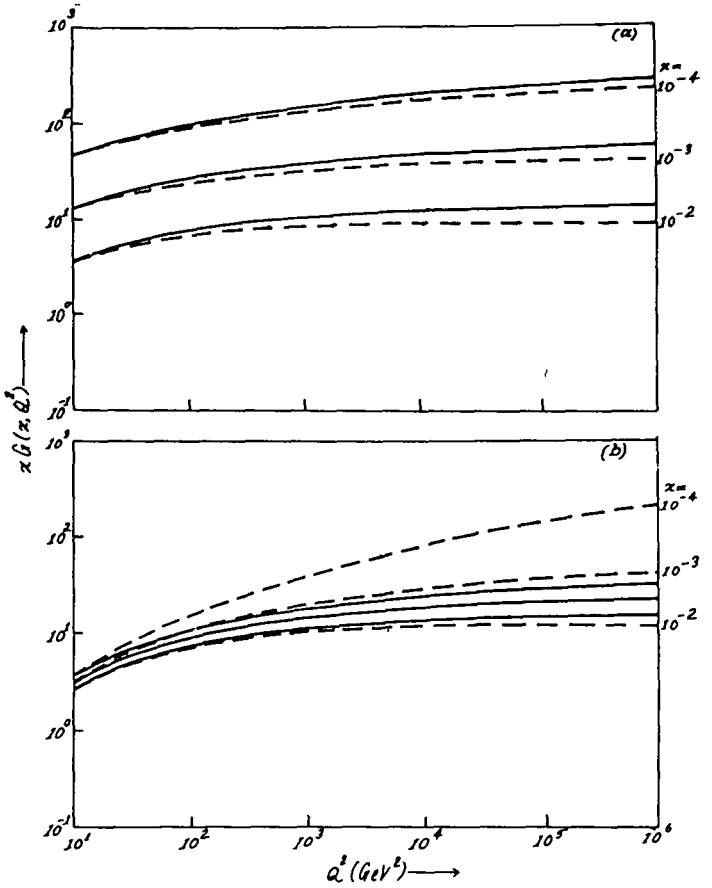

Fig. 4(a) and **Fig. 4(b).** Q^2-evolutions of $xG(x,Q^2)$ for EHLQ Set-1(a) and Set-1(b) respectively (dashed lines) for $x = 10^{-2}, 10^{-3}$ and 10^{-4} alongwith the corresponding predictions (solid lines) from equation (23) as indicated in Fig. 3(a) and Fig. 3(b).

The results of these changes are presented in Fig. 4(a) and Fig. 4(b) for set-1(a) and set-1(b) respectively for $x = 10^{-2}, 10^{-3}$ and 10^{-4} alongwith our corresponding predictions.

DFLM [M. Diemoz, F. Ferroni, E. Long, G. Martineli, 1986;1988] also proceed in the same manner to parametrize the data from the nutrino expreiments BEBC'85 [D. Alasia et al, 1985] CCFRR'83 [D. MacFarlane et al, 1983] CHARM'83 [F. Bergsma et al, 1983] and CDHS'83 [H. Abramowicz et al, 1983] at $Q_0^2 = 10\text{GeV}^2$. For the set DFLM-2 they consider gluon function to be

$$xG(x, Q^2) \sim (1 - 0.18x)(1 - x)^{5.06},$$

with $\lambda_{\overline{\text{MS}}} = 300\text{MeV}$. Here the next to leading order QCD calculation is performed. The result is given in the figure for $x = 10^{-1}, 10^{-2}, 10^{-3}$ and 10^{-4} by dashed lines. Our result from the equation (23) is given by solid lines taking inputs as before.

The role of absorptive corrections in the small-x behaviour of deep inelastic gluon structure functions $xG(x, q^2)$ is widely discussed now [A. Ali and J. Bartels, 1991] due to the new generation of accelerators HERA [A. Ali, J. Bartels 1991 and F Eisale and F.W. Brasse 1992] LHC [G. Jarlskog and D. Rein 1990] SSC [J.H. Mullvey 1987] etc. Kim and Ryskin estimated [V.T. Kim and M.G. Ryskin 1991] the non-linear absorption corrections with the parametrization used in semihard phenomenology [E.M. Levin and M.G. Ryskin, 1990]. As non-linear absorption effect are essentially at very small-x only [L.V. Gribov, E.M. Levin and M.G. Ryskin 1983], they decided to use the standard GLAP equation [G. Altarelli and G. Parisi 1977; V.N. Gribov and L.N. Lipatov 1972; Yu.L. Dokshitzer 1977] in region of interest ($x > 10^{-6}, q^2 < 10^5\text{GeV}^2$) i.e. $x > x_0(q^2)$ where $\ln \tilde{x}_0 = (1/12.7)\ln^2(q^2/\Lambda^2)$. But in this case they are to add a new boundary condition

$$xG(x, q^2), \; = \; aq^2 \tag{A}$$

on the line $x = x_0(q^2)$, where $a = x_0 G(x_0, q^2)q^2$, which is fixed by the initial condition

$$xG(x) \; = \; A(1 - x^3)x^{-w_0} \tag{B}$$

at $q_*^2 = 4\,\text{GeV}^2$. The coefficient A is fixed by the normalization $\int xG(x)dx = 0.55$ and $w_0 = (1/\pi)N_c\alpha_s(q_*^2) \times 4\ln 2$ corresponds to the QCD pomeron singularity given by the summation of leading-log contributions $\left(\alpha_s \ln \frac{1}{x}\right)^n$ [25], $N_c = 3$ be the number of colours Absorption corrections reveal itself due to this new boundary condition. Kim and Ryskin obtain numerical solution of linear GLAP equation. The boundary condition corresponds to a strong correlation between gluons inside the proton. Gluons group in a small "h-" spots" [E.M. Levin and M.G. Ryskin 1990; A.H. Muller and J. Qiu 1986] with radius $R_s \sim 0.2$ Fm ($x = 1/3$). If gluons are distributed uniformly inside the proton the screening would be smaller and non-linear effect reveals itself at smaller x. For this case $R_s \sim 0.7\text{Fm} \sim R_n(x_0 = 0.0035)$. In the Fig. 6(a) the x dependence of gluon structure functions $xG(x, q^2)$ at $q^2 = 10, 100$ and 1000GeV^2 is given by the curves 1, 4, 7; 2, 5, 8 and 3, 6, 9 respectively. Solid

curves are the ordinary linear GLAP evolution; long dashed curves take into account the absorption corrections through the new boundary condition (A) for $R_s \sim 0.2$ Fm. Short dashed is the same for $R_s \sim R_n$. Here $\Lambda = 200$ MeV. In the Fig. 6(b) the difference between linear (solid curves) GLAP and non linear (dashed curves) GLR [L.V. Gribov and E.M. Levin; M.G. Ryskin 1983] evolution is given. The curves 1, 4; 2, 5 and 3, 6 correspond to $Q^2 = 10, 100$ and 1000GeV^2 respectively. The new and old initial conditions (A) and (B) at $q_s^2 = 4\text{GeV}^2$ are shown by dotted and dot-dashed curves, respectively. Here $\Lambda = 200$ MeV. In both the figures, the shaded areas are our predictions from the equation (25) with upper and lower boundaries corresponding to $K = 1$ and 100 respectively. In both cases gluon distribution functions $xG(x_0Q^2)$ for linear GLAP equation at $x_0 = 10^{-2}$ are taken as inputs; because, it is almost same for all curves.

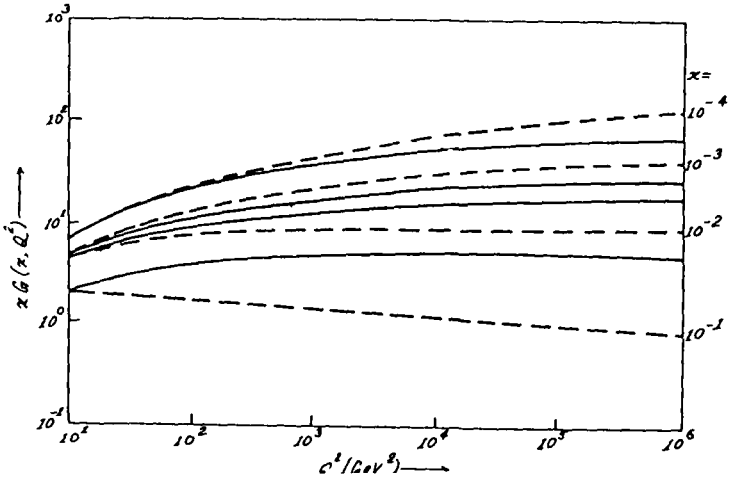

Fig. 5. Q^2-evolutions of $xG(x, Q^2)$ for DFLM 2 (dashed lines) for $x = 10^{-1}$, 10^{-2}, 10^{-3} and 10^{-4} alongwith the corresponding predictions (solid lines) from equation (23) as indicated in Fig. 3(a) and Fig. 3(b).

In the leading $\log(1/x)$ [LL$(1/x)$] approximation of QCD it is expected that the gluon distribution will grow indefinitely as

$$xg(x, Q^2) \sim x^{-\lambda}, \qquad \text{(C)}$$

in the small-x limit [J. Kwiecinski, A.D. Martin and P.J. Sutton 1991] with $\lambda \simeq 0.5$. This increase with decreasing x, will of course eventually be tamed by screening corrections which give rise to non-linear terms in the QCD evolution equations. The approximate framework is provided by the Lipatov equation [Ya.Ya. Balitskij and L.N. Lipatov 1978; S. Catani, F. Fiorani, G. Marchesini and G. Oriani 1990] with the addition of the non-linear shadowing term. This is known as 'GLR' equation. The radius parameter R in the shadowing term characterises the area πR^2 in which the gluons are concentrated within the proton. We would expect R to be approximately equal to the radius of the proton i.e. $R \simeq 5\text{GeV}^{-1}$, although it has been argued that

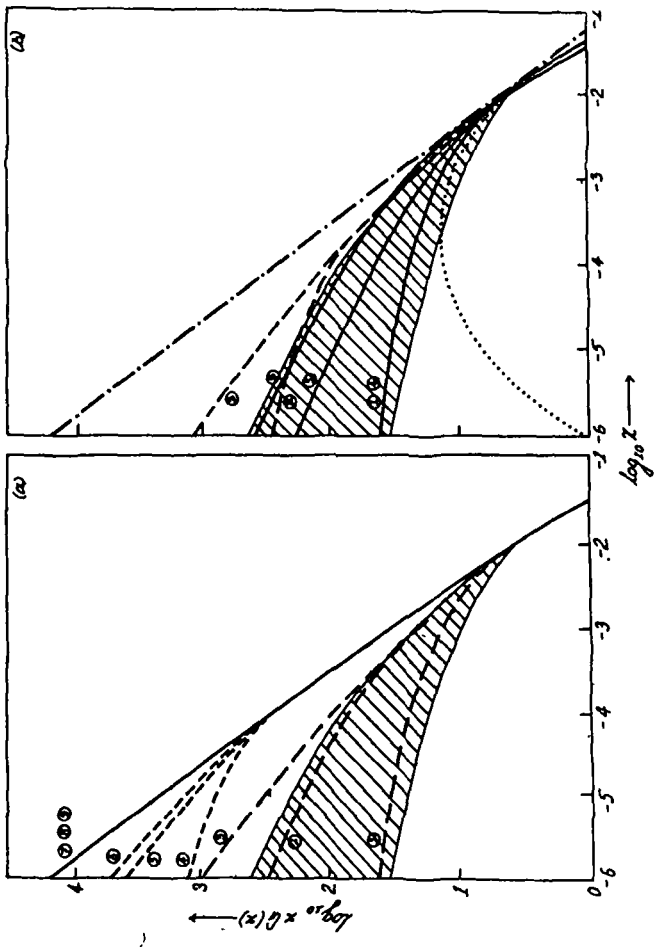

Fig. 6(a) x-evolutions of $xG(x,q^2)$ at $q^2 = 10, 100$ and $1000GeV^2$ are given by curves 1,4,7; 2,5,8 and 3,6,9 respectively. Solid curves are GLAP evolution; long-dashed curves take into account the absorption corrections through (a) for $R_a \sim 0.2F_m$: short dashed are the same for $R_a \sim R_n$. The shaded area is the prediction from equation (25) with upper and lower boundaries corresponding to $K = 1$ and 100 respectively.

(b) Difference between GLAP (solid curves) and GLR (dashed curves) equations. The curves 1,4; 2,5 and 3.6 correspond to $q^2 = 10, 100$ and 1000GeV^2 respectively. Initial conditions (A) and (B) are shown by dotted and dot-dashed curves respectively. The shaded area is same as in (a).

the gluons may be concentrated in "hot spots" within the proton. So, the results for $R = 2\text{GeV}^{-1}$ are also shown. The non-linear integro-differential Lipatov equation can now be solved numerically [J. Kwiecinski, A.D. Martin and P.J. Sutton 1991] with the analysis entirely confined to the small-x region $x < x_0$. It is informative to compare the above results with the gluon distributions to set B_- of partons obtained in the KMRS [J. Kiecinski, A.D. Martin, R.G. Roberts and W.J. Stirling 1990] global structure function analysis which attempted to incorporate both the Lipatov and shadowing effects, albeit in an approximate manner. KMRS evolved the starting distributions up from $Q^2 = 4\,\text{GeV}^2$ using the next-to-leading order AP equations. In the Fig. 7 the continuous curves are the values of $xg(x,Q^2)$ determined by solving the Lipatov equation for $Q^2 = 100$ and 1000GeV^2. The dashed curves are $xg(x,Q^2)$ of set B_- of the KMRS next-to-leading order structure function analysis. In each case three curves are in descending order the solution with shadowing neglected and the solutions with the shadowing term included with $R = 5\text{GeV}^{-1}$ and $R = 2\text{GeV}^{-1}$. The shaded areas are our predictions described before. $xg(x,Q^2)$ at $x = 10^{-2}$ for Lipatov equation are taken as inputs. They are almost same for all the curves.

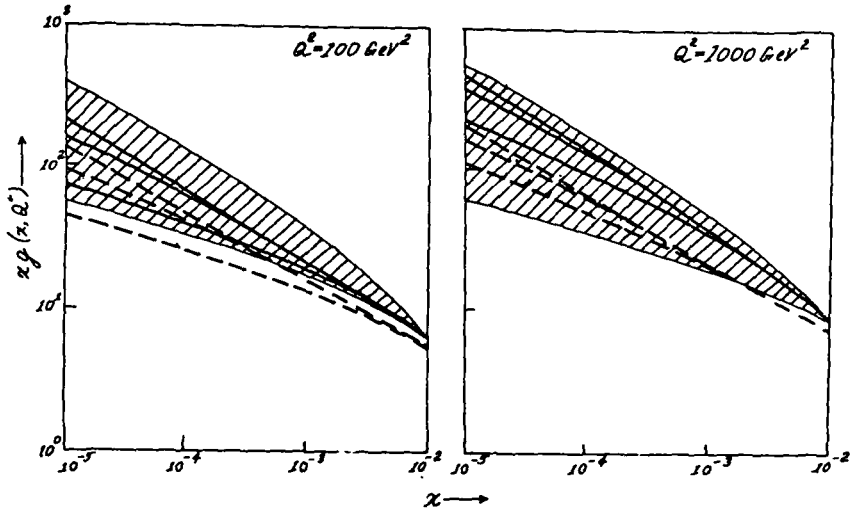

Fig. 7. x-evolutions of $xg(x,Q^2)$ of Lipatov for $Q = 100$ and $1000GeV^2$ (solid curves). The dashed curves are $xg(x,Q^2)$ of KMRS set B$_-$. In each three curves in descending order are the solutions with shadowing neglected, solutions with $R = 5GeV^{-1}$ and $R = 2GeV^{-1}$ respectively. The shaded area is same as in Fig. 6(a).

6. It is clear from the figures that our t-evolutions conform with those of EHLQ set-1, EHLQ set-2 and DFLM 2 parametrizations for $x < 10^{-2}$ but do not conform for $x > 10^{-2}$. But they conform excellently with set-1(a) whereas differ badly with set-1(b). The bands in all the figures gives our predictions for x-evolutions

for $1 < K < 100$. Our predictions conform well with those of others. It can be inferred from our predictions that screening correction at verylow-x is more likely. To conclude, our simple approximate analytical solution of AP equation for gluon structure function gives satisfactory predictions in HERA range. The qualitative predictions of our results conform to those of several other authors. AP equation in present form thus stands as a viable alternative to Lipatov and GLR predictions at least in the x and Q^2 range under study.

References

[1] J.K. Sarma and B. Das, *Phys. Lett.*, **B126**(1993) 323.

[2] L.F. Abbot, W.B. Atwood and R.N. Barnett, *Phys. Rev.*, **D22**(1980) 582.

[3] G. Altarelli and G. Parisi, *Nucl. Phys.*, **B126** (1977) 298.

[4] F.J. Yadurain, *Quantum Chromodynamics*, Springer-Verlag, New York, 1983.

[5] I.S. Granshteyn and I.M. Ryzhik, *Tables of Integrals, Series and Products*, ed. Alen Geffrey, Academic Press, New York, 1965.

[6] L.A. Pipes and L.R. Harvill, *applied Mathematics for Engineersand Physicians*, Mc Graw-Hill Bokk Company, New York, 1970.

[7] I. Sneddon, *Elements of Partial Differential Equations*, Mc Graw-Hill, New York, 1957.

[8] E. Eichen, Z. Hinchliffe, K. Lane and C. Quigg, *Rev. Mod. Phus.* **56**(1984) 579.

[9] H. Abramowicz et al. (CDHS '83), *Z. Phys.*, **C17** (1983) 283.

[10] M. Diemoz, F. Ferroni, E. Long and G. Martinelli, (DFLM) *Z. Phys.*, **C39** (1988) 21.

[11] M. Diemoz, F. Ferroni and E. Long, *Phys. Rep.*, **130**(1986) 293.

[12] D. Alasia et al., (BEBC '85) *Z. Phys.*, **C28** (1985) 321.

[13] D. Mac Farlane et al., (CCFRR '83), Fermilab-pub-83, 108-exp. (1983).

[14] F. Bergsma et al., (CHARM '83), *Phys. Lett.*, **123** (1983) 269.

[15] See for example *Proceeding of the DESY topical meeting in the small-x behaviour of deep inelastic structure function in QCD*, eds. A Ali and J. Bartels. North Holland, 1991.

[16] F. Eisale and F.W. Brasse, DESY 92-140, October, 1992.

[17] See for example *Proceeding of Large Hadron Collider Workshop*, Vol. II, CERN 90-10, eds. G.Jarlskog and D. Rein, 1990.

[18] See for example *Proceedings of the Workshop on Physics at future accelerators*. Vol. I, CERN 87-07, eds. J.H. Mulvey, 1987.

[19] V.T. Kim and M.G. Ryskin, DESY 91-064, June, 1991.

[20] E.M. Levin and M.G. Ryskin, *Phys. Rep.*, **189** (1990) 267.

[21] L.V. Gribov, E.M. Levin and M.G. Ryskin, *Phys. Rep.*, **100** (1983) 1.

[22] V.N. Gribov and L.N. Lipatov, *Sov. J. Nucl. Phys.*, **15** (1972) 438.

[23] L N Lipatov *Sov J Nucl Phys* **20** (1975) 94

[24] Yu L Dokshitzer *Sov Phys JETP* **46** (1977) 641

[25] E A Kuraev L N Lipatov and V S Fadin *Sov Phys JETP* **45** (1977) 199

[26] A H Mueller and J Qiu *Nucl Phys* **B268** (1986) 427

[27] J Kwiecinski A D Martin and P J Sutton Durham Preprint DTP/91/12 April 1991

[28] Ya Ya Balitski and L N Lipatov *Sov J Nucl Phys* **28** (1978) 822

[29] L N Lipatov in *Perturbation QCD* ed A H Mueller World Scientific Singapore 1989

[30] L N Lipatov *Phys Lett* **B251** (1990) 284

[31] L N Lipatov and R Kirschner *Z Phys* **C45** (1990) 477

[32] N Cafalonis *Nucl Phys* **B296** (1988) 49

[33] S Catani F Fiorani G Marchesini and G Oriani *Cavendish Lab* Preprint HEP 90 21 (1990)

[34] J Kwiecinski A D Martin R G Roberts and W J Stirling (KMRS) *Phys Rev* **D42** (1990) 3645

Reprinted from

PHYSICS LETTERS B

Physics Letters B 403 (1997) 139–144

x-distribution of deuteron structure function at low-x

J.K. Sarma [a,1,2], D.K. Choudhury [b,3], G.K. Medhi [c]

[a] *Electronics Science Department, Gauhati University, Guwahati 781014, Assam, India*
[b] *Physics Department, Gauhati University, Guwahati 781014, Assam, India*
[c] *Physics Department, Birjhora Mahavidyalaya, Bongaigaon 783380, Assam, India*

Received 25 February 1997
Editor H Georgi

ELSEVIER

PHYSICS LETTERS B

Aims and Scope
Physics Letters B ensures the rapid publication of letter-type communications in the fields of Nuclear Physics/Intermediate Energy Physics, High Energy Physics and Field Theory

Abstracted/indexed in:
Current Contents Physical Chemical & Earth Sciences INSPEC

Subscription Information 1997
PHYSICS LETTERS A (ISSN 0375-9601) and PHYSICS LETTERS B (ISSN 0370 2693) will each be published weekly For 1997 13 volumes volumes 224–236 (78 issues altogether) of Physics Letters A have been announced For 1997 26 volumes volumes 390–415 (104 issues altogether) of Physics Letters B have been announced The subscription prices for these volumes are available upon request from the Publisher PHYSICS REPORTS (ISSN 0370-1573) will be published approximately weekly For 1997 14 volumes volumes 277–290 (84 issues altogether) of Physics Reports have been announced The subscription price for these volumes is available upon request from the Publisher
A combined subscription to the 1997 issues of Physics Letters A Physics Letters B and Physics Reports is available at a reduced rate
Subscriptions are accepted on a prepaid basis only and are entered on a calendar year basis Issues are sent by SAL (Surface Air Lifted) mail wherever this service is available Airmail rates are available upon request
For orders claims, product enquiries (no manuscript enquiries) please contact the Customer Support Department at the Regional Sales Office nearest to you

New York, Elsevier Science, P O Box 945, New York, NY 10159-0945 USA Tel +1 212 633 3730, [Toll free number for North American customers 1 888 4ES INFO (437 4636)], Fax +1 212 633 3680, E-mail usinfo-f@elsevier com
Amsterdam, Elsevier Science, P O Box 211, 1000 AE Amsterdam The Netherlands Tel +31 20 485 3757 Fax +31 20 485 3432, E-mail nlinfo-f@elsevier nl
Tokyo, Elsevier Science, 9 15 Higashi-Azabu 1-chome Minato ku, Tokyo 106, Japan Tel +81 3 5561 5033 Fax +81 3 5561 5047 E mail kyf04035 @niftyserve or jp
Singapore, Elsevier Science No 1 Temasek Avenue #17-01 Millenia Tower Singapore 039192 Tel +65 434 3727, Fax +65 337 2230 E mail asiainfo@elsevier com sg
Claims for issues not received should be made within six months of our publication (mailing) date

Advertising Offices
International Elsevier Science, Advertising Department The Boulevard Langford Lane Kidlington, Oxford OX5 1GB UK Tel +44 1865 843565, Fax +44 1865 843976
USA and Canada Weston Media Associates, Dan Lipner P O Box 1110 Greens Farms, CT 06436-1110 USA Tel +1 203 261 2500 Fax +1 203 261 0101
Japan Elsevier Science Japan Marketing Services 1 9 15 Higashi-Azabu, Minato-ku Tokyo 106, Japan Tel +81 3 5561 5033, Fax +81 3 5561 5047

U.S mailing notice – Physics Letters B (ISSN 0370-2693) is published weekly by Elsevier Science B V , P O Box 211, 1000 AE Amsterdam, The Netherlands Annual subscription price in the USA is US$ 6917 00 (valid in North, Central and South America only), including air speed delivery Periodicals postage paid at Jamaica, NY 11431
USA POSTMASTERS Send address changes to Physics Letters B, Publications Expediting, Inc , 200 Meacham Avenue, Elmont, NY 11003
AIRFREIGHT AND MAILING in the USA by Publications Expediting, Inc , 200 Meacham Avenue, Elmont, NY 11003

♾ The paper used in this publication meets the requirements of ANSI/NISO Z39 48-1992 (Permanence of Paper)

Printed in The Netherlands

North-Holland, an imprint of Elsevier Science

ELSEVIER

19 June 1997

PHYSICS LETTERS B

Physics Letters B 403 (1997) 139–144

x-distribution of deuteron structure function at low-x

J K Sarma [a,1,2], D K Choudhury [b,3], G K Medhi [c]

[a] *Electronics Science Department, Gauhati University, Guwahati 781014, Assam, India*

[b] *Physics Department, Gauhati University, Guwahati 781014, Assam, India*

[c] *Physics Department, Barpeta Mahavidyalaya, Bongaigaon 783380, Assam, India*

Received 25 February 1997

Editor: H. Georgi

Abstract

An approximate solution of the Altarelli–Parisi (AP) equation is presented and the x distribution of the deuteron structure function is calculated at the low x limit. The results are compared with the EMC, NA 28 experiment data. © 1997 Published by Elsevier Science B.V.

1. Introduction

The Altarelli–Parisi (AP) equations [1] are the basic tools to study the Q^2-evolution of structure functions. Even though alternative evolution equations [2] have been proposed and pursued in recent years to study structure functions especially at low-x, the AP equations have been the basic tools in studying double asymptotic scaling (DAS) [3] or extracting the gluon density from the slope of the structure functions at low-x [4].

Based on QCD studies Ball and Forte show [3] that evolving a flat input distribution at $Q_0^2 = 1\ \mathrm{GeV}^2$ with the AP equations leads to a strong rise of F_2 at low-x in the region measured by HERA. An interesting feature is that if QCD evolution is the underlying dynamics of the rise perturbative QCD predicts that at large Q^2 and small x the structure function exhibits double scaling in the two variables

$$\sigma = \sqrt{\log(x_0/x)\ \log(t/t_0)} \qquad \rho \equiv \sqrt{\frac{\log(x_0/x)}{\log(t/t_0)}}$$

with $t \equiv \log(Q^2/\Lambda^2)$. This follows from a computation of the asymptotic form of the structure function $F_2(x, Q^2)$ at small-x and relies only on the assumption that any increase in $F_2(x, Q^2)$ at small x is generated by perturbative QCD evolution.

It implies that the AP equations have characteristic x-evolution at low x. The present paper reports calculation of x-evolutions for singlet, non-singlet and deuteron structure functions at low x from the same equations. It is based on the approximate solutions of AP equation using Taylor expansion at low-x. The formalism was used earlier [5] to the low-x EMC and Fermilab data with reasonable phenomenological success. It was a natural improvement of an earlier analysis at intermediate x [6]. In the present paper in Section 2 we discuss the necessary theory in short. Section 3 gives the result and the discussion.

[1] E-mail: jks@gu.ernet.in

[2] E-mail: jks@unighy.ren.nic.in

[3] E-mail: dilip@gu.ernet.in

PII S0370-2693(97)00483-8

2. Theory

Though the theory is discussed earlier [5] yet we have mentioned the essential steps here again for clarity.

The AP equation for the singlet structure function has the standard form [7]

$$\frac{\partial F_2^s(x,t)}{\partial t} - \frac{A_f}{t}\Bigg[\{3+4\ln(1-x)\}F_2^s(x,t) + 2\int_x^1 \frac{dw}{(1-w)}\{(1+w^2)F_2^s(x/w,t) - 2F_2^s(x,t)\} + \tfrac{3}{2}N_F\int_x^1 \{w^2+(1-w)^2\}G(x/w,t)dw\Bigg] = 0, \tag{1}$$

where $A_f = 4/(33-2N_f)$, N_f being the number of flavour and $t = \ln(Q^2/\Lambda^2)$. Defining

$$I_1^s(x,t) = 2\int_x^1 \frac{dw}{(1-w)}\{(1+w^2)F_2^s(x/w,t) - 2F_2^s(x,t)\} \tag{2}$$

and

$$I_2^s(x,t) = \tfrac{3}{2}N_f\int_x^1 \{w+(1-w)^2\}G(x/w,t)dw, \tag{3}$$

one can recast (1) as

$$\frac{\partial F_2^s(x,t)}{\partial t} - \frac{A_f}{t}[\{3+4\ln(1-x)\}F_2^s(x,t) + I_1^s(x,t) + I_2^s(x,t)] = 0. \tag{4}$$

Let us introduce the variable $u = 1-w$ and note that

$$\frac{x}{(1-u)} = x\sum_{k=0}^{\infty} u^k. \tag{5}$$

The series (5) is convergent for $|u| < 1$. Since $x < w < 1$, so $0 < u < 1-x$ and hence the convergence criterion is satisfied. Using (5) we can rewrite,

$$F_2^s(x/w,t) = F_2^s\left(x + x\sum_{k=1}^{\infty} u^k, t\right) = F_2^s(x,t) + x\sum_{k=1}^{\infty} u^k \frac{\partial F_2^s(x,t)}{x} + \tfrac{1}{2}x^2\left(\sum_{k=1}^{\infty} u^k\right)^2 \frac{\partial^2 F_2^s(x,t)}{\partial x^2} + \ldots, \tag{6}$$

which covers the whole range of u, $0 < u < 1-x$.

Neglecting higher order terms, $F_2^s(x/w,t)$ can then be approximated for low x as

$$F_2^s(x/w,t) \simeq F_2^s(x,t) + x\sum_{k=1}^{\infty} u^k \frac{\partial F_2^s(x,t)}{x}. \tag{7}$$

Putting (5) and (7) in (2) and (3) and performing u-integrations we get,

$$I_1^s(x,t) = [-(1-x)(3+x)]F_2^s(x,t) + \{x(1-x^2) + 2x\ln(1/x)\}\frac{\partial F_2^s(x,t)}{\partial x} \tag{8}$$

and

$$I_2^s(x,t) = N_f\Bigg[\tfrac{1}{3}(1-x)(2-x+2x)G(x,t) + \{-\tfrac{1}{2}x(1-x)(5-4x+2x^2) + 2x\ln(1/x)\}\frac{\partial G(x,t)}{\partial x}\Bigg], \tag{9}$$

where we have used the identity

$$\sum_{k=1}^{\infty}\frac{u^k}{k} = \ln 1/(1-u). \tag{10}$$

Using (8) and (9) in (4) we obtain

$$\frac{\partial F_2^s(x,t)}{\partial t} - \frac{A_f}{t}\Bigg[A(x)F_2^s(x,t) + B(x)\frac{\partial F_2^s(x,t)}{\partial x} + C(x)G(x,t) + D(x)\cdot\frac{\partial G(x,t)}{\partial x}\Bigg] = 0, \tag{11}$$

where

$$A(x) = 3+4\ln(1-x) - (1-x)(3-x), \tag{12}$$

$$B(x) = x(1-x^2) + 2x\ln(1/x)\,, \tag{13}$$

$$C(x) = \tfrac{1}{3}N_f(1-x)(2-x+2x^2)\,, \tag{14}$$

$$D(x) = -\tfrac{1}{2}N_f(1-x)(5-4x+2x^2) + 2x\ln(1/x) \tag{15}$$

In order to solve (11), we need to relate the singlet distribution $F_2^s(x,t)$ with the gluon distribution $G(x,t)$. For small x and high Q^2, the gluon is expected to be more dominant than the sea. For lower Q^2 ($Q^2 \simeq \Lambda^2$), however, there is no such clear cut distinction between the two. For simplicity, we therefore, assume,

$$G(x,t) = KF_2^s(x,t)\,, \tag{16}$$

where K is a parameter to be determined from experiments. But the possibility of the breakdown of relation (16) also can not be ruled out.

Then from Eq. (11) we get

$$\frac{\partial F_2^s(x,t)}{\partial t} - \frac{A_f}{t}\left[L(x,K)F_2^s(x,t) + M(x,K)\frac{\partial F_2^s(x,t)}{\partial x}\right] = 0\,, \tag{17}$$

where

$$L(x,K) = A(x) + KC(x)\,, \tag{18}$$

$$M(x,K) = B(x) + KD(x) \tag{19}$$

The general solution of (17) can now be obtained by recasting it in the standard form

$$P(x,t,F_2^s)\frac{\partial F_2^s}{\partial x} + Q(x,t,F_2^s)\frac{\partial F_2^s}{\partial t} = R(x,t,F_2^s)\,, \tag{20}$$

where

$$P(x,t,F_2^s) = A_f M(x,K)\,,$$

$$Q(x,t,F_2^s) = -t\,, \tag{21}$$

and

$$R(x,t,F_2^s) = -A_f L(x,K)F_2^s(x,t)$$

The general solution of (20) is

$$F(u,V) = 0\,, \tag{22}$$

where F is an arbitrary function and

$$u(x,t,F_2^s) = C_1$$

and

$$V(x,t,F_2^s) = C_2 \tag{23}$$

form a solution of the equations

$$\frac{dx}{P(x,t,F_2^s)} = \frac{dt}{Q(x,t,F_2)} = \frac{dF_2^s}{R(x,t\ F_2)} \tag{24}$$

Solving (24) one obtains

$$u(x,t,F_2^s) = tX^s(x) \tag{25}$$

and

$$V(x,t,F_2^s) = F_2^s(x,t)Y^s(x)\,, \tag{26}$$

where

$$X^s(x) = \exp\left[1/A_f \int dx/M(x)\right] \tag{27}$$

and

$$Y^s(x) = \exp\left[\int L(x)/M(x)dx\right] \tag{28}$$

Thus the structure function $F_2^s(x,t)$ has to satisfy (22) with u and V given by (25) and (26), respectively. It thus has no unique solution. The simplest possibility is that a linear combination of u and V is to satisfy (20) so that

$$A_s u + B_s V = 0 \tag{29}$$

Putting the values of u and V in (29) we obtain

$$F_2^s(x,t) = -\frac{A_s}{B_s}\ t\ \left[\frac{X^s(x)}{Y^s(x)}\right] \tag{30}$$

Defining

$$F_2^s(x,t_0) = -\frac{A_s}{B_s}\ t_0\ \left[\frac{X^s(x)}{Y^s(x)}\right] \tag{31}$$

one then has

$$F_2^s(x,t) = F_2^s(x,t_0)\ \ (t/t_0)\,. \tag{32}$$

which gives the t-evolution of singlet structure function $F_2^S(x,t)$. Again defining

$$F(x_0,t) = \frac{A_f}{B_f} \cdot t \cdot \left[\frac{X'(x)}{Y'(x)}\right]_{x=x_0} \tag{33}$$

one then has

$$F_2^S(x,t) = F_2(x_0,t) \cdot \frac{\left[\frac{X'(x)}{Y'(x)}\right]}{\left[\frac{X'(x)}{Y'(x)}\right]_{x=x_0}}$$

so that

$$F_2^S(x,t) = F_2^S(x_0,t) \times \exp\left[\int_{x_0}^{x}\left\{\frac{1}{A_f M(x)} - \frac{L(x)}{M(x)}\right\}dx\right], \tag{34}$$

which gives the x-evolution of $F_2^S(x,t)$.

On the other hand, the AP equation for the non-singlet structure function

$$\frac{\partial F^{NS}(x,t)}{\partial t} - \frac{A_f}{t}\left[\{3+4\ln(1-x)\}F_2^{NS}(x,t) + 2\int_x^1 \frac{dw}{(1-w)}\{(1+w^2)F_2^{NS}(x/w,t) - 2F_2^{NS}(x,t)\}\right] = 0 \tag{35}$$

can be written as

$$\frac{\partial F_2^{NS}(x,t)}{\partial t} - \frac{A_f}{t}\left[A(x)F_2^{NS}(x,t) + B(x)\frac{\partial F_2^{NS}(x,t)}{\partial x}\right] = 0 \tag{36}$$

which is free from the additional assumption (16). Using the same procedure as for the singlet equation, Eq. (36) yields

$$F_2^{NS}(x,t) = F_2^{NS}(x,t_0) \cdot (t/t_0) \tag{37}$$

and

$$F_2^{NS}(x,t) = F_2^{NS}(x,t_0) \times \exp\left[\int_{t_0}^{t}\{1/A_f B(x) - A(x)/B(x)\}dx\right]. \tag{38}$$

which give the t and x-evolutions of non-singlet structure function F_2^{NS}.

The F_2 deuteron and proton structure functions measured in deep inelastic electro-production can be written in terms of singlet and non-singlet quark distribution functions as

$$F_2^d = \tfrac{5}{9}F_2^S \tag{39}$$

and

$$F_2^p = \tfrac{3}{18}F_2^{NS} + \tfrac{5}{18}F_2^S. \tag{40}$$

Using (32) and (34) in (39) we will get the t and x-evolutions of the deuteron structure function at low x as

$$F_2^d(x,t) = F_2^d(x,t_0) \cdot (t/t_0) \tag{41}$$

and

$$F_2^d(x,t_0) = F_2^d(x_0,t) \times \exp\left[\int_{t_0}^{t}\{1/A_f M(x) - L(x)/M(x)\}dx\right] \tag{42}$$

using the input functions

$$F_2^d(x,t_0) = \tfrac{5}{9}F_2^S(x,t_0)$$

and

$$F_2^d(x_0,t) = \tfrac{5}{9}F_2^S(x_0,t).$$

Similarly using (32) and (37) in (40) we have the t-evolution of the proton structure function at low x as

$$F_2^p(x,t) = F_2^p(x,t_0) \cdot (t/t_0) \tag{43}$$

using the input functions

$$F_2^p(x,t_0) = \tfrac{3}{18}F_2^{NS}(x,t_0) + \tfrac{5}{18}F_2^S(x,t_0)$$

But the x-evolution of the proton structure function like those of the deuteron structure function is not possible by this methodology; because to extract the

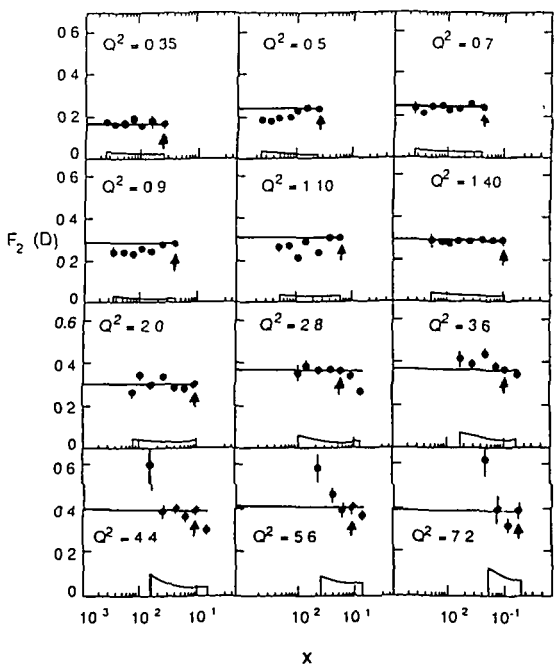

Fig 1 Nucleon structure function, $F_2(D)$ obtained by EMC NA 28 from deuteron as a function of x for different intervals of Q^2 (in GeV^2) Statistical errors are indicated by bars, systematic errors are shown by the bands beneath In addition to the marked errors there is an overall normalization error of 7% Here solid lines are our results (Eq (42) for $N_f = 4$ and $K \simeq 10$–10^{12} Input data points are given by arrow heads.

x-evolution of the proton structure function we are to put (34) and (38) in (40). But as the functions inside the integral sign of Eqs. (34) and (38) are different, we need to separate the input functions $F_2^S(x_0, t)$ and $F_2^{NS}(x_0, t)$ from the data points to extract the x-evolution of the proton structure function, which is not possible.

3. Results and discussion

In our earlier analyses [5] we observed the excellent phenomenological success of the t-evolutions of deuteron and proton structure functions. Here we analyse the x-evolutions of the deuteron structure function. For a quantitative analysis we evaluate the integrals that occurred in (42) for $N_f = 4$ and present the results in Fig. 1 (solid lines) for EMC NA 28 deuteron data [8] in the $K \simeq 10$–10^{12} range. Input data points indicated by arrow heads are taken from experiments.

It is seen that our integrals are almost independent of the K-values particularly in the $x \lesssim 0.1$ range. These results conform well to the data especially for $Q^2 < 2$ GeV^2; but for $Q^2 > 2$ GeV^2, F_2^d grows faster as x decreases. This is a possible indication of the breakdown of (16) at high-Q^2. A clearer testing of our result is actually the relation (38) which is free from the additional assumption (16). But non-singlet data is not sufficiently available at low x to test our result – Eq. (38)

Generally the x-distributions of structure functions are assumed at a fixed low $Q^2 = Q_0^2$ value by various experimental and theoretical constraints and there is no universal agreement among these different assumptions. Then the values of structure functions at higher Q^2 values are calculated from evolution equations. But here we present a method to calculate the x-distribution of the deuteron structure function for any value of Q^2. By knowing the value of the structure function at a fixed value of $x = x_0$, we can evaluate it for other values of x in the low-x region. This is a possible alternative to the various other phenomenological x-distributions discussed in the literature.

Traditionally the AP equations provide a means of calculating the manner in which the parton distributions change at fixed x as Q^2 varies. This change comes about because of the various types of parton branching emission processes and the x-distributions are modified as the initial momentum is shared among the various daughter partons. However the exact rate of modifications of x-distributions at fixed Q^2 cannot be obtained from the AP equations since it depends not only on the initial x but also on the rates of change of parton distributions with respect to x, $d^n F(x)/dx^n$ ($n = 1$ to ∞), upto infinite order. Physically this implies that at high x, the parton has a large momentum fraction at its disposal and as a result radiates partons (including gluons) in innumerable ways, some of them involving complicated QCD mechanisms. However for low x, many of the radiation processes will cease to occur due to momentum constraints and the x-evolutions get simplified. It is then possible to visualise a situation in which the modification of the x-distribution simply depends on its initial value and its first derivative. In this simplified situation, the AP equations give information on the shapes of the x-distribution as demonstrated in this paper. Our result also indicates that the shapes of the x-distributions of all the structure func-

tions at low x which are some combinations of non-singlet and singlet structure functions, are the same for all values of Q^2. This is observed in all data including the HERA data.

References

[1] G Altarelli and G Parisi Nucl Phys B 12 (1977) 298
G Altarelli Phys Rep 81 (1981) 1
V N Gribov and L N Lipatov Sov J Nucl Phys 20 (1975) 94
Y L Dokshitzer Sov Phys JETP 46 (1977) 641

[2] Y Y Balitsky and L N Lipatov Sov J Nucl Phys 28 (1978) 822
E A Kuraev L N Lipatov and Fadin Sov Phys JETP 45 (1977) 199
L V Gribov E M Zevin and M G Ryskin Phys Rep 100 (1983) 1 Nucl Phys B 188 (1981) 555

[3] R D Ball and S Forte Phys Lett B 335 (1994) 77 B 336 (1994) 77,
A De Rujula S L Glashow H D Politzer S B Treiman F Wilczek and A Zee Phys Rev D 10 (1974) 1649
A Zee F Wilczek and S B Treiman Phys Rev D 10 (1974) 2881

[4] K Prytz Phys Lett B 311 (1993) 286 332 (1994) 393
Kalpana Bora and D K Choudhury Phys Lett B 354 (1995) 151
A V Kotokov and G Parente Phys Lett B 379 (1996) 195

[5] D K Choudhury and J K Sarma Pramana J Phys 38 (1992) 481 39 (1992) 273
J K Sarma and B Das Phys Lett B 304 (1993) 323

[6] D K Choudhury and A Saikia Pramana J Phys 29 (1987) 385 33 (1989) 359 34 (1990) 85

[7] L F Abbott W B Atwood and R M Barnett Phys Rev D 22 (1980) 582

[8] EMC NA 28 M Arneodo et al Nucl Phys B 333 (1990) 1 Phys Lett B 211 (1988) 493

PHYSICS LETTERS B

Instructions to Authors (short version)

(A more detailed version of these instructions is published in the preliminary pages to each volume)

Submission of papers

Manuscripts (one original + two copies), accompanied by a covering letter, should be sent to one of the Editors indicated on page 2 of the cover

Original material By submitting a paper for publication in Physics Letters B the authors imply that the material has not been published previously nor has been submitted for publication elsewhere and that the authors have obtained the necessary authority for publication

Refereeing Submitted papers will be refereed and, if necessary, authors may be invited to revise their manuscript If a submitted paper relies heavily on unpublished material, it would be helpful to have a copy of that material for the use of the referee

Types of contributions

Letters The total length of the paper should preferably not exceed six journal pages equivalent to ten typewritten pages with double spacing including the list of authors abstract, references, figure captions and three figures In the case that more figures are required the text should be shortened accordingly As proofs will *not* be sent authors should check their papers carefully before submission

Manuscript preparation

All manuscripts should be written in good English The paper copies of the text should be prepared with double line spacing and wide margins on numbered sheets See notes opposite on electronic version of manuscripts

Structure Please adhere to the following order of presentation Article title Author(s), Affiliation(s), Abstract Classification codes and keywords Main text Acknowledgements, Appendices, References Figure captions Tables

Corresponding author The name complete postal address, telephone and fax numbers and the e mail address of the corresponding author should be given on the first page of the manuscript

Classification codes/keywords Please supply one to four classification codes (PACS and/or MSC) and up to six keywords of your own choice that describe the content of your article in more detail

References References to other work should be consecutively numbered in the text using square brackets and listed by number in the Reference list Please refer to the more detailed instructions for examples

Illustrations

Illustrations should also be submitted in triplicate one master set and two sets of copies The *line drawings* in the master set should be original laser printer or plotter output or drawn in black india ink with careful lettering large enough (3–5 mm) to remain legible after reduction for printing The *photographs* should be originals, with somewhat more contrast than is required in the printed version They should be unmounted unless part of a composite figure Any scale markers should be inserted on the photograph not drawn below it

Colour plates Figures may be published in colour, if this is judged essential by the Editor The Publisher and the author will each bear part of the extra costs involved Further information is available from the Publisher

After acceptance

Notification You will be notified by the Editor of the journal of the acceptance of your article and invited to supply an electronic version of the accepted text, if this is not already available

Copyright transfer You will be asked to transfer the copyright of the article to the Publisher This transfer will ensure the widest possible dissemination of information

No proofs In order to speed up publication, all proofreading will be done by the Publisher and proofs are *not* sent to the author(s)

Electronic manuscripts

The Publisher welcomes the receipt of an electronic version of your accepted manuscript (preferably encoded in LaTeX) If you have not already supplied the final accepted version of your article to the journal Editor you are requested herewith to send a file with the text of the accepted manuscript directly to the Publisher by e mail or on diskette (allowed formats 3 5' or 5 25 MS-DOS, or 3 5 Macintosh) to the address given below Please note that no deviations from the version accepted by the Editor of the journal are permissible without the prior and explicit approval by the Editor Such changes should be clearly indicated on an accompanying printout of the file

Author benefits

No page charges Publishing in Physics Letters B is free

Free offprints The corresponding author will receive 50 offprints free of charge An offprint order form will be supplied by the Publisher for ordering any additional paid offprints

Discount Contributors to Elsevier Science journals are entitled to a 30% discount on all Elsevier Science books

Contents Alert Physics Letters B is included in Elsevier's pre publication service Contents Alert

Further information (after acceptance)

Elsevier Science B.V., Physics Letters B
Issue Management
Physics and Materials Science
P.O. Box 2759, 1000 CT Amsterdam
The Netherlands
Tel.: + 31 20 485 2634
Fax: + 31 20 485 2319
E-mail: NHPDFSKED@ELSEVIER.NL

North-Holland, an imprint of Elsevier Science